Somatostatin analogues as drug delivery systems for receptor-targeted cancer therapy

Anna Escolà Jané

Somatostatin analogues as drug delivery systems for receptor-targeted cancer therapy

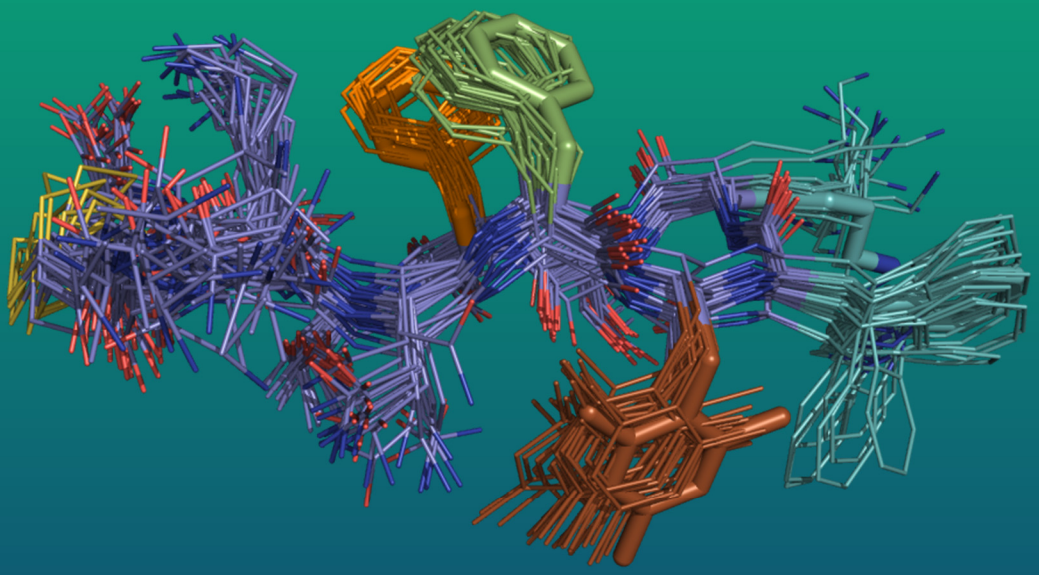

Universitat de Barcelona

Anna Escolà Jané

Barcelona, 2018

Organic Chemistry PhD program

Somatostatin analogues as drug delivery systems for receptor-targeted cancer therapy

Anna Escolà Jané

Organic Chemistry PhD Program

Inorganic and Organic Chemistry Department

University of Barcelona

Thesis director

Dr. Antoni Riera Escalé

Inorganic and Organic Dpt. UB

IRB Barcelona

UNIVERSITAT DE BARCELONA

IRB BARCELONA

INSTITUTE FOR RESEARCH IN BIOMEDICINE

Memòria presentada per Anna Escolà Jané per a optar al grau de DOCTOR en Química per la Universitat de Barcelona.

Anna Escolà Jané

Revisada per:

Dr. Antoni Riera Escalé

Barcelona, Setembre de 2018

Aquest treball s'ha realitzat des del Gener de 2014 fins al Setembre de 2018 amb el suport econòmic del *Ministerio Español de Economía y Competitividad* amb una beca de *Formación del Personal Investigador en un centro de Excelencia Severo Ochoa* (FPI Severo Ochoa). La tasca s'ha finançat amb els projectes de recerca del *Ministerio Español de Economía y Competitividad* CTQ2014-56361 i CTQ2017-87840-P

El treball experimental s'ha dut a terme en el laboratori de la Unitat de Recerca en Síntesi Asimètrica (URSA) de l'Institut de Recerca Biomèdica de Barcelona (IRB Barcelona), ubicat al Parc Científic de Barcelona (PCB).

We've all been sorry, we've all been hurt
But how we survive is what makes us who we are
Survive, **Rise Against**

Agraïments

Abans de començar una tesi no t'imagines amb la quantitat de gent que et creuaràs durant els 4 anys; algunes persones hi són des del principi i t'ajuden a començar aquest llarg camí, altres apareixen més endavant i es queden al teu costat fins al final i altres, simplement, estan de pas. Una tesi és un procés molt llarg en el que hi intervenen moltíssimes persones a qui s'ha de donar les gràcies; espero no deixar-me a ningú...

Primer de tot voldria donar les gràcies al Dr. Antoni Riera, per donar-me l'oportunitat de treballar a URSA. Tot i que el meu background no era orgànic m'he acabat adaptant bastant bé. Al Dr. Xavier Verdaguer per tots els consells durant aquests quatre anys. A la Dra. María Macías, per tot el suport pel que fa als RMN de pèptids i per resoldre'm dubtes sempre que ho he necessitat.

Als membres del meu TAC: al Dr. Àngel Messeguer, al Dr. Vicente Marchán i a la Dra. Natàlia Carulla; per tots els suggeriments que m'heu fet en les comissions de seguiment, per la vostra passió i entusiasme per la ciència i per donar-me sempre ànims quan els resultats no acompanyaven gens.

Al Dr. Álvaro Rol, aunque para mí siempre vas a ser sólo Álvaro. Gracias por el tiempo compartido en la vitrina, (fue bastante duro, ¡la verdad!), por todos los "acompáñame a fumar", "vamos fuera", "moneypenny!" y "las paredes tienen ojos" que me has dedicado todo este tiempo. Por ser un amigo de verdad, escuchar mis tonterías, darme buenos consejos y decirme las verdades a la cara sin ningún tipo de problema. Te he echado de menos estos dos últimos años.

Als ex-URSA members; Àlex, per ser un pilar fonamental al principi de la tesi, sense la teva ajuda moltes coses no m'haurien sortit mai. A un dels meus guiris preferits, Dan, per tots els "ets un pesao", les bromes, riures i converses de tornada cap a casa quan vivia a Barcelona; saps que ets una persona molt important per mi. A l'Edgar, per fer-me veure que els companys de lab també poden ser amics. A Helea, por tu pasión por la ciencia, por enseñarme que con constancia las cosas acaban saliendo. A la Sílvia, per fer-me veure que tot l'esforç acaba tenint la seva recompensa. A la Núria, per fer-me de guia els primers dies de tesi. To Chris, for your passion when teaching science. A Ale, por todos los consejos recibidos en el tiempo que coincidimos. A Toni Todorovski, gracias por estar siempre dispuesto a ayudar.

Als URSA-members actuals; Craig, my other guiri, you are a real URSA (yoU aRe So Aweseome!), thank you for making the lab-work less hard and for sharing the experience of having not-so-good results; once we joined forces, everything went better. The word friend really makes sense with you. A l'Ernest, per totes les discussions sobre català i per ser tant transparent; ets molt bona gent! Al Pep, per haver-te convertit en una persona important; saps que els meus "ets tan..." no són sempre de veritat. A la Marta, per fer del laboratori un lloc més alegre i per compartir amb mi la passió pel ball. A l'Albert, per haver-me ensenyat que hi pot haver ordre dins el caos i per tots els Aaaaaaaannaaa! que has dit en aquests anys cada cop que entrava per la porta. Al Joan, el meu successor en SPPS, pels riures i les abraçades. A l'Enric, per aportar un toc de color pink (pink para Enric! pink para Enric!) i d'alegria al laboratori. A l'Amparo per fer-me veure que les coses sempre poden canviar cap a millor. A Caro, por aportar un toque de humor antes de salir de trabajar. Al Rubén, una de les últimes incorporacions, per les duríssimes crítiques. A Elia, per portare umorismo e un tocco "italianini", rustico e moderno in laboratorio. Ciao bello. Al Juanjo, per ser tan "moniii".

Al Pol, per entendre'ns amb una mirada, pels riures i somriures, els memes i l'alegria que desprens i contagies a la gent, ets genial! Al Sergi, per "bajarse de la vida" amb només 21 anys. A la Roberta i el Pedro, per demostrar-me que la paciència és la mare de la ciència. Als estudiants de pas Elsa, Ronald, Tiffaine, Samuel, Iris, Eva, María, Joan, Pol, Martí, Lorenzo, Laura, Nico i Martí, per ser una font d'anècdotes.

A la Helen, una ex-URSA, per escoltar-me sempre (que no és poc!). Per estar sempre disposada a organitzar trobades i sortides. Ets un amor! En tu he trobat una gran amiga.

Tampoc puc oblidar-me de donar les gràcies a l'Arnald, per tot el suport durant aquests anys de doctorat (ha sigut dur, ho sé!), pels consells i pels sopars! A l'Albert Gallén, per entrar al laboratori sempre amb un somriure a la cara. Molta sort en la recta final!

Com podria oblidar dels meus inicis en la ciència; gracias Margarita por todo lo que me enseñaste durante el máster, ha sido de gran ayuda para los años que han venido después; seguro que sin tus consejos y tu dirección ahora no estaría presentando esta tesis. A Lucía, compañera de laboratorio y una gran amiga. Gracias por las risas aseguradas cada vez que nos vemos, por los ánimos y por estar siempre aunque sea en la distancia.

A la Judith, per tots els moments compartits, per mantenir la tradició començada a l'APS i continuar fent gran la nostra col·lecció de fotos. Per ser les iaies amb més ganes de festa. Tot i la distància saps que aquí hi tens una amiga. A l'Helena, per ajudar-me en tot allò referent a pèptids i desproteccions. A Gianmarco, por estar siempre dispuesto a ir a tomar un café. Al lunch team: Laura, Gemma, Jordi, Jürgen, Ricardo i Cris, per fer els migdies més agradables.

A Montse, por ser igual de perseverante (o quizá igual de cabezota) que yo, por demostrarme que las cosas acaban saliendo y por toda la ayuda estos años. Sin ti parte de esta tesis no habría sido posible. A Nacho, por estar siempre dispuesto a ayudar. A Mónica, por toda la ayuda y la paciencia que has tenido conmigo y con los experimentos con células.

A la Mar, per rebre'm sempre amb un somriure i ajudar-me amb els espectres de masses, no sempre ha sigut fàcil. A l'Irene i la Laura, per tota la vostra ajuda. Al Jordi i al Pau per l'ajuda amb els RMN de pèptids. Al Jesús, per tenir sempre bones paraules. Al personal d'Enantia S.L., en especial a la Montse, el Toni, l'Esther i l'Adela per l'ajuda i els consells. A BCN Peptides S.A., per la col·laboració en aquesta tesis.

A la Vicky i l'Anna, pels berenars, els riures, els brainstormings i tots els moments viscuts amb vosaltres (i els que ens queden!!). Sense vosaltres no hagués sigut el mateix.

A les de tota la vida; Laia, Clara M., Clara C. i Laura, per ser-hi sempre, passi el que passi.

Al Mario, pel suport incondicional durant tots aquests anys. Sé que no ha sigut gens fàcil... Però si hem superat això, res ens aturarà. Sense tu aquesta tesi tampoc hagués sigut possible.

A "La Famiglia", pels valors que m'heu donat i per ser-hi sempre. Sense vosaltres segur que no hauria arribat fins aquí. Sou la millor família que podria tenir. A les iaies, per cuidar-me sempre i per preocupar-vos per com em va "el col·legi". Als avis, per tot el que em vau ensenyar des de petita; us porto sempre amb mi.

Table of contents

Abbreviations and units

ACH	α-Cyano-4-hydroxycinnamic acid	DEA	Diethanolamine
ACN	Acetonitrile	DIEA	N,N-Diisopropylethylamine
aa	Amino acid	DME	Dimethoxyethane
AcO^-	Acetate ion	DMF	Dimehtylformamide
AcOH	Acetic acid	DMSO	Dimethylsulfoxide
Ac_2O	Acetic anhydride	D_2O	Deuterated water
anh.	anhydrous	ee	Enantiomeric excess
API	Active pharmaceutical ingredient	*et. al*	et alia
aq	Aqueous	Et_3N	Triethylamine
BF_4^-	Tetrafluoroborate ion	EtOH	Ethanol
Boc	tert-Butyloxycarbonyl	Et_2O	Diethyl ether
cAMP	Cyclic adenosine monophosphate	ESI	Electrospray ionisation
CD_3Cl	Deuterated chloroform	eq	equivalent
CD_3OD	Deuterated methanol	FA	Formic acid
$-CH_3$	Methyl group	FDA	Food and Drug Administration
CHO-K1	Chinese hamster ovarian cell line	Fmoc	Fluorenylmethyloxycarbonyl
cm-1	Wavenumber unit	Fmoc-AA-OH	Fmoc-protected amino acid
CNS	Christallography & NMR system	FmocOSu	Fmoc-Succinimide
DAD	Diode array detector	g	grams
DBU	1,8-Diazabicyclo[5.4.0]undec-7-ene	GH	Growth Hormone
DCM	Dichloromethane	GHIH	Growth Hormone-inhibiting hormone

GIT	Gastrointestinal tract	$KMnO_4$	Potassium permanganate
GnRH	Gonadotropin-releasing hormone	kV	Kilovolt
GP	Generic peptides	LHRH	Luteinizing Hormone Releasing Hormone
GPCR	G-protein coupled receptor	MALDI	Matrix Assisted Laser Desorption/Ionization
h	hours	MAPK	Mitogen-activated protein kinase
H_{Ar}	Aromatic proton	MeI	Methyl iodide
HATU	1-[Bis(dimethylamino)methylene]-1H-1,2,3-triazolo[4,5-b]pyridinium 3-oxid hexafluorophosphate	MeOH	methanol
HCl	Hydrochloric acid	MeONa	Sodium methoxide
H_2O	water	mg	Milligrams
HMBC	Heteronuclear Multiple Bond Correlation	MHz	Megahertz
HOBt	Hydroxybenzotriazole	Milli-Q Water	Ultrapure water, Type 1
HR-MS	High-resolution mass spectrometry	min	Minutes
H_2SO_4	Sulfuric acid	mL	Millilitre
HSQC	Heteronuclear single quantum correlation	mm	Millimetre
Hz	Hertz	mmol	Millimol
I_2	Iodine	MP	Melting point
IPA	Isopropanol	ms	Milliseconds
K_2CO3	Potassium carbonate	MS	Mass spectrometry
KCN	Potassium cyanide	MS/MS	Tandem mass spectrometry
Ke	Decay constant	m/z	Mass/charge ratio
Ki	Inhibition constant	N_2	Nitrogen
KI	Potassium iodide	Na	Sodium

Na_2CO_3	Sodium carbonate	T	Temperature
$NaNO_3$	Sodium nitrate	t	Time
NH_4HCO_3	Ammonium bicarbonate	$t_{1/2}$	Half-life
nm	Nanometre	^{t}Bu	Tert-butyl
nM	Nano molar	TFA	Trifluoroacetic acid
NMR	Nuclear magnetic resonance spectroscopy	TFA^-	Trifluoroacetate ion
ns	Nano seconds	TFE	2,2,2-Trifluoroethanol
NOE	Nuclear overhauser effect	THF	Tetrahydrofuran
NOESY	Nuclear overhauser effect spectroscopy	TIS	Triisopropylsilane
PBS	Phosphate-buffered saline	TMD	Trans-membrane domain
PTP	Phosphotyrosine phosphatase	$TMS\text{-}CHN_2$	Trimethylsilyldiazomethane
ppm	Parts per million	TOF	Time-Of-Flight detector
$Pd(OAc)_2$	Palladium acetate	TOCSY	Total correlated spectroscopy
rpm	Revolutions per minute	trt	Trityl group
RP-UPLC	Reverse-phase UPLC	t_R	Retention time
r.t.	Room temperature	UPLC	UltraPerformance Liquid Chromatography
SiO_2	Silicon dioxide	UPLC-MS	UPLC-Mass spectrometry
SPPS	Solid phase peptide synthesis	UV	Ultraviolet
SPS	Solvent purification system	WT	Wild type cells
SRIF	Somatotropin release-inhibiting factor	λ	wavenumber
SST	Somatostatin	μL	Microlitre
SST14	14-aa somatostatin	μM	Micro molar
SST28	28-aa somatostatin	μm	Micrometre
SSTR	Somatostatin receptor	2-CTC	2-chlorotrityl chloride
ST	SSTR2-overexpressing cell type	°C	Degree Celsius

Chapter 1

Introduction and objectives

Somatostatin (SST) is an endogenous hormone which was first discovered in its tetradecapeptidic form from bovine hypothalamic extracts[1] in 1973 (Figure 1.1). It inhibited the secretion of somatotropin (or growth hormone, GH) in somatotrope cells. Due to this discovery, it was called *Somatotropin Release-Inhibiting Factor* (SRIF) or *Growth Hormone-Inhibiting Hormone* (GHIH). Subsequently, somatostatin was found to be secreted by a broad range of tissues, including pancreas, intestinal tract and regions of the central nervous system outside the hypothalamus.[2]

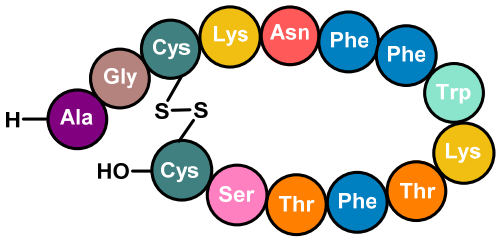

Figure 1.1. 14-amino acid Somatostatin structure (SRIF structure).

Since its initial isolation, the 14-amino acid peptide (SRIF14) has been the most studied form of SRIF although its prehormone of 28 amino acids (SST28) is also biologically active.[3] SRIF (or SST14) is involved in multiple biological functions which include the inhibition of secretion of endogenous factors such as the above-mentioned growth hormone, insulin, glucagon or gastrin, and the inhibition of exogenous secretion of gastric acid or pancreatic enzymes.[4] All these functions are mediated by direct interactions with at least five characterised G-protein-coupled receptors, named SSTR1-

[1] a) P. Brazeau, W. Vale, R. Burgus, N. Ling, M. Butcher, J. Rivier, R. Guillemin, *Science*, **1973**, *179*, 77 - 79; b) R. Burgus, N. Ling, M. Butcher, R. Guillemin, *Proc. Natl. Acad. Sci. U.S.A.*, **1973**, *70*, 684 - 688.

[2] a) E. Tousson; K. Abou-Easa. *J. Am. Sci.*, **2010**, 6, 91-98. J. b) Morisset, *Pancreas*, **2017**, *46*, 8 - 18.

[3] a) A. V. Schally, A. Dupont, A. Arimura, T. W. Redding, G. L. Linthicum, *Fed. Proc. Fed. Am. Soc. Exp. Biol.*, **1975**, *34*, 584; b) A. Arimura, H. Sato, A. Dupont, N. Nishi, A. V. Schally, *Science*, **1975**, *189*, 1007 - 1009; c) A. V. Schally, A. Dupont, A. Arimura, T. W. Redding, N. Nishi, G. L. Linthicum, D. H. Schlesinger, *Biochemistry*, **1976**, *15*, 509 - 514; d) L. Pradayrol, H. Jornvall, V. Mutt, A. Ribet, *FEBS Lett*, **1980**, *109*, 55 - 58.

[4] a) T. Hokfelt, S. Effendic, C. Hellerstrom, O. Johansson, R. Luft, A. Arimura, *Acta Endocrinol.*, **1975**, *80*, 5 - 41; b) Y. C. Patel, S. Reichlin, *Endocrinology*, **1978**, *102*, 523 - 530; c) S. Reichlin, *N. Engl. J. Med.*, **1983**, *309*, 1495 - 1501, 1556 - 1563.

5,[5] which differ in their tissue distribution and pharmacological properties.[5f] A large number of studies deleting residues were performed with the aim of identifying the active site of the peptide. Through these, the molecule-crucial region for the interaction with the receptors (pharmacophore) was identified as the fragment that included Phe7-Trp8-Lys9-Thr10 residues.[6] It was also hypothesised that those residues form a β-hairpin stabilised by aromatic interactions between Phe6 and Phe11 side chains.[7]

Somatostatin (SRIF14) is secreted throughout the central nervous system[8], in the gastrointestinal tract, retina, peripheral neurones and the pancreatic islets of Langerhans[9] and has anti-secretory, anti-proliferative and anti-angiogenic effects. Although SRIF14 is efficacious in certain conditions, the therapeutic use of the native peptide is limited by its very short plasma half-life (< 3 min), the broad spectrum of biological responses and the lack of selectivity over its different receptors.[10]

With the aim of overcoming these drawbacks, the synthesis of SRIF analogues has focused on progressively shortening the peptides but maintaining the annular structure and the pharmacophore region to create analogues with higher selectivity against some SSTRs and higher plasma half-life. Due to somatostatin's mode of action, it has been tested against several dysfunctions such as hypersecretory tumours (GH-secreting pituitary

[5] a) Y. C. Patel, K. K. Murthy, E. Escher, D. Banville, J. Spiess, C. B. Srikant, *Metabolism*, **1990**, *39*, 63 - 69; b) Y. C. Patel, *Basic. Clin. Asp. Neurosci.*, **1992**, *4*, 1 - 16; c) Y. C. Patel, M. T. Greenwood, R. Panetta, L. Demchyshyn, H. Niznik, C. B. Srikant, *Life Sci*., **1995**, *57*, 1249 - 1265; d) J. C. Reubi, U. Horisberger, A. Kappeler, J. A. Laissue, *Blood*, **1998**, *92*, 191 - 197; e) A. Schonbrunn, A. H. Tashjian, *J. Biol. Chem.*, **1978**, *253*, 6473 - 6483. f) D. Hoyer *et al.*, *Trends Pharmacol. Sci.*, **1995**, *16*, 86 - 88.

[6] a) W. Bauer, U. Briner, W. Doepfner, R. Halber, R. Huguenin, P. Marbach, T. J. Petcher, J. Pless, *Life Sci*., **1982**, *31*, 1133 - 1140; b) D. Veber, R. Saperstein, R. Nutt, R. Friedinger, S. Brady, P. Curley, D. Perlow, W. Palveda, C. Colton, A. Zacchei, D. Tocco, D. Hoff, R. Vandlen, J. Gerich, L. Hall, L. Mandarino, E. Cordes, P. Anderson, R. Hirschmann, *Life Sci.*, **1984**, *34*, 1371 - 1378; c) J. E. Taylor, D. H. Coy, *J. Endocrinol. Invest.*, **1997**, *20*, 8 - 10.

[7] M. Knappenberg, A. Michel, A. Scarso, J. Brison, J. Zanen, K. Hallenga, P. Deschrijver, G. Van Binst, *Biochim.Biophys.Acta, Protein Struct.Mol.Enzymol.*, **1982**, *700*, 229 - 246.

[8] U. Kumar, M. Grant; *Results Probl. Cell Differ*, **2010**, *50*, 137 - 184.

[9] U. Rai, T. R. Thrimawithana, C. Valery, S. A. Young; *Pharmacol. Ther*, **2015**, *152*, 98 - 110.

[10] G. Weckbecker, I. Lewis, R. Albert, H. A. Schmid, D. Hoyer, C. Bruns. *Nature Reviews Drug Discovery,* **2003**, *2*, 999 - 1017.

adenomas and gastrinomas), diabetes type I and II and gastrointestinal disorders (bleeding ulcers or pancreatitis).[4c] Out of all the somatostatin analogues developed, only four reached the market for the treatment of different metabolic diseases; octreotide (commercial name: Sandostatin®)[6a,11], lanreotide (Somatuline®)[12] and vapreotide (Sanvar®)[13], octapeptides which maintain the disulphide bridge and pasireotide (Signifor®)[14] a cyclic hexapeptide. Their structures are shown in Figure 1.2. As it can be seen in the structures, they share the fragment including Phe/Tyr/Phg7_D-Trp8_Lys9_Thr/Val10.

Since the discovery of SSTRs in the 1990's,[5f,15] exhaustive research of SRIF analogues' binding properties has been investigated. Through these binding assays, the behaviour of both octreotide and lanreotide against SSTRs was established; showing a marked increase in the selective pharmacological profile for the binding with SSTR2 and SSTR5.[16] In light of these findings, research on somatostatin analogues focused on shorter peptide synthesis mimicking octreotide, a potential hit-to-lead in drug discovery. Some modifications used to synthesise new shorter analogues were ring size adjustment, exchange of amino acids, disulphide bridge modification and multiple N-methylation.[17] Peptides containing some of these modifications were found to improve the properties of the natural hormone.

[11] S. W. J. Lamberts, A. J. van der Lely, W. W. de Herder, *N. Eng. J. Med*., **1996**, *334*, 246 - 254.

[12] J. Marek, V. Hána, M. Kršek, V. Justová, F. Catus, F. Thomas, *Eur.J. Endocrinol.*, **1994**, *131*, 20 - 26.

[13] P. M. Girard, E. Goldschmidt, D. Vittecoq, P. Massip, J. Gastiaburu, M. C. Meyohas, J. P. Coulaud, A. V. Schally, *AIDS*, **1992**, *6*, 715 - 718.

[14] C. Bruns, I. Lewis, U. Briner, G. Meno-Tetang, G. Weckbecker, *Eur. J. Endocrinol.*, **2002**, *146*, 707 - 716.

[15] Y. C. Patel, C. B. Srikant, *Endocrinology*, **1994**, *135*, 2814 - 2817.

[16] C. Bruns, F. Raulf, D. Hoyer, J. Schloos, H. Lubbert, G. Weckbecker, *Metabolism*, **1996**, *45*, 17 - 20.

[17] a) C. R. R. Grace, J. Erchegyi, S. C. Koerber, J. C. Reubi, J. Rivier, R. Riek, *J. Med. Chem.,* **2006**, *49*, 4487 - 4496; b) A. Di Cianni, A. Carotenuto, D. Brancaccio, E. Novellino, J. C. Reubi, K. Beetschen, A. M. Papini, M. Ginanneschi, *J. Med. Chem.,* **2010**, *53*, 6188 - 6197; c) J. Chatterjee, B. Laufer, J. G. Beck, Z. Helyes, E. Pintér, J. Szolcsányi, A. Horvath, J. Mandl, J. C. Reubi, G. Kéri, H. Kessler, *ACS Med. Chem. Lett.*, **2011**, *2*, 509 - 514; d) M. Morpurgo, C. Monfardini, L. J. Hofland, M. Sergi, P. Orsolini, J. M. Dumont, F. M. Veronese, *Bioconjugate Chem.*, **2002**, *13*, 1238 - 1243.

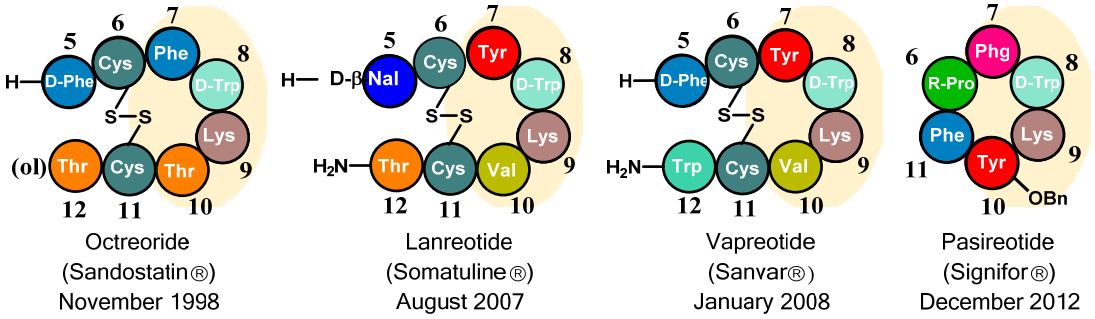

Figure 1.2. Commercially available SRIF analogues where the pharmacophore region (aa7 to aa10) is highlighted. The date of FDA approval is also shown. D-β-Nal: 3-(2'-naphthyl)-D-alanine. Phg: L-Phenylglycine. R-Pro: 3-[(2-aminoethyl)amino-carbonyloxy]-L-proline.

The flexible structure of the native somatostatin14 made it impossible to determine its major structure in solution. It has been proved that SRIF14 shows an equilibrium state between different conformations,[18] some of which are partially structured. SRIF has a disulphide bridge which provides conformational restriction but further to that, the existence of aromatic interactions between Phe6, Phe7 and Phe11 was proposed.[19] When residues 6 and 11 are substituted by alanine the biological activity is completely lost,[20] whereas if the substitution is made by cysteines linked by a disulphide bridge, the biological activity is retained.[19] In light of these findings, it was established that the aromatic interactions between these residues (Phe 6 and 11) play a key role in the stabilisation of the hormone.[19] Initial bi-dimensional nuclear magnetic resonance (NMR) studies suggested that the interaction was taking place between residues 6 and 7 as there

[18] a) K. Hallenga, G. Van Binst, A. Scarso, A. Michel, M. Knappenberg, C. Dremier, J. Brison, J. Dirkx, *FEBS Lett.*, **1980**, *119*, 47 - 52; b) M. Knappenberg, A. Michel, A. Scarso, J. Brison, J. Zanen, K. Hallenga, P. Deschrijver, G. Van Binst, Biochim. Biophys. Acta, *Protein Struct. Mol. Enzymol.*, **1982**, *700*, 229 - 246; c) L. A. Buffington, V. Garsky, J. Rivier, W. A. Gibbons, *Biophys. J.*, **1983**, *41*, 299 - 304; d) L. A. Buffington, V. Garsky, J. Rivier, W. A. Gibbons, *Int. J. Pept. Protein Res.*, **1983**, *21*, 231 - 241.

[19] a) J. E. Rivier, M. R. Brown, W. W. Vale, *J. Med. Chem.*, **1976**, *19*, 1010 - 1013; b) D. F. Veber, F. W. Holly, W. J. Paleveda, R. F. Nutt, S. J. Bergstrand, M. Torchiana, M. S. Glitzer, R. Saperstein, R. Hirschmann, *Proc. Natl. Acad. Sci. U.S.A.*, **1978**, *75*, 2636 - 2640.

[20] W. W. Vale, C. Rivier, M. R. Brown, J. E. Rivier, *Hypothalamic Peptide Hormones and Pituitary Regulation, Advances in Experimental Medicine and Biology*. Plenum Press **1977**, 123 - 156.

were no ^{1}H-^{1}H NOE signals corresponding to the interaction of Phe11 with other aromatic protons.[21]

The fact that the octapeptides with a disulphide bridge between residues 6 and 11 (Figure 1.2) maintained the biological activity against SSTR2 directed the synthesis to the derivatives of eight residues and to the theory of 6-11 interaction over the 6-7 interaction model. Rivier *et al.* carried out the substitution of each residue by Tyr (*Tyr-Scan*) and it was suggested that Phe6 is functionally involved in the receptor activation process, while Phe7 internally stabilises SST tertiary structure through the stacking of aromatic rings.[19]

Some years ago, the significant advances in solid-phase peptide synthesis (SPPS) led us to consider the SRIF14 scaffold in the design of new analogues with higher stability and receptor selectivity. We hoped to overcome some drawbacks of octapeptides such as the loss of activity towards some receptors. Furthermore, the design of novel tetradecapeptidic analogues would enable us to remain closer to the natural hormone in terms of structure, pharmacokinetics, etc. Structurally more rigid SRIF14-analogues will allow us to characterise their main conformation. For that reason, our group, in collaboration with BCN peptides, began researching the development of new tetradecapeptidic somatostatin derivatives.

The first modifications were performed by Rosario Ramón.[22] She did the first thesis of our group in this project by synthesising two new SRIF analogues introducing the amino acids L and D-3-(3'-quinolyl)-alanine, [L-Qla8]-SRIF and [D-Qla8]-SRIF. This amino acid has a similar size when compared to Trp but with inverse electronic properties of the aromatic ring. Furthermore, Qla lacks the N-H bond which has been proposed to be the key to the

[21] a) A. W. H. Jans, K. Hallenga, G. Van Binst, A. Michel, A. Scarso, J. Zanen, *Biochim. Biophys. Acta, Protein Struct. Mol. Enzymol.*, **1985**, *827*, 447 - 452; b) E. M. M. Van den Berg, A. W. H. Jans, G. Van Binst, *Biopolymers*, **1986**, *25*, 1895 - 1908; c) J. E. Rivier, M. R. Brown, W. W. Vale, *J. Med. Chem.*, **1976**, *19*, 1010 - 1013.

[22] R. Ramón, Doctoral thesis *Síntesis de aminoácidos no naturales y aplicación a la síntesis de péptidos con interés farmacológico*, University of Barcelona, **2009**.

SSTRs activation.[23] In both cases, the peptides obtained were less rigid and showed a different biological activity towards the SSTRs. While [L-Qla8]-SRIF was active against SSTR1 and 3 but not towards SSTR2, 4 and 5, [D-Qla8]-SRIF resembled octreotide for the binding with SSTR5,[24] was active in front of SSTR1 and 3 but not against SSTR2 and SSTR4.

Next modification was the substitution of the disulphide bridge between Cysteines 3 and 14 by a C-C double bond.[25] This was meant to study the impact on the stability and biological activity. The peptide containing the non-natural amino acid L-allylglycine in both positions 3 and 14 was synthesised and then cyclised by metathesis, mimicking the strategy followed when cyclising octa-analogues via an alkene.[26] As a result, the carbaSOM showed more conformational flexibility than the natural hormone whilst the binding affinity was maintained for SSTR1 and SSTR5 but it decreased for the other three receptors with SSTR2 being the one with the lowest affinity values.

The most important modification was the substitution of phenylalanines for the non-natural amino acid L-β-mesitylalanine (Msa), studied in Pablo Antonio Martín-Gago's thesis,[27] which led us to a deeper understanding of somatostatin. Furthermore, he also introduced the non-natural amino acid D-Tryptophan (D-Trp) instead of L-Tryptophan

[23] B. H. Hirst, B. Shaw, C. A. Meyers, D. H. Coy, *Regul. Pept.*, **1980**, *1*, 97 - 113.

[24] R. Ramón, P. Martín-Gago, X. Vedaguer, M. J. Macias, P. Martín-Malpartida, J. Fernández-Carneado, M. Gómez-Caminals, B. Ponsati, P. López-Ruiz, M. A. Cortés, B. Colás, A. Riera, *ChemBioChem*, **2011**, *12*, 625 - 632.

[25] P. Martín-Gago, R. Ramón, E. Aragón, J. Fernández-Carneado, P. Martín-Malpartida, X. Vedaguer, P. López-Ruiz, B. Colás, M. A. Cortés, B. Ponsati, M. J. Macias, A. Riera, *Bioorg. & Med. Chem Lett.*, **2014**, *24*, 103 - 107.

[26] a) R. F. Nutt, D. F. Veber, R. Saperstein, *J. Am. Chem. Soc.*, **1980**, *21*, 6539 - 6545; b) V. M. Garsky, D. E. Clark, N. H. Grant, *Biochem. Biophys. Res. Commun.*, **1976**, *4*, 911 - 916; c) D. F. Veber, R. G. Strachan, S. J. Bergstrand, F. W. Holly, C. F. Homnick, R. Hirschmann, M. L. Torchiana, R. Saperstein, *J. Am. Chem. Soc.*, **1976**, *8*, 2367 - 2369; d) A. N. Whelan, J. Elaridi, R. J. Mulder, A. J. Robinson, W. R. Jackson, *Can. J. Chem.*, **2005**, 6 -7, 875 - 881; e) D. D'Addona, A. Carotenuto, E. Novellino, V. Piccand, J. C. Reubi, A. di Cianni, F. Gori, A. M. Papini, M. Ginanneschi, *J. Med. Chem.*, **2008**, *51*, 512 - 520; f) A. di Cianni, A. Carotenuto, D. Brancaccio, E. Novellino, J. C. Reubi, K. Beetschen, A. M. Papini, M. Ginanneschi, *J. Med. Chem.*, **2010**, *53*, 6188 - 6197.

[27] P. A. Martín-Gago, doctoral thesis *Synthesis of highly structured and receptor-selective tetradecapeptidic analogs of somatostatin: Fine tuning the non-covalent interactions among their aromatic residues*, Univeristat de Barecelona, 2013.

(L-Trp) in position 8 to depict its role in the stabilization of the structure's β-turn. By doing that, it has been observed that using the D-isomer ([D-Trp8]-SRIF) triggers an increase in the biological activity of the peptide due to the stronger aromatic-aliphatic interaction with Lysine 9 (Lys9).[28] Moreover, the replacement of Phe6, Phe7 or Phe11 for L-Msa, in addition to the change of L-Trp for D-Trp, provided highly structured peptides. The structure in solution was determined by NMR for the first time (Figure 1.3). The higher rigidity, when compared to the natural hormone, comes from the enhanced aromatic interactions provided by the higher electronic density and the higher steric hindrance of the mesityl aromatic ring.

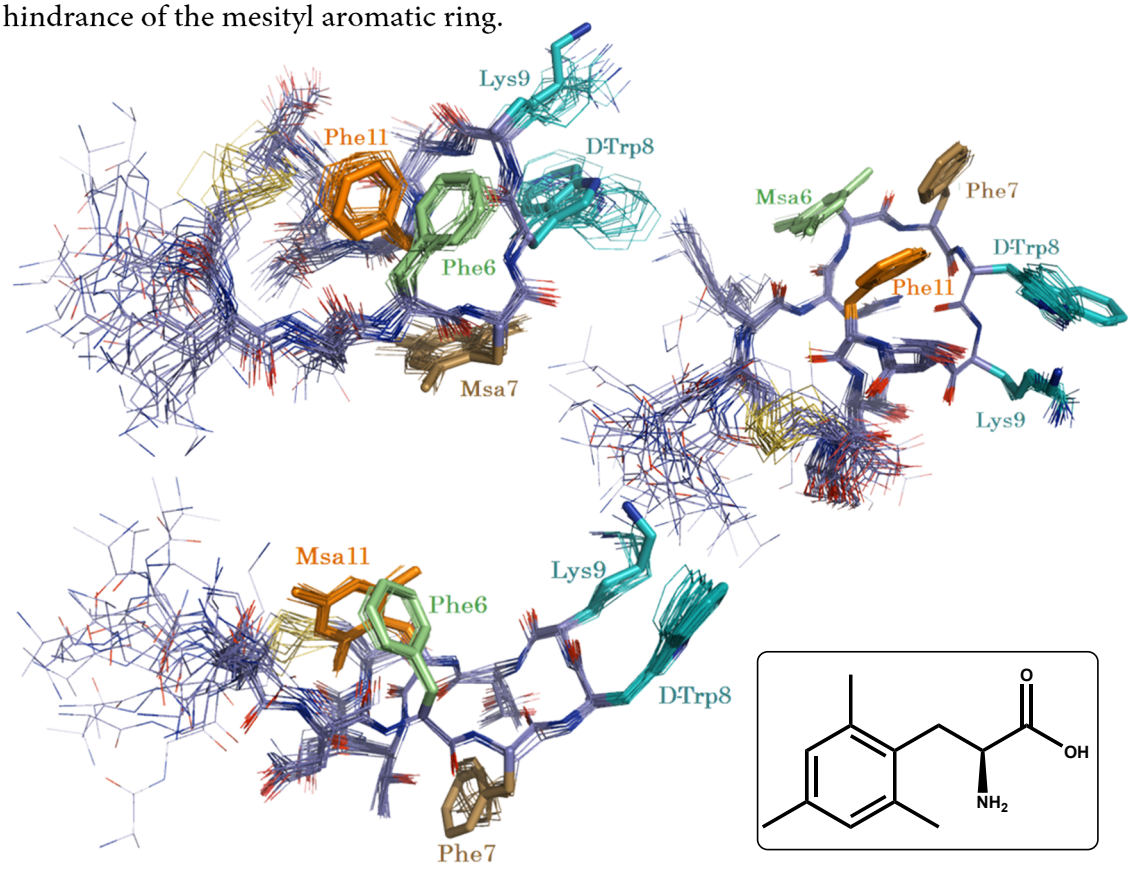

Figure 1.3. SRIF-analogues' 3D structures obtained by NMR. [Msa7_D-Trp8]-SRIF (top, left) has an edge-to-face interaction between Phe6 and Phe11, [Msa6_D-Trp8]-SRIF (top, right) has an aromatic cluster with the three aromatic rings interacting with each other and [Msa11_D-Trp8]-SRIF (bottom, left) has and offset-tilted orientation between residues 6 and 11. Msa structure is shown for a better understanding.

[28] a) B. H. Arison, R. Hirschmann, D. F. Veber, *Bioorg. Chem.*, **1978**, *7*, 447 - 451; b) O. Ovadia, S. Greenberg, B. Laufer, C. Gilon, A. Hoffman, H. Kessler, *Expert Opin. Drug Discov.*, **2010**, *5*, 655 - 671.

When comparing the structures obtained, it can be seen that in both [Msa6_D-Trp8]-SRIF and [Msa11_D-Trp8]-SRIF, the non-natural amino acid is directly involved in the π - π aromatic interaction, while in the [Msa7_D-Trp8]-SRIF analogue the Msa is placed on the other side of the molecule which enables the Phe6 and Phe11 to be closer in space to each other and making the π - π aromatic interaction stronger.

The affinity of these three compounds for the SSTRs was measured; the analogue with Msa in position 7 showed outstanding results for the SSTR2 with the affinity for that receptor being even higher than that of octreotide and resembling SRIF14. The opposite behaviour was observed for the analogues with Msa in position 6 and 11, which displayed higher affinity for both SSTR3 and SSTR5.[27,29]

To have a better understanding of the π - π aromatic interactions between the residues forming the pharmacophore region of the molecule and its effect on the biological activity, some additional modifications of the residues Phe6, Phe7 and Phe11 were implemented in Alvaro Rol's thesis.[30] He studied the effect of introducing electron poor amino acids into the SRIF14 sequence. As stated before, the introduction of Msa into the natural sequence led to more rigid structures.[29] Hence, it was hypothesised that the pharmacological profile could also be modified by tuning the π - π aromatic interactions. The modifications consisted of the introduction of non-natural amino acids with electron-poor aromatic rings to determine its influence in the stabilisation of the major structure in solution. The amino acids used were L-β-3',5'-difluoro-phenylalanine,[29] L-β-3'-pyridylalanine and L-β-4'-pyridylalanine. L-β-mesitylalanine was introduced in position 7 in some selected derivatives as an amino acid with an electron rich aromatic ring. Structures of these four amino acids are shown in Figure 1.4 and Figure 1.5 (left).

[29] P. Martín-Gago, M. Gómez-Caminals, R. Ramón, X. Verdaguer, P. Martín-Malpartida, E. Aragón, J. Fernández-Carneado, B. Ponsati, P. López-Ruiz, M. A. Cortés, B. Colás, M. J. Macias, A. Riera, *Angew. Chem. Int. Ed.*, **2012**, *51*, 1820-1825.

[30] A. Rol Rúa, doctoral thesis *Análogos de somatostatina y cortistatina. Efectos de las interacciones aromáticas en sus estructuras y en la actividad biológica.* Universitat de Barcelona, 2015.

The selection of Msa was due to two main factors; a) the electronic effect, making the aromatic ring richer in electrons as a result of the electron donating character of the methyl groups and b) the steric effect that these two methyl groups in *ortho* positions confer to the amino acid, thus preventing the rotation around the phenylic bond (Figure 1.5).

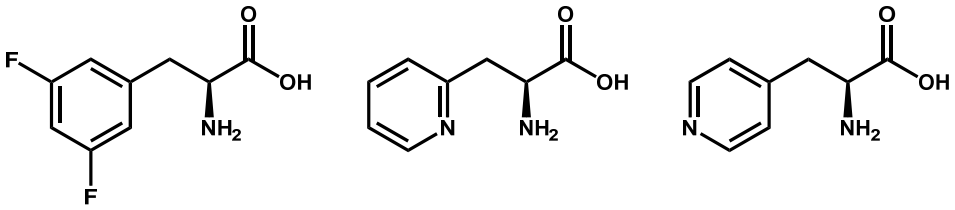

Figure 1.4. Structures of the non-natural amino acids selected to be used as a modification in the natural sequence. L-β-3',5'-difluoro-phenylalanine (left), L-β-3'-pyridylalanine (middle), L-β-4'-pyridylalanine (right).

In the present thesis, we planned to deeply explore the effects of the aromatic interaction by substituting the above-mentioned phenylalanines for an electron-rich aromatic ring but with less steric hindrance than Msa: L-3-(3',5'-dimethylphenyl)-alanine (Dmp) (Figure 1.5). While Msa has a restricted rotation around the phenylic bond due to the two methyl groups in the *ortho* positions, Dmp is less sterically hindered and is more prone to rotate around this bond.

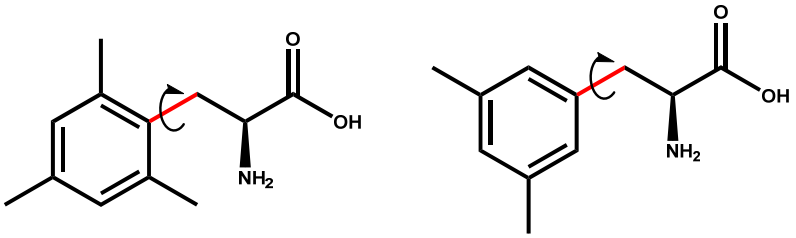

Figure 1.5. Structure comparison between the two non-natural electron-rich amino acids L-β-mesitylalanine (left) and L-3-(3',5'-dimethylphenyl)-alanine (right). In red, phenylic bonds.

In order to compare these results with those previously obtained when introducing Msa in the same positions, the synthesis of Dmp, the synthesis of new somatostatin analogues,

the structure determination of these peptides and the binding studies will be described in **Chapter 3**.

To complete the family of analogues started by Dr. Álvaro Rol[30], we will also study the effect of introducing 3'Pya and 4'Pya (amino acids with an electron-poor aromatic ring) in position 7, usually occupied by an electron-rich aromatic amino acid (normally Phe or Msa) while Msa is placed in position 6. The results obtained for these new analogues concerning 3D structures and binding affinity will be outlined in **Chapter 4**.

Somatostatin, its functions and its binding with the SSTRs have been studied extensively, however the relevance of the Trp residue to the biological activity is not well understood despite numerous publications where the clarification of its role were attempted.[31] As stated previously, Rosario Ramon,[22] also tried to clarify the exact role of that amino acid by substituting it with L or D-Qla. At that point, good binding results were obtained against receptors SSTR1 and SSTR3 but the 3D structures couldn't be determined and that didn't allow us to elaborate a full-working hypothesis that corroborates all the experimentally observed facts.

To additionally study the role of the amino acid in position 8, we thought that it could be useful to substitute the Phe7 for the well-known Msa as it gives highly structured peptides,[27] in addition to the introduction of either L or D-Qla in position 8. We hopped that the combination of these two modifications would afford more constrained peptides from which the 3D structure could be determined by 2D NMR. With these analogues we also expected to have a binding affinity for SSTR1 and SSTR3 similar to that exhibited by [L-Qla8]-SRIF and [D-Qla8]-SRIF. The NMR and binding results will be discussed in **Chapter 5**.

[31] a) C. A. Meyers, D. H. Coy, W. Y. Huang, A. V. Schally, T. W. Redding, *Biochemistry*, **1978**, *17*, 2326-2331; b) B. H. Hirst, B. Shaw, C. A. Meyers, D. H. Coy, *Regul. Pept.*, **1980**, *1*, 97–113; c) V. Prasad, E. T. Birzin, C. T. McVaugh, R. D. van Rijn, S. P. Rohrer, G. Chicchi, D. J. Underwood, E. R. Thornton, A. B. Smith, R. Hirschmann, *J. Med. Chem.*, **2003**, *46*, 1858 –1869.

As stated before, SRIF14 can be used effectively in certain conditions but its therapeutic use has been limited due to its very short half-life (< 3 min), its lack of selectivity against the five receptor sub-types and the broad range of biological responses. To overcome these challenges, we aimed to synthesise longer-living, and receptor-selective somatostatin analogues. To achieve stability against proteases and aminopeptidases, the enzymes responsible for the degradation of peptides and proteins, the introduction of D-amino acids is a methodology that has to be considered. Until now, some shorter analogues with D-amino acids replaciong key L-aa have been synthesised.[14,26e,32] Some of these analogues are commercially available treatments such as octreotide, lanreotide and vapreotide (Figure 1.2). Our group sought to find a full-length SRIF-analogue with enhanced stability and defined 3D structure in solution. We, indeed, synthesised highly structured analogues containing D-Trp in position eight (one example can be seen in Figure 1.6) but even though we observed an improvement in the half-life when compared to the natural hormone, the analogues were still less stable than octreotide.

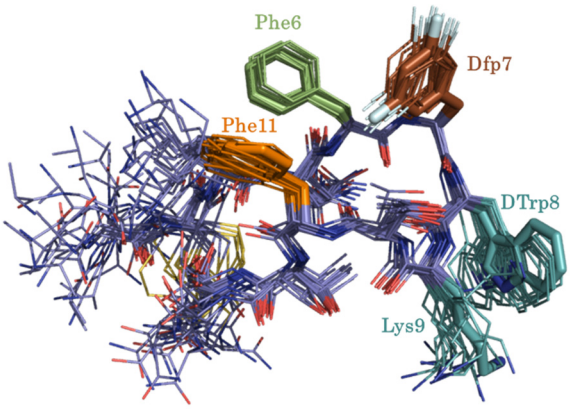

Figure 1.6. [L-Dfp7_D-Trp8]-SRIF structure obtained by NMR with a cluster interaction between the three aromatic rings.

[32] a) N. Viguerie, N. Tahiri-Jouti, A. M. Ayral, C. Cambillau, J. L. Scemama, M. J. Bastié, S. Knuhtsen, J. P. Estève, L. Pradayrol, C. Susini, *Endocrinology*, **1989**, *124*, 1017-1025; b) G. Weckbecker, F. Raulf, B. Stolz, C. Bruns, *Pharmacol. Ther.*, **1993**, *60*, 245-264; c) D. H. Coy, J. E. Taylor, *Metabolism*, **1996**, *45*, 21-23; d) H. A. Schmid, *Mol. Cell. Endocrinol.*, **2008**, *286*, 69-74; e) S. Lesche, D. Lehmann, F. Nagel, H. A. Schmid, S. Schulz, *J. Clin. Endocrinol. Metab.*, **2009**, *94*, 654-661.

To overcome this weakness, we performed a series of substitutions in crucial positions of somatostatin and assessed their impact on the stability and 3D structure. The results obtained with each modification and its influence on the half-life when compared to SRIF14 will be discussed in **Chapter 6**.

A long-term objective when obtaining a selective, structured and long-lived SRIF14 analogue is to be able to attach a cargo at the *N*-terminus such as a fluorescent probe, a drug, a cytotoxic or a p38α inhibitor, to induce a targeted response or effect inside the cell. In recent years, receptor-targeted cancer therapy has gained considerable interest as certain receptors have been found to be aberrantly overexpressed in cancer cells compared to normal cells[33] and could be exploited to overcome the major obstacle of cancer therapy; the low internalization rate into cells. Hence, somatostatin analogues that selectively bind to membrane-associated SSTRs could be a potencial tool for different and numerous actions such as selective delivery into tumor cells,[34] selective labeling of malignant cells and as triggers of an inhibitory response depending on the molecule that is bound at the *N*-terminus. Furthermore, the emerging field of biomedical optical imaging[35] has awakened a great deal of interest due to the relevance of developing new optical contrast agents.[36]

To further study the role of SRIF analogues as imaging agents, carriers and/or drug delivery systems we postulated that a fluorophore, an inhibitor or a photo-labile and photo-switchable compound could be coupled to the *N*-terminus of a peptide. With this, we hope to disclose their rate of internalisation as well as their potential to be used as selective carriers and fuorescent probes for different imaging techniques. The ability to

[33] L. C. Sun, D. H. Coy, *Curr. Drug Delivery*, **2011**, *8*, 2 -10.

[34] W. Mier, R. Eritja, A. Mohammed, U. Haberkorn, M. Eisenhut, *Bioconjugate Chem.*, **2000**, *11*, 855 - 860.

[35] E. B. De Haller, *J. Biomed. Opt.*, **1996**, *1*, 7 -17.

[36] G. A. Wagnières, W. M. Star, B. C. Wilson, *Photochem. Photobiol.*, **1998**, *68*, 603 - 632.

bind the receptor, their capacity as inhibitors and their ease of release once inside the cell will be assessed in **Chapter 7**.

To summarise, the main objectives of the present Doctoral Thesis are:

- Synthesis, binding studies and structural elucidation in solution of tetradecapeptidic somatostatin analogues with the non-natural amino acid L-3-(3',5'-dimethylphenyl)-alanine (Dmp). Analysis of the importance of steric and electronic effects imposed by Dmp in order to obtain a predominant structure in solution.

- Synthesis, binding and NMR studies of SRIF analogues presenting L-β-3'-pyridylalanine and L-β-4'-pyridylalanine. Study of the importance of amino acids with electron-poor aromatic rings in position 7 in combination with L-β-mesitylalanine (an electron-rich one) in position 6 to evaluate how they tune the π - π aromatic interactions to obtain the final 3D structure.

- Synthesis of peptides containing the non-natural amino acids L-3-(3'-quinolyl)-alanine and L-β-mesitylalanine maintaining the good binding profile of the structureless analogues previously synthesised with only L-3-(3'-quinolyl)-alanine.

- Search for a stable SRIF analogue introducing D-amino acids in key points of the natural hormone. Study of the importance of each modification.

- Incorporation of a molecule at the *N*-terminus of a SRIF analogue to be used in different biological assays; fluorescence assays, inhibition assays and light assisted release assays.

Chapter 2

Background

2.1 SRIF14 previous analogues

SRIF14 was considered a potential novel therapeutic agent for the treatment of endocrine diseases since the discovery of its potential as an inhibitor of other endogenous hormones. However, this role as a therapeutic agent was hampered because of SRIF14 low half-life in blood (less than three minutes). This guided the design of new analogues with longer plasmatic half-lives, higher inhibitory potency and more specific physiological actions.

Substitution of L-Trp for D-Trp (Figure 2.1) was the first modification made in the natural hormone's structure giving a more resistant analogue (higher half-life in plasma) which maintained similar binding profile against SSTRs. The stabilisation of the peptide was predicted to be due to the D-amino acid introduced in the natural sequence. Many studies ascertained that [D-Trp8]-SRIF14 analogue was 5 to 8 times more potent *in vitro* in the releasing of GH, insulin and glucagon than natural SRIF.[1]

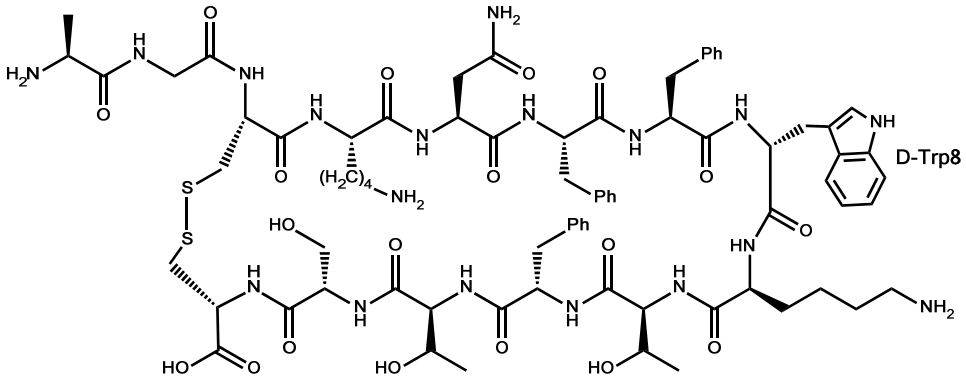

Figure 2.1 [D-Trp8]-SRIF14 chemical structure.

Further studies found that the stabilisation of the peptide was due to a closer spatial proximity of D-Trp8 and Lys9 than that which takes place with L-Trp8 in the natural

[1] a) J. Rivier, M. Brown, W. Vale, *Biochem. Biphys. Res. Commun.*, **1975**, *66*, 746 - 751; b) D. H. Coy, E. J. Coy, C. Meyers, J. Drouin, L. Ferland, A. Gómez-Pan, A.V. Schally, *Endocrinology*, **1976**, *98*, 305A. c) B. H. Hirst, B. Shaw, C. A. Meyers, D. H. Coy, *Regulatory Peptides*, **1980**, *1*, 97 - 113.

hormone. This shorter distance between these two amino acids and the presence of the D-amino acid made the aliphatic-aromatic interaction stronger thus enhancing the stability of the β-turn as the two side chains approached each other.[2]

Another series of analogues included the introduction of a D-Cys in position 14 and a L-Ala in position 2. Vale[3] and co-workers showed that [D-Cys14]-SRIF14 better inhibited the secretion of GH and glucagon when compared to the inhibition of insulin. Likewise, Meyers *et al.*[4] reported a similar behaviour of the [L-Ala2_D-Cys14]-SRIF14 analogue. When using [D-Trp8_D-Cys14]-SRIF14 the inhibitory selectivity was further increased which made that peptide a promising therapeutic agent for the treatment of Diabetes Mellitus type II.[3,5]

Simultaneously, Vale *et al.*[6] reported the substitution of each individual amino acid for L-Ala. The effects of substituting Gly2, Lys4, Asn5, Thr10, Thr12 and Ser13 for L-Ala were comparable to those obtained for the natural hormone as the inhibition of GH, glucagon and insulin release did not decrease. However, when the substitution was performed on Phe6, Phe7, Trp8, Lys9 and Phe11 resulting analogues had an inhibitory capacity over GH of less than 4%.

Even though all these analogues had a longer plasmatic half-life *in vitro* than natural SRIF, they were discarded as potential therapeutics due to their rapid metabolic degradation *in*

[2] a) B. H. Arison, R. Hirschmann, D. F. Veber, *Bioorg. Chem.*, **1978**, *7*, 447 - 451; b) O. Ovadia, S. Greenberg, B. Laufer, C. Gilon, A. Hoffman, H. Kessler, *Expert Opin. Drug Discov.*, **2010**, *5*, 655 - 671.

[3] M. Brown, J. Rivier, W. Vale, *Science*, **1977**, *196*, 1467 - 1469.

[4] C. Meyers, A. Arimura, A. Gordin, R. Fernández-Durango, D. H. Coy, A. V. Schally, J. Drouin, L. Ferland, M. Beaulie, F. Labrie, *Biochem. Biophys. Res. Commun.*, **1975**, *65*, 176.

[5] C. Meyers, A. Arimura, A. Gordin, R. Fernández-Durango, D. H. Coy, A. V. Schally, J. Drouin, L. Ferland, M. Beaulie, F. Labrie, *Biochem. Biophys. Res. Commun.*, **1977**, *74*, 630 - 636.

[6] a) W. Vale, P. Brazeau, C. Rivier, M. Brown, B. Boss, J. Rivier, R. Burqus, N. Ling, R. Guillemin, *Recent Prog. Horm. Res.*, **1975**, *31*, 365 – 397; b) M. Brown, J. Rivier, W. Vale, *Endocrinology*, **1976**, *98*, 336 - 343.

vivo which decreased its hypothetical efficacy. To overcome this drawback, a large family of shorter analogues began growing rapidly.

One of the first discovered peptides that was shorter than natural SRIF14 and maintained the inhibitory effect over the release of GH was c[Cys_Phe_D-Trp_Lys_Thr_Cys]. Vale *et al.*[7] gained deeper knowledge into somatostatin's structure through the deletion of key residues until they synthesised the above mentioned active peptide. From these studies, they stated that an important region of the molecule was formed by residues 6 to 11 and from this knowledge, they synthesised a library of octa and nonapeptides containing Phe_D-Trp_Lys_Thr, the key fragment for the intrinsic inhibitory effect.[8] This 4 amino acid motif, the one in the β-turn of the peptide, was predicted to conform the pharmacophore region of the molecule.[9] However, some modifications have been made to that region, but only to Phe7 and Thr10 which do not compromise the biological activity whereas changes in both positions 8 and 9 do. The only modification in within the β-turn which does not affect the biological activity is the substitution of L-Trp8 for its optical isomer. Due to its efficacy, D-Trp has been a used as a recurrent modification and introduced in the vast majority of the analogues synthesised until now.

Having seen Rivier and co-workers' peptide, c[Cys_Phe_D-Trp_Lys_Thr_Cys], and noticing the absence of the Phe6_Phe7 pair, Bauer *et al.* [9a] decided to introduce a D-Phe at the *N*-terminal part to emulate the presence of an aromatic ring present in the natural hormone. Furthermore, they introduced a reduced Thr residue at the *C*-terminal part to emulate Thr12 of SRIF14. Therefore, D-Phe_c[Cys_Phe_D-Trp_Lys_Thr_Cys]_Thr(ol) was the final sequence. This new analogue, initially called SMS 201-995, was then named

[7] W. Vale, M. Brown, C. Rivier, M. Perrin, J. Rivier, *Brain Peptides: A New Endocrinology*, **1979**, 71 - 88.

[8] W. Vale, C. Rivier, J. Rivier, M. Brown, *Medicinal Chemistry V*, **1977**, 25 - 62.

[9] a) W. Bauer, U. Briner, W. Doepfner, R. Halber, R. Huguenin, P. Marbach, T. J. Petcher,a J. Pless, *J. Life Sci.*, **1982**, *31*, 1133 - 1140; b) J. E. Taylor, D. H. Coy, *J. Endocrinol. Invest.*, **1997**, *20*, 8 - 10.

as octreotide (Figure 2.2) and was commercialised by Novartis (Sandoz at that time) as Sandostatin®.

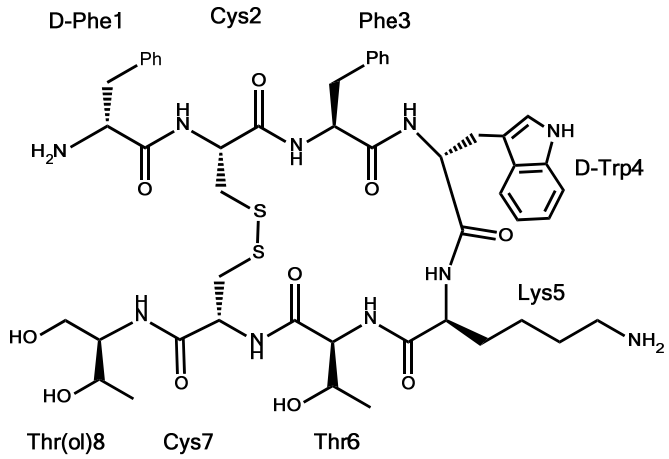

Figure 2.2 Octreotide's structure. D-Phe_c[Cys_Phe_D-Trp_Lys_Thr_Cys]_Thr(ol).

Octreotide turned out to be more potent than the natural somatostatin in terms of inhibition of GH liberation but not against insulin and glucagon release. Furthermore, its half-life higher than SRIF14 (117 min[10] for octreotide and less than 3 min for somatostatin) made octreotide an analogue with higher overall activity than the natural hormone.[9a] This increase in the half-life was due to the *N*-terminal and *C*-terminal protection with non-natural amino acids which make it more difficult for the proteases to cleave the amide bonds. For these reasons, in 1988, octreotide was the first somatostatin analogue to be commercialised for the treatment of acromegaly and gastrointestinal and pancreatic tumours.

This event triggered deeper investigation into octapeptides with a similar structure to octreotide and some more analogues reached the market in the subsequent years. Vapreotide (RC-160 or Sanvar®, Figure 2.3) with the sequence D-Phe_c[Cys_Tyr_D-Trp_ Lys_Val_Cys]_Trp(NH_2), was discovered by Schally and co-workers[11] to be more

[10] a) P. Marbach, U. Briner, M. Lemaire, A. Schweizer, T. Terasaki, *Metab. Clin. Exp.*, **1992**, *41*, 7 - 10; b) A. Janecka, M. Zubrzycka, *Endocr. Regul.*, **2001**, *35*, 75 - 79.

[11] a) R. Z. Cai, B. Szoke, R. Lu, D. Fu, T. W. Redding, A. V. Schally, *Proc. Natl. Acad. Sci. U.S.A.*, **1986**, *83*, 1896 - 1900; b) R. Z. Cai, T. Karashima, J. Goutch, B. Szoke, D. Olsen, A. V. Schally, *Proc. Natl. Acad. Sci. U.S.A.*, **1987**, *84*, 2502 - 2506.

selective against the inhibition of GH release than glucagon, insulin and gastric secretion. This analogue was commercialised by Debiopharm Group.

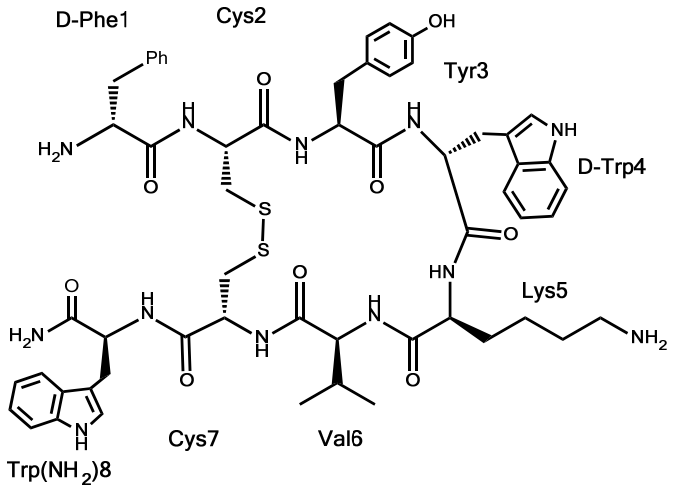

Figure 2.3 Vapreotide's structure. D-Phe_c[Cys_Tyr_D-Trp_Lys_Val_Cys]_Trp(NH_2).

Shortly after this analogue was released onto the market, another compound was discovered by Shally, Coy and co-workers;[12] Lanreotide (BIM - 23014, Somatuline®,) with the sequence D-Nal_c[Cys_Tyr_D-Trp_Lys_Val_Cys]_ Thr(NH_2) (Figure 2.4).

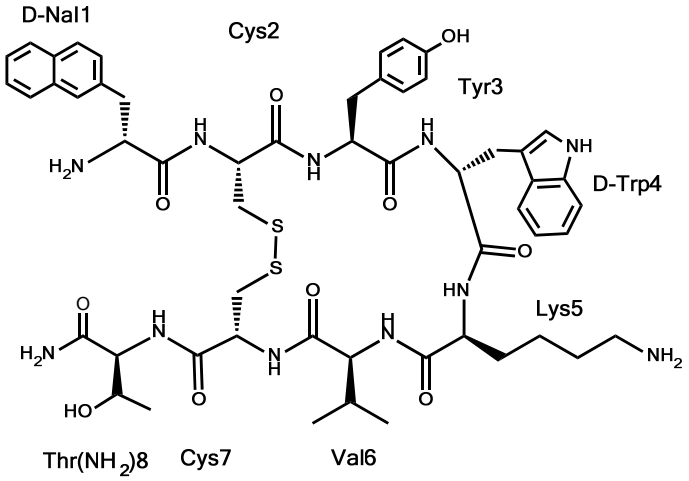

Figure 2.4 Lanreotide's structure. D-NaI_c[Cys_Tyr_D-Trp_Lys_Val_Cys]_Thr(NH_2).

[12] a) W. A. Murphy, V. A. Lance, S. Moreau, J. P. Moreau, D. H. Coy, *Life Sci.*, **1987**, *40*, 2515 - 2522; b) J. E. Taylor, A. E. Bodgen, J. P. Moreau, D. H. Coy, *Biochem. Biophys. Res. Commun.*, **1988**, *153*, 81 - 86; c) K. Raynor, W. Murphy, D. H. Coy, *Mol. Pharmacol.*, **1993**, *43*, 838 - 844.

Lanreotide, commercialised by Ipsen, turned out to be an excellent analogue for the treatment of acromegaly, as was vapreotide.

Simultaneously to the discovery of these active peptides, somatostatin receptors were being described and referred to as SSTRs. Their sequences remained unaltered during vertebrate evolution and even though each receptor seems to be overexpressed in one tissue type and perform some specific actions, most tissues co-express more than one SSTR subtype. This suggests that the precise actions of somatostatin are dependent on its interaction with the receptors expressed in each cell.[13] Furthermore, these receptors differ in their pharmacological properties and tissue distribution. Receptor subtype populations were discovered in different organs such as brain, pituitary, intestine, pancreas, thyroid, kidneys, immune system cells and different cancer cell lines using different techniques. [14]

To date, five different subtype receptors have been described for humans as well as for other mammalian species (murine, bovine and porcine).[15]

[13] a) Y. C. Patel, *Front. Neuroendocrinol.*, **1999**, *20*, 157 - 198; b) L. N. Moller, C. E. Stidsen, B. Hartmann, J. J. Holst, *Biochim. Biophys. Acta*, **2003**, *1616*, 1 - 84.

[14] a) Y. C. Patel, K. K. Murthy, E. Escher, D. Banville, J. Spiess, C. B. Srikant, *Metabolism*., **1990**, *39*, 63 - 69; b) Y. C. Patel, M. T. Greenwood, R. Panetta, L. Demchyshyn, H. Niznik, C. B. Srikant, *Life Sci*., **1995**, *57*, 1249 - 1265; c) T. Reisine, G. I. Bell, *Endocr. Rev*., **1995**, *16*, 427 - 442; d) Y. C. Patel, *J. Endocrinol. Invest.*, **1997**, *20*, 348 -367; e) Y. C. Patel, C. B. Srikant, *Trends Endocrinol. Metab.*, **1997**, *8*, 398 - 405; f) J. C. Reubi, U. Horisberger, A. Kappeler, J. A. Laissue, *Blood*, **1998**, *92*, 191 - 197.

[15] a) J.F. Bruno, Y. Xu, J. Song, M. Berelowitz, *Proc. Natl. Acad. Sci U.S.A.*, **1992**, *89*, 11151 - 11155; b) J. D. Corness, L. L. Demchyshyn, P. Seeman, H. H. M. van Tol, C. B. Srikant, G. Kent, Y.C. Patel, H. B. Niznik, *FEBS Lett.*, **1993**, *321*, 279 - 284; c) L. L. Demchyshyn, C. B. Srikant, R. K. Sunahara, G. Kent, P. Seeman, H. H. M. van Tol, R. Panetta, Y. C. Patel, H. B. Niznik, *Mol. Pharmacol.*, **1993**, *43*, 894 - 890; d) X. J. Li, M. Forte, R. A. North, C. A. Ross, S. H. Snyder, *J. Biol. Chem.*, **1992**, *267*, 21307 - 21312; e) W. Meyerhof, I. Wulfsen, C. Schonrock, S. Fehr, D. Richter, *Proc. Natl. Acad. Sci. U.S.A.*, **1992**, *89*, 10267 - 10271; f) A. M. O'Carroll, S. J. Lolait, M. Konig, L. C. Mahan, *Mol. Pharmacol.*, **1992**, *42*, 939 - 946; g) R. Panetta, M. T. Greenwood, A. Warszynska, L. L. Demchyshyn, R. Day, H. B. Niznik, C. B. Srikant, Y. C. Patel, *Mol. Pharmacol.*, **1994**, *45*, 417 - 427; h) L. Rohrer, F. Raulf, C. Bruns, R. Buettner, F. Hofstaedter, R. Schule, *Proc. Natl. Acad. Sci. U.S.A.*, **1993**, *90*, 4196 - 4200; i) Y. Yamada, T. Reisine, S. F. Law, Y. Ihara, A. Kubota, S. Kagimoto, M. Seino, Y. Seino, G. I. Bell, S. Seino, *Mol. Endocrinol.*, **1993**, *6*, 2136 - 2142; j)) K. Yasuda, S. Rens-Domiano, C. D. Breder, S. F. Law, C. B. Saper, T. Reisine, G. I. Bell, *J. Biol. Chem.*, **1992**, *267*, 20422 - 20428.

All five receptors share common signalling pathways such as the inhibition of adenylyl cyclase, activation of phosphotyrosine phosphatase (PTP), and modulation of mitogen-activated protein kinase (MAPK) through G-protein-dependent mechanisms. Some of the subtypes are also coupled to inward rectifying K^+ channels (SSTR2, 3, 4, 5), to voltage-dependent Ca^{2+} channels (SSTR1, 2), a Na^+/H^+ exchanger (SSTR1), AMPA/kainate glutamate channels (SSTR1, 2), phospholipase C (SSTR2, 5), and phospholipase A_2 (SSTR4). SSTRs block cell secretion by inhibiting intracellular cAMP and Ca^{2+} and by a receptor-linked distal effect on exocytosis.[13]

Somatostatin receptors are seven trans-membrane domain (TMD) G protein coupled receptors (GPCRs) which has made it difficult to characterize them. Knowing their structure would have been useful to synthesise peptidic compounds with a concrete structure to target only one of the receptors and make therapeutic agents more selective and specific. As the structure of the SSTRs has not been elucidated yet, the design of new somatostatin analogues focused on obtaining a structure-activity-affinity relationship in an indirect way. Several *in vitro* and *in vivo* studies have been performed from which it has been stated that SSTR2 is the most important receptor from the SSTRs family. It inhibits endocrine secretion of GH, insulin, glucagon, gastrin secretion and gastrointestinal tract exocrine secretion. Furthermore, SSTR2 is present in gastroenteropancreatic tumours and epilepsy and pain processes. From the rest of the receptors, SSTR5 is more implicated in the inhibition of insulin release than SSTR2 but less implicated in GH release. SSTR4 is implicated in the inhibition of glucagon and insulin release whereas the role of SSTR3 and SSTR1 is not as clear as the others, although they are suspected to be implicated in cellular apoptosis and vision, respectively.[16]

[16] a) A. Vezzani, D. Hoyer, *Eur. J. Neurosci.*, **1999**, *11*, 3767 - 3776; b) G. Weckbecker, I. Lewis, R. Albert, H. A. Schmid, D. Hoyer, C. Bruns, *Nat. Rev. Drug Discov.*; **2003**, *2*, 999 - 1017; c) A. Rubio, J. Ávila, L. de Lecea, *Expert Opin. Ther. Targets*, **2007**, *11*, 1 - 9.

Patel and his group designed a strategy to determine the affinity of a peptide against all five different SSTRs and applied this same methodology for somatostatin analogues previously mentioned;[17] octreotide, vapreotide and lanreotide (Table 2.1).

	SSTR1 (nM)	**SSTR2 (nM)**	**SSTR3 (nM)**	**SSTR4 (nM)**	**SSTR5 (nM)**
Somatostatin-14	0.1-2.26	0.2-1.3	0.3-1.6	0.3-1.8	0.2-0.9
Somatostatin-28	0.1-2.20	0.2-4.1	0.3-6.1	0.3-7.9	0.05-0.4
Octreotide	290-1140	0.4-2.1	4.4-34.5	$>10^3$	5.6-32
Vapreotide	$>10^3$	5.4	31	45	0.7
Lanreotide	500-2330	0.5-1.8	43-107	66-2100	0.6-14

Table 2.1 Binding selectivity (Ki values) of selected endogenous somatostatin-like peptides against SSTR1-5. Ki values express inhibition in a competitive assay of somatostatin analogues against radio-labelled SRIF obtained by Patel *et al.*[17]

Binding affinity of somatostatin analogues against SSTR1, SSTR4 and SSTR3 to a lesser extent, decreases when compared to somatostatin whilst the affinity for SSTR2 and SSTR5 increases indirectly due to the loss of activity in the other receptors. It has been hypothesised and accepted that this fact is caused by the higher rigidity of the cycle, the lack of extracyclic amino acids or a combination of both.

This data by itself alone does not clarify if there is a structure-activity relationship that drives a concrete peptide towards a specific SSTR. However, what has been extrapolated from this data is that residues Phe6 and Phe11 have to be in the spatial proximity (in shorter analogues forced to be closer by a disulfide bridge) as that shorter distance gives the analogues an appropriate pharmacological profile for SSTR2.

In recent years, the vast majority of analogues synthesised have been shorter peptides (octa and hexapeptides) focused on the achievement of a better pharmacological profile and higher potency and selectivity against SSTR2 being the tetradecapeptidic analogues a minority.

[17] Y. C. Patel, C. B. Srikant, *Endocrinology*, **1994**, *135*, 2814 - 2817.

2.2 Previous SRIF14 analogues studied in our group

BCN Peptides S.A., funded in 1989, focus on manufacturing Generic Peptides (GP) as Active Pharmaceutical Ingredients (APIs). The company started selling products in Europe where it is nowadays very well positioned in the GP market, being the only producer of sterile grade peptides. Over the years, the company broadened its range of activities involving itself in custom manufacturing services.

Since its discovery, somatostatin (SRIF14) has generated great interest both for its research purposes and its pharmacological properties. BCN Peptides S.A. developed a synthetic strategy for this natural hormone that was patented in 1999. Simultaneously, our group was focused on the development of bioactive compounds; such as non-natural amino acids. To gain knowledge into somatostatin structure and to develop new somatostatin analogues a collaboration between BCN Peptides S.A. and our lab was set up. The main objective was to study the effect of introducing different non-natural amino acids in the hormone sequence maintaining the 14 residue scaffold.

The first experimental results in this project were obtained by Dr. Rosario Ramón. In her doctoral thesis,[18] she asymmetrically synthesised both enantiomers of the non-natural amino acid 3-(3'-quinolyl)-alanine (L-Qla and D-Qla) as Trp analogues.

However, the electronic properties of Trp and Qla are completely opposite as can be seen in Figure 2.5. Whilst the indole ring from Trp is electron rich due to the electron donating character of the pyrrole ring, the pyridine ring in Qla confers more acceptor character as

[18] R. Ramón, Doctoral thesis *Síntesis de aminoácidos no naturales y aplicación a la síntesis de péptidos con interés farmacológico*, University of Barcelona, **2009**.

a consequence of the free electron pair. Another key difference between both amino acids is the lack of the N-H bond of Qla.

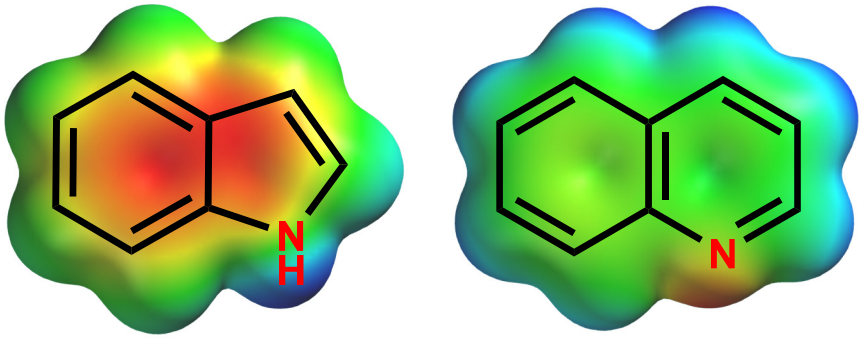

Figure 2.5 Electronic densities of the indole (left) and quinoline (right) rings. Spartan calculation (semi-empiric AM1).[19] Red = high electronic density; Green/Blue = low electronic density.

Based upon this difference in the electronic properties, and the importance of Trp for the maintenance of somatostatin's activity, two analogues were synthesised substituting L-Trp8 for L and D-Qla8 (Figure 2.6). This modification was performed to establish whether the electronic properties of this key amino acid affect the rigidity of the molecule and its pharmacological profile.

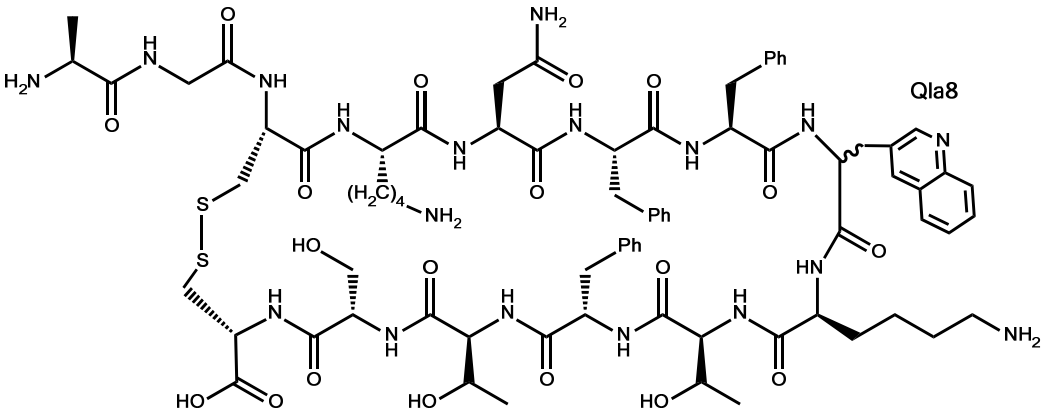

Figure 2.6 [L-Qla8]-SRIF and [D-Qla8]-SRIF structures, with the non-natural amino acid L and D-Qla substituting Trp8.

[19] Spartan '10 v 1.1.0 (Wavefunction)

2D NOESY experiments were performed for both peptides and it was concluded that both analogues showed higher conformational flexibility due to the low density of NOE signals observed in the H_{Ar}-H_{Ar} interaction region (Figure 2.7)

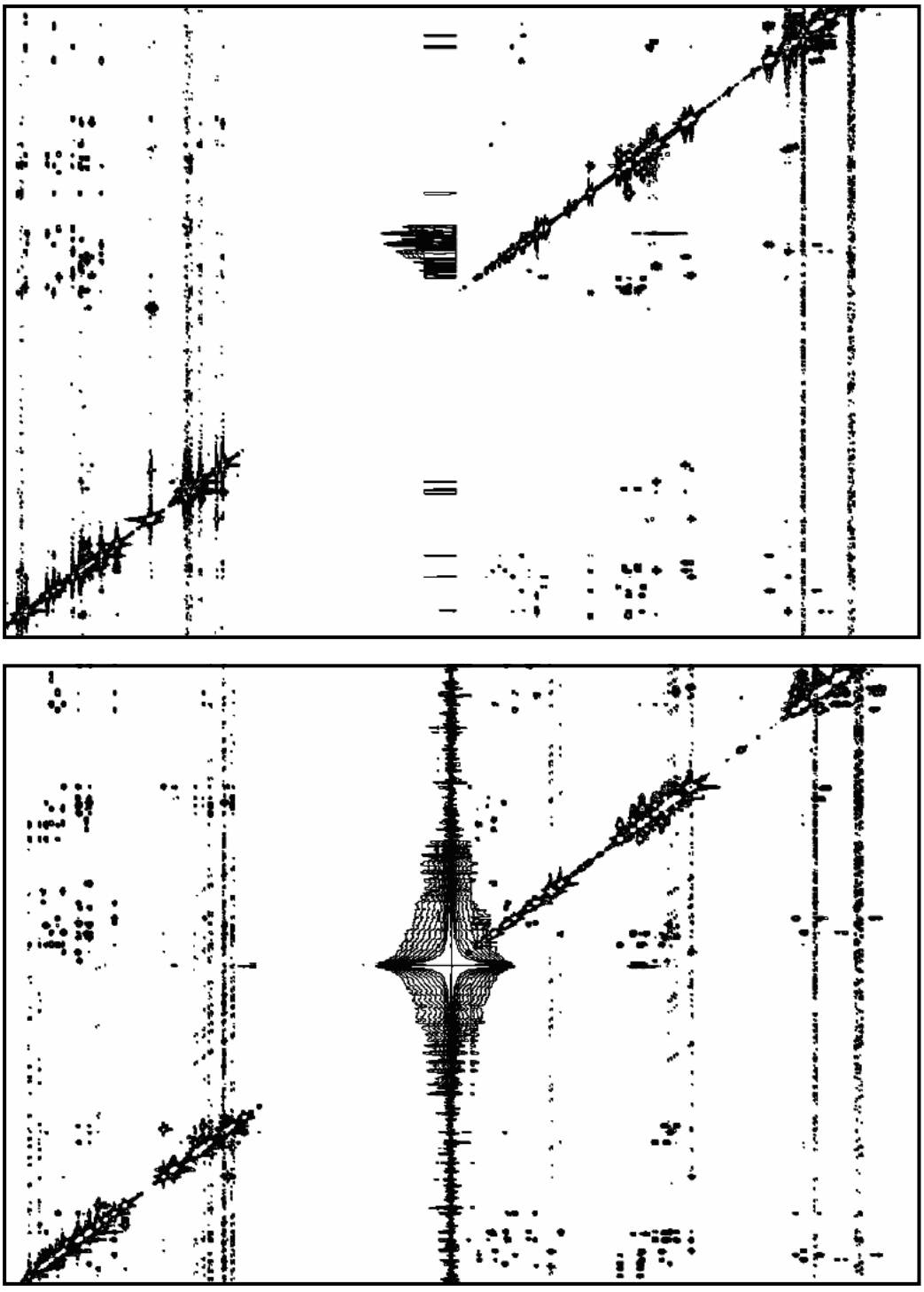

Figure 2.7 Homonuclear 2D NOESY 200ms spectra of [L-Qla8]-SRIF (top) and [D-Qla8]-SRIF (bottom) acquired in a Bruker Avance III spectrometer.[18]

It was postulated that the loss of the indolic N-H proton would be the cause of the less rigid structures obtained for these two compounds as it can interact with surrounding residues. Furthermore, the obtained pharmacological profile against SSTRs was different (Table 2.2).

	SSTR1 (nM)	SSTR2 (nM)	SSTR3 (nM)	SSTR4 (nM)	SSTR5 (nM)
Somatostatin-14	0.43	0.0016	0.53	0.74	0.23
[D-Trp8]-SRIF	0.32	0.0010	0.61	5.83	0.46
Octreotide	300	0.053	15.2	$>10^3$	11.5
[L-Qla8]-SRIF	1.33	$>10^3$	1.95	$>10^3$	$>10^3$
[D-Qla8]-SRIF	13.6	1.16	0.65	$>10^30$	14.5

Table 2.2 Binding selectivity (Ki values) of [L-Qla8]-SRIF, [D-Qla8]-SRIF and selected reference peptides against SSTR1-5 obtained in collaboration with BCN Peptides S.A.[18]

As can be seen in the Table 2.2, both [L-Qla]-SRIF and [D-Qla]-SRIF have similar activity to natural SRIF against SSTR3. The analogue with the L enantiomer resembles somatostatin in the binding with SSTR1 while the peptide with the D isomer reaches values closer to the octreotide range for SSTR5. The loss of rigidity of the structure could be related to a higher selectivity against some of the SSTRs and the maintenance of the activity in some of them. This work was published in 2011.[18]

The next modification done by BCN Peptides S.A. was the introduction of mesitylalanine (Msa) in the search for more stable and selective analogues. This amino acid was chosen for its steric and electronic properties; the side chain size is bigger as a consequence of the three methyl groups which gives greater steric hindrance in the amino acid surroundings. Furthermore, the electron-donor character of these methyl groups transform the aromatic ring in an electron rich ring when compared to the natural Phenylalanine (Figure 2.8).

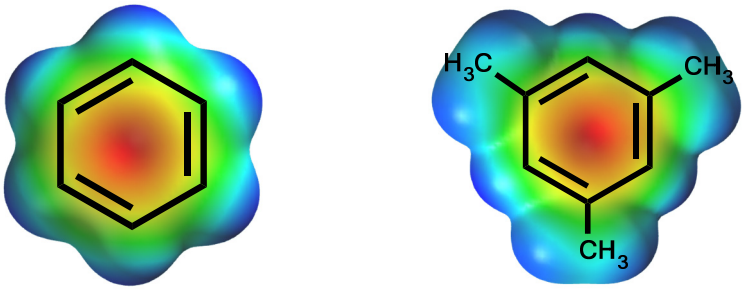

Figure 2.8 Electronic densities of the benzene (left) and mesityl (right) rings. Spartan calculation (semi-empiric AM1).[19] Red = high electronic density; Green/Blue = low electronic density.

Pablo Antonio Martín-Gago, in his doctoral thesis,[20] started the synthesis of different 14-residue somatostatin analogues containing this non-natural amino acid and D-Trp in position 8. He synthesised three different somatostatin analogues introducing these two modifications: [L-Msa6_D-Trp8]-SRIF, [L-Msa7_D-Trp8]-SRIF and [L-Msa11_D-Trp8]-SRIF. These three peptides showed higher rigidity leading to more structured analogues. The nine methyl protons of the Msa aromatic ring together with its highly shielded aromatic protons enabled to obtainment of information upon the residue's spatial contact by analysing the TOCSY and NOESY spectra. Furthermore, the 2D NMR spectra obtained showed a high density of NOE signals which indicated high spatial ordering.

[L-Msa6_D-Trp8]-SRIF analogue (Figure 2.9) showed a cluster interaction in which the three aromatic rings of Msa6, Phe7 and Phe11 are implicated and are facing the same side of the molecule. From the three aromatic rings, Msa6 and Phe11 are the ones which are closer in space and bear a strong *face to face* interaction. In addition to that, the D-Trp8-Lys9 pair is facing the same side of the molecule than the cluster.

[20] P. A. Martín-Gago, doctoral thesis *Synthesis of highly structured and receptor-selective tetradecapeptidic analogs of somatostatin: Fine tuning the non-covalent interactions among their aromatic residues*, Univeristat de Barecelona, 2013.

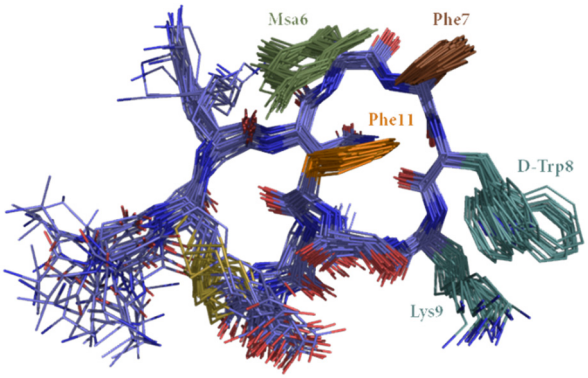

Figure 2.9 Superimposition of the 20-25 most stable 3D structures obtained by NMR of [L-Msa6_D-Trp8]-SRIF, showing a *face to face* interaction between Msa6 and Phe11.

The analogue [L-Msa7_D-Trp8]-SRIF holds a different structure than the analogue with the Msa residue in position 6. As seen in Figure 2.10, the most stable conformations in solution bear an *edge to face* interaction between Ph6 and Phe11 while residue Msa7 does not interact and is placed in the other side of the molecule. It was supposed that the strong interaction between 6 and 11 was potentiated by the indirect action of Msa7 being in the opposite site of the peptide. In this case, the D-Trp8-Lys9 pair is oriented towards the outside of the peptidic backbone.

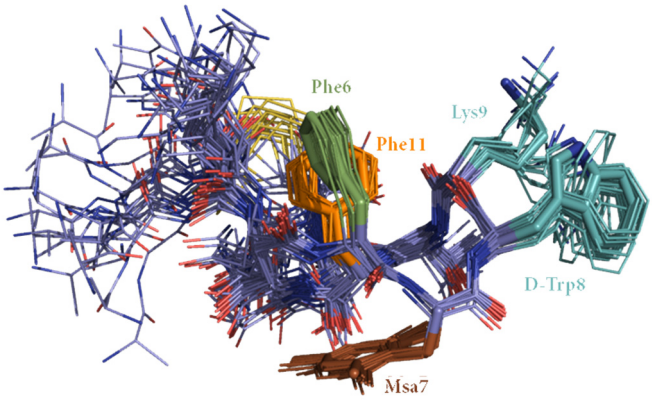

Figure 2.10 Superimposition of the 20-25 most stable 3D structures obtained by NMR of [L-Msa7_D-Trp8]-SRIF with an *edge to face* interaction between Phe6 and Phe11.

Finally, the most stable structures of the [L-Msa11_D-Trp8]-SRIF analogue showed an aromatic interaction between Phe6 and Msa11 with a *face to face* geometry (Figure 2.11).

As with the previous analogue, the aromatic amino acid in position 7 is placed on the opposite site of the molecule, being closer to Asn5, Thr10 and Thr12.

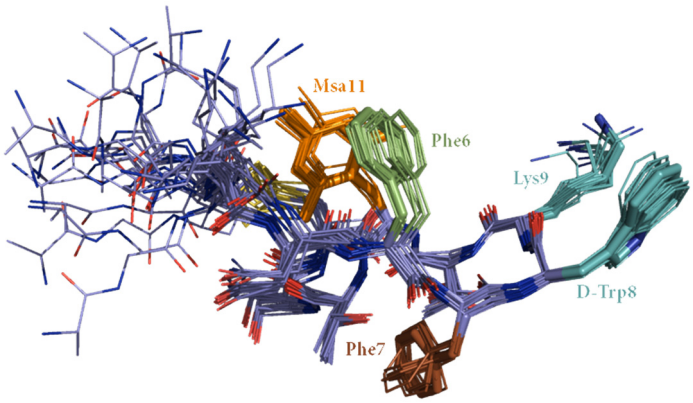

Figure 2.11 Superimposition of the 20-25 most stable 3D structures obtained by NMR of [L-Msa11_D-Trp8]-SRIF analogue with a *face to face* interaction between Phe6 and Msa11.

Due to the absence of NOE signals between D-Trp8-Lys9 pair and the rest of the molecule, these two residues are shown to be oriented towards the outside of the peptidic backbone as it happened with [L-Msa7_D-Trp8]-SRIF.

The aim of the group was to depict structure-activity relationship patterns against the five different SSTRs by studying well-structured peptides. These 3D structures enabled the group to start thinking of a correlation between conformation and activity. Binding studies were performed for these three new analogues and compared with natural SRIF, octreotide and [D-Trp8]-SRIF; the results can be seen in Table 2.3.

The data obtained showed that [L-Msa6_D-Trp8]-SRIF analogue resembles the natural hormone's activity against SSTR3 and SSTR5 but the activity against SSTR2 is completely lost. This fact is in disagreement with Hirschmann's hypothesis which stated that the amino acid in position 6 was interacting with receptor 2 via the π-donor capability of the side chain (Table 2.3).[21]

[21] S. Neelamkavil, B. Arison, E. Birzin, J. Feng, K. Chen, A. Lin, F. Cheng, L. Taylor, E. R. Thornton, A. B. Smith III, R. Hirschmann *J. Med. Chem.*, **2005**, *48*, 4025 - 4030.

	SSTR1 (nM)	SSTR2 (nM)	SSTR3 (nM)	SSTR4 (nM)	SSTR5 (nM)
Somatostatin-14	0.43	0.0016	0.53	0.74	0.23
[D-Trp8]-SRIF	0.32	0.0010	0.61	5.83	0.46
Octreotide	300	0.053	15.2	$>10^3$	11.5
[L-Msa6_D-Trp8]-SRIF	3.08	4.55	0.78	4.70	0.36
[L-Msa7_D-Trp8]-SRIF	0.33	0.0024	7.49	$>10^3$	$>10^3$
[L-Msa11_D-Trp8]-SRIF	3.35	0.14	1.31	$>10^3$	0.73

Table 2.3 Binding selectivity (Ki values) of [L-Msa6_D-Trp8]-SRIF, [L-Msa7_D-Trp8]-SRIF, [L-Msa11_D-Trp8]-SRIF and selected reference peptides against SSTR1-5 obtained in collaboration with BCN Peptides S.A.[22]

[L-Msa7_D-Trp8]-SRIF displayed an excellent binding affinity for SSTR2 (picomolar range), that was greater than octreotide and resembling the one of the natural hormone. Furthermore, it maintained the activity against SSTR1 (same range as SRIF14) but it decreased the activity against SSTR3 and the activity is completely lost against SSTR4 and SSTR5. These experimental results were in agreement with the pharmacophore proposed for SSTR1 by Kaupmann where the affinity of [L-Msa7_D-Trp8]-SRIF against that receptor would be increased due to the π-π interaction of Msa7 and Phe195 of SSTR1.[23]

The binding affinity of the [L-Msa11_D-Trp8]-SRIF analogue for SSTR5 was maintained but the activity against SSTR1, SSTR2 and SSTR3 decreased and the one against SSTR4 was completely lost as it happened with the previous analogue (Msa in position 7). The orientation of 6 and 11 to one side of the molecule and residue 7 to the other side of the peptidic backbone confers the analogue an orientation restriction that may be the cause of the loss of the binding affinity against SSTR4.

These promising results published in 2012 settled the basis for further research as they offered a new tool for the study of 14-amino acid somatostatin analogues.[22] Well-defined

[22] P. Martín-Gago, M. Gómez-Caminals, R. Ramón, X. Verdaguer, P. Martín-Malpartida, E. Aragón, J. Fernández-Carneado, B. Ponsati, P. López-Ruiz, M. A. Cortés, B. Colás, M. J. Macías, A. Riera, *Angew. Chem. Int. Ed.*, **2012**, *51*, 1820 - 1825.

[23] K. Kaupmann, C. Bruns, F. Raulf, H. P. Weber, H. Mattes, H. Lubbert, *EMBO J.*, **1995**, *14*, 727 - 735.

structures in solution were obtained for the first time and they were vital in establishing activity patterns against SSTR1-5.

Dr. Álvaro Rol, during his thesis,[24] continued working in the field of structure-activity relationships. He synthesised other analogues using a non-natural electron-poor aromatic amino acid. This work was done by He introduced the L-3-(3', 5'-difluorophenyl)-alanine (Dfp) in positions 6, 7 and 11 on the natural SRIF14 sequence. The selection of this amino acid was due to its capacity to modulate the chemical properties of the peptidic sequences or proteins in which it is introduced.[25]

Dfp was also chosen because fluorinated aliphatic residues can stabilise protein structures[26] and modulate the action on enzymatic recognition sites[27] but little is known about the role of aromatic fluorinated amino acids in the stabilisation of proteins, a topic which is under study.[28] All things considered, the substitution of two protons of an aromatic ring for fluorine atoms does not trigger a big steric perturbation as the radius of fluorine and hydrogen are relatively similar. However, that substitution can produce an increase in the aromatic interactions with other aromatic rings due to an increase of the hydrophobicity of the ring and the π - π interactions.[29] Furthermore, the inclusion of two fluorine atoms induces a change in the quadrupole moment as a result of the high

[24] A. Rol Rúa, doctoral thesis *Análogos de somatostatina y cortistatina. Efectos de las interacciones aromáticas en sus estructuras y en la actividad biológica.* Universitat de Barcelona, 2015.

[25] a) S. Purser, P. R. Moore, S. Swallow, V. Gouverneur, *Chem. Soc. Rev.*, **2008**, *37*, 320 - 330; b) M. Salwiczek, E. K. Nyakatura, U. I. M. Gerling, S. Ye, B. Koksch, *Chem. Soc. Rev.*, **2012**, *41*, 2135 - 2171.

[26] a) J. Horng, D. P. Raleigh, *J. Am. Chem. Soc.*, **2003**, *125*, 9286 - 9287; b) C. Jäckel, M. Salwiczek, B. Koksch, *Angew. Chem. Int. Ed.*, **2006**, *45*, 4198 - 4203.

[27] B. Bilgiçer, K. Kumar, *Proc. Natl. Acad. Sci. U.S.A.*, **2004**, *101*, 5324 - 15329.

[28] a) J. S. Thoron, E. Chapman, E. C. Murphy, P. G. Schultz, J. K. Judice, *J. Am. Chem. Soc.*, **1995**, *117*, 1157 - 1158; b) H. Chiu, Y. Suzuki, D. Gullickson, R. Ahmad, B. Kokona, R. Fairman, R. P. Cheng, *J. Am. Chem. Soc.*, **2006**, *128*, 15556 - 15557.

[29] J. C. Horng, D. P. Raleigh, *J. Am. Chem. Soc.*, **2003**, *125*, 9286 - 9287.

electronegativity of these halogens which moves the π electronic density towards their positions as it can be seen in Figure 2.12.

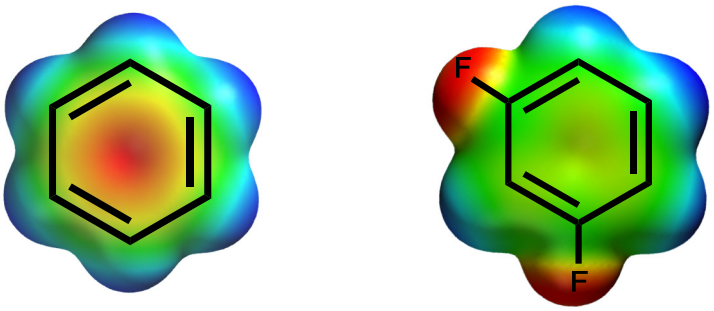

Figure 2.12 Electronic densities of benzene (left) and 3', 5'-difluorophenyl (right) rings. Spartan calculation (semi-empiric AM1).[19] Red = high electronic density; Green/Blue = low electronic density.

To this end, Álvaro Rol synthesised six different SRIF14 analogues containing Dfp in different positions. A part from that modification, all newly synthesised peptides included D-Trp in positon 8 and some of the analogues included Msa in position 7 as it was known to potentiate conformational restriction and trigger the activity and selectivity towards SSTR2. All six new peptides displayed well-dispersed 2D NMR data which were used to obtain the main conformations in aqueous solution. Although it has been postulated that electron-deficient aromatic residues in position 11 destabilise the fold of the analogue due to their limited capacity to shield residue 6,[30] Álvaro Rol found a strong aromatic interaction between the aromatic rings of Phe6 and Dfp11 in one of his analogues, [L-Dfp11_D-Trp8]-SRIF (Figure 2.13, top). Moreover, this analogue was active and selective for SSTR2. However, when Dfp was placed in position 7, [L-Dfp7_D-Trp8]-SRIF (Figure 2.13, bottom), the analogue turned out to be selective for SSTR3 (Table 2.4).[31]

[30] M. Salwiczek, E. K. Nyakatura, U. I. M. Gerling, S. Ye, B. Koksch, *Chem. Soc. Rev.*, **2012**, *41*, 2135 - 2171.

[31] P. Martín-Gago, Á. Rol, T. Todorovski, E. Aragón, P. Martin-Malpartida, X. Verdaguer, M. Vallès Miret, J. Fernández-Carneado, B. Ponsati, M. J. Macias, A. Riera, *Scientific Reports*, **2016**, *6*, 27285.

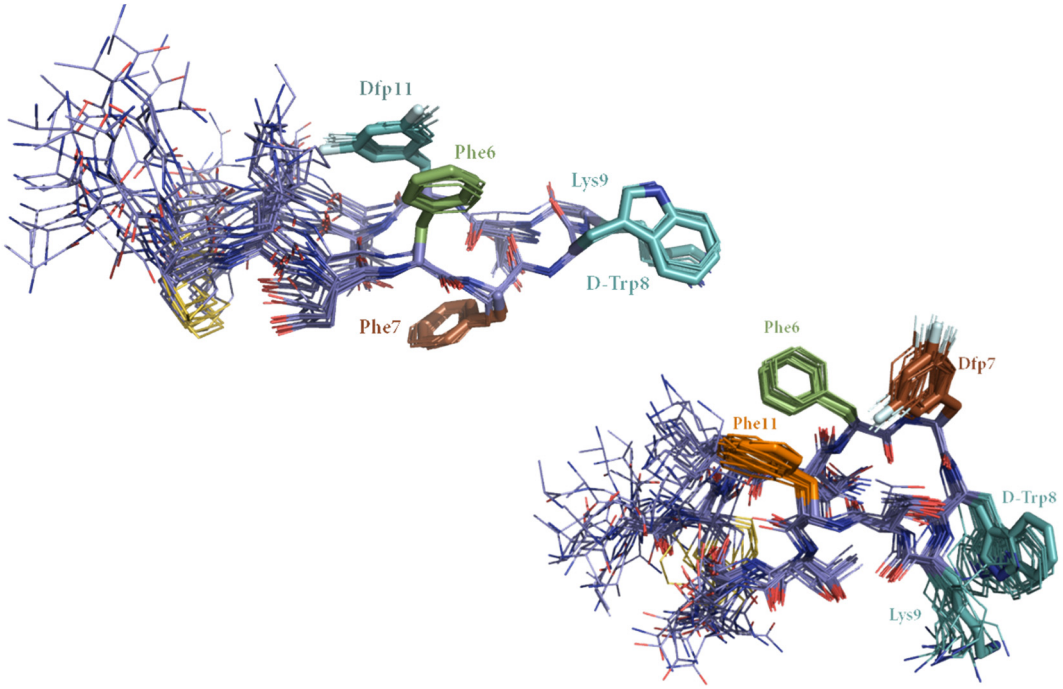

Figure 2.13 3D structures obtained by NMR of [L-Dfp11_D-Trp8]-SRIF analogue with an *offset stacked* interaction between Dfp6 and Phe11 (top) and [L-Dfp7_D-Trp8]-SRIF analogue with a *face to face* interaction between Phe6 and Dfp7 and the approximation of residue 7 to Phe11 through the F atom (bottom).

Dr. Rol also synthesised analogues containing both Dfp in different positions and Msa in position 7. Even though these analogues displayed a well-defined structure in solution (Figure 2.14), the binding affinities against SSTR1-5 of these new peptides were not as good as the ones without Msa (Table 2.4).

	SSTR1 (nM)	**SSTR2 (nM)**	**SSTR3 (nM)**	**SSTR4 (nM)**	**SSTR5 (nM)**
Somatostatin-14	1.88	0.016	0.25	1.55	0.76
Octreotide	480	0.77	13.0	>1000	21.0
[L-Dfp7_DTrp8]-SRIF	14.0	0.36	1.10	12.0	2.10
[L-Dfp11_DTrp8]-SRIF	14.0	0.066	3.81	11.0	5.00
[L-Dfp6_L-Msa7_D-Trp8]-SRIF	38.0	0.17	5.46	150	82.0
[L-Dfp11_L-Msa7_D-Trp8]-SRIF	19.0	0.26	23.0	62.0	31.0

Table 2.4 Binding selectivity (Ki values) of [L-Dfp7_D-Trp8]-SRIF, [L-Dfp11_D-Trp8]-SRIF, [L-Dfp6_L-Msa7_D-Trp8]-SRIF, [L-Dfp11_L-Msa7_D-Trp8]-SRIF and selected reference peptides against SSTR1-5.[31]

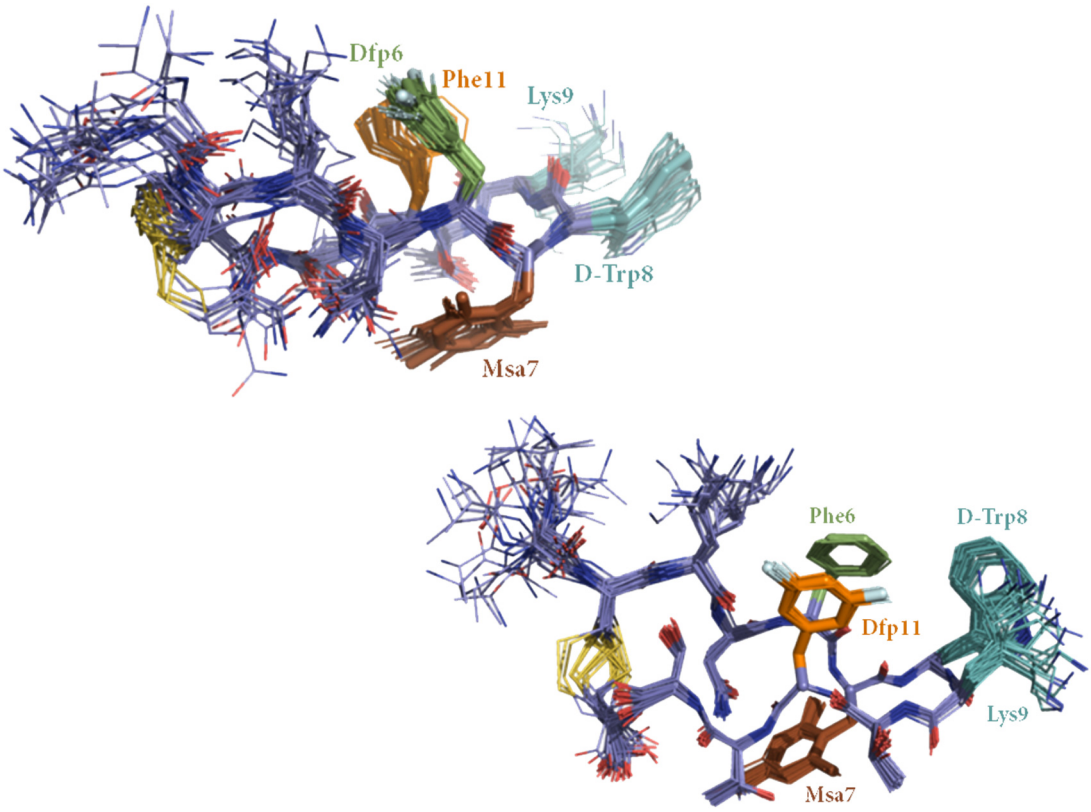

Figure 2.14 3D structures obtained by NMR of [L-Dfp6_L-Msa7_D-Trp8]-SRIF analogue with an *offset stacked* interaction between Dfp6 and Phe11 (top) and [L-Dfp11_L-Msa7_D-Trp8]-SRIF analogue with a *face to face* interaction between Phe6 and Dfp11 (bottom).

All these results, published between 2012 and 2016,[22, 31] opened up the field of study of 14 amino acid somatostatin analogues as conformationally structured peptides in solution. These compounds also enabled the establishment of binding activity trends against SSTR1-5. These results encouraged us not only to deepen our knowledge on this topic, trying to establish a substitution pattern which reinforced our effort to predict the selectivity of new analogues against SSTRs but to go one step further and try to find a structured, selective and long-lived 14-amino acid somatostatin analogue, which can also act as a carrier for a variety of molecules in the *N*-terminus.

Chapter 3

SRIF analogues with L-Dmp-OH

3.1 Introduction

The use of non-natural amino acids into biologically active peptides has been one of the most frequently used approaches to the development of novel peptides and peptide analogues with improved properties.[1]

Non-natural dimethyl phenyl alanines have been already implemented in the synthesis of opioid peptides. These peptides are endogenous substances that exhibit the pharmacological properties of morphine, an alkaloid analgesic isolated from opium. Opioid peptides are involved in many physiological actions and are implicated in the mechanisms of pain, addiction, stress, depression, and mental illness.

Tyr1, Phe3 and Phe4 are key amino acids in opioid peptides as they interact with opioid receptors (G-protein-coupled receptors). For that reason, Sasaki and Ambo decided to substitute them for the non-natural amino acid 2',6'-dimethylphenylalanine (^{2,6}Dmp).[2] In most of their analogues the substitution of Phe3 for this amino acid produced analogues with higher binding affinity and selectivity, whereas when substituting Phe4 for ^{2,6}Dmp, the obtained analogues had reduced their activity. When substituting Tyr1, the obtained compounds showed unexpectedly high binding affinity or just a slight drop in bioactivity.[2]

Okada and co-workers[3] used the same amino acid in another family of opioid peptides and obtained an increase of the binding affinity against the opioid receptors when introducing ^{2,6}Dmp.

[1] T. Li, Y. Tsuda, K. Minoura, Y. In, T. Ishida, L. H. Lazarus, Y. Okada, *Chem. Pharm. Bull.*, **2006**, *54*, 873 - 877.

[2] Y. Sasaki, A. Ambo, *Int. J. Med. Chem.*, **2012**, article ID: 498901.

[3] T. Li, K. Shiotani, A. Miyazaki, Y. Tsuda, A. Ambo, Y. Sasaki, Y. Jinsamaa, E. Marczak, S. D. Bryant, L. H. Lazarus, Y. Okada, *J. Med. Chem.*, **2007**, *50*, 2753 - 2766.

In our research group, Pablo Antonio Martín-Gago,[4] introduced 2,4,6-trimethyl-phenylalanine (Msa) in various somatostatin analogues. He found that the introduction of Msa, an amino acid with higher electronic density and higher steric hindrance, induced a conformational restriction depending on which Phe was it substituting in the native SRIF14 sequence (seen in section 2.2 of the present doctoral thesis).

L-3-(3',5'-dimethylphenyl)-alanine (L-3-(3',5'-dimethylphenyl)alanine, L-^{3,5}Dmp-OH or Dmp, the L enantiomer unless otherwise specified) is a non-natural amino acid (Figure 3.1) that has been under study due to the higher electronic density that the methyl groups give to the aromatic ring and the reduced mobility of the Dmp aromatic ring when compared to phenylalanine (Phe).[5]

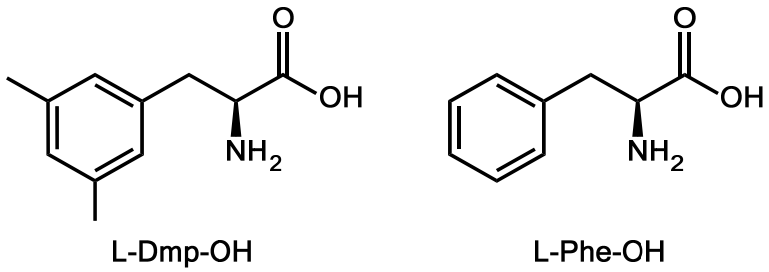

Figure 3.1. Structural comparison between L-3-(3',5'-dimethylphenyl)alanine, Dmp (left) and L-phenylalanine, Phe (right).

From the electronic perspective, the aromatic π-π interactions should be favoured with respect to the ones established between the two plain benzene aromatic rings of Phe. The intrinsic rigidity of Dmp could displace the conformational equilibrium to the formation of more rigid conformations.[6]

[4] P. A. Martín-Gago, doctoral thesis *Synthesis of highly structured and receptor-selective tetradecapeptidic analogs of somatostatin: Fine tuning the non-covalent interactions among their aromatic residues*, Univeristat de Barecelona, 2013.

[5] P. Martín-Gago, M. Gómez-Caminals, R. Ramón, X. Verdaguer, P. Martín-Malpartida, E. Aragón, J. Fernández-Carneado, B. Ponsati, P. López-Ruiz, M. A. Cortés, B. Colás, M. J. Macias, A. Riera Angew. Chem. Int. Ed., **2012**, *51*, 1820 –1825.

[6] Martín-Gago, P.; Aragón, E.; Gomez-Caminals, M.; Fernández-Carneado, J.; Ramón, R.; Martin-Malpartida, P.; Verdaguer, X.; López-Ruiz, P.; Colás, B.; Cortes, M.A.; Ponsati, B.; Macias, M.J.; Riera, R. *Molecules*, **2013**, *18*, 14564-14584.

The aromatic interactions are produced by a combination of Van der Waals, electrostatic and hydrophobic forces but the contribution of each one has not been determined with precision yet.[7] Nevertheless, it has been demonstrated that the aromatic interaction is enhanced in aqueous media due to hydrophobic effects.[8] This fact is important as the aromatic interactions in proteins are determined in aqueous media. The substitution of two hydrogen atoms of the Phe aromatic ring for two methyl groups creates a significant difference when talking about steric hindrance due to the bigger radius of the methyl group when compared to the hydrogen atom. However, Dmp is capable of fostering the π-π aromatic interactions with other aromatic rings because of an increased hydrophobicity of its ring (theoretical logP, hydrophobicity parameter, of Dmp aromatic ring is 3.01 whilst logP of Phe ring is 2.03).[9] Although the steric hindrance of Dmp is enhanced when compared to the natural Phe, their quadrupole moment is virtually the same which implies that the electron density stays on the aromatic ring, as can be seen in Figure 3.2.

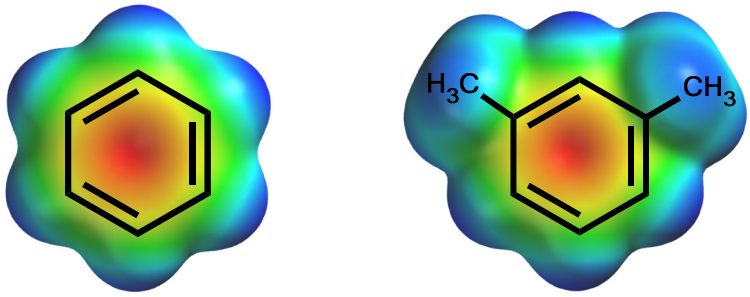

Figure 3.2. Electron densities of the benzene (left) and dimethyl (right) rings. Spartan calculation (semi-empiric AM1).[10] Red = high electronic density; Green/Blue = low electronic density.

Furthermore, the electronic density of the aromatic ring of the non-natural amino acid (Dmp) is higher than that of Phe due to the electron-donor character of the two methyl

[7] C. A. Hunter, K. R. Lawson, J. Perkins, C. J. Urch, *J. Chem. Soc. Perkin. Trans.*, **2001**, *5*, 651 - 669.

[8] M. D. Sindkhedkar, H. R. Mulla, A. Cammers-Goodwin, *J. Am. Chem. Soc.*, **2000**, *122*, 9271 - 9277.

[9] logP calculated with Spartan (semi-empiric AM1 calculations).

[10] Spartan '10 v 1.1.0 (Wavefunction)

groups. As stated earlier, this characteristic would foster the aromatic interactions with other aromatic rings of the molecule.

To the best of our knowledge, Dmp has never been used in peptidic sequences nor in somatostatin analogues. With its introduction into the somatostatin sequence we intended to determine whether the methyl groups in the ortho positions of Msa are key to obtain structured and selective peptides. Through the insertion of Dmp we hoped not only to disclose the importance of both steric and electronic effects on the obtainment of structured peptides but to see if a more hydrophobic amino acid would enhance the π-π interactions with other aromatic residues. As the aromatic ring of Dmp has four more protons than Phe we would be able to determine its spatial proximity with the other amino acids of the molecule by analysing the 2D homonuclear ^{1}H-^{1}H NMR (TOCSY and NOESY) and to establish the major set of conformations in solution. Moreover, to try to clarify the structure-activity relationship through sequence modifications we would also perform the binding affinity assays against SSTRs.

3.2 Synthesis of SRIF14 analogues containing L-Dmp-OH

Somatostatin analogues containing L-Dmp-OH were synthesised by an individual and systematic substitution of the aromatic residues (Phe6, Phe7 and Phe11) for the non-natural amino acid (Figure 3.3). D-Trp was introduced in position 8 in all the analogues as it is known to enhance the activity of the peptides which contain it in the sequence by increasing their half-lives and it also contributes directly to the stabilization of the β-turn.[11] In the search for new and more stable analogues, the substitution of L-Trp for its D-enantiomer was a constant modification.

[11] a) B. H. Arison, R. Hirschmann, D. F. Veber, *Bioorg. Chem.*, **1978**, *7*, 447 - 451; b) O. Ovadia, S. Greenberg, B. Laufer, C. Gilon, A. Hoffman, H. Kessler, *Expert Opin. Drug Discov.*, **2010**, *5*, 655 - 671.

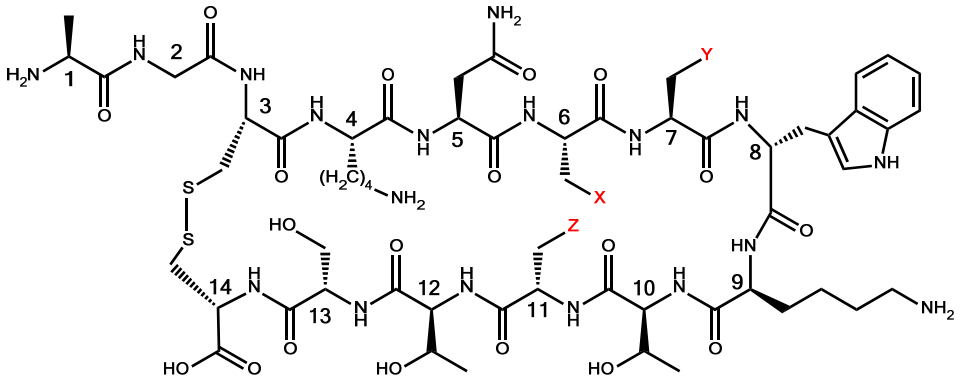

	6	**7**	**8**	**11**
[L-Dmp6_D-Trp8]-SRIF14 (1)	Dmp	Phe	D-Trp	Phe
[L-Dmp7_D-Trp8]-SRIF14 (2)	Phe	Dmp	D-Trp	Phe
[L-Dmp11_D-Trp8]-SRIF14 (3)	Phe	Phe	D-Trp	Dmp

Figure 3.3. Somatostatin derivatives containing Dmp in different positions that will be presented in this chapter.

Even though Fmoc-L-Dmp-OH is a commercial amino acid, its preparation has never been published with the exception of the synthesis of the unprotected L-Dmp-OH performing the asymmetric hydrogenation with DIPAMP.[1] However, the enantiomeric excess of this transformation was not described.

As our group has remarkable knowledge in asymmetric synthesis and in the development of new catalysts, we thought that it would be a good strategy to synthesise Fmoc-L-Dmp-OH by asymmetric hydrogenation using Rh-MaxPHOS, a catalyst previously developed in our group.[12] For that reason a retrosynthetic analysis was performed (Scheme 3.1), the key step being the obtainment of the achiral dehydroamino acid, to obtain the non-natural amino acid Fmoc-L-Dmp-OH.

[12] a) M. Revés, C. Ferrer, T. León, S. Doran, P. Etayo, A. Vidal-Ferran, A. Riera, X. Verdaguer, *Angew. Chem. Int. Ed.*, **2010**, *49*, 9452 - 9455; b) E. Cristóbal-Lecina, P. Etayo, S. Doran, M. Revés, P. Martín-Gago, A. Grabulosa, A. R. Costantino, A. Vidal-Ferran, A. Riera, X. Verdaguer, *Adv. Synth. Catal.*, **2014**, *356*, 795 - 804.

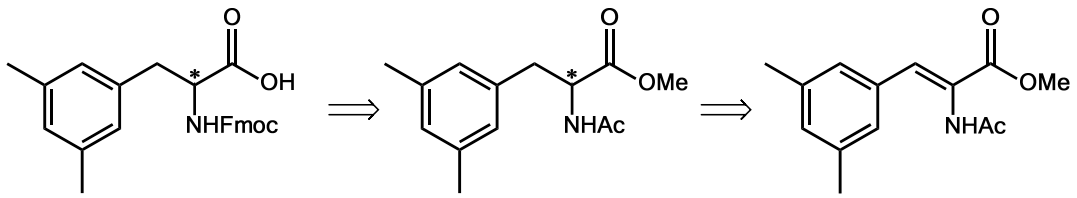

Scheme 3.1. Retrosynthetic analysis for the obtainment of the chiral Fmoc-L-Dmp-OH starting from the achiral dehydroamino acid.

The synthesis of the dehydroamino acid could be performed through two different synthetic pathways (Figure 3.4). The first one consisted in the methanolysis of the azalactone intermediate[5] and the second one through a Heck reaction.[1] *N*-acetylglycine and 3,5-dimethylbenzaldehyde underwent a condensation to form the corresponding azalactone in the presence of acetic anhydride (Route 1). Subsequent ring opening (MeONa/MeOH) produced the desired dehydroamino acid in a total 56% yield. The E isomer was not detected by either TLC or ^{1}H-NMR.

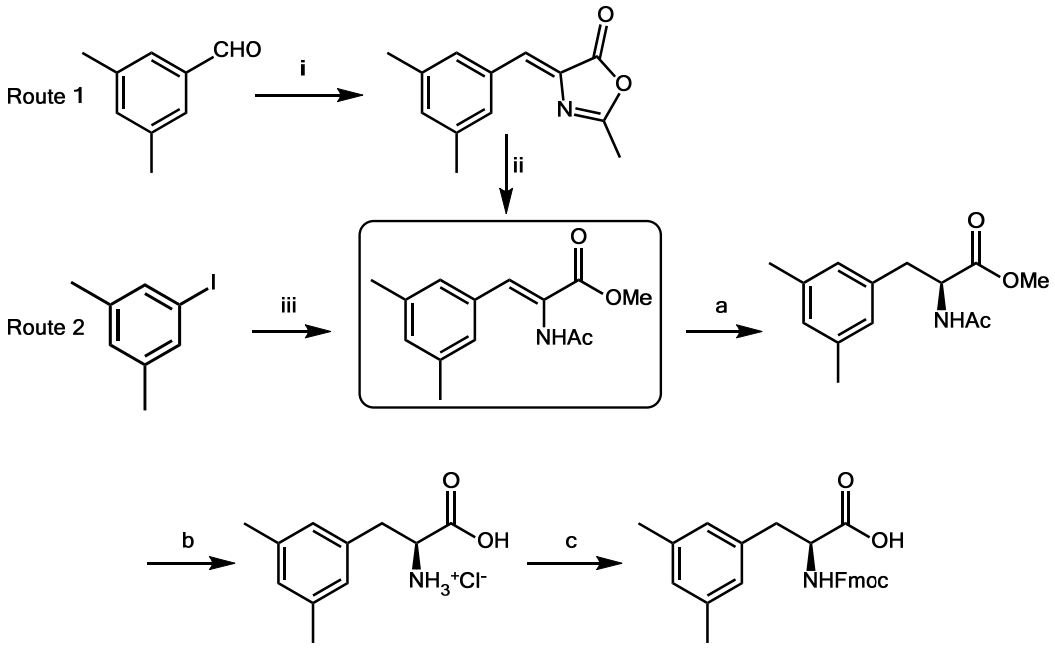

Figure 3.4. Synthesis of Fmoc-L-Dmp-OH. **Route 1** through an azalactone intermediate: i) *N*-Ac-Gly-OH, AcONa, Ac_2O, 100°C, 2h; ii) MeONa, MeOH, 70°C, 2h. **Route 2** through a Heck reaction: iii) *N*-Ac-dehydro-Ala-OMe, tri-(o-tolyl)phosphine, $Pd(OAc)_2$, Et_3N, ACN, 100°C, 48h. a) MaxPHOS-Rh cat 3%, H_2 (5 bar), MeOH, 48h, rt; b) HCl aq, reflux, 6h; c) FmocOSu, Na_2CO_3, H_2O, acetone, 0°C to rt, 24h.

The synthesis of the dehydroamino acid via the Heck reaction (Route 2) took place uneventfully in an 86% conversion and a 51% yield using a similar procedure as the one previously described by Pablo Martín-Gago.[4]

Following the designed route (Schem3.1), the next step was the asymmetric hydrogenation of the dehydroamino acid; for that particular reaction a 3% MaxPHOS catalyst loading was used. The reaction reached full conversion and the desired product was achieved with an 82% yield and an enantiomeric excess greater than 99%, calculated by HPLC (Scheme 3.2).

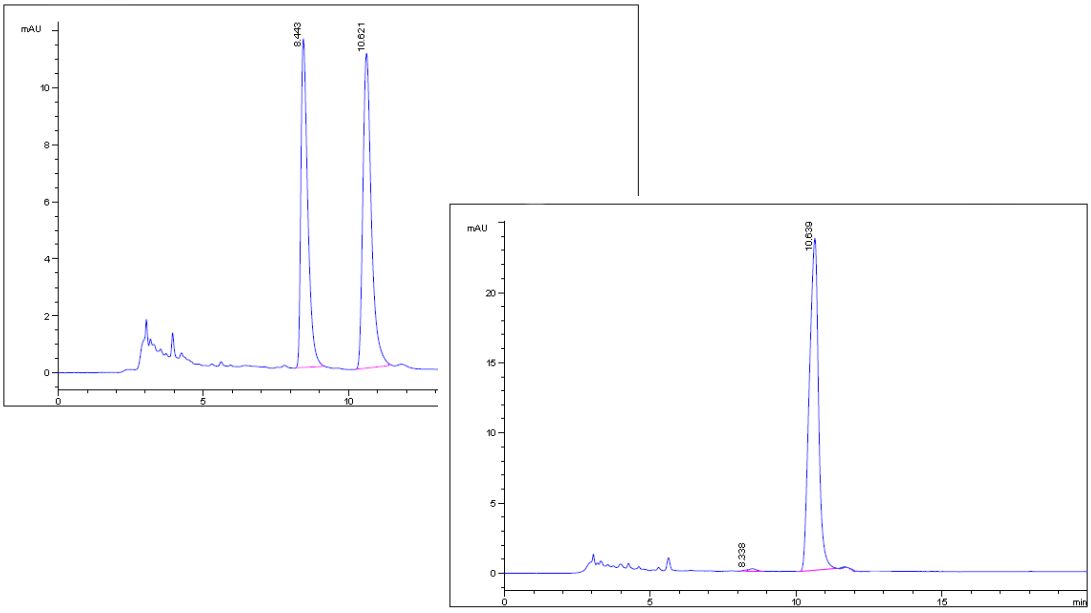

Peak	t_R	Width	Area	Height	Area (%)
1	8.338	0.176	1.057	0.100	0.196
2	10.639	0.373	531.386	23.742	98.628

Scheme 3.2. Analytical HPLC after the asymmetric hydrogenation reaction. Conditions used: Heptane/IPA (90:10), T = 20 ºC, flow rate = 1 mL/min, column: Chiralpak IA, stop time = 20 min.

Once the chirality was introduced, a hydrolysis needed to be done to obtain the free amino acid itself as a chlorine salt and then the Fmoc protection of the amino moiety was performed. Both reactions reached full conversion and the obtained yields were excellent, being >99% for the hydrolysis and >90% for the Fmoc protection. The enantiomeric

excess obtained through the asymmetric hydrogenation was maintained until the obtainment of the final Fmoc-L-Dmp-OH.

The rest of the amino acids, including Fmoc-D-Trp(Boc)-OH, were commercially available from different suppliers.

All three peptides presented in this chapter were synthesised by solid phase peptide synthesis (SPPS) following the well-known Fmoc/^{t}Bu strategy using a 2-chlorotrytyl chloride resin. The synthesis of [L-Dmp6_D-Trp8]-SRIF14 (**1**) is shown as a general example in Scheme 3.3.

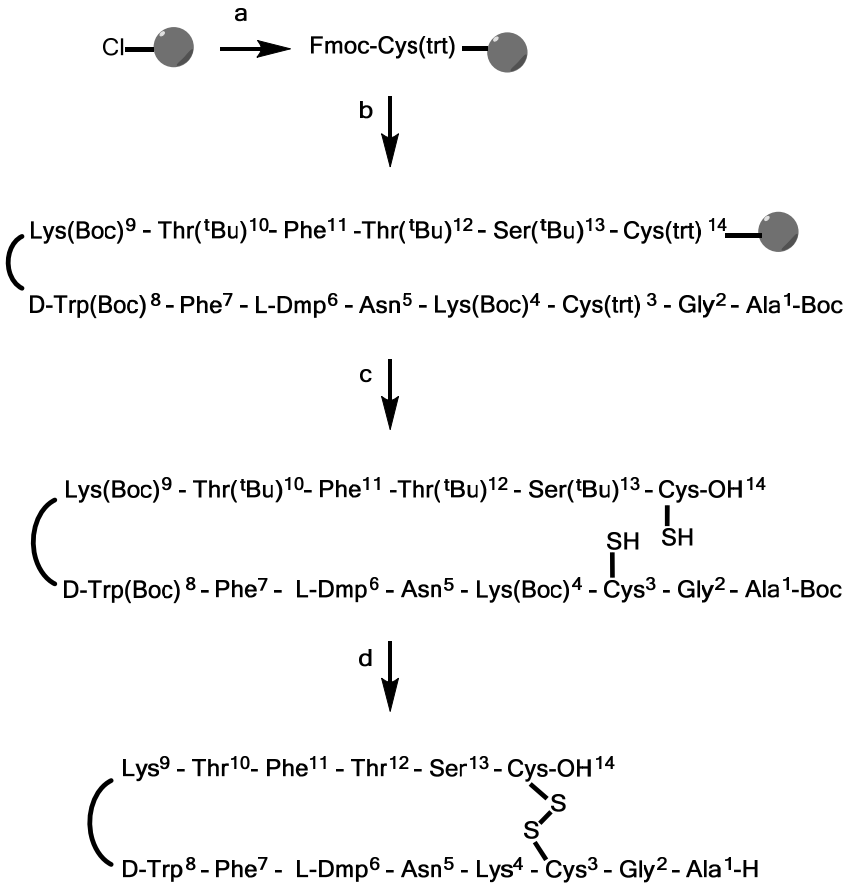

Scheme 3.3. SPPS of [L-Dmp6_D-Trp8]-SRIF14 (**1**). a) 1. Fmoc-Cys(trt)-OH (3eq), DIEA (3eq), 2. MeOH; b) 1. Piperidine 20% in DMF, 2. Fmoc-AA-OH (1.5-3eq), DIPCIDI (3eq), HOBt (3eq), DMF; 3. Piperidine 20% in DMF, 4. Boc-Ala-OH (3eq), DIPCIDI (3eq), HOBt (3eq), DMF, c) DCM/TFE/AcOH, d) 1. I_2, 2. TFA/DCM/anisole/H_2O.

During the synthesis of the analogue [L-Dmp11_D-Trp8]-SRIF14 (**3**), the coupling of Fmoc-Asn-OH in position 5 was problematic; for that reason a recoupling with HATU (stronger coupling reagent) was necessary. This difficulty to couple that amino acid was observed previously by Hirschmann[13] during the synthesis of [L-Pyz11_D-Trp8]-SRIF14.

3.3 NMR studies and structure determination

The peptides presented in this chapter were characterised by nuclear magnetic resonance (NMR). To this end, samples were dissolved in phosphate buffer at pH=6.5 with 10% D_2O and the corresponding homonuclear mono and bidimensional spectra (^1H-^1H TOCSY and NOESY 200ms and 350ms, 600 MHz) were acquired for each analogue.

Each TOCSY experiment contains all cross peaks due to protons of the same spin system. It should be noted that protons from different amino acids always belong to different spin systems, because there is no scalar coupling across the amide bond. That way we can identify characteristic signals for each amino acid corresponding to the protons of the same side chain.

Cross peaks in the NOESY are due to dipolar couplings resulting from interactions of spins via space and hence only depend on the distance but not on the number of intervening bonds. The NOESY not only contains peaks from which distances are derived for the structure calculation but is also heavily used during the sequential resonance assignment process. Considering that scalar couplings are restricted to protons within a single amino acid, sequential correlations (correlations between protons of neighbouring amino acids) need to be taken from the NOESY.

Through these two different experiments, the chemical shift of each proton present in the molecule were assigned as well as the relation between two protons. In all the cases, the

[13] S. Neelamkavil, B. Arison, E. Birzin, J. Feng, K. Chen, A. Lin, F. Cheng, L. Taylor, E. R. Thornton, A. B. Smith III, R. Hirschmann, *J. Med. Chem.*, **2005**, *48*, 4025 - 4030.

process starts by assigning the sequential TOCSY and NOESY signals. To be more precise, the first ones to be identified are the amidic protons and the ones located in Cα and Cβ.

Spectra were analysed until all resonance signals corresponding to each amino acid were identified as well as the medium and long distance NOE peaks which define the different conformations of each molecule. Spectra were processed using XwinNMR and analysed using CARA software.[14]

After these, medium and long distance NOE signals were assigned using the Wuethrich protocol.[15] All protons from the amino acids used are represented in the following figure (Figure 3.5) with their corresponding nomenclature.

Each proton was assigned following the IUPAC nomenclature for amino acid side chains (α, β, γ, δ,…) depending on the proton position with respect to the C of the carboxylic acid. If a pair of protons appear to be non-equivalent in the spectra, they were distinguished by a number.

At first sight, it can be distinguished if a peptide is prone to have a defined 3D structure in solution or not by simple observation of the NOESY spectrum. If the density of long distance NOE signals is low, it indicates that the peptide has a flexible sequence without a preferred 3D ordering in solution. However, if the density of signals is high, it probably has a preferred conformation in solution so it is possible to obtain the major 3D structure in solution. This fact can be seen in Figures 3.6 and 3.7 where NOESY spectra of SRIF14 and [L-Dmp11_D-Trp8]-SRIF (**3**) are shown. SRIF-14 spectra display a low volume of signals but sufficient enough to assign all the protons of its sequence. However, the absence of medium and long-distance NOE signals implies a high flexibility in solution.

[14] CARA for OS X systems, v. 1.9, R. L. J. Keller, The Computer Aided Resonance Assignment Tutorial, 1st Ed. Cantina Verlag, **2004**.

[15] K. Wuethrich, G. Wider, G. Wagner, W. Braun, J. Mol. Biol., **1982**, *155*, 311 - 319.

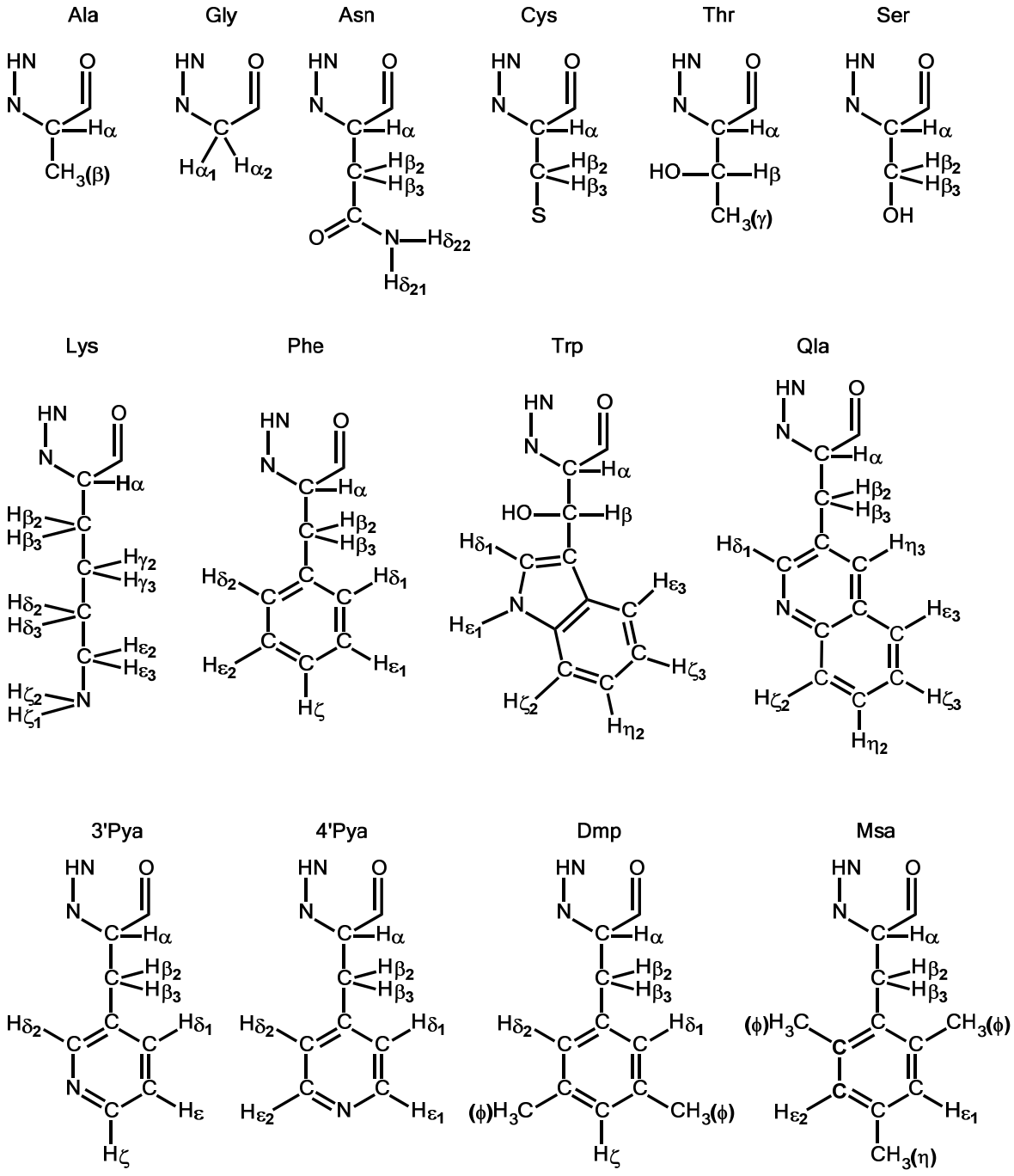

Figure 3.5. Amino acids used during this thesis and nomenclature of each of its protons.

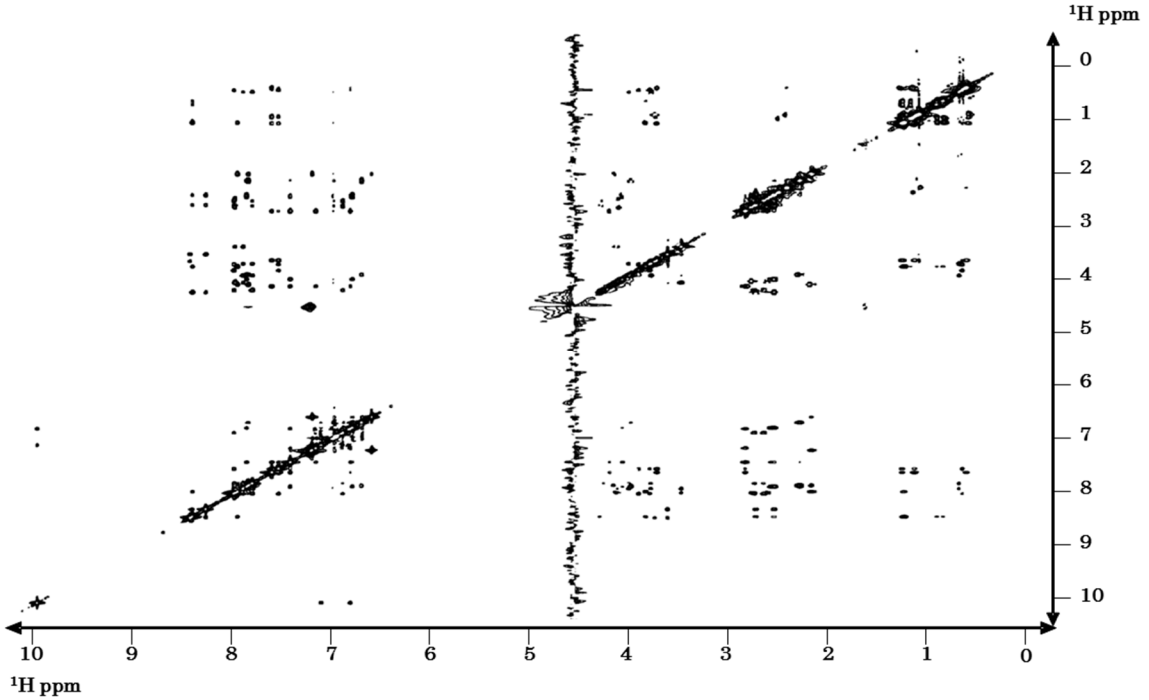

Figure 3.6. NOESY 200 ms spectrum for SRIF14 with low density of NOE signals.

As it can be seen in the NOESY spectrum of the analogue **3** (Figure 3.7), there is a high density of long and medium-distance NOE signals which will be useful to determine the major conformation in solution.

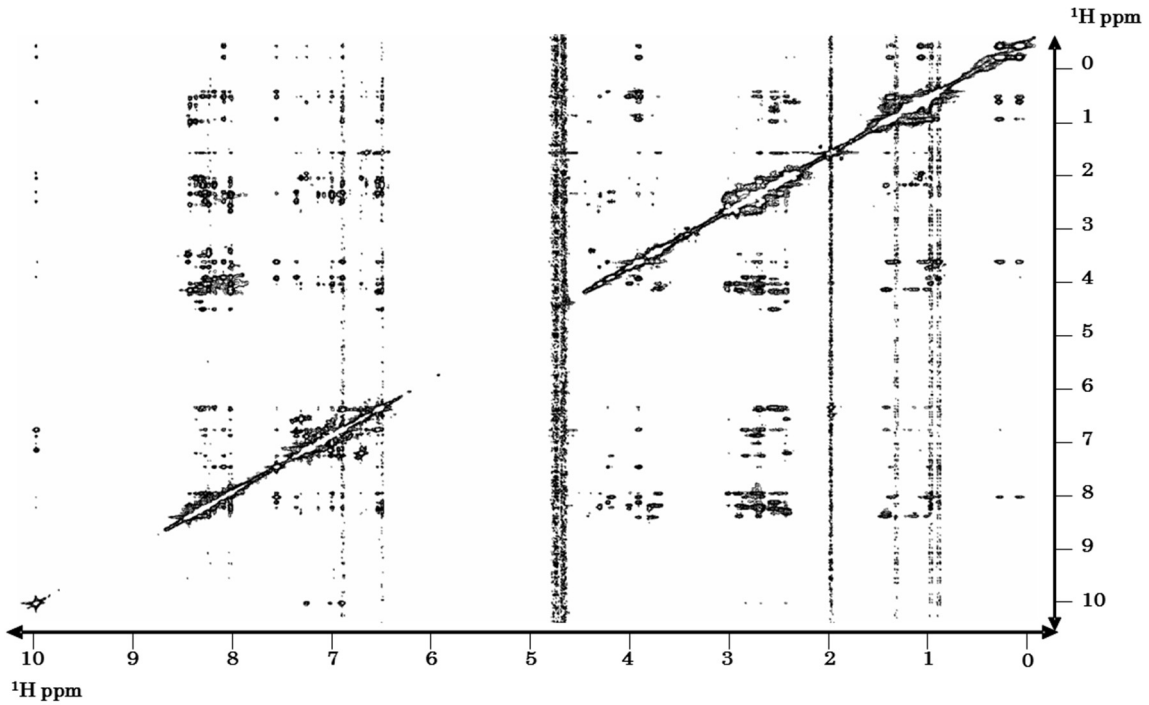

Figure 3.7. Bidimensional homonuclear NOESY 350 ms spectrum for [L-Dmp11_D-Trp8]-SRIF (**1**) with high density of NOE signals.

Once all the signals were identified and assigned, the peaks were integrated to obtain the peak volume for each NOE signal. This information was processed via the CNS program (Christallography & NMR System)[16] through the StructCalc platform.[17] CNS program allowed us to refine the structure using restrictions coming from the PARALLHDG Force Field[18] (which contains previously observed and verified experimental data and theoretical calculations) and from our NMR spectra. That way, the theoretical structures obtained can be modulated through distance restrictions coming from the NOE signals. A variable number of calculations were set up until the lower energy structures were convergent, coherent with the experimental values and the dihedral angles did not violate the Ramachandran diagrams.[19]

The results obtained from the CNS program were visualised with PyMOL program.[20] The starting calculations returned structures with low convergence but some patterns could be elucidated. However, as more corrections related to NOE signals which violate the distances were introduced, more convergent structures were obtained. At that point, when the lower energy structures were highly convergent, the structure was considered validated and definitive.

Our peptides (**1**-**3**) showed a major set of conformations in solution. The general inclusion of D-Trp in position 8 enhanced the aliphatic-aromatic interaction between D-Trp8_Lys9, which was translated into a higher shielding of Hγ of Lys9 and triggered the stabilization of the β-turn of the peptide.[5, 11]

[16] A. T. Brunger, P. D. Adams, G. M. Clore, W. L. DeLano, P. Gros, R. W. Grosse-Kunstleve, J. S. Jiang, J. Kuszewski, M. Nilges, N. S. Pannu, R. J. Read, L. M. Rice, T. Simonson, G. L. Warren, *Acta Crystallogr. D Biol. Crystallogr.*, **1998**, *54*, 905 - 921.

[17] P. Martín-Malpartida, M. J. Macias, unpublished data.

[18] J. P. Linge, M. Nilges, *J. Biomol. NMR*, **1999**, *13*, 51 - 59.

[19] G. N. Ramachandran, C. Ramakrishnan, V. Sasisekharan, *J. Mol. Biol.*, **1963**, *7*, 95 - 99.

[20] W. L. DeLano. The Pymol molecular graphics system. Palo Alto, CA: DeLano Scientific, **2002**, USA.

We observed that L-β-3', 5'-dimethylphenylalanine helped in the structural determination of the molecule not only via direct or indirect aromatic interactions which is translated into a major ordering in the structure but through the six protons of the methyl groups which, together with the highly shielded Hζ proton, nourish the spectra with a higher volume of NOE interactions. All this information helps obtain a major 3D conformation in solution once introduced in the calculation program.

3.3.1 Structure of [L-Dmp11_D-Trp8]-SRIF14 (1)

[L-Dmp11_D-Trp8]-SRIF14 (**1**) was the first analogue to be studied. The acquired NMR data clearly showed that peptide **1** was more rigid than the natural SRIF in solution due to the high density of NOE signals (Figure 3.7). Even though there was some conformational variability of the extracyclic side chains, the 30 lower energy conformations showed high degree of convergence of both the peptidic backbone and the side chains (Figure 3.8).

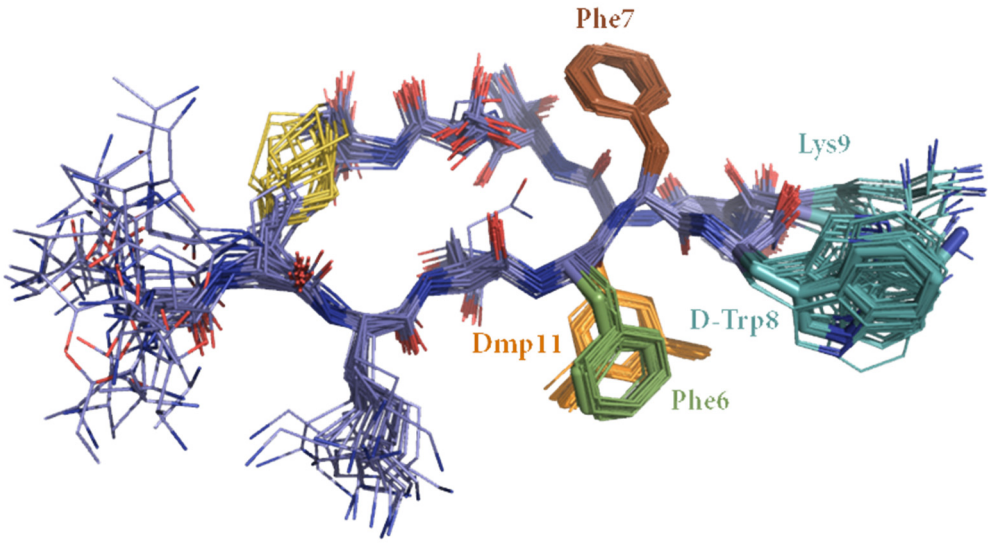

Figure 3.8. Superimposition of the 30 lower energy structures of [L-Dmp11_D-Trp8]-SRIF (**1**) which are in agreement with experimental NMR data.

It has to be noted that there is a geometrical feature which stands out above the rest; the π-π aromatic interaction that takes place between Phe6 and Dmp11 in a *face to face* geometry. That approach is not completely flat due to the proximity of the Hβ of Dmp11 with the H_{AR} of Phe6 (Figure 3.9). Simultaneously, Phe7 does not participate in this

aromatic interaction and is placed on the other side of the molecule with a similar orientation than the Phe6-Dmp11 pair. This orientation was supported by some long-distance NOE signals: interaction of Hβ of Asn5 with Hδ of Phe7, Hε and Hδ of Phe7 with Hγ of Thr12 and Thr10.

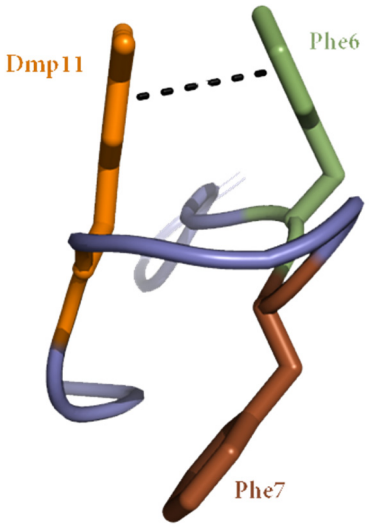

Figure 3.9. Lateral view of the *face to face* π-π aromatic interaction between Phe6 and Dmp11.

Contrary to what happened with the Msa analogues synthesised by Dr. Martín-Gago,[4, 21] the ineraction between 6 and 11 of this Dmp-containing analogue takes place on the side below the peptidic backbone (as depicted in Figure 3.8). Moreoever, the geometry of the spatial aproximation between residues 11 and 6 is also different from Dr. Martín-Gago's [Msa11_D-Trp8]-SRIF14 analogue; whilst he found an *offset-tilted* interaction, Dmp11_DTrp8-SRIF14 showed a *face to face* π-π aromatic interaction.

Furthermore, the D-Trp8_Lys9 pair shows high density of NOE signals between them which is translated in a closer proximity in space. As a consequence of the little volume of NOE signals between that pair and the rest of the molecule D-Trp8_Lys9 face the outside of the peptidic backbone. Due to this lack of NOE signals, two different orientations of the pair were found, with the one which was oriented to the same side of the molecule that Phe6 and Dmp11, being most populated.

[21] To keep the structures consistent, we have always plotted them with the residues 1-7 in front of the residues 10-14 while 8 and 9 form the β turn and are located on the right side.

3.3.2 Structure of [L-Dmp7_D-Trp8]-SRIF14 (2)

Peptide **2** also displayed sufficient information in the bidimensional NMR experiments to assume that it would display a major set of conformations in solution. In this case, the lower energy conformations showed a π-π aromatic interaction between the Phe6 and Phe11 while residue 7 was found at the other side; below the peptidic backbone (Figure 3.10). This spatial disposition appeared to be the contrary to the one found for **1** and with a perpendicular orientation of Msa7 with respect to the peptidic backbone. The difference between **1** and **2** lies in the different spatial geometry of the interaction. While in peptide **1** Dmp6 and Phe11 showed a *face to face* interaction and were placed below the backbone, in peptide **2** the same residues (Phe11 and Phe6) were placed in a marked *edge to face* geometry and above the backbone (Figure 3.11).

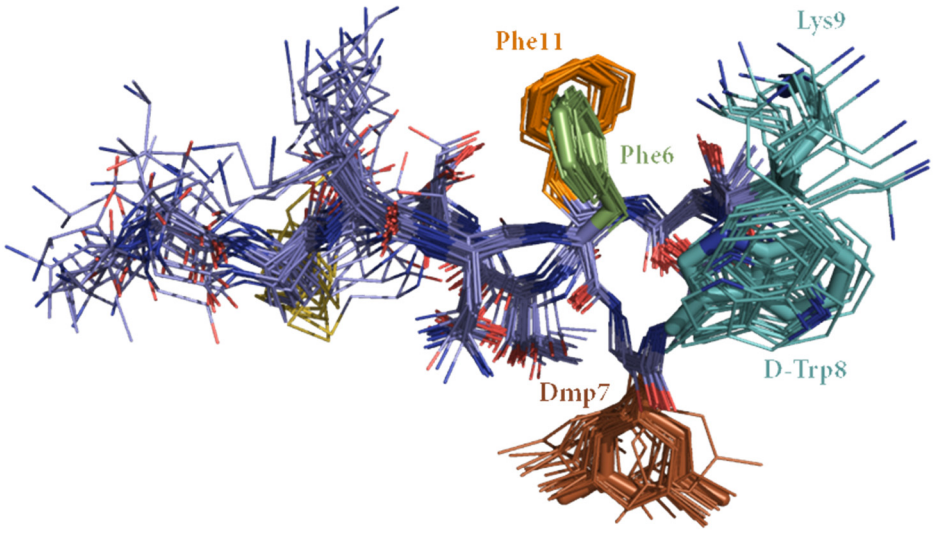

Figure 3.10. Superimposition of the 22 lower energy structures of [L-Dmp7_D-Trp8]-SRIF (**2**) which are in agreement with experimental NMR data.

This geometry was supported by some detected long-distance NOE signals: interaction of Hδ of Phe11 with HN, Hα, Hδ and Hζ of Phe 6 and Hζ of Phe11 with Hδ of Phe6. Moreover, the D-Trp8_Lys9 pair shows high denisity of NOE signals between them which is translated into a closer proximity in space. Contrary to what happened with **1**, some

NOE signals between the pair and other residues of the molecule were detected; which led it to adopt an orientation similar to the Phe6-Phe11 π-π aromatic interaction.

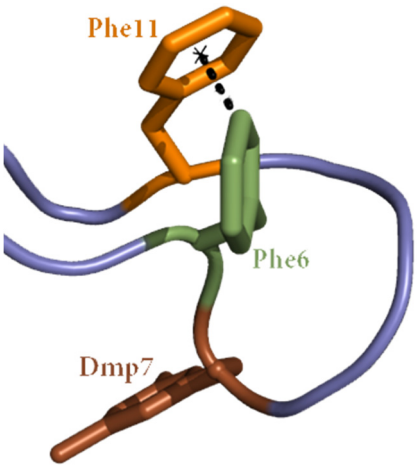

Figure 3.11. View of the *edge to face* π-π aromatic interaction between Phe6 and Phe11.

However, the NOEs detected between the pair itself and the pair and the rest of the molecule were not enough to avoid having two different orientations of the D-Trp8 being the most populated the one in which the N atom was oriented to the same side of the molecule that Phe6 and Phe11.

This particular set of conformations of peptide **2** was seen to be similar for the analogue [L-Msa7_D-Trp8]-SRIF14,[4] in which Phe6 and Phe11 were also interacting above the peptidic backbone while Msa7 was placed below with a flat orientation and facing the inner part of the molecule thus facilitating the interaction between Phe6 and Phe11 by steric repulsion. The interaction between residues 6 and 11 of **2** was found to be an *edge to face* as in the Msa analogue (Figure 3.12).

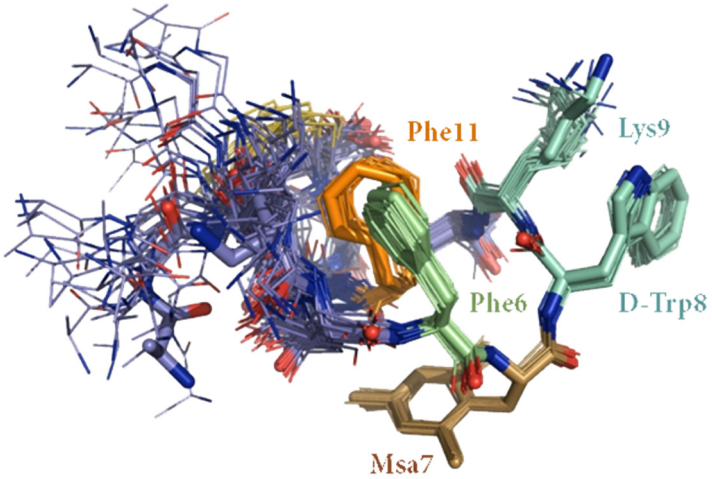

Figure 3.12. Superimposition of the lowest energy conformers of [L-Msa7_D-Trp8]-SRIF, previously synthesised in our group.[4]

3.3.3 Structure of [L-Dmp6_D-Trp8]-SRIF14 (3)

The third analogue studied from this family was [L-Dmp6_D-Trp8]-SRIF14 (**3**). In this case, two different major conformations were observed (Figure 3.13). The lower intensity of the NOE signals corresponding to each conformation when compared to other signals, implies a bigger difficulty to obtain a set of convergent structures even when dihedral angle restrictions were introduced for some amino acids.

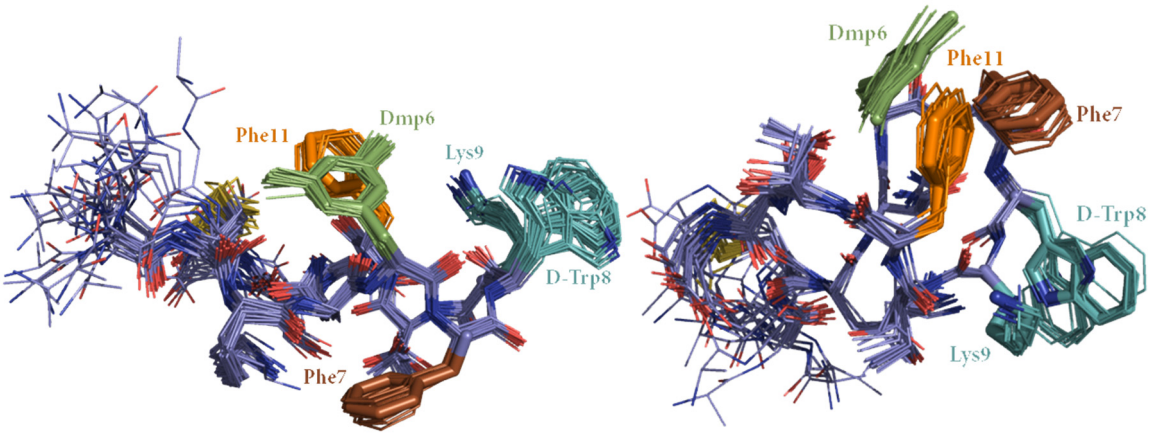

Figure 3.13. Two major conformations in solution obtained for peptide **3**.

For the first conformation (Figure 3.14) a 6-to-11 interaction was found with an *edge to face* geometry between Dmp6 and Phe11 (Figure 3.15). In that case Phe7 was placed below the peptidic backbone with a similar orientation to the aromatic interaction. Resembling peptide **2**, this spatial disposition is the opposite of the one happening in analogue **1**, where Phe7 was facing the upper part of the molecule and the interaction between 6 and 11 was placed below the backbone. The low volume of NOE signals of the D-Trp8_Lys9 pair cause it to face the outside of the peptidic backbone but with a small inclination towards the Dmp6_Phe11 interaction.

This conformation was found to be similar to the previously obtained for [L-Msa7_D-Trp8]-SRIF14 and described by Dr. Martín Gago,[4] with the aromatic interaction between residues 6 and 11 taking place above the peptidic backbone wile residue 7 is placed below and does not directly participate in the π- π interaction.

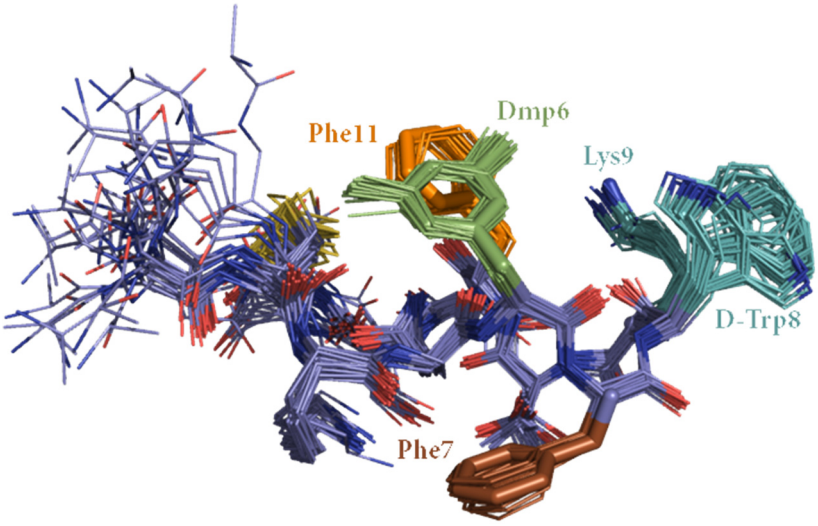

Figure 3.14. Superimposition of the 32 lower energy structures of [L-Dmp6_D-Trp8]-SRIF (**3**) which are in agreement with experimental NMR data for a 6-to-11 interaction.

Furthermore, we could also observe two different orientations of the D-Trp8 which came from the lack of NOE signals with the other side chains of the residues present in the molecule.

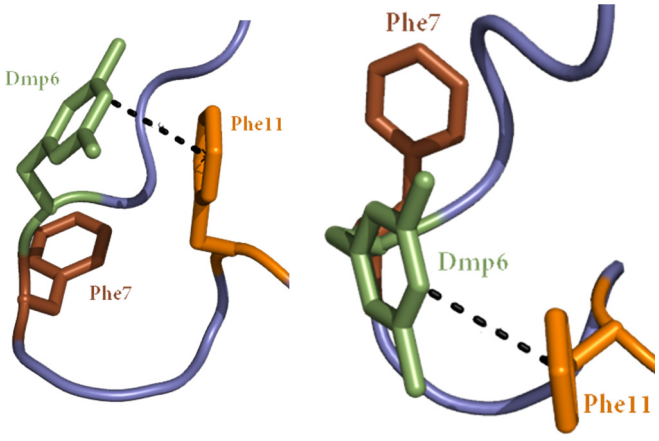

Figure 3.15. Side views of the *edge to face* π-π aromatic interaction between Dmp6 and Phe11.

This 6-to-11 conformation was also supported by long-range NOE signals: interaction of Hδ of Dmp6 with HN, Hβ, Hε and Hδ of Phe11, interaction of Hζ of Dmp6 with Hβ and Hε of Phe11 and interaction of Hδ of Phe11 with Hα of Dmp6.

The second set of conformations were found to form a cluster interaction between Dmp6, Phe7 and Phe11 (Figure 3.16) which was completely different from the structures of [L-Dmp11_D-Trp8]-SRIF14 (**1**) and [L-Dmp7_D-Trp8]-SRIF14 (**2**).

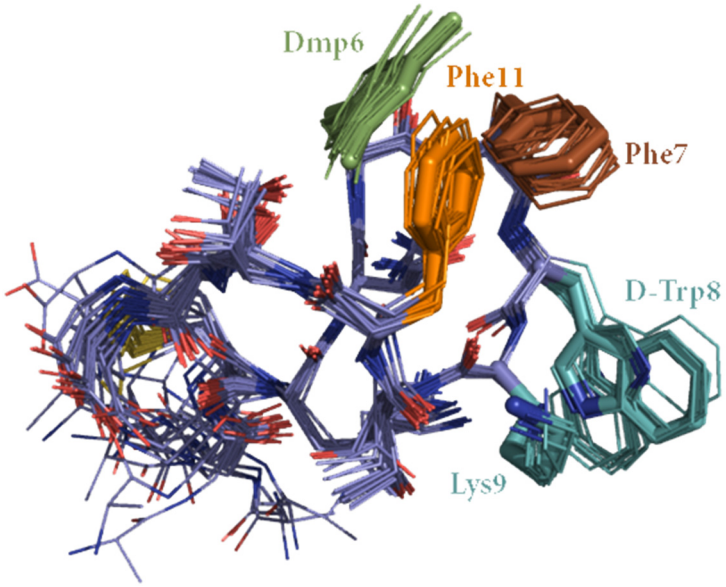

Figure 3.16. Superimposition of the 32 lower energy structures of [L-Dmp6_D-Trp8]-SRIF (**3**) which are in agreement with experimental NMR data for a cluster interaction.

This conformation was also supported by long-distance NOE signals: interaction of Hδ of Phe7 with Hβ and Hε of Phe11, Hδ of Phe7 with Hβ of Dmp6 and Hε of Phe7 with Hε of Dmp6. As can be seen in the figure, the three aromatic rings are interacting with each other with different geometries; Dmp6 and Phe7 show an *offset-stacked* geometry while Dmp6 is interacting with Phe11 via an *edge to face* spatial disposition. At the same time, Phe11 also interacts with Phe7 with an *edge to face* geometry (Figure 3.17).

Due to the cluster interaction between all three aromatic residues, the peptidic backbone adopts a different conformation which resembles a clamp. In this new spatial disposition, the D-Trp8_Lys9 pair is facing the opposite side of the molecule than the π-π aromatic interaction. Furthermore, the pair D-Trp8_Lys9 pair shows high denisity of NOE signals between the two residues which is translated into a closer proximity in space. As with the other cases, the low volume of NOE peaks between the D-Trp8_Lys9 pair and the rest of the molecule detected in the experimental NMR spectrum make it difficult to determine the major orientation of D-Trp8 in the peptide.

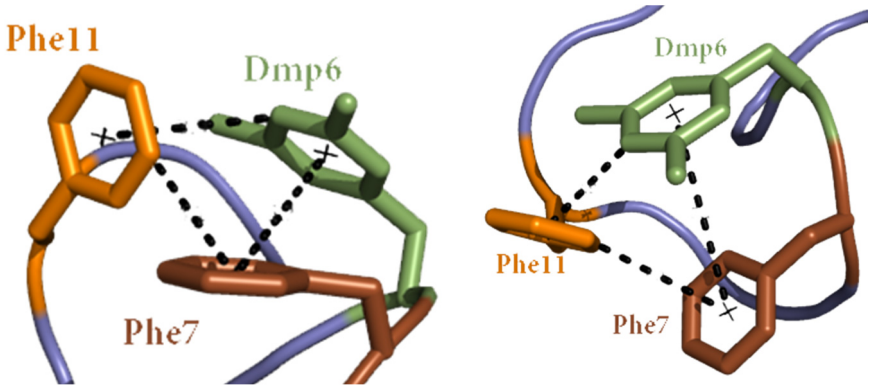

Figure 3.17. Simplified views of the cluster aromatic interaction of [L-Dmp6_D-Trp8]-SRIF (**3**) analogue. Dmp6-Phe7 show a π-π *offset-stacked* aromatic interaction and Phe7-Phe11 and Dmp6-Phe11 an *edge to face* aromatic interaction.

This cluster-type conformation was similar to the one obtained for the Msa analogue [L-Msa6_D-Trp8]-SRIF14,[4] in which the three aromatic residues were also interacting with each other.

3.4 Binding assays

To try to establish a relationship between the 3D structure and the pharmacological profile we needed to perform binding assays against all five somatostatin receptors (SSTR1-5). They were performed following the protocol designed by Rens-Domiano *et al.*[22] where the Chinese Hamster Ovarian-K1 (CHO-K1) cell line was transfected with a plasmid containing one of the SSTRs, causing the cells to overexpress the receptor. In total, five different subtype cell lines were obtained, each one expressing only one of the receptors. This cell line was chosen due to its low level of expression of constitutional membrane proteins. For the assays it was necessary to separate the membranes from the rest of the cell. Once this was achieved, a competition assay between an analogue and the radioactively labelled somatostatin, [^{125}I-Tyr11]-SRIF14, was performed by maintaining a constant concentration of the radioactive compound and the extracted membranes. The analogue to be tested was added in variable concentrations. After incubation in the

[22] S. Rens-Dominano, S. F. Law, Y. Yamada, S. Seino, G. I. Bell, T. Reisine, *Mol. Pharmacol.*, **1992**, *42*, 28 - 34.

corresponding media, the displacement of radioactively labelled SRIF14 could be observed. This displacement enabled to obtain the inhibition curves from which the Ki values could be obtained for a concrete SSTR. These assays were performed by Eurofins Scientific.[23]

During the present doctoral thesis, we have measured the binding profile of the somatostatin analogues in several occasion along these years. We have observed differences in the Ki values of the same compound and, therefore, natural somatostatin was introduced in each set of compounds as a control. Since the values found for our control varied from one set of measurements to another, a correction needed to be made to compare the results. The best option would have been doing several replicates of each sample but due to the high economic cost of each measure, it was not possible. Taking this into account, we thought that the best option would be to use the average of several measures of SRIF14 as a standard.

To obtain good average values, we used 6 measures of SRIF14 for each receptor,[24] taken on different occasions along these years. As shown in Table 3.1, values that were abnormally high or low when compared to the already published ones,[5] were excluded from the average.

Once the average value was obtained, the Ki values for all the peptides had to be normalised. To do that we used the following equation:

$$Ki\ analogue = Ki\ analogue\ (observed)\ \frac{Ki\ (average\ for\ SRIF14)}{Ki\ (observed\ for\ SRIF14)}$$

[23] Eurofins Panlabs Taiwan Ltd., 158 Lide Road Beitou, District 112, Taipei, Taiwan. www.eurofins.com

[24] These average values will also be used in the following chapters of this thesis.

	SSTR1 (nM)	**SSTR2 (nM)**	**SSTR3 (nM)**	**SSTR4 (nM)**	**SSTR5 (nM)**
Somatostatin 1	1.88	0.016	0.25	1.55	~~**0.76**~~
Somatostatin 2	2.74	0.055	0.43	2.91	2.28
Somatostatin 3	4.18	~~**0.30**~~	0.77	5.73	2.48
Somatostatin 4	2.88	~~**0.21**~~	0.99	4.18	2.00
Somatostatin 5	~~**0.75**~~	0.036	0.20	1.20	1.11
Somatostatin 6	3.68	~~**0.20**~~	~~**1.10**~~	6.94	4.64
Average	3.07	0.036	0.53	3.75	2.50

Table 3.1 Average Ki values for somatostatin. In bold and crossed out, values that were excluded from the average calculation due to abnormality.

The average value of SRIF14 for each SSTR was divided by the data obtained for the same receptor in a particular measurement giving a correction factor. That factor was then multiplied for each Ki value of the different analogues. That way, we could obtain the normalised Ki values shown in Table 3.2.[25]

$$Ki\ analogue = Ki\ analogue\ (observed) * correction\ factor$$

Binding affinity values of the three analogues from the Dmp family together with the ones for the natural SRIF14, expressed as Ki values, are shown in Table 3.2.

	SSTR1 (nM)	**SSTR2 (nM)**	**SSTR3 (nM)**	**SSTR4 (nM)**	**SSTR5 (nM)**
Somatostatin-14 (average)	3.07	0.036	0.53	3.75	2.50
[Dmp11_D-Trp8]-SRIF14 (1)	5.07	0.14	1.10	22.44	4.78
[Dmp7_D-Trp8]-SRIF14 (2)	1.81	0.094	0.36	17.86	1.98
[Dmp6_D-Trp8]-SRIF14 (3)	8.03	0.58	0.41	6.30	2.55

Table 3.2 Normalised binding selectivity values (Ki values) of Dmp somatostatin analogues against SSTR1-5. Ki values express inhibition in a competitive assay of somatostatin analogues against radio-labelled SRIF. Due to the small number of repetitions, the values are shown without their error. Raw data is shown in Chapter 9, section 9.2.4.

[25] Ki values of Table 4.1 and 6.9 have been obtained with the same normalization protocol.

On one hand, both analogues **1** and **2** show a binding affinity against SSTR1 and SSTR5 which resembles the one of the natural hormone. However, while **2** maintains its affinity for SSTR2 and SSTR3, **1** loses part of its activity against these same receptors. Moreover, both analogues are less effective when talking about SSTR4.

On the other hand, [Dmp6_D-Trp8]-SRIF14 (**3**) only loses part of its affinity for SSTR2 while the Ki values for the other four receptors are in the same order of magnitude as the natural hormone being the Ki value for SSTR3 even better than the one for SRIF14.

These results, together with the ones obtained from the NMR spectroscopy experiments, will be discussed in the following section.

3.5 Discussion

We have studied three different somatostatin analogues containing the non-natural amino acid Dmp in their sequence.

As for the analogues where Phe was substituted by Msa, the peptides presented in this chapter have reached a rigid-enough 3D structure in solution when containing the non-natural amino acid Dmp as demonstrated by the NMR spectroscopy experiments. This supports the statement that electron-rich aromatic and hydrophobic amino acids are able to restrict peptides' structure by enhancing the π-π aromatic interactions.

For analogue **1,** an interaction between Phe6 and Dmp11 has been detected through the NMR data. Contrary to what was expected, the π-π aromatic interaction took place below the peptidic backbone while residue 7 was placed at the other side of the molecule. The interaction between both aromatic residues was found to bear a *face to face* geometry. The binding profile of this analogue against the different SSTRs was shown in Table 3.1. While the affinity for SSTR1 and SSTR5 was maintained, its binding activity for SSTR2 and SSTR3 was partially lost and completely lost for SSTR4.

Analogue **2** also displayed an interaction between the Phe6 and Phe11 as it has been detected through the NMR data. Contrary to what happened for analogue **1**, the aromatic interaction took place above the peptidic backbone while Dmp7 was placed below. Furthermore, the π-π interaction was found to bear an *edge to face* spatial disposition being Phe6 the one which approaches the centre of Phe11. This conformation and spatial disposition was found to be similar to the one obtained for the Msa7 analogue.[4] In this case, the binding affinity for SSTR2 was seen to resemble that of the natural hormone as it also happened for the [Msa7_D-Trp8]-SRIF14 analogue. However, only the activity against SSTR4 was lost while the binding for SSTR1, SSTR3 and SSTR5 was maintained.

For analogue **3**, two major structures in solution were found; one with a 6-to-11 interaction and a second structure in which all three aromatic residues were interacting to form an aromatic cluster. The cluster set of conformations resembled the one obtained for the Msa6 analogue.[4] As a consequence of this duality of conformations, the binding profile of the [Dmp6_D-Trp8]-SRIF14 (**3**) analogue showed a broad range of activity, resembling the natural hormone for all the receptors with the exception of SSTR2, for which the affinity decreased. The best Ki values were obtained for SSTR3 (Table 3.1) which could be attributed to the presence of a cluster aromatic interaction as it has been seen before for the [Msa6_D-Trp8]-SRIF14 analogue.[4]

Furthermore, this duality in the structures while introducing Dmp in positon 6 could be explained by the absence of methyl groups in the ortho positions. This could make the peptide less rigid than the one containing Msa in the same position. This absence of the ortho methyl groups also enabled peptide **3** to adopt both structures in solution. It should be noted that the special disposition (*edge to face*) of the residues 6 and 11 would not be possible if Msa was placed in position 6 due to the methyl group in the para positions.

3.6 Conclusions

The introduction of the non-natural electron-rich aromatic amino acid L-3-(3',5'-dimethylphenyl)-alanine (Dmp) favours the conformational restriction of the 14-amino acid somatostatin analogues in aqueous solution. The higher electronic density coming from the inductive effect of the two methyl groups directly bonded to the aromatic ring, the higher hydrophobicity and the higher rigidity of the amino acid (compared to the natural Phe), favour the formation of π-π aromatic interactions with different geometries; *edge to face*, *offset-stacked* or *face to face*.

However, when these peptides are compared to the ones containing the electron-rich aromatic amino acid Msa, also studied in our group, Dmp makes the structures less rigid. This could be one of the causes of the lower selectivity of these analogues against SSTRs.

The substitution of the Phe6 by a more electron-rich aromatic amino acid (Dmp) favours the formation of both a cluster structure and a 6-to-11 interaction. The obtainment of a cluster interaction when the substitution was made in position 6 was also seen for the analogue containing Msa in the same position.[4] This cluster spatial disposition favoured the selectivity for SSTR3 when Msa was present which was partly achieved also in the Dmp analogue **3** (Table 3.1) as the value for that receptor is even lower than the one for the natural hormone. The duality in structures could be responsible for the lack of selectivity that this analogue has shown against all SSTRs.

Both [Dmp11_D-Trp8]-SRIF14 (**1)** and [Dmp7_D-Trp8]-SRIF14 (**2)** analogues display a binding affinity for SSTR2 that resembles SRIF14 while [Dmp6_D-Trp8]-SRIF14 (**3**) is less selective for that same receptor. Thus, the inclusion of Dmp does not imply an increased selectivity for SSTR2. However, its inclusion in positions 11 and 7 (analogues **1** and **2**) triggers a loss of selectivity for SSTR4, as happened when Msa was present in these same positions.[4]

Chapter 4

SRIF analogues with L-Msa-OH in position 6 and L-Pya-OH in position 7

4.1 Introduction

L-3-(3'-pyridyl)-alanine (L-3'Pya-OH or 3'Pya) and L-3-(4'-pyridyl)-alanine (L-4'Pya-OH or 4'Pya) are non-natural amino acid that have been widely used in the last decades in peptide analogues (Figure 4.1).[1]

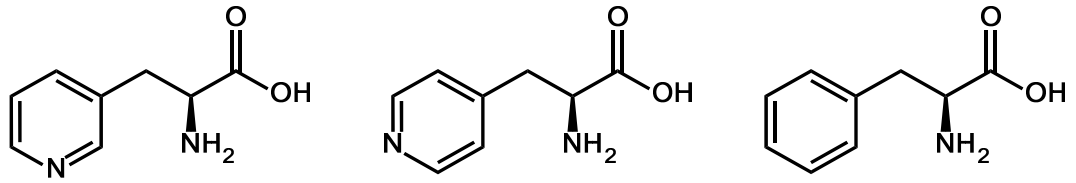

Figure 4.1. Structural comparison between L-3'Pya-OH (left), L-4'Pya-OH (centre) and L-Phe-OH (right).

Pyridylalanines are well-known antagonists of phenylalanine in the prevention of bacterial growth[2] and have been used as feedback inhibitors and in enzyme specificity studies.[2c] Moreover, these molecules are capable of inhibiting the histidine decarboxylase.[3]

Their major use is as residues in anti-ovulatory drugs through an antagonist action to the gonadotropin-releasing hormone (GnRH or Luteinizing Hormone-Releasing Hormone,

[1] a) P.J. Lea, R. D. Norris, *Phytochemistry*, **1976**, *15*, 585 - 595; b) D. C. Roberts, F. Vellaccio, *Peptides*, **1983**, *5*, 341 - 449; c) M. J. Wilson, D. L. Hatfield, *Biochim. Biophys. Acta*, **1984**, *781*, 205 - 215; d) H. Wang, Y. Byun, C. Barinka, M. Pullambhatla, H. C. Bhang, J. J. Fox, J. Lubkowski, R. C. Measem, M. G. Pomper, *Bioorg. Med. Chem. Lett.*, **2010**, *20*, 392 - 397; e) H. Xiao, F. B. Peters, P.-Y. Yang, S. Reed, J. R. Chittuluru, P. G. Schultz, *ACS Chem. Biol.*, **2014**, *9*, 1092 - 1096; f) M. Mansha, U. U. Kumari, Z. Cournia, N. Ullah, *Eur. J. Med. Chem.*, **2016**, *124*, 666 - 676; g) P. A. Mroz, D. Perez-Tilve, F. Liu, V. Gelfanov, D. DiMarchi, J. P. Mayer, *J. Med. Chem.*, **2016**, *59*, 8061 - 8067; h) K. D. Barnash, J. The, J. L. Norris-Drouin, S. H. Cholensky, B. M. Worley, F. Li, J. I. Stuckey, P. J. Brown, M. Vedadi, C. H. Arrowsmith, S. V. Frye, L. I. James, *ACS Comb. Sci.*, **2017**, *19*, 161 - 172; i) F. Gan, R. Liu, F. Wang, P. G. Schhultz, *J. Am. Chem. Soc.*, **2018**, *140*, 3829 - 3832; j) N. Canu, P. Belin, R. Thai, I. Correia, O. Lequin, J. Seguin, M. Moutiez, M. Gondry, *Angew. Chem. Int. Ed.*, **2018**, *57*, 3118 - 3122.

[2] a) C. Niemann, R. N. Lewis, J. T. Hays, *J. Am. Chem. Soc.*, **1942**, *64*, 1678 - 1682; b) D. F. Elliot, A. T. Fuller, C. R. Harrington, *J. Chem. Soc.*, **1948**, *0*, 85 - 89, ; c) E. M. Lansford Jr., W. Shive, *Arch. Biochem. Biophys.*, **1952,** *38*, 347 - 351; d) P. T. Sullivan, M. Kester, S. J. Norton, *J. Med. Chem.*, **1968**, *11*, 1172 - 1176.

[3] G. W. Chang, E. E. Snell, *Biochemistry*, **1968**, *7*, 2005 - 2012.

LHRH) where 3'Pya excels over 2'Pya and 4'Pya.[4] Other peptide analogues include antibacterial and anti-inflammatory drugs,[5] vasopressin, angiotensin II and ribonuclease analogues.[6]

L-3'Pya and L-4'Pya share some characteristics; the decreased electronic density of the aromatic ring due to the N atom when compared to L-phenylalanine which increases the hydrophilicity of the above mentioned ring (theoretical logP, hydrophobicity parameter, of 3'Pya and 4'Pya aromatic rings is 0.7 whilst logP of Phe ring is 2.03).[7] Although both Pya aromatic rings show the same logP value, the charge distribution moment is different in each case due to the different position of the N atom (Figure 4.2). This difference in the N_{AR} position creates a dissymmetry in the 3'Pya electronic density that is not present in the 4'Pya ring where Hδ are equivalent as well as both Hε.

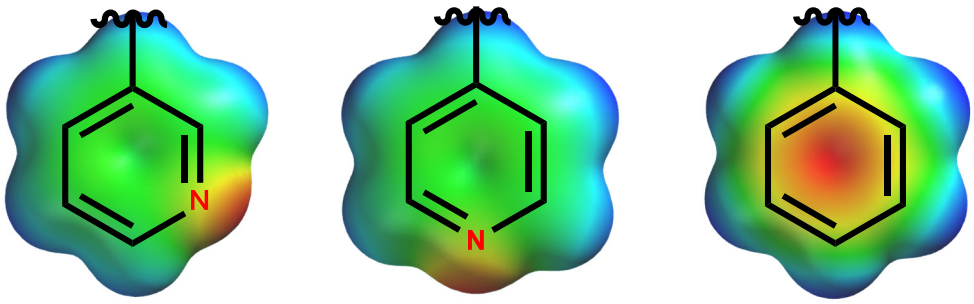

Figure 4.2. Electronic densities of the 3'Pya (left), 4'Pya (middle) and phenyl (right) rings. Spartan calculation (semi-empiric AM1).[8] Red = high electronic density; Green/Blue = low electronic density.

[4] a) K. Folkers, C. Y. Bowers, T. M. Kubiak, J. Stepinski, *Biochem. Biophys. Res. Commun.*, **1983**, *111*, 1089 - 1095; b) J. E. Rivier, J. Porter, C. L. Rivier, M. Perrin, A. Corrigan, W. A. Hook, R. P. Siraganian, W. W. Vale, *J. Med. Chem.*, **1986**, *29*, 1845 - 1851.

[5] a) Japan Patent JP 60/130591 A2, **1985**; b) European Patent EP 98609/A2, **1984**; c) H. Shimeno, S. Soeda, A. Nagamatsu, *Chem. Pharm. Bull.*, **1977**, *25*, 2983 - 2987.

[6] a) M. Sobocinska, I. Derdowska, J. Schwarts, G. Kupryszewski, *Peptides*, **1995**, *16*, 389 - 393; b) K. Heieh, E. C. Jorgensen, *J. Med. Chem.*, **1979**, *22*, 1199 - 1206; c) O. D. Van Batenburg, I. Vosluyl-Holtcamp, C. Schattenkerk, K. Hoes, K. E. T. Kerling, E. Havinga, *Biochem. J.*, **1977**, *163*, 385 - 387; d) C. Hoes, J. Flaap, W. Bloemhoff, K. E. T. Kerling, *Recl. Trau. Chim. Pays-Bas*, **1980**, *99*, 99.

[7] logP calculated with Spartan (semi-empiric calculations).

[8] Spartan '10 v 1.1.0 (Wavefunction)

These non-natural electron-poor aromatic amino acids have been previously used in our group together with Msa to explore the effect of an electron-deficient aromatic ring in the formation of π-π aromatic interactions in 14-residue somatostatin analogues. Álvaro Rol, in his doctoral thesis,[9] described that the replacement of a Phe for one of these non-natural amino acids triggers the formation of stable-enough 3D structures in solution. The geometry of the formed π-π aromatic interaction changes depending on the Phe that has been substituted by either 3'Pya or 4'Pya.

During his thesis,[9] Álvaro Rol also synthesised several analogues combining 3'Pya or 4'Pya and Msa. In these analogues, Msa was always placed in position 7 so as to assure a stronger π-π interaction between residues 6 and 11 and a more potent binding for SSTR2. From the two families of peptides synthesised with Msa in position 7, the analogue that bore a strong and marked binding affinity for SSTR2 was [L-4'Pya6_Msa7_D-Trp8]-SRIF14 (Figure 4.3, bottom) whereas the binding for the other receptors decreased.

A similar set of conformations was obtained when the electron-deficient amino acid 3'Pya was introduced in position 6; the obtained structure showed a 6-to-11 interaction with an *edge to face* (Figure 4.3, top). In both analogues Msa was placed below the peptidic backbone while the aromatic interaction was placed upwards. However, when 3'Pya or 4'Pya replaced the phenylalanine in position 7, an aromatic cluster was obtained with different geometries for the interaction between the three aromatic rings.

In light of these findings, we thought that it could be interesting to study the effects of introducing Msa in position 6 instead of in position 7, as previously done in our group, in combination with the introduction of either 3'Pya or 4'Pya in position 7. Our aim was to check if Msa in position 6 caused the same stabilisation than when being introduced in position 7. Its three methyl groups help in the stabilisation of the peptide through direct and indirect aromatic interactions which lead to more constrained conformations.

[9] A. Rol Rúa, doctoral thesis *Análogos de somatostatina y cortistatina. Efectos de las interacciones aromáticas en sus estructuras y en la actividad biológica.* Universitat de Barcelona, 2015.

Moreover, the density of signals of its nine methyl protons together with the highly shielded Hε nourish the spectra with a higher volume of NOE signals. When introduced in the computational program, all this new experimental information may be determinant in the obtainment of a major conformation in solution.

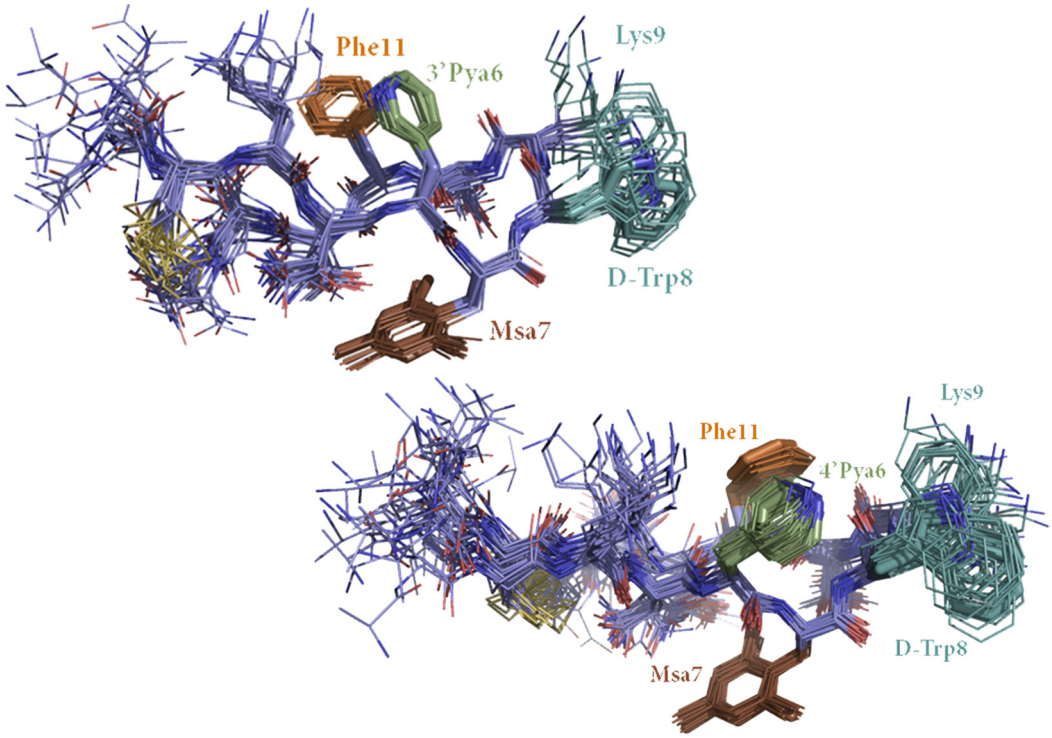

Figure 4.3. Superimposition of the 25 lower energy structures of [L-3'Pya6_Msa7_D-Trp8]-SRIF (top) and [L-4'Pya6_Msa7_D-Trp8]-SRIF (bottom) which are in agreement with experimental NMR data for a 6-to-11 interaction.[9]

4.2 Synthesis of SRIF14 analogues with L-Msa-OH and an L-Pya-OH in position 7

To study the effects on the aromatic interactions of introducing a non-natural electron-poor aromatic amino acid in position 7 in combination with the introduction of Msa (an electron rich aromatic amino acid) in position 6 of the natural SRIF14 structure, we synthesised two new peptides; one containing L-3'Pya-OH in position 7 and the other with L-4'Pya-OH in the same position. These analogues have been synthesised by substituting the aromatic residue Phe7 for one of the two electron-deficient non-natural amino acids and Phe6 for Msa (Figure 4.4). D-Trp has been maintained as a fixed

substitution in position 8 in both analogues as it is known to enhance the biological activity by increasing the half-life and it also contributes directly in the stabilization of the β-turn.[10]

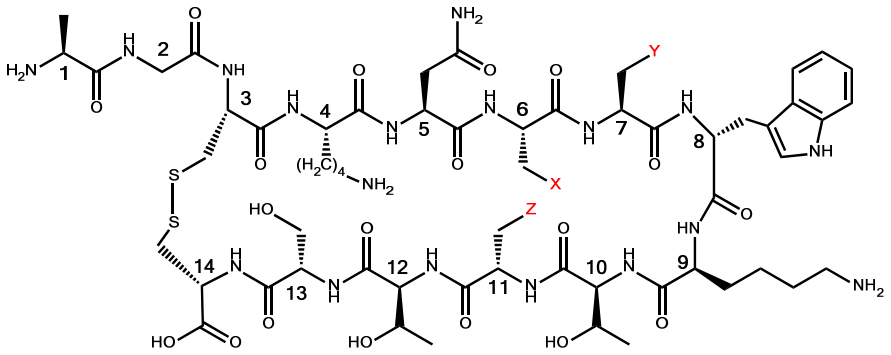

	6	7	8	11
[Msa6_L-4'Pya7_D-Trp8]-SRIF14 (4)	Msa	4'Pya	D-Trp	Phe
[Msa6_L-3'Pya7_D-Trp8]-SRIF14 (5)	Msa	3'Pya	D-Trp	Phe

Figure 4.4. Somatostatin derivatives containing 3'Pya and 4'Pya in position 7 and Msa in positon 6 that will be presented in this chapter.

Fmoc-L-Msa-OH was synthesised following the asymmetric synthesis protocol previously developed in our group (Figure 4.5).[11]

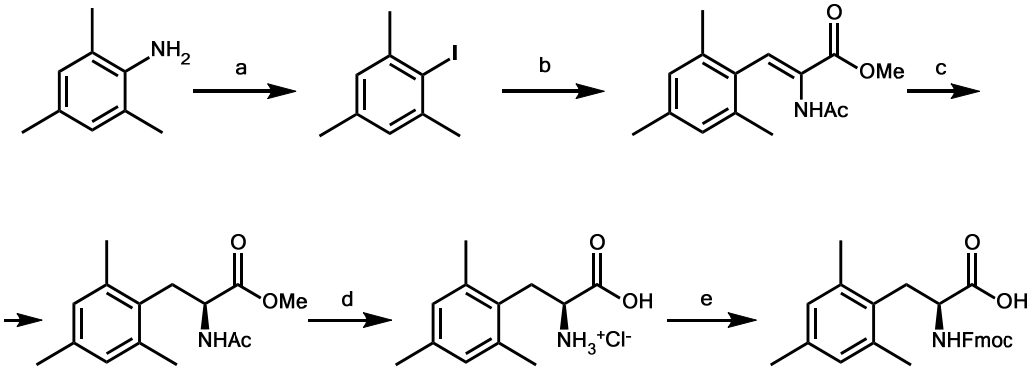

Figure 4.5. Synthesis of Fmoc-L-Msa-OH. a) HCl aq, $NaNO_2$, KI, 0°C, 18h; b) *N*-Ac-dehydro-Ala-OMe, tri-(o-tolyl)phosphine, $Pd(OAc)_2$, Et_3N, 100°C, 10h; c) MaxPHOS-Rh cat 3%, H_2 (50 bar), MeOH, 24h, rt; d) HCl aq, reflux, 6h; e) Fmoc-OSu, Na_2CO_3, H_2O, acetone, 0°C to rt, 24h.

[10] a) B. H. Arison, R. Hirschmann, D. F. Veber, *Bioorg. Chem.*, **1978**, *7*, 447 - 451; b) O. Ovadia, S. Greenberg, B. Laufer, C. Gilon, A. Hoffman, H. Kessler, *Expert Opin. Drug Discov.*, **2010**, *5*, 655 - 671.

[11] R. Ramón, M. Alonso, A. Riera, *Tetrahedron: Asymmetry*, **2007**, *18*, 2797 - 2802.

As depicted in Figure 4.5, the first step for the synthesis of the final chiral amino acid was the obtainment of the 2-iodo-1,3,5-trimethylbenzene through a diazonium salt. The iodinated compound was achieved with a 60% yield. The subsequent step of the synthesis was the Heck reaction to obtain the dehydroamino acid which took place in 81% yield using a similar procedure as the one described by Dr. Martin-Gago.[12] The dehydroamino acid was then asymmetrically reduced using a 3% MaxPHOS catalyst loading. The reaction reached full conversion and the desired product was achieved with a 77% yield and an enantiomeric excess greater than 99%, calculated by HPLC (Scheme 4.1).

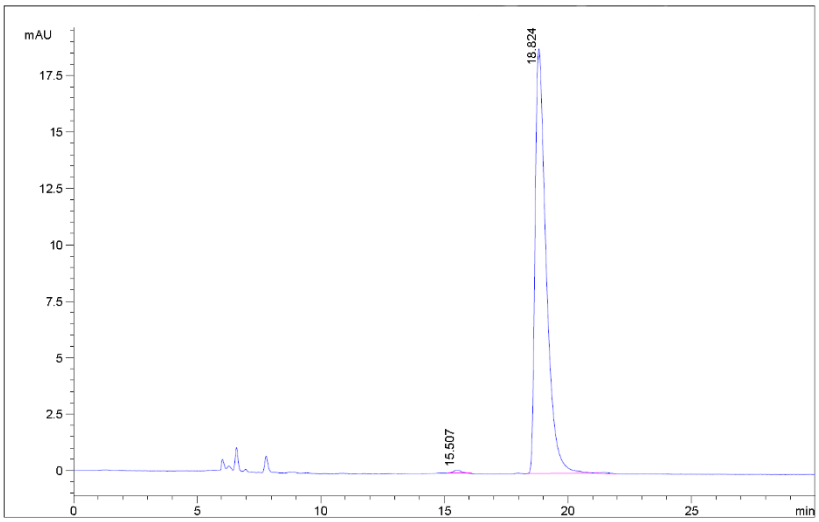

Peak	t_R	Width	Area	Height	Area (%)
1	15.507	0.420	3.226	0.128	0.542
2	18.824	0.520	586.783	18.821	98.539

Scheme 4.1. Analytical HPLC after the asymmetric hydrogenation reaction. Conditions used: Heptane/IPA (90:10), T = 25 ºC, flow rate = 0.5 mL/min, column: Chiralpak IA, stop time = 30 min.

Once the chirality was introduced, a hydrolysis was performed to obtain the free amino acid itself as a chlorine salt and then the Fmoc protection of the amino moiety was performed. Both reactions reached full conversion and the obtained yields were brilliant,

[12] P. A. Martín-Gago, doctoral thesis *Synthesis of highly structured and receptor-selective tetradecapeptidic analogs of somatostatin: Fine tuning the non-covalent interactions among their aromatic residues*, Univeristat de Barecelona, 2013.

(>99% for the hydrolysis and >90% for the Fmoc protection). The enantiomeric excess obtained through the asymmetric hydrogenation was maintained until the obtainment of the final Fmoc-L-Msa-OH. The rest of amino acids, including Fmoc-D-Trp(Boc)-OH, were commercially available from different suppliers.

Both peptides presented in this chapter (**4** and **5**) were synthesised by solid phase peptide synthesis (SPPS) following the well-known Fmoc/^{t}Bu strategy using a 2-chlorotrytyl chloride resin. The synthesis of [Msa6_L-4'Pya7_D-Trp8]-SRIF14 (**4**) is shown as a general example in Scheme 4.2.

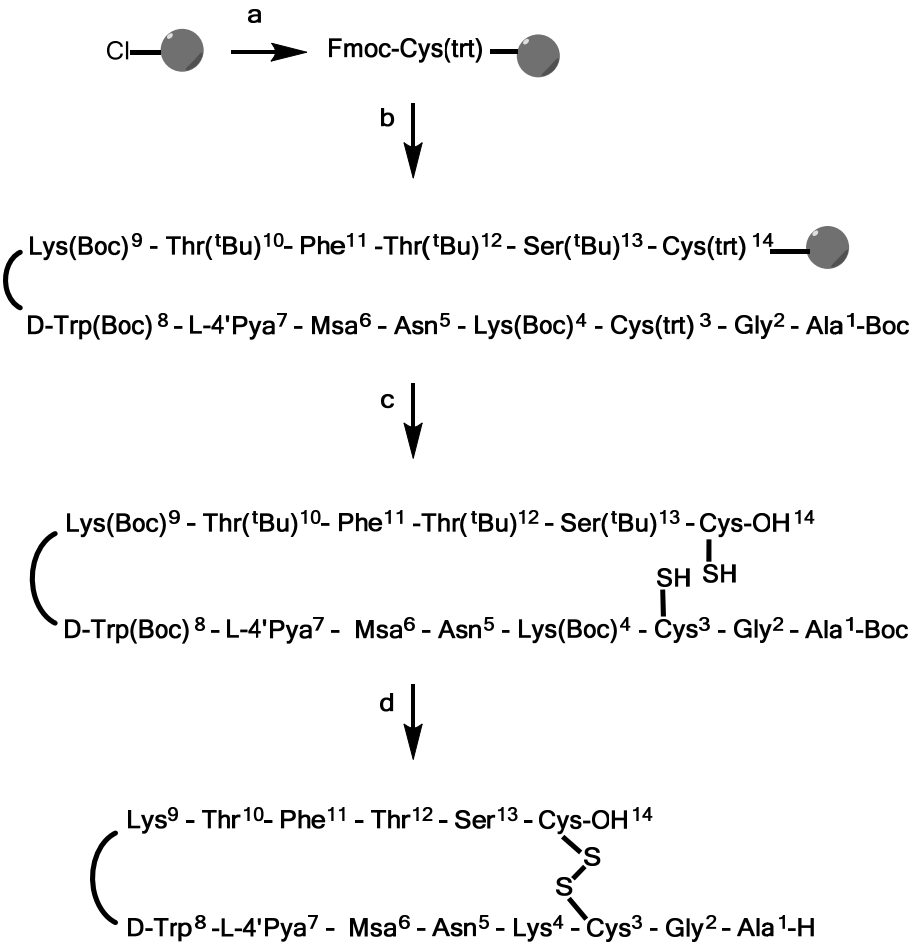

Scheme 4.2. SPPS of [Msa6_L-4'Pya7_D-Trp8]-SRIF14 (**4**). a) 1. Fmoc-Cys(trt)-OH (3eq), DIEA (3eq), 2. MeOH; b) 1. Piperidine 20% in DMF, 2. Fmoc-AA-OH (1.5-3eq), DIPCIDI (3eq), HOBt (3eq), DMF; 3. Piperidine 20% in DMF, 4. Boc-Ala-OH (3eq), DIPCIDI (3eq), HOBt (3eq), DMF, c) DCM/TFE/AcOH, d) 1. I_2, 2. TFA/DCM/anisole/H_2O.

During the synthesis of the analogue [Msa6_L-3'Pya7_D-Trp8]-SRIF14 (**5**), the coupling of Fmoc-Asn-OH in position 5 was problematic; for that reason a recoupling with HATU (stronger coupling reagent) was necessary. This difficulty was also encountered during the synthesis of [L-Dmp11_D-Trp8]-SRIF14 (**3**) and observed previously by Hirschmann[13] during the synthesis of [L-Pyz11_D-Trp8]-SRIF14.

4.3 Structure determination

The two analogues, with a TFA^- counter ion, synthesised in this chapter were analysed by NMR in phosphate buffer at pH = 6.5 and both bidimensional homonuclear ^1H-^1H TOCSY and ^1H-^1H NOESY were obtained. The followed process was the one described in chapter 3.3 of the present doctoral thesis. After identifying all the NOE signals,[14] peaks were integrated and the volumes introduced in the CNS program[15] using the StructCalc platform.[16] A variable number of calculations were set up until the lower energy structures were convergent, coherent with the experimental values and the dihedral angles did not violate the Ramachandran diagrams.[17] In both cases a major 3D set of structures in solution could be obtained.

4.3.1 Structure of [Msa6_L-4'Pya7_D-Trp8]-SRIF1 (4)

The NMR data of [Msa6_L-4'Pya7_D-Trp8]-SRIF14 analogue (**4**) clearly showed that it was more rigid than the natural SRIF in solution due to the high density of NOE signals. Even though there was some conformational variability of the extra cyclic side chains, the major set of conformations in solution could be elucidated with high convergence of the

[13] S. Neelamkavil, B. Arison, E. Birzin, J. Feng, K. Chen, A. Lin, F. Cheng, L. Taylor, E. R. Thornton, A. B. Smith III, R. Hirschmann, *J. Med. Chem.*, **2005**, *48*, 4025 - 4030.

[14] K. Wuethrich, G. Wider, G. Wagner, W. Braun, *J. Mol. Biol.*, **1982**, *155*, 311 - 319.

[15] A. T. Brunger, P. D. Adams, G. M. Clore, W. L. DeLano, P. Gros, R. W. Grosse-Kunstleve, J. S. Jiang, J. Kuszewski, M. Nilges, N. S. Pannu, R. J. Read, L. M. Rice, T. Simonson, G. L. Warren, *Acta Crystallogr. D Biol. Crystallogr.*, **1998**, *54*, 905 - 921.

[16] P. Martín-Malpartida, M. J. Macias, unpublished data.

[17] G. N. Ramachandran, C. Ramakrishnan, V. Sasisekharan, *J. Mol. Biol.*, **1963**, *7*, 95 - 99.

peptidic backbone and intracyclic side chains. As Figure 4.6 shows, there was a π-π aromatic interaction between Msa6 and Phe11 while 4'Pya7 was placed at the other side of the molecule. As for **2** and one of the conformations of **3**, the aromatic interaction took place above the peptidic backbone while residue 7 was placed below. The geometry of the 6-to-11 interaction was different from the ones observed until now; an *offset-stacked* geometry which was not completely flat due the a close spatial proximity between Hβ of Phe11 and one of the methyl groups of Msa6. At the same time, 4'Pya7 did not take part in the aromatic interaction and was placed underneath the backbone of the molecule with an oposite orientation than the Msa6_Phe11 pair.

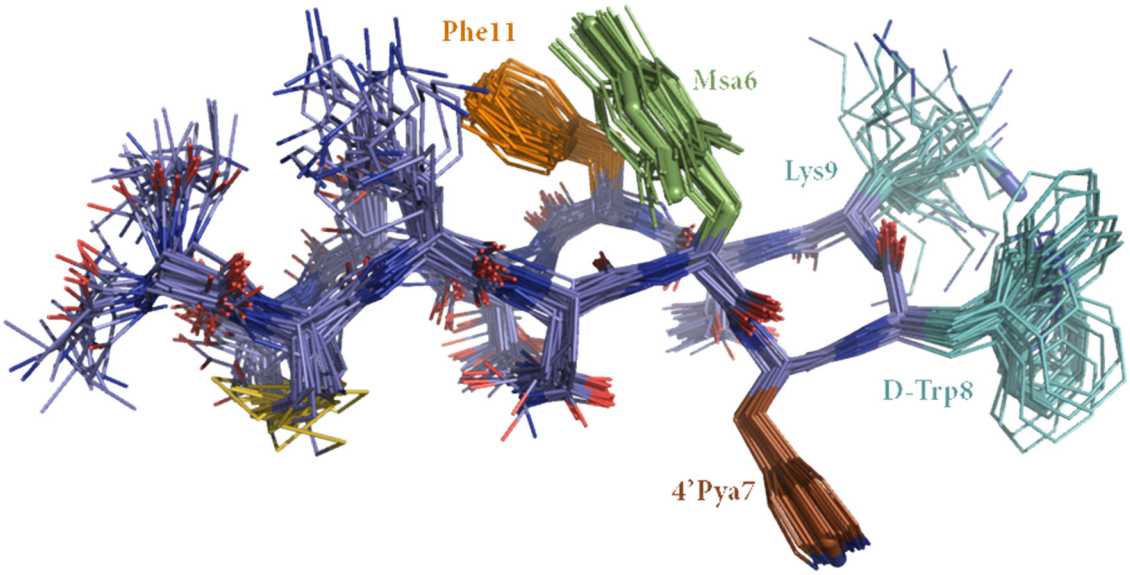

Figure 4.6. Superimposition of the 30 lower energy structures of [Msa6_4'Pya7_D-Trp8]-SRIF (**4**) which are in agreement with experimental NMR data for a 6-to-11 interaction.

This orientation was supported by some long-distance NOE signals: interaction of Hβ of 4'Pya7 with Hδ of Asn5, Hδ of 4'Pya7 with Hγ of Thr12 and Hε of 4'Pya7 with HN of Thr10. Furthermore, the D-Trp8_Lys9 pair shows high denisity of NOE signals between them which is translated in a closer proximity in space. As a consequence of the little volume of NOE signals between that pair and the rest of the molecule D-Trp8_Lys9 face the outside of the peptidic backbone.

4.3.2 Structure of [Msa6_L-3'Pya7_D-Trp8]-SRIF14 (5)

The NMR data of [Msa6_L-3'Pya7_D-Trp8]-SRIF14 analogue (**5**) clearly showed that it was more rigid than the natural SRIF in solution due to the high density of NOE signals. Even though there were sufficient NOE peaks in the ^{1}H-^{1}H NOESY spectra to determine that the peptide should have a defined structure in solution, we could not obtain a convergent conformation through computational studies.

The impossibility of the calculated structures to converge may be attributed to the existence of more than one major conformation in solution. Peaks corresponding to both conformations were observed which may have driven the calculations into a more complicated scenario. This duality of major conformations is, normally, translated into a higher volume of NOE peaks which can lead to some confusion between both structures. For that reason, it was impossible to obtain a definite 3D structure.

4.4 Binding assays

As previously described for the Dmp peptide family, the binding activity against all five somatostatin receptors (SSTR1-5) for these two new analogues was measured. They were performed following the protocol designed by Rens-Domiano *et al.*[18] as previously mentioned. Using isolated CHO-K1 cell membranes overexpressing the five different SSTRs, the Ki value for each analogue was determined by a competition assay against radio-labelled [^{125}I-Tyr11]-SRIF14 which had previously been incubated with each receptor. These assays were performed externally by Eurofins Scientific.[19] As it happened with the binding assays of the Dmp family, the raw data obtained for these two SRIF14 analogues containing 3'Pya and 4'Pya had to be normalised.[20] Binding affinity values of

[18] S. Rens-Dominano, S. F. Law, Y. Yamada, S. Seino, G. I. Bell, T. Reisine, *Mol. Pharmacol.*, **1992**, *42*, 28 - 34.

[19] Eurofins Panlabs Taiwan Ltd., 158 Lide Road Beitou, District 112, Taipei, Taiwan. www.eurofins.com

[20] Ki values have been normalised using the protocol described in Chapter 3.4. Ki values of Table 3.2 and 6.9 have been obtained with the same normalization protocol.

the two analogues from the Pya family together with the ones for the natural SRIF14, expressed as Ki values, are shown in Table 4.1.

	SSTR1 (nM)	**SSTR2 (nM)**	**SSTR3 (nM)**	**SSTR4 (nM)**	**SSTR5 (nM)**
Somatostatin-14	3.07	0.036	0.53	3.75	2.50
[Msa6_4'Pya7_D-Trp8]-SRIF14 (4)	34.13	0.74	2.59	13.28	4.35
[Msa6_3'Pya7_D-Trp8]-SRIF14 (5)	74.14	12.52	2.24	8.07	6.09

Table 4.1. Normalised binding selectivity values (Ki values) of 3'Pya and 4'Pya somatostatin analogues against SSTR1-5. Ki values express inhibition in a competitive assay of somatostatin analogues against radio-labelled SRIF. Due to the small number of repetitions, the values are shown without their error. Raw data is shown in Chapter 9, Section 9.2.4.

Normalised data illustrates that both analogues **4** and **5** show a binding affinity against SSTR5 which resembles the one of the natural hormone for the same receptor while the activity against the other receptors decreases significantly. The only exception is the binding affinity that compound **5** displays for SSTR4, which also resembles SRIF14.

4.5 Discussion

As it happened when Phe7 was substituted by Msa, one of the peptides presented in this chapter (**4**) has reached a rigid-enough 3D structure in solution when containing the non-natural amino acid 4'Pya. This supports the statement that not only the electron-rich aromatic amino acids are able to restrict peptides' structure by enhancing the π-π aromatic interactions but the electron-poor aromatic amino acids too. Furthermore, the enhanced hydrophilicity of the both 3'Pya and 4'Pya aromatic ring would lead to a decrease in the π-π aromatic interactions but this effect would be counteracted by the higher number of aromatic interactions created by the different distribution of the electronic density within the aromatic ring of Pya when compared to Phe.

NMR spectra of analogue **4** displayed a marked interaction between residues 6 and 11. After performing structure calculations, we were able to confirm the existence of this

interaction and determine its geometry; an *offset-stacked*. Contrary to what happened when introducing Dmp in position seven, 4'Pya7 oriented itself to the D-Trp8_Lys9 pair and not to the π-π aromatic interaction that was occurring between the aromatic rings of Msa6 and Phe11. When comparing analogue **4** with peptides previously synthesised in our group,[9,21] which included L-4'Pya or Msa together with D-Trp in position 8, the structure, the interaction and the geometry obtained for the aromatic interaction was completely different. Whilst [Msa6_D-Trp8]-SRIF14 displayed a cluster interaction between all three aromatic rings, **4** held a 6-to-11 π-π aromatic interaction with an *offset-stacked* geometry. However, the major conformation obtained for analogue **4** was seen to be similar to that obtained for the [4'Pya7_D-Trp8]-SRIF14 analogue in which the aromatic interaction also took place between residues 6 and 11 but with the geometry being *edge to face*.

Even though the ^{1}H-^{1}H TOCSY and ^{1}H-^{1}H NOESY spectra of peptide **5** indicated that the peptide should display a rigid-enough conformation in solution (the spectra showed high volume of NOE peaks), we were not able to disclose its major set of 3D conformations by structure calculations and further analysis of the NOE signals. We suggest that this difficulty in the obtainment of the major structure could be due to the existence of at least two major stable conformations (6-to-11 type interaction and cluster-type interaction). This hypothesis was then verified by long and medium-distance NOE interactions.[22] At that point, one possible solution to this problem could be performing the NMR experiments again but at lower temperatures so that the peptide would be less prone to the exchange between both major conformations. However, by lowering the temperature the shift of the equilibrium to one concrete set of conformations is not guaranteed.

[21] P. Martín-Gago, M. Gómez-Caminals, R. Ramón, X. Verdaguer, P. Martín-Malpartida, E. Aragón, J. Fernández-Carneado, B. Ponsati, P. López-Ruiz, M. A. Cortés, B. Colás, M. J. Macias, A. Riera Angew. Chem. Int. Ed., **2012**, *51*, 1820 –1825.

[22] Long-distance NOE for a cluster-type interaction: Hβ of Phe11 with Hε of 3'Pya7, Hδ of Phe11 with Hε of 3'Pya7 and Hφ of Msa6 and Hδ of 3'Pya7 with Hφ of Msa6 and Hζ Phe11. Long-distance NOE for a 6-to-11 type interaction: Hε of Msa6 with Hδ, Hζ and Hε of Phe11, Hδ of Phe11 with Hφ and Hη of Msa6 and Hδ of Asn5 with Hβ of 3'Pya7.

Both analogues **4** and **5**, displayed lower binding affinity for receptors SSTR1, SSTR2 and SSTR3 when compared to natural SRIF14 but the activity was maintained for the receptor five as shown in Table 4.1. The only difference between both analogues was the affinity for receptor four; while the analogue with 4'Pya in position 7 (**4**) lost its activity for that receptor becoming a selective analogue for SSTR5, the analogue with 3'Pya in the same position (**5**), maintained its binding affinity for SSTR4 thus being a selective analogue for both SSTR4 and SSTR5. With these results in hand, we could hypothesise that the analogue **5** should have a similar set of major conformations in solution than analogue **4** as the pharmacological profiles are similar in terms of potency and binding activity. However, this hypothesis should be validated by further 2D NMR experiments and structure calculations.

4.6 Conclusions

We have studied two different somatostatin analogues containing the non-natural amino acids L-4'Pya and L-3'Pya in combination with L-β-3'-mesitylalanine (Msa) in its sequence and we have been able to verify that the introduction of these non-natural electron-poor amino acids favour a conformational restriction of the 14-amino acid somatostatin analogues in aqueous solution. Although the enhanced hydrophilicity of the Pya rings lead to a decrease in the π-π aromatic interactions, the difference in the electronic density distribution when compared to Phe counteracts that decrease, leading to highly structured analogues.

The analogue [Msa6_4'Pya7_D-Trp8]-SRIF14 (**4)** displayed a rigid-enough 3D set of conformations in which the π-π aromatic interaction took place between residues 6 and 11 which are interacting trough an *offset-stacked* geometry. Even though we have not been able to elucidate the structure of analogue **5** due to the duality between 6-to-11 and cluster conformations, we have verified that the introduction of an electron-deficient aromatic amino acid gives the peptides a sufficient rigidity to characterise them by NMR spectroscopy as seen for analogue **4**.

However, when these peptides are compared to the ones which only contain one modification (a part from D-Trp in position 8) the aromatic interaction geometry change thus obtaining a *offset-stacked* 6-to-11 interaction but with residue 7 facing the D-Trp8_Lys9 pair and not the one composed by Msa6_Phe11.

Both [Msa6_4'Pya7_D-Trp8]-SRIF14 (**4)** and [Msa6_3'Pya7_D-Trp8]-SRIF14 (**5)** analogues display a high binding affinity for SSTR5 that resembles SRIF14 being analogue **4** quite selective for that particular receptor. Furthermore, [Msa6_3'Pya7_D-Trp8]-SRIF14 (**5)** also bore a good binding affinity for SSTR4 which could be due to the hypothesised duality in structures that has been observed through the NMR experiments.

Chapter 5

SRIF analogues with L-Qla-OH

5.1 Introduction

L-3-(3'-quinolyl)-alanine, L-Qla-OH or Qla (L enantiomer unless otherwise specified) and its enantiomer D-3-(3'-quinolyl)-alanine (D-Qla-OH or D-Qla) are a non-natural aromatic amino acids which belongs to the derivatives of phenylalanine. In peptide analogues, they can be used to substitute either Phe or Trp. However, our aim was to introduce them instead of Trp8 on somatostatin analogues to elucidate their role in the stabilisation of a set of major conformations in solution and to depict the effect of the N-H bond in the interaction with the SSTRs (Figure 5.1).

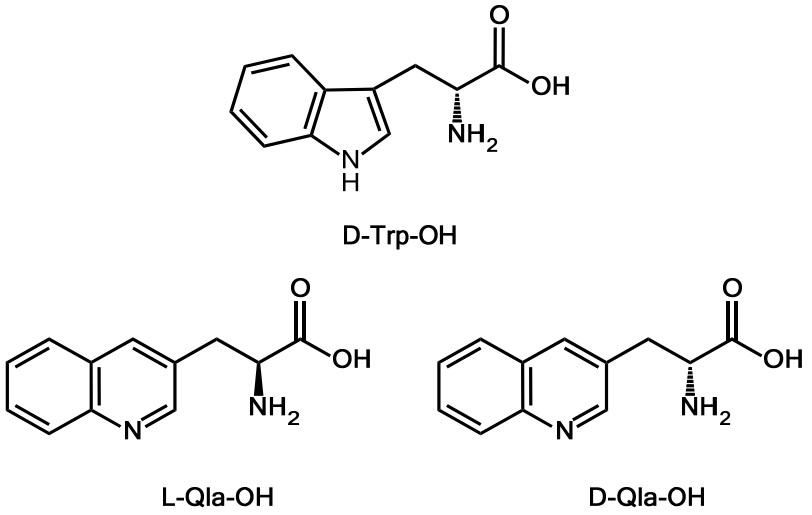

Figure 5.1. Structural comparison between D-Trp-OH (top), L-Qla-OH (bottom, left) and D-Qla-OH (bottom, right).

The relevance of Trp to the biological activity of natural SRIF and SRIF14 analogues is not yet well understood even though some attempts to clarify its role have been performed.[1] Coy and co-workers concluded that the N-H bond of the indole ring plays a crucial role in the biological activity by measuring gastric acid and pepsin inhibitory activities of different analogues that bore modifications in the Trp8 residue.[2] Despite all the experiments performed, the impact of the electronic effects in the obtainment of a

[1] C. A. Meyers, D. H. Coy, W. Y. Huang, A. V. Schally, T. W. Redding, *Biochemistry*, **1978**, *17*, 2326 - 2331.

[2] B.H. Hirst, B. Shaw, C. A. Meyers, D. H. Coy, *Regul. Pept.*, **1980**, *1*, 97 - 113.

rigid-enough 3D structure is still under study and the effect of having an electron-deficient heterocycle remains unclear.[3] Previous studies in our group enabled us to deepen our knowledge in the effect of substituting L/D-Trp by an electron-deficient non-natural amino acid. L/D-Qla was chosen as a possible substituent for L/D-Trp due to the similarity in shape but the opposed electronic properties and lack of the N-H bond present in the indole ring (Figure 5.2). This bond is believed to be essential for the biological activity of the molecule due to either its binding to the receptors or its implication in the formation of a biologically active conformation.[2]

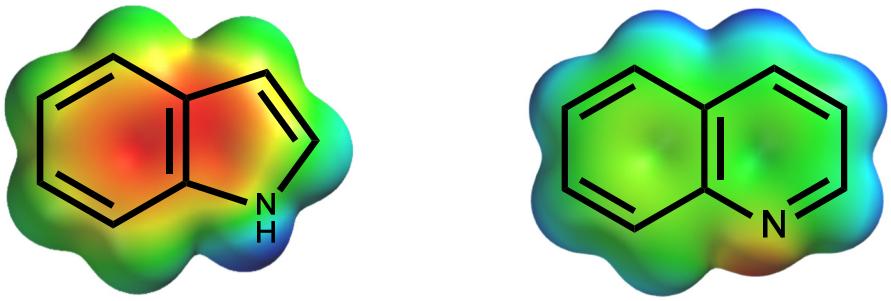

Figure 5.2. Electronic densities of the tryptophan (left) and quinolyl (right) rings. Spartan calculation (semi-empiric AM1).[4] Red = high electronic density; Green/Blue = low electronic density.

Ramón *et al.*[5] synthesised both [L-Qla8]-SRIF14 and [D-Qla8]-SRIF14 to elucidate the role of the amino acid in position 8 in both conformation stabilisation and receptor recognition. When homonuclear ^{1}H-^{1}H TOCSY and NOESY NMR experiments were acquired and analysed, none of the Qla analogues were rigid enough to adopt a preferred 3D conformation in solution. However, the binding was very interesting as both analogues showed good binding affinity for SSTR3 while the biological activity for SSTR2 was completely lost. Furthermore, [L-Qla8]-SRIF14 also showed a good binding affinity for SSTR1.

[3] V. Prasad, E. T. Birzin, C. T. McVaugh, R. D. van Rijn, S. P. Rohrer, G. Chicchi, D. J. Underwood, E. R. Thornton, A. B. Smith III, R. Hirschmann, *J. Med. Chem.*, **2003**, *46*, 1858 - 1869.

[4] Spartan '10 v 1.1.0 (Wavefunction)

[5] R. Ramón, P. Martín-Gago, X. Verdaguer, M. J. Macias, P. Martin-Malpartida, J. Fernández-Carneado, M. Gomez-Caminals, B. Ponsati, P. López-Ruiz, M. A. Cortés, B. Colás, A. Riera, *ChemBioChem*, **2011**, *12*, 625 - 632.

Contrary to what was seen in the NMR spectra for these two Qla-containing somatostatin analogues, the NMR of the natural hormone showed many contacts involving different side chains which helped in the stabilisation of the β-turn; Trp8_Lys9 pair displayed a high number of NOE signals and interactions between the aromatic residues in position 6 and 11 with Trp8 were also detected. Furthermore, NOE signals between both Phe6 and Phe11 with Lys9 side chain were stronger in SRIF14 than in both Qla analogues were these signals were weak ([L-Qla8]-SRIF14) or inexistent ([D-Qla8]-SRIF14).

In addition to this, NH-NH and Hα-HN contacts were detected across the turn in the natural hormone spectra while they were inexistent in both Qla analogues. Taking these results into account, the idea that Qla analogues will not induct the formation of a rigid-enough conformation gained acceptance and it was further supported by the lack of medium- and long-distance NOE signals between L/D-Qla and Lys9 side chains.

Knowing the importance of Msa in the obtainment of stable conformations in solution due to its particular steric and electronic properties[6] we thought that introducing it in position 7 together with Qla in position 8 could be a worth-to-try combination to finally obtain a viable and rigid-enough structure of a peptide containing Qla. Moreover, the introduction of an electron-poor aromatic amino acid could also trigger the formation of π-π aromatic interactions which could lead to the formation of a major 3D structure in solution. For that reason, the introduction of the non-natural 3'Pya and 4'Pya in positon 11 in combination with Qla8 will be also studied in this chapter.

Our aim was to understand the importance of both electronic and steric effects as well as the role of the N-H bond in the binding affinity of SRIF14 analogues against the different SSTRs.

[6] Its ring size is bigger as a consequence of the three methyl groups which is translated into a more steric hindrance in the amino acid surroundings. Furthermore, the electron-donor character of these methyl groups transform the aromatic ring in an electron rich one when compared to the natural Phenylalanine. This effect is thought to potentiate the aromatic interactions between the aromatic residues Phe6, Phe7 and/or Phe11.

5.2 Synthesis of the non-natural amino acid L-Qla-OH

The racemic synthesis of Qla-OH has been described previously[7] as well as its enzymatic resolution.[8] However, we aimed to perform the synthesis in an enantiomerically pure pathway. As previously mentioned, our group has remarkable knowledge in asymmetric synthesis so we designed a strategy to synthesise Fmoc-L-Qla-OH by asymmetric hydrogenation using Rh-MaxPHOS.[9] For that reason a retrosynthetic analysis was performed (Scheme 5.1), the key step being the obtainment of the achiral dehydroamino acid (as for the Dmp synthesis), to obtain the non-natural amino acid Fmoc-L-Qla-OH.

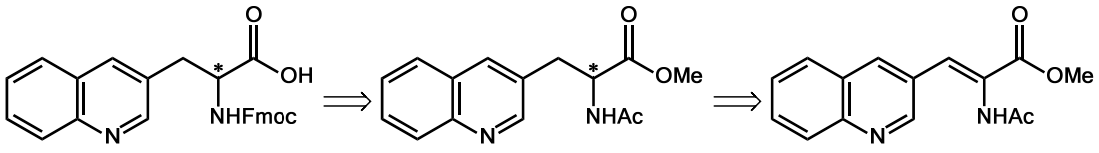

Scheme 5.1. Retrosynthetic analysis for the obtainment of the chiral Fmoc-L-Qla-OH starting from the achiral dehydroamino acid.

The L enantiomer was synthesised following two different synthetic methodologies (Figure 5.3). The first one consisted in the synthetic route previously described[10] but with the modifications developed in our group by Martín-Gago in his doctoral thesis.[11] The second synthetic protocol used was the asymmetric protocol fully developed and

[7] D. E. Levy, F. Lapierre, W. Liang, W. Ye, C. W. Lange, X. Li, D. Grobelny, M. Casabonne, D. Tyrrell, K.Holme, A. Nadzan, R. E. Galardy, *J. Med. Chem.*, **1998**, *41*, 199 - 223.

[8] a) S. A. Thomas, T. Li, K. W. Woods, X. Song, G. Packard, J. P. Fischer, R. B. Diebold, X. Liu, Y. Shi, V. Klinghofer, E. F. Johnson, J. J. Boudka, A. Olson, R. Guan, S. R. Magnone, K. Marsh, Y. Luo, S. H. Rosenber, V. L. Giranda, Q. Li, *Bioorg. Med. Chem. Lett.*, **2006**, *16*, 3740 - 3744; b) E. Dyer, W. Yokayama, *J. Org. Chem.*, **1961**, *26*, 2124 - 2125; c) U. Jacoby, F. Zymalkowski, *Arch. Pharm. Ber. Dtsch. Phrm. Ges.*, **1971**, *304*, 271 - 277.

[9] a) M. Revés, C. Ferrer, T. León, S. Doran, P. Etayo, A. Vidal-Ferran, A. Riera, X. Verdaguer, *Angew. Chem. Int. Ed.*, **2010**, *49*, 9452 - 9455; b) E. Cristóbal-Lecina, P. Etayo, S. Doran, M. Revés, P. Martín-Gago, A. Grabulosa, A. R. Costantino, A. Vidal-Ferran, A. Riera, X. Verdaguer, *Adv. Synth. Catal.*, **2014**, *356*, 795 - 804.

[10] T. Li, Y. Tsuda, K. Minoura, Y. In, T. Ishida, L. H. Lazarus, Y. Okada, *Chem. Pharm. Bull.*, **2006**, *54*, 873 - 877.

[11] P. A. Martín-Gago, doctoral thesis *Synthesis of highly structured and receptor-selective tetradecapeptidic analogs of somatostatin: Fine tuning the non-covalent interactions among their aromatic residues*, Univeristat de Barecelona, 2013.

described in our group by Rosario Ramón in her doctoral thesis.[12] Although the Fmoc-Qla-OH had been previously synthesised in our group, we have encountered several problems through its synthesis following Route 1. The azalactone formation took place without major problems and with a 73% yield. However, the first difficulty we had to face was the azalactone ring opening. For that particular step, we obtained low yields (≤ 33%) without being able to detect other organic products by NMR. After some attempts to elucidate the possible cause of the problem without success, we decided to perform the reaction in anhydrous conditions and generating the MeONa *in situ* to avoid problems coming from the starting materials.

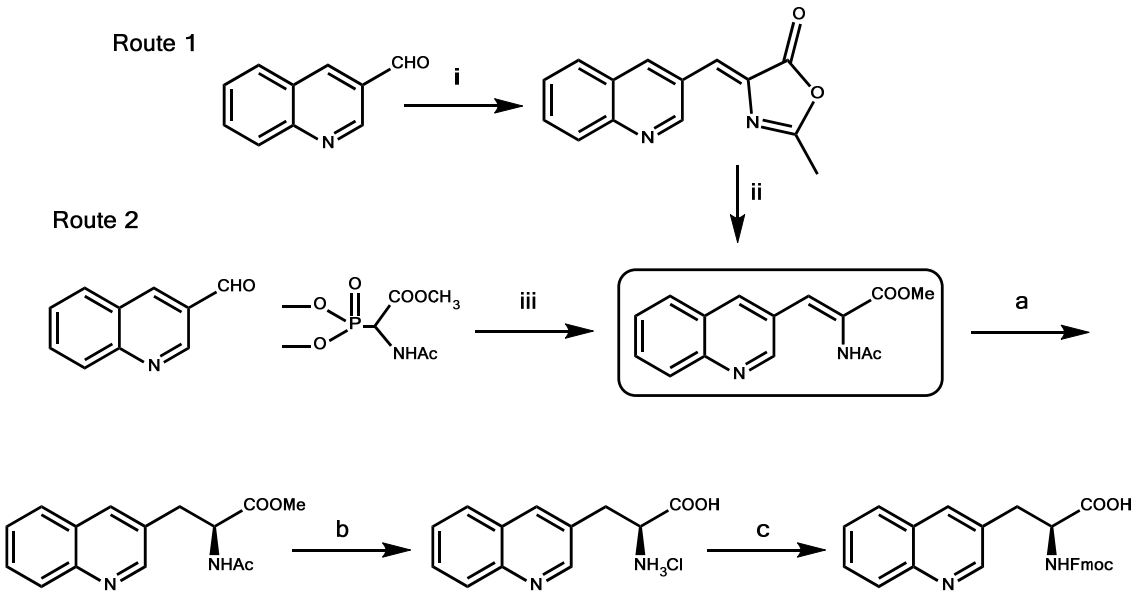

Figure 5.3. Synthesis of Fmoc-L-Qla-OH. **Route 1** through an azalactone intermediate: i) N-Ac-Gly-OH, AcONa, Ac_2O, 85°C, 24h; ii) MeONa, MeOH, 70°C, 16h. **Route 2** through a Horner-Wadswoth-Emmons reaction: iii) DBU, anhydrous CH_2Cl_2, rt, 3.5h. a) MaxPHOS-Rh cat 3%, H_2 (10 bar), MeOH, 24h, rt; b) HCl aq, reflux, 6h; c) Fmoc-OSu, Na_2CO_3, H_2O, dioxane, 0°C to rt, 48h.

[12] R. Ramón, Doctoral thesis *Síntesis de aminoácidos no naturales y aplicación a la síntesis de péptidos con interés farmacológico*, University of Barcelona, **2009**.

We have also distilled the commercially available anhydrous MeOH over Na to avoid having traces of water in the solution which could led to some kind of hydrolysis of the desired product. After performing the reaction under these conditions, we did not obtain the desired ester product but the acid as the major product with a 93% yield (Figure 5.4).

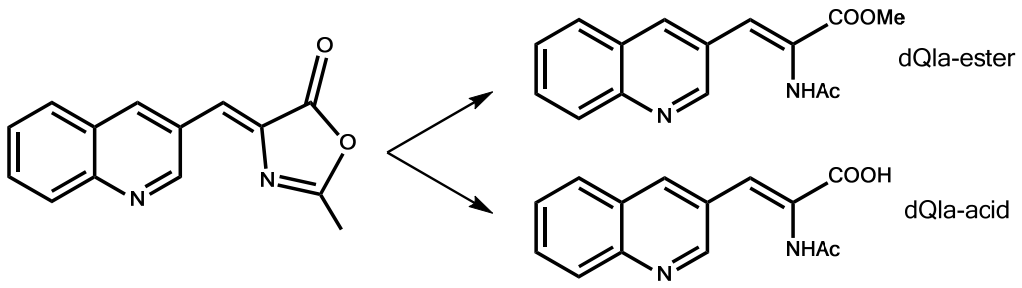

Figure 5.4. Two possible products of the azalactone ring opening reaction with MeONa in MeOH; **dQla-ester** (top) and **dQla-acid** (bottom).

The formation of the **dQla-acid** product proceeded with a 100% conversion which was checked by ^{1}H-NMR where no signals from the starting material were observed (Figure 5.5).

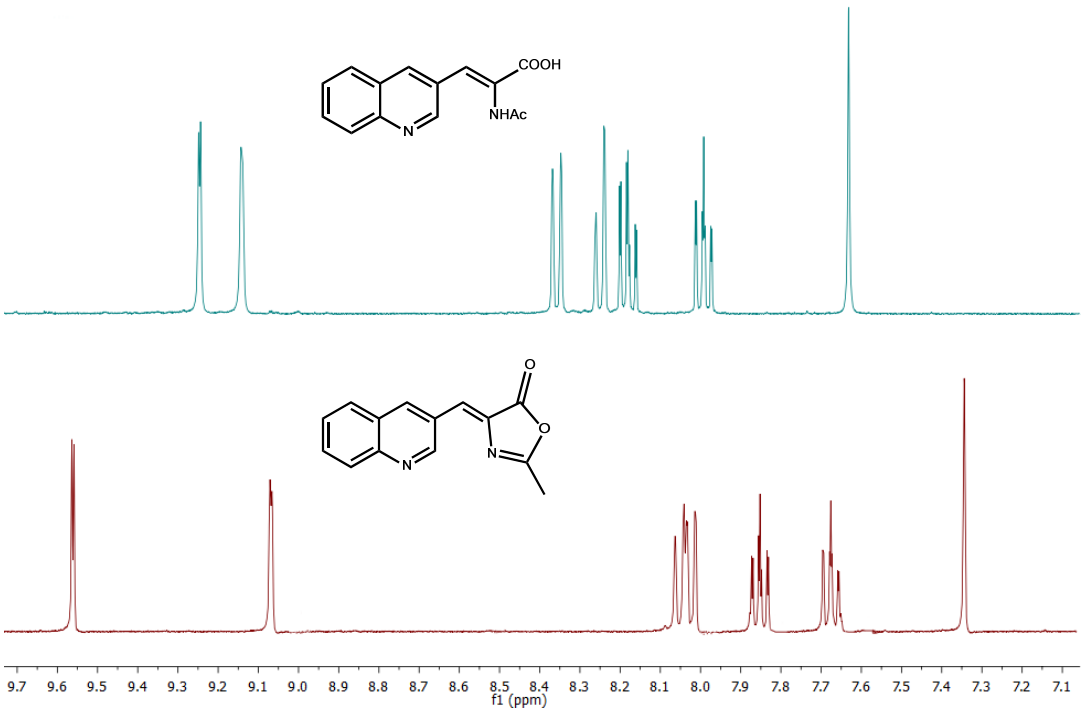

Figure 5.5. Comparison between the aromatic regions of the ^{1}H-NMR of the azalactone (bottom) and the obtained product corresponding to the dQla-acid (top) and not to the dQla-ester compound.

Furthermore, the signal from the methyl group of the ester was not present in the final product ^{1}H-NMR spectrum (Figure 5.6). This absence of the methyl ester signal enabled us to corroborate our acid formation hypothesis.

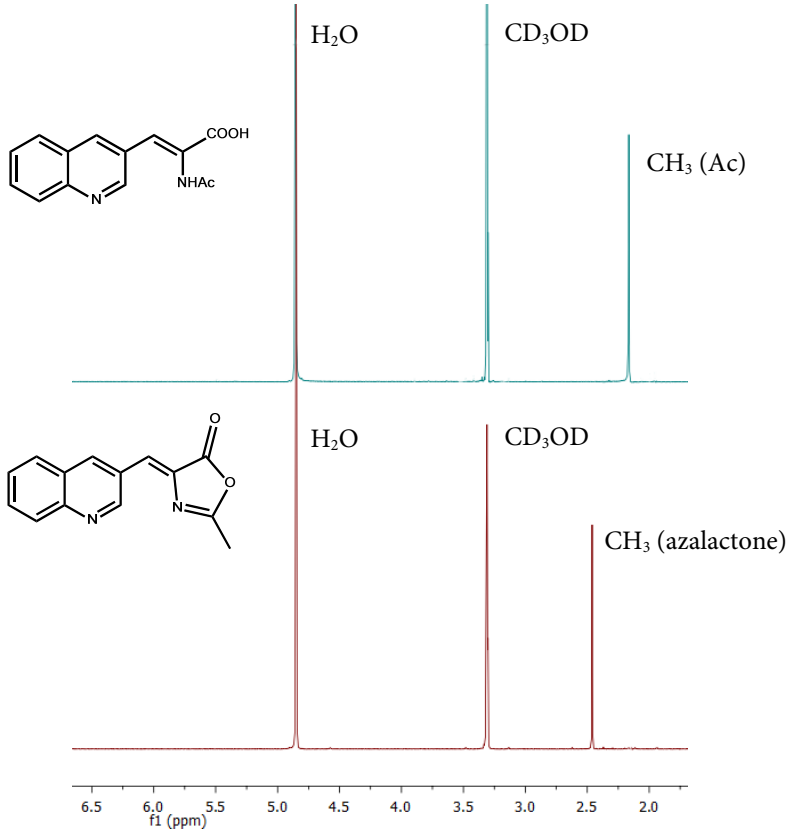

Figure 5.6. Comparison between the aliphatic regions of the ^{1}H-NMR of the azalactone (bottom) and the obtained product corresponding to the dQla-acid compound (top).

Seeing that the obtained product was the dQla-acid and not the dQla-ester, we decided to do an esterification so as to follow the previously developed synthetic strategy.[5,12] Three different reaction conditions were tested (Table 5.1) without being able to obtain the dQla-ester compound. When working with the **entry 1** conditions, we observed the esterification product but with the quinoline N being methylated too. When testing conditions of the **entry 2**, no reaction took place after 16h so we decided to stop it and try the **entry 3** conditions. Fisher esterification is a well-known methodology for the esterification of acids with primary alcohols (MeOH in our case) but in that case the reaction did not work either after 16h.

Entry	Reagents	Solvent	T (ºC)
1	MeI, K_2CO_3	Acetone	65
2	TMS-CHN_2	Toluene/MeOH (4:1)	rt
3	H_2SO_4	MeOH	90

Table 5.1. Tested conditions for the esterification of the dQla-acid obtained compound. Reaction time for all of them was ~16h.

In light of these results and due to the high yield of the dQla-acid formation, we thought that it could be useful to hydrogenate the acid directly with the methodology developed in our group by Dr. Cristóbal-Lecina.[13] During his thesis, Edgar Cristóbal performed the hydrogenation of the model substrate (E)-2-acetamido-3-phenylacrylic acid with Rh-MaxPHOS[14] obtaining full conversion and an enantiomeric excess of 99%.

Following the same experimental methodology,[15] some attempts to hydrogenate the dQla-acid had been performed but no successful results were obtained. The products of the hydrogenation reaction showed medium conversion rates and low enantiomeric excesses which made us move to the synthesis of the Fmoc-L-Qla-OH through **Route 2** (Figure 5.3).

Through this synthetic protocol we obtained the final Fmoc-L-Qla-OH with good yields and an enantiomeric excess ≥ 99%. However, the synthesis of the final amino acid did not proceed without difficulties. The dehydroamino acid (dQla) was facile achieved through a Horner-Wadsworth-Emmons reaction with a 73% yield. After being purified, the dQla

[13] E. Cristóbal, Doctoral thesis *Catálisis Asimétrica con complejos de rodio e iridio. Aplicación en síntesis de compuestos biológicamente activos*, University of Barcelona, **2014.**

[14] E. Cristóbal-Lecina, P. Etayo, S, Doran, M. Revés, P. Martín-Gago, A. Grabulosa, A. R. Costantino, A. Vidal-Ferran, A. Riera, X. Verdaguer**,** *Adv. Synth. Catal.*, **2014**, *356*, 795 - 804.

[15] H_2, P = 3 bar, MeOH, 1% Rh-MaxPHOS, room temperature.

was reduced to obtain the corresponding ester. Different conditions were tested to obtain the desired product with good yields and high-enough enantiomeric excess (Table 5.2).

Entry	P H_2 (bar)	T (ºC)	η (%)	Conversion (%)	ee (%)
1	50	rt	95	100	83
2	20	rt	94	100	90
3	**10**	**rt**	**96**	**100**	**96**
4	5	rt	95	100	93

Table 5.2. Tested conditions for the dQla reduction. All the reactions were stirred for 24h using anhydrous and degassed MeOH as a solvent.

Even though the best conditions seemed to be the ones from entry 3 (Table 5.2), we decided to try to reduce the tetrafluoroboric salt of the dQla (dQla-BF_4^-) as it is known to facilitate the hydrogenation for some substrates. The results of the reduction of the dQla-BF_4^- are shown in Table 5.3 being entry 3 the one which gave better results reaching the same enantiomeric excess we obtained when reducing the dQla.

Entry	P H_2 (bar)	T (ºC)	η (%)	Conversion (%)	ee (%)
1	10	rt	94	35	88
2	50	rt	86	100	95
3	**10**	**65**	**86**	**100**	**96**

Table 5.3. Tested conditions for the dQla- BF_4^- reduction. All the reactions were stirred for 24h using anhydrous and degassed MeOH as a solvent.

As the same enantiomeric excess was obtained, we decided to continue the synthesis through the reduction of the dQla as it needed milder conditions than the reduction of the tetrafluoroboric salt that needed heating up to 65ºC. Furthermore, the yield of dQla salt reduction was lower than the one of the dQla. In our particular case, the usage of the BF_4^- salt did not improve the reduction of the double bond nor the enantiomeric excess.

The following ester hydrolysis proceeded as expected obtaining quantitative yields. The final Fmoc protection step was key in the obtainment of the desired compound; it is known that this protections could improve the enantiomeric excess of the final product. In our case, after 48h of reaction the Fmoc-L-Qla-OH was obtained with 98% yield and 99% enantiomeric excess (Scheme 5.2).

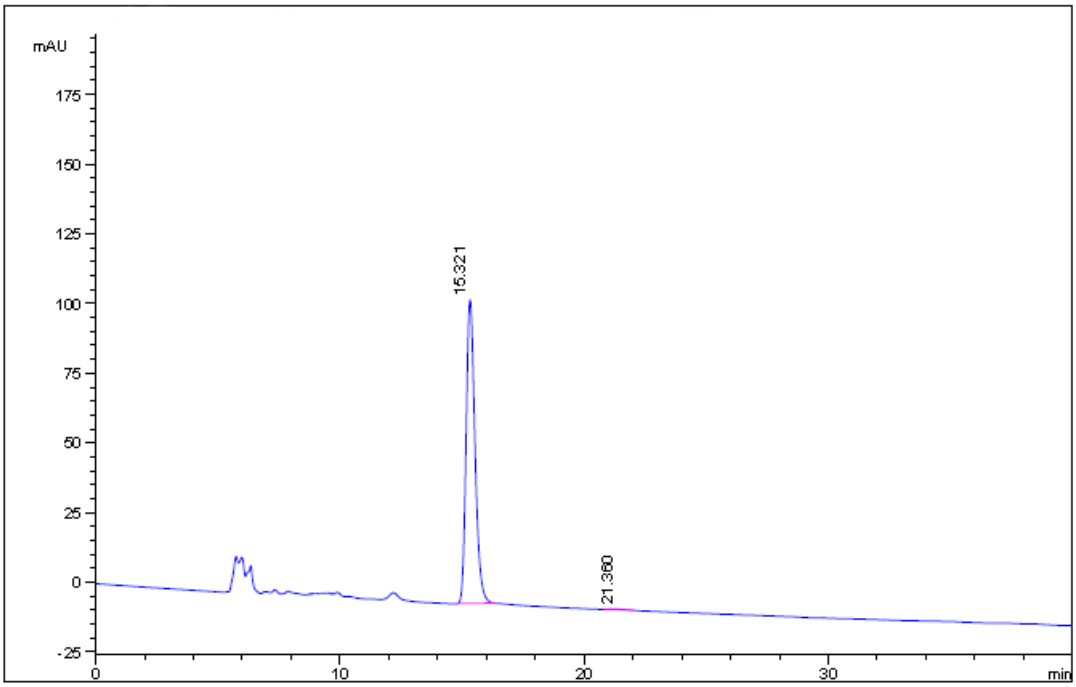

Peak	t_R	Width	Area	Height	Area (%)
1	15.321	0.388	2750.749	108.941	99.596
2	21.360	0.719	11.165	0.259	0.404

Scheme 5.2. Analytical HPLC of the final Fmoc-L-Qla-OH. Conditions used: Heptane/EtOH-0.2% TFA (60:40), T = 25 ºC, flow rate = 0.5 mL/min, column: Chiralcel OJ, stop time = 40 min.

To conclude, after testing different conditions, the final compound was obtained with good yields and good enantiomeric excess following the previously described **Route 2** even if that was more expensive than Route 1 due to the usage of the Methyl 2-acetamido-2-(dimethoxyphosphoryl)acetate. Furthermore, the cause of the abnormally low yields when performing the opening of the azalactone have been disclosed and directed to the obtainment of one single product (dQla-acid) with an outstanding yield.

5.3 Synthesis of SRIF14 analogues with L-Qla-OH

Somatostatin analogues containing L-Qla-OH were synthesised by an individual and systematic substitution of the aromatic residue Phe11 for the non-natural amino acids 3'Pya and 4'Pya while replacing the Trp8 by L-Qla (Figure 5.7). Through that analogues we expect to be able to disclose the role of residue 8 both in the half-life of the peptide and the activity against SSTRs. Furthermore, we believe these analogues will also help in explaining the role of the N-H bond of the Trp in the binding with the SSTRs.

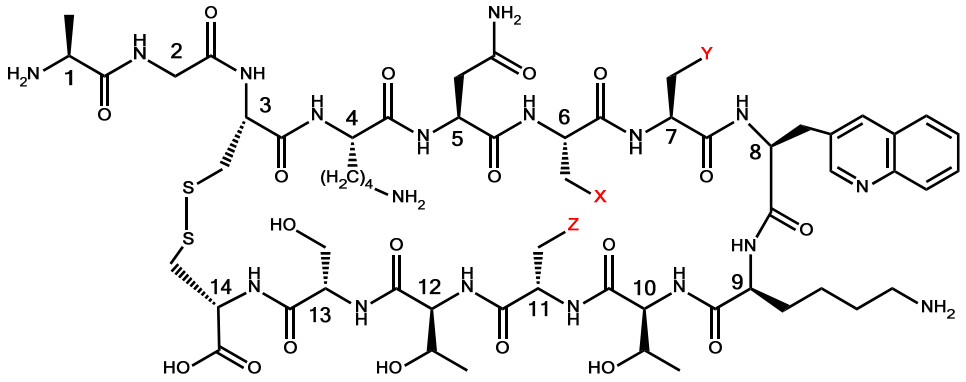

	6	**7**	**8**	**11**
[Msa7_L-Qla8]-SRIF14 (6)	Phe	Msa	L-Qla	Phe
[L-Qla8_4'Pya11]-SRIF14 (6.1)	Phe	Phe	L-Qla	4'Pya
[L-Qla8_3'Pya11]-SRIF14 (6.2)	Phe	Phe	L-Qla	3'Pya

Figure 5.7. Somatostatin derivatives containing L-Qla in position 8 and 4'Pya and 3'Pya in position 11 that will be presented in this chapter.

Fmoc-L-Qla-OH was synthesised following the methodology described above (Chapter 5.2). The rest of amino acids were commercially available from different suppliers. All three peptides were synthesised by solid phase peptide synthesis (SPPS) following the Fmoc/^{t}Bu strategy using a 2-chlorotrytyl chloride resin. The synthesis of [Msa7_L-Qla8]-SRIF14 (**6**) is shown as a general example in Scheme 5.3.

During the synthesis of the analogue **6**, the coupling of Fmoc-L-Qla-OH in position 8 was problematic; for that reason a second coupling with HOBt was necessary.

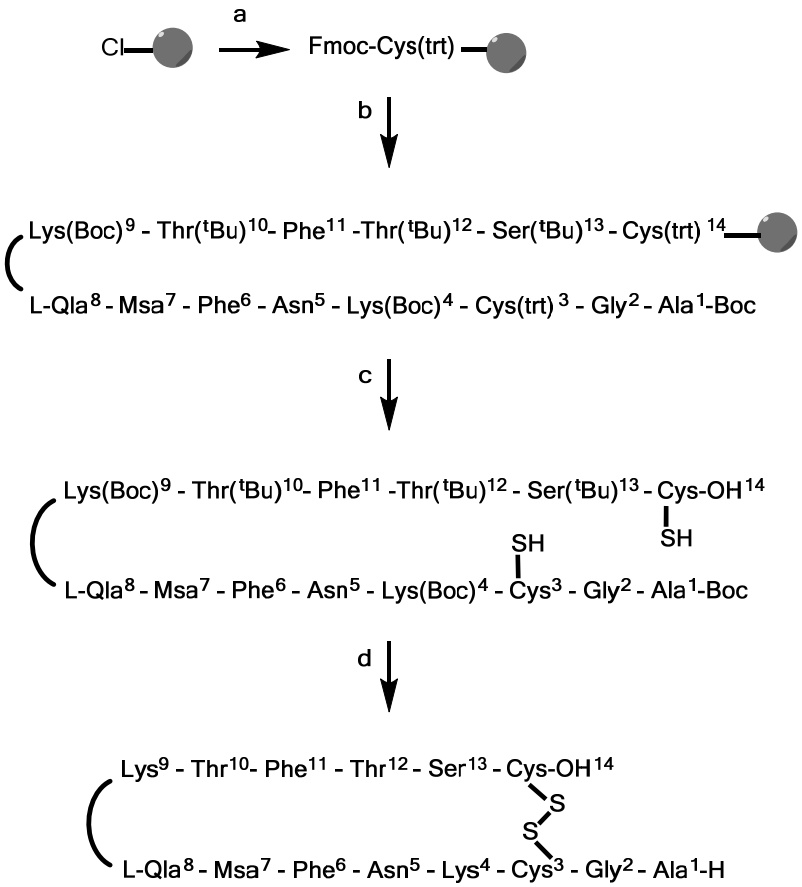

Scheme 5.3. SPPS of [Msa7_L-Qla8]-SRIF14 (**6**). a) 1. Fmoc-Cys(trt)-OH (3eq), DIEA (3eq), 2. MeOH; b) 1. Piperidine 20% in DMF, 2. Fmoc-AA-OH (1.5-3eq), DIPCIDI (3eq), HOBt (3eq), DMF; 3. Piperidine 20% in DMF, 4. Boc-Ala-OH (3eq), DIPCIDI (3eq), HOBt (3eq), DMF, c) DCM/TFE/AcOH, d) 1. I_2, 2. TFA/DCM/anisole/H_2O.

5.4 NMR studies and structure determination

Two of the three analogues (with a TFA^- counter ion) presented in this chapter were analysed by NMR spectroscopic techniques in phosphate buffer (pH = 6.5) and bidimensional homonuclear ^1H-^1H TOCSY and ^1H-^1H NOESY were obtained. The process followed was the one described in Chapter 3.3 of the present doctoral thesis. However, for none of the two peptides analysed by NMR (**6** and **6.1**) a structure could be obtained as the density of medium and long-distance NOE was really low but enough signals were detected to assign the protons of the sequence of analogue **6** (the chemical shifts are shown in Chapter 9).

At that point, it was a surprising result that **6** did not display a major conformation in solution as the peptide [Msa7]-SRIF14 previously synthesised in our group was rigid-enough to adopt a definite structure in solution with the only substitution of Phe7 by Msa (Figure 5.8).[11]

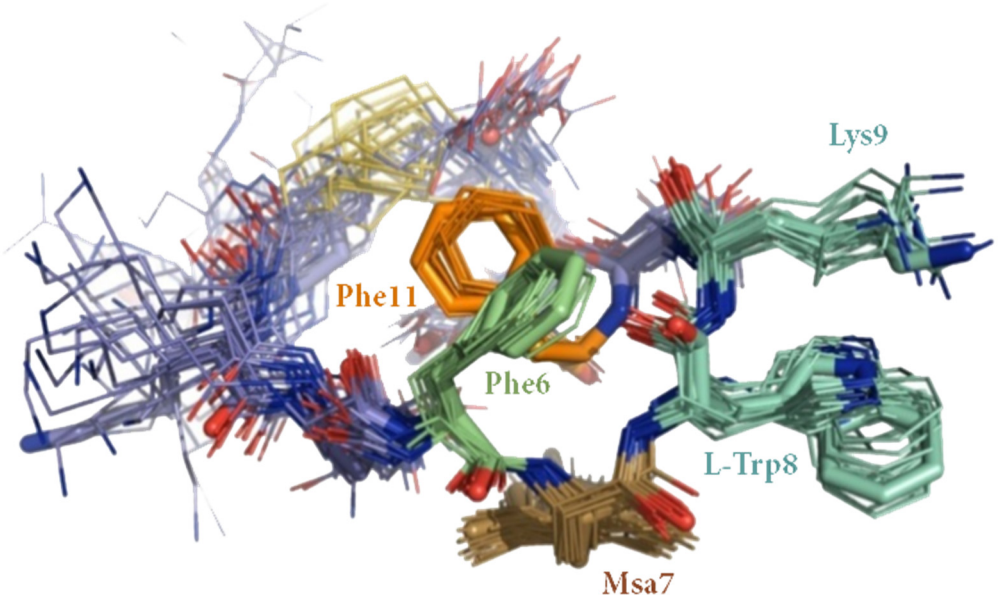

Figure 5.8. Superimposition of the lower energy structures of [Msa7]-SRIF which are in agreement with experimental NMR data for a 6-to-11 interaction.

With these results in hand in combination with the lack of time and the low chances of improvement due to the low change in the structural and electronic properties of 3'Pya when compared to 4'Pya, we decided not to acquire the NMR spectra of the peptide **6.2**.

5.5 Conclusions

We were able to synthesise the non-natural amino acid Fmoc-L-3-(3'-quinolyl)-alanine with good yields and enantiomeric excess through Route 2 although being a more expensive synthetic pathway due to the usage of a particular reagent; methyl 2-acetamido-2-(dimethoxyphosphoryl)acetate. The use of the BF_4^- salt in the asymmetric reduction of the dQla did not improve the enantiomeric excess results so we performed the synthesis of the final Fmoc-L-Qla-OH by reducing the dQla to the corresponding Qla-ester.

Conversely, we did not synthesise the amino acid through Route 1 as different problems occurred during the synthesis. However, we were able to identify the main byproduct of the dQla formation which was the dQla-acid. After different attempts to perform an esterification we did not succeed. In addition to that, the direct hydrogenation of the dQla-acid did not proceed as expected thus obtaining medium conversion rates and low enantiomeric excesses. With these results in hand, we synthesised the Fmoc-L-Qla-OH through Route 2.

Contrary to what happened in the previous chapters, the peptides presented herein were not rigid-enough to obtain a major set of 3D conformations in solution when containing the non-natural amino acids L-Qla and 3'Pya or 4'Pya as demonstrated by the NMR spectroscopy experiments. Due to the impossibility to obtain a definite structure, we did not perform the binding studies for these peptides as we would only have information about their potency and activity but we would not be able to relate them with their structures.

Chapter 6

SRIF analogues with D amino acids: half-lives and fragmentations

6.1 Introduction

Somatostatin (SRIF14), a broad inhibitory neuropeptide, and its analogues have been used in the treatment of different types of tumours and other diseases over the years. However, the role of native SRIF14 as a therapeutic agent was hampered by its low half-life (less than three minutes in plasma), which forced a constant infusion of the drug. The broad spectrum of biological responses and the lack of selectivity over its different receptors made treatments difficult to optimise.[1] This fact guided the synthesis of analogues towards the obtainment of longer plasmatic half-lives, higher inhibitory potency and more precise physiological actions.

As for other naturally occurring peptides, the low plasma half-life of SRIF14 is due to the degradation by endogenous peptidases, the degradation by proteolytic enzymes, the rapid renal and hepatic clearance and the destruction of the peptide by the phagocytes as part of the immune response.[2] All these mechanisms of degradation prevent SRIF14 from many therapeutic uses. Although the majority of peptides have to be delivered intravenous or subcutaneous, the oral route of administration is recognised to be the preferred one for drug delivery systems as it is the most pleasant for the patients.[3] A drug is supposed to fulfil the criteria of Lipinski's "Rule of five" in which both chemical and physical properties of a drug are evaluated in order to decide if a compound is likely to be given orally or not.[4] These rules state that, in general, an orally active drug should have no more than one violation of the following criteria: a) not having more than **5** donor

[1] G. Weckbecker, I. Lewis, R. Albert, H. A. Schmid, D. Hoyer, C. Bruns., *Nature Reviews Drug Discovery*, **2003**, *2*, 999 - 1017.

[2] a) G. Prevost, L. Israel, *Recent Results Cancer Res.*, **1993**, *129*, 63 - 70; b) F. Boccardo, D. Amoroso, *Chemotherapy*, **2001**, *47*, 62 - 77 (suppl. 2); c) R. J. Solá, K. Griebenow, *BioDrugs*, **2010**, *24*, 9 - 21; d) J. Rafferty, H. Nagaraj, A. P. McCloskey, R. Huwaitat, S. Porter, A. Albadr, G. Laverty, *Curr. Med. Chem.*, **2016**, *23*, 4231 - 4259.

[3] a) B. J. Bruno, G. D. Miller, C. S. Lim, *Ther. Deliv.*, **2013**, *4*, 1443 - 1467; b) J. H. Hamman, G. M. Enslin, A. F. Kotzé, *BioDrugs,* **2005**, *19*, 165 - 177.

[4] a) C. A. Lipinski, F. Lombardo, B. W. Dominy, P. J. Feeney, *Adv. Drug Delivery Rev.*, **2001**, *46*, 3 - 26; b) C. A. Lipinski, *Drug Discov. Today Technol.*, **2004**, *1*, 337 - 341.

hydrogen bonds, b) not having more than **10** acceptor hydrogen bonds, c) having a molecular mass of less than **500** Da and d) having an octanol-water partition coefficient (log *P*) not greater than **5**.[5] However, peptides normally do not fulfil Lipinski's criteria.[4a] Peptide degradation in the gastrointestinal tract (GIT) is the consequence of a variety of actions occurring at the same time; cleavage by proteases and peptidases and a harsh degradative acidic environment. Furthermore, the dramatic change in the pH values from highly acidic to slightly basic could also lead to peptides with lessened bioactivity.[2c] Moreover, these extreme pH values could lead to oxidation, deamidation and/or hydrolysis of the peptide primary structure.[6,7]

Different strategies have been employed to improve the bioavailability and stability of peptides for its use in humans; chemical modifications and the usage of carriers and delivery systems, among others. However, variations of the peptide motif could result in an alteration of the physicochemical and biochemical properties of the peptide itself; conformational structure, chemical, physical and biochemical properties and biological function *in vivo*.[8]

One of the widely-followed strategies to improve the biostability of peptides has been the cyclisation of the primary amino acid motif which was seen to confer the peptide a higher resistance to proteolysis. Peptides are outstanding candidates to be cyclised as they hold a potential for both side-chain (disulphide or amide bond between two residues) and backbone cyclization (involves the introduction of a short sequence that connects both the *C*- and *N*-terminal parts of the peptide).[9] To further stabilise peptides, lipidation has

[5] Note that all numbers are multiples of five, which is the origin of the rule's name.

[6] X. Wang, Q. Zhang, *Eur. J. Pharm. Biopharm.*, **2012**, *82*, 219 - 229.

[7] L. D. M. Leite, E. Barbu, G. J. Pilkington, *Curr. Top. Med. Chem.*, **2015**, *15*, 2277 - 2289.

[8] S. V. Moradi, W. M. Hussein, P. Varamini, P. Simerska, I. Toth, *Chem. Sci.*, **2016**, *7*, 2492 - 2500.

[9] a) I. Avan, C. D. Hall, A. R. Katritzky, *Chem. Soc. Rev.*, **2014**, *43*, 3575 - 3594; b) A. C. Conibear, S. Chaousis, T. Durek, K. J. Rosengren, D. J. Craik, C. I. Schroeder, *Biopolymers*, **2016**, *106*, 89 - 100.

also been tested by conjugating lipids (fatty acids) to the *N*-terminal part of the peptides, which resulted in an improvement of the enzymatic degradation ratio.[10]

N-methylation of peptides has also been tested as a way to block their enzymatic recognition by reducing proteolytic cleavage by steric hindrance. Cyclosporine A would be a good example of this procedure as it holds seven *N*-methylated peptide bonds which confer it the aptitude to be administered orally even violating Lipinski's "Rule of 5".[4a, 11] However, the *N*-methylation has an important drawback; racemization can occur in certain cases during the synthesis of the amino acid due to acidic and basic conditions used within SPPS.[12] Although some methodologies have been developed to synthesise these amino acids in an enantiomerically pure way,[13] some complications are still encountered when *N*-methylating functionalised amino acids such as histidine, tryptophan and cysteine where side chains can also undergo *N*-methylation.[14] An example would be the *N*-methylation of some amino acids of the native SRIF14 sequence which lowered the biodegradation of the synthesised analogues and therefore increased their bioavailability.[15]

Among all the modifications, the most commonly employed has been the substitution of the naturally occurring L-amino acids by their unnatural D-enantiomers. This strategy has been reported to be effective in the reduction of the enzymatic recognition and cleavage of peptides upon exposure to proteolytic enzymes (chymotrypsin, pepsin, trypsin…).[16] Another alternative would be substituting natural amino acids by unnatural variants as proteolytic enzymes possess decreased ability to recognise these moieties.

---

[10] M. J. Hackett, J. L. Zaro, W. C. Shen, P. C. Guley, M. J. Cho, *Adv. Drug Deliv. Rev.*, **2013**, *65*, 1331 - 1339.

[11] J. Chatterjee, F. Rechenmacher, H. Kessler, *Angew. Chem. Int. Ed.*, **2013**, *52*, 254 - 269.

[12] C. Gilon, M. A. Dechantsreiter, F. Burkhart, A. Friedler, H. Kessler, *Methods of Organic Chemistry: Synthesis of Peptides and Peptidomimetics*, **2003**, *22*, 215 - 271.

[13] One example would be the reduction of 5-oxazolidienes developed by Freidinger.

[14] J. R. McDermott, N. L. Benoiton, *Can. J. Chem.*, **1973**, *51*, 2562 - 2570.

[15] R. M. J. Liskamp, D. T. S. Rijkers, J. A. W. Kruijtzer, J. Kemmink, *ChemBioChem*, **2011**, *12*, 1626 - 1653.

[16] S. M. Miller, R. J. Simon, S. Ng, R. N. Zuckermann, J. M. Kerr, W. H. Moos, *Drug Dev. Res.*, **1995**, *35*, 20 - 32.

Moreover, the incorporation of some of these non-natural amino acids onto the peptide sequence tend to trigger positive effects on their stability.[17]

To deeply explore the effects of the small modifications in the obtainment of more structured and stable analogues, we considered that it could be useful to substitute key amino acids for their D-enantiomer, in order to compare these results with the ones obtained for the parent native SRIF14. The synthesis of the somatostatin analogues, the structure determination results together with the binding studies to determine the affinity against the different SSTRs, the half-lives and the fragmentation patters will be discussed in this chapter.

The increase in the bioavailability of our compounds will be studied by measuring their half-lives. They will be determined by incubating the peptides with human serum, taking aliquots at previously determined time points and then analysing them by RP-UPLC.[18] Half-lives of peptides in human serum will be calculated as described in **Chapter 9.2.7** of the present doctoral thesis. However, we were not only focused on the obtainment of peptides with higher half-lives but on the identification of the crucial breakage points so as to introduce modifications that prevent cleavage from happening. The key point for performing these studies has been the establishment of a collaboration between Lead Molecular Design S.L. (Molecular Discovery Ltd, Middlesex, UK), Gabrielle Cruciani's research group in the University of Perugia (Italy) and our group. They suggested analysing the half-life samples (aliquots from the incubations) by RP-HPLC together with tandem mass spectrometry (MS/MS) in order to separate the formed metabolites and determine the most prone to hydrolyse bonds.

[17] A. Murza, K. Belleville, J. M. Longpré, P. Sarret, É. Marsault, *Biopolym.*, **2014**, *102*, 297 - 303.

[18] RP-UPLC conditions: Thermo Scientific Ultimate 3000 ultra-performance liquid chromatography equipped with a Zorbax Eclipse Plus C18 column (150 x 2.1 mm, 1.8 μm) using H_2O-0.1%TFA and ACN-0.1%TFA as eluents over 20 min.

6.2 Synthesis of SRIF14 analogues

Somatostatin analogues containing D-amino acids were synthesised by individual and systematic substitution of key amino acids (Figure 6.1). D-Trp was introduced in position 8 in all the analogues as it is known to enhance the activity of the peptides which contain it by increasing their half-lives and stabilizing the β-turn.[19] As for the analogues **1**-**5**, the substitution of L-Trp for its D-enantiomer has been a constant modification.

D-amino acids were introduced in different positions of the SRIF14 natural sequence which are known to be the key for the stability of the peptide with the aim of disclosing their importance within the enzymatic recognition pathway. The introduction of such amino acids would enable the resulting peptide to resist proteolytic degradation and avoid triggering an immune response.[20]

The non-natural amino acid mesitylalanine (Msa) was introduced in position 7 in all the analogues synthesised as it has been demonstrated that it helps in the obtainment of more structured peptides. As seen in our group, introduction of Msa in position 7 in somatostatin analogues containing allowed to determine its 3D structures in solution for the first time.[21] As exposed in Chapter 2 of the present doctoral thesis, peptide **7**[22] was the first analogue which displayed conformational stability and a selective binding affinity against SSTR2 which resembled the one of the natural hormone.

---

[19] a) B. H. Arison, R. Hirschmann, D. F. Veber, *Bioorg. Chem.*, **1978**, *7*, 447 - 451; b) O. Ovadia, S. Greenberg, B. Laufer, C. Gilon, A. Hoffman, H. Kessler, *Expert Opin. Drug Discov.*, **2010**, *5*, 655 - 671.

[20] M. Uppalapati, D. J. Lee, K. Mandal, H. Li, L. P. Miranda, J. Lowitz, J. Kenney, J. J. Adams, D. Ault-Riché, S. B. H. Kent, S. S. Sidhu, *ACS Chem. Biol.*, **2016**, *11*, 1058 - 1065.

[21] P. Martín-Gago, M. Gómez-Caminals, R. Ramón, X. Verdaguer, P. Martín-Malpartida, E. Aragón, J. Fernández-Carneado, B. Ponsati, P. López-Ruiz, M. A. Cortés, B. Colás, M. J. Macías, A. Riera, *Angew. Chem. Int. Ed.*, **2012**, *51*, 1820 - 1825.

[22] P. A. Martín-Gago, doctoral thesis *Synthesis of highly structured and receptor-selective tetradecapeptidic analogs of somatostatin: Fine tuning the non-covalent interactions among their aromatic residues*, Univeristat de Barecelona, 2013.

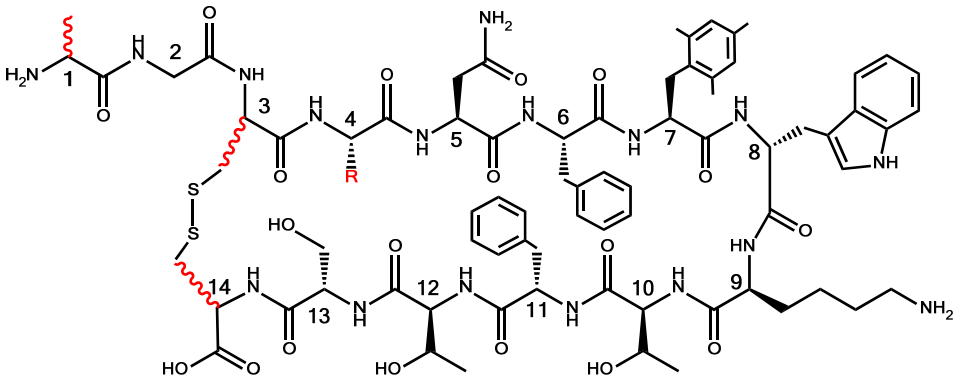

	1	3	4	7	8	14
[Msa7_D-Trp8]-SRIF14 (7)*	L-Ala	L-Cys	L-Lys	Msa	D-Trp	L-Cys
[Msa7_D-Trp8_D-Cys14]-SRIF14 (8)	L-Ala	L-Cys	L-Lys	Msa	D-Trp	**D-Cys**
[D-Ala1_Msa7_D-Trp8_D-Cys14]-SRIF14 (9)	**D-Ala**	L-Cys	L-Lys	Msa	D-Trp	**D-Cys**
[D-Cys3,14 _Msa7_D-Trp8]-SRIF14 (10)	L-Ala	**D-Cys**	L-Lys	Msa	D-Trp	**D-Cys**
[D-Ala1_D-Cys3,14_Msa7_D-Trp8]-SRIF14 (11)	**D-Ala**	**D-Cys**	L-Lys	Msa	D-Trp	**D-Cys**
[L-Orn4_Msa7_D-Trp8]-SRIF14 (12)	L-Ala	L-Cys	**L-Orn**	Msa	D-Trp	L-Cys
[L-Orn4_Msa7_D-Trp8_D-Cys14]-SRIF14 (13)	L-Ala	L-Cys	**L-Orn**	Msa	D-Trp	**D-Cys**

Figure 6.1. Somatostatin derivatives containing D-amino acids in different positions that will be presented in this chapter. *Peptide previously synthesised by Dr. Martín-Gago.[22]

As previously mentioned in Chapter 4, Fmoc-L-Msa-OH was synthesised following the asymmetric synthesis protocol previously developed in our group (Scheme 4.1, page 73)[23] while the rest of amino acids, including Fmoc-D-Trp(Boc)-OH, Fmoc-D-Ala-OH and Fmoc-L-Orn-OH, were commercially available from different suppliers.

All seven peptides presented in this chapter were synthesised by solid phase peptide synthesis (SPPS) following the well-known Fmoc/^{t}Bu strategy using 2-chlorotrytyl chloride resin. The synthesis of [D-Ala1_D-Cys3,14_Msa7_D-Trp8]-SRIF14 (**11**) is shown as a general example in Scheme 6.1

[23] R. Ramón, M. Alonso, A. Riera, *Tetrahedron: Asymmetry*, **2007**, *18*, 2797 - 2802.

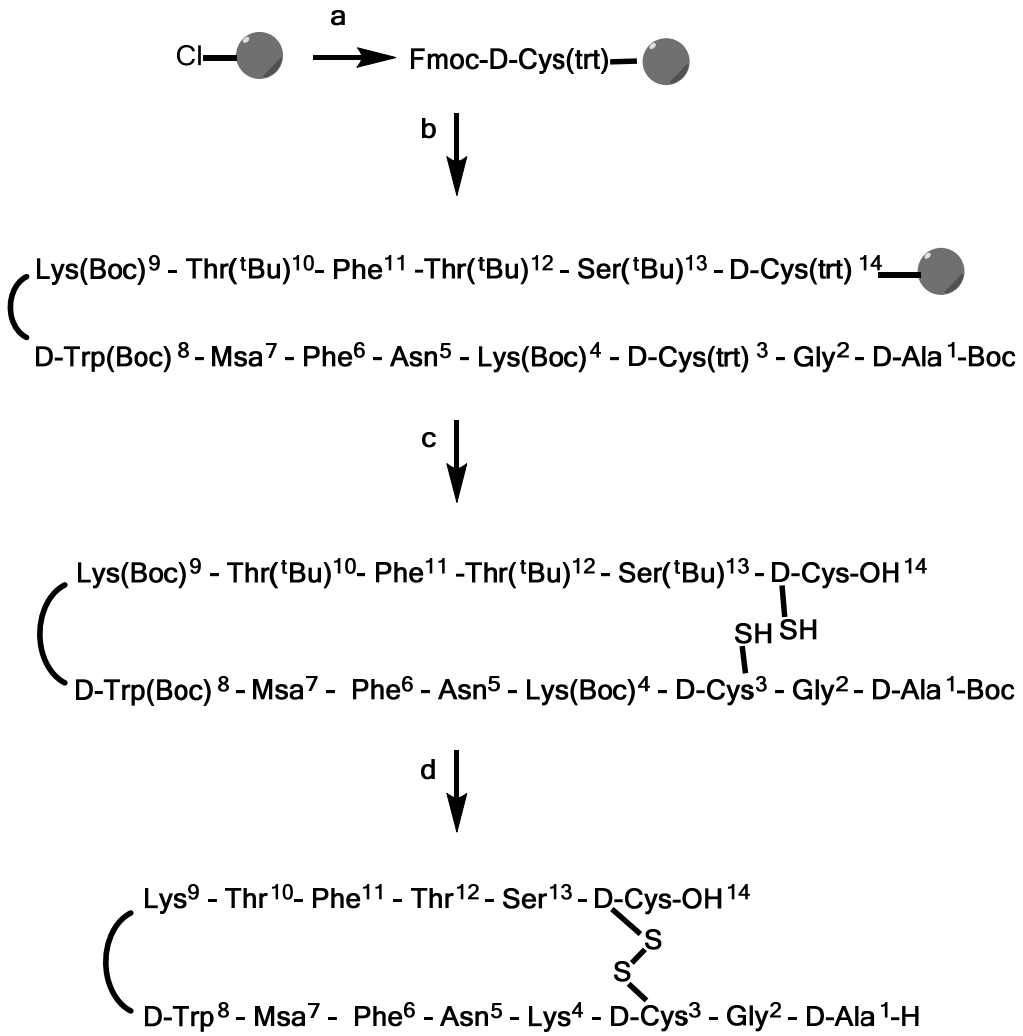

Scheme 6.1. SPPS of [D-Ala1_D-Cys3,14_Msa7_D-Trp8]-SRIF14 (**11**). a) 1. Fmoc-D-Cys(trt)-OH (3eq), DIEA (3eq), 2. MeOH; b) 1. Piperidine 20% in DMF, 2. Fmoc-AA-OH (1.5-3eq), DIPCIDI (3eq), HOBt (3eq), DMF; 3. Piperidine 20% in DMF, 4. Boc-D-Ala-OH (3eq), DIPCIDI (3eq), HOBt (3eq), DMF, c) DCM/TFE/AcOH, d) 1. I_2, 2. TFA/DCM/anisole/H_2O.

Contrary to what happened during the synthesis of [L-Dmp11_D-Trp8]-SRIF14 (**3**) and [Msa6_L-3'Pya7_D-Trp8]-SRIF14 (**5**), the coupling of Fmoc-Asn-OH in position 5 in the D-amino acid containing sequences was not problematic so the recoupling step was not needed.

6.3 Half-lives and fragmentation studies

Peptides have always been considered to be well-suited compounds for their use in the treatment of diseases where the target is a protein-protein interaction.[24] Somatostatin analogues are known to have a great potential as drugs due to their high specificity for the SSTRs which are a subclass of G-protein-coupled receptors (GPCRs). A 14-amino acid somatostatin analogue with a high-enough half-life has never been obtained before even though several strategies have been followed.[9-11,16,17] For that reason, we synthesised six new analogues (plus peptide **7** previously synthesised in our group[22]) using at least one of the mentioned modifications.

All seven peptides (**7**-**13**) were synthesised with the aim of increasing their half-life when compared to the natural hormone ($t_{1/2}$ < 3 min) and becoming promising drug candidates. Until now, the best methodology to study the metabolic stability of peptides was the usage of HPLC-MS to follow the decrease of the peak corresponding to the starting peptide. However, it has been proven that these MS-based proteomic approaches experience difficulties when sequencing cyclic peptides in addition to being limited to the 20 standard amino acids. [25,26]

To overcome these drawbacks, Lead Molecular Design S.L. (Molecular Discovery Ltd, Middlesex, UK) developed a new approach that used LC-MS/MS data from metabolic stability experiments to determine specific cleavage sites which can be applied to cyclic peptides and can also include non-natural amino acids.

Using their methodology, half-lives and fragmentations of both somatostatin14 and our seven analogues were measured as described in the following sections. All peptides

[24] a) M. C. Manning, D. K. Chou, B. M. Murphy, R. W. Payne, D. S. Katayama, *Pharm. Res.*, **2010**, *27*, 544–575; b) L. Di, *AAPS J.*, **2015**, *17*, 134–143.

[25] C. Xu and B. Ma, *Drug Discov. Today*, **2006**, *11*, 595 - 600.

[26] a) D. J. Craik, D. P. Fairlie, S. Liras, D. Price, *Chem. Biol. Drug Des.*, **2013**, *81*, 136 - 147; b) A. S. Bayden, E. F. Gomez, J. Audie, D. K. Chakravorty, D. J. Diller, *Biopolymers*, **2015**, *104*, 775 - 789; c) T. H. J. Niedermeyer, M. Strohalm, *PLoS One*, **2012**, *7*, e44913.

(SRIF14 and **7**-**13**) were studied through UPLC-MS/MS techniques and further analysed with the software designed by Lead Molecular Design S.L.[27] Half-life values were calculated from the UPLC data[28] obtained and using a linear regression of the natural logarithm of the percentage of peak area integration *versus* time. To obtain the fragmentation patterns, serum-stability samples were analysed using the data-dependent MS/MS method developed by Lead Molecular Design S.L.[29] MS/MS data for each analogue was acquired up to one time point higher of the obtained $t_{1/2}$ value.

6.3.1 Somatostatin

Somatostatin was the first of the eight peptides to be studied. The UPLC data showed that SRIF14 had a half-life in human serum of **15 min** which correlated with the low half-life that the natural hormone displays in human plasma ($t_{1/2}$ < 3 min). The fact that $t_{1/2}$ in human serum is higher than the one obtained for the same hormone in human plasma is related to the lack of clotting agents in the human serum which would make the degradation faster.

The degradation pattern of the native somatostatin14 was obtained and ten metabolites were detected and characterised (Figure 6.2). Among these metabolites, first, second and third generation metabolites were formed during the incubation of SRIF14 in human serum over 48h and were identified by a subsequent revision of the results. The MS/MS data acquired for the first four time points (t = 0 min, 5 min, 10 min and 30 min) as somatostatin's half-life was established to be of around 15 min. As it can be seen in Figure 6.2, the first metabolites formed correspond to the loss of the extracyclic amino acids of the molecule either sequentially or together (metabolites **a** and **b**) thus indicating that they conform the part of the sequence which is easier to hydrolyse. Other important formed metabolites were the ones which were obtained after the ring opening next to either Lys4

[27] WebMetabase and Mass MetaSite.

[28] UPLC data was acquired and analysed as described in Chapter 9.2.7 of the present doctoral thesis.

[29] As described in Chapter 9.2.8.

or Lys9 (metabolites **c** and **d** appearing at t = 0 min and t = 5 min, respectively). Through deletion of single amino acids, metabolites **e**, **f**, **g**, **h**, **i**, and **j** were formed.

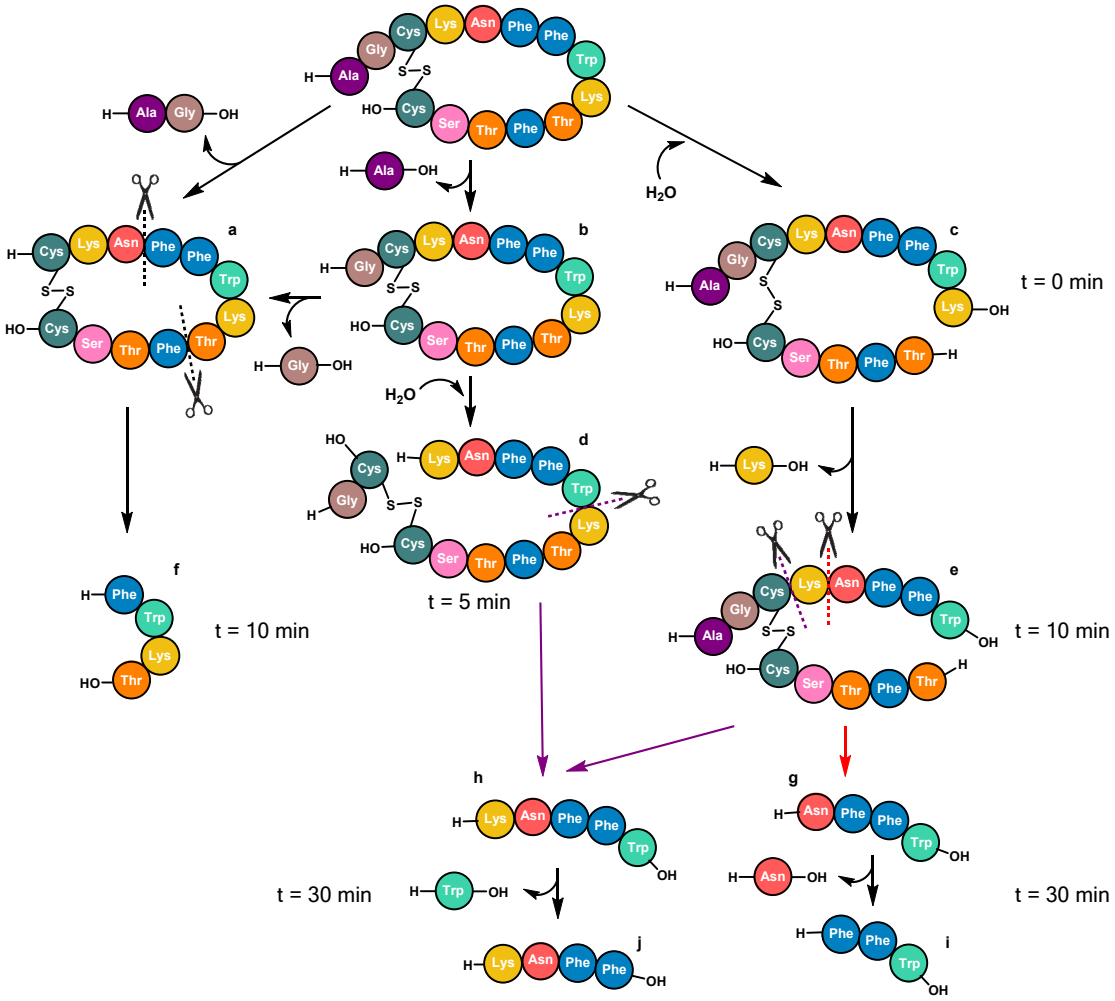

Figure 6.2. Proposed metabolites of somatostatin14 at different times after incubations in human serum detected using UPLC-MS/MS and analysed with WebMetabase and Mass MetaSite. **a**: M-128; **b**: M-71; **c**: M+18; **d**: M-53; **e**: M-110; **f**: M-1056; **g**: M-1024; **h**: M-896; **i**: M-1138; **j**: M-1082.

From the ten metabolites formed, three of them were detected for the first time at t = 0 min, one after 5 min, two after 10 min and four at the time point t = 30 min. For the metabolites formed prior to t = 30 min, a multiple detection in various time points was seen as shown in Table 6.1. The first four metabolites (**a**, **b**, **c** and **d**) were also detected and identified at t = 10 min and t = 30min. Metabolites **e** and **f** were also detected at t = 30 min. However, we could not determine if these metabolites would have been detected at higher incubation times.

Metabolite	Detection time (min)		
a: M-Gly2_Ala1	0	10	30
b: M-Ala1	0	10	30
c: ring opening Lys9	0	10	30
d: M-Ala1 + ring op. Cys3	5	10	30
e: M-Lys9	-	10	30
f: Phe7-Thr10	-	10	30
g: Asn5-Trp8	-	-	30
h: Lys4-Trp8	-	-	30
i: Phe6-Trp8	-	-	30
j: Lys4-Phe7	-	-	30

Table 6.1. Time of appearance and other detection times of the ten metabolites detected for the natural hormone SRIF14.

6.3.2 [L-Orn4_Msa7_D-Trp8]-SRIF14 (12)

Trying to overcome the ring opening through the Lys4, we decided to substitute that amino acid by a one-carbon shorter natural non-proteinogenic amino acid, L-Orn. [L-Orn4_Msa7_D-Trp8]-SRIF14 (**12**) was studied and the obtained half-life in human serum was around **15 min** resembling the one of the natural hormone and thus, indicating that the degradation pattern should be similar to the one of SRIF14.

Five different metabolites were detected and characterised for the analogue **12** (Figure 6.3) among which first, second and third generation metabolites were identified. Similar to the natural hormone, the MS/MS data was only acquired for the samples of the first four time points. Contrary to what was expected, the substitution of L-Lys4 by L-Orn4 was not a good modification to increase the half-life of the analogues since the ring opening next to this amino acid was observed after 5 min of incubation (metabolite **d**). The two first-formed metabolites were the ones in which the extracyclic part was lost (**a** and **b**) as happened in the natural hormone. Furthermore, the ring opening through Lys9 and the subsequent loss of that amino acid was also observed after 30 min of incubation (metabolite **c**). The other two metabolites were formed after the cleavage of one or two

amide bonds; Cys3_L-Orn4 (metabolite **d**, after 5 min of incubation) and Phe6_Msa7 and Thr12_Ser13 (metabolite **e**, after 30 min).

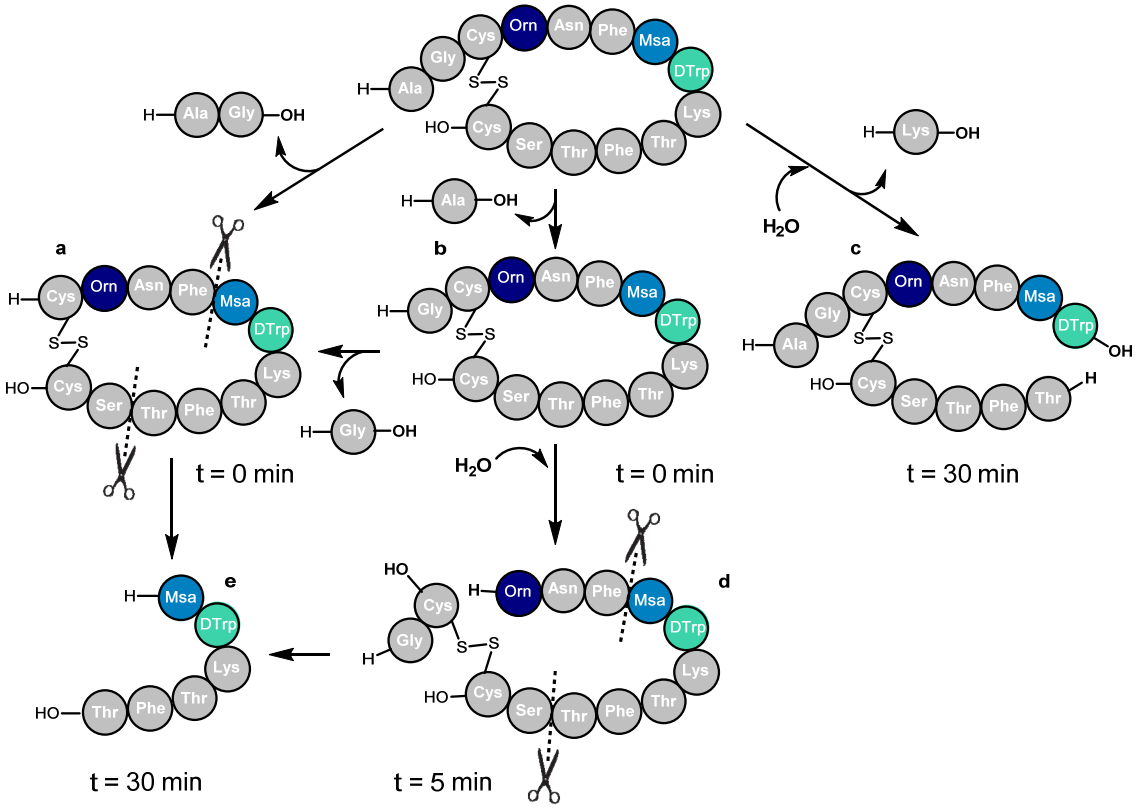

Figure 6.3. Proposed metabolites of [L-Orn4_Msa7_D-Trp8]-SRIF14 (**12**) at different times after incubations in human serum detected using UPLC-MS/MS and analysed with WebMetabase and Mass MetaSite. **a**: M-128; **b**: M-71; **c**: M-53; **d**: M-110; **e**: M-647.

With that results in hand, we hypothesised that the metabolites that would have been formed at higher incubation times (t > 30 min) would be fragments of the bigger ones, i.e. fragments of metabolites **c** and **d** which were the ones that had experienced less fragmentation upon t = 30 min.

From the five metabolites formed, two of them were detected for the first time at t = 0 min, one after 5 min, and two at the time point t = 30 min. Some of the metabolites formed within the first minutes of the incubation of the peptide with human serum, were also detected at higher time points. As it can be seen in the Table 6.2, metabolites **a, b** and **c** were also detected at t = 10 min and t = 30 min.

Metabolite	Detection time (min)		
a: M-Gly2_Ala1	0	10	30
b: M-Ala1	0	10	30
c: M-Lys9	5	10	30
d: M-Ala1 + ring. op Cys3	-	-	30
e: Msa7-Thr12	-	-	30

Table 6.2. Time of appearance and other detection times of the five metabolites detected for the [L-Orn4_Msa7_D-Trp8]-SRIF14 (**12**) somatostatin analogue.

6.3.3 [L-Orn4_Msa7_D-Trp8_D-Cys14]-SRIF14 (13)

With the aim of obtaining an analogue with a high-enough half-life and with the capacity to avoid the ring opening through Lys4 present in the native sequence, analogue **13** was synthesised.

[L-Orn4_Msa7_D-Trp8_D-Cys14]-SRIF14 (**13**) was studied and the obtained half-life in human serum was established to be **13 min** being slightly lower than the one of the natural hormone and thus, indicating that the degradation pattern should be comparable to the one obtained for SRIF14 and **12**.

Analogue **13** displayed four different metabolites which were detected and characterised using the previously described methodology (Figure 6.4).[29] In this case, only first and second generation metabolites were identified and the MS/MS data was only acquired for the samples of the first four time points.

The introduction of D-Cys in position fourteen did not help in increasing the half-life of the analogue and the inclusion of L-Orn dit not prevent the ring from opening between the amino acids in positions three and four. Similar to what happened for **12**, two of the first formed metabolites were the ones losing the extracyclic amino acids (**a** and **c**). Moreover, the other two metabolites detected were the ones in which the ring opened through the L-Orn4 (metabolite **b**) and Lys9 (with the subsequent loss of the amino acid, metabolite **d**).

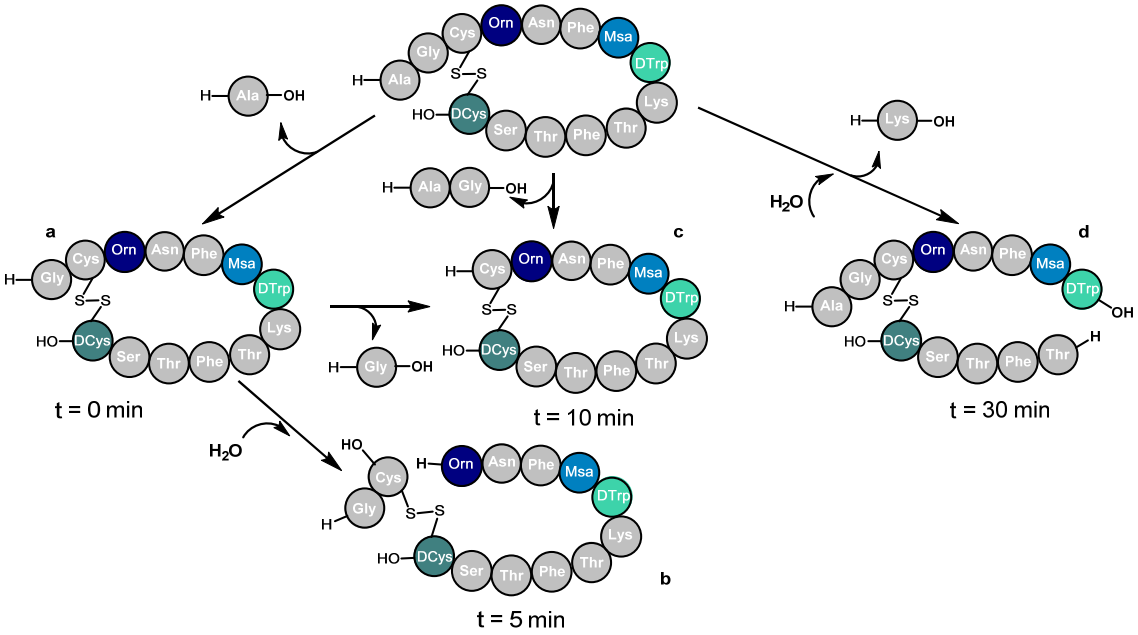

Figure 6.4. Proposed metabolites of [L-Orn4_Msa7_D-Trp8_D-Cys14]-SRIF14 (**13**) at different times after incubations in human serum detected using UPLC-MS/MS and analysed with WebMetabase and Mass MetaSite. **a**: M-71; **b**: M-53; **c**: M-128; **d**: M-110.

From the four metabolites formed, one was detected for the first time at t = 0 min, one after 5 min, one at the time point t = 10 min and the last one after 30 min of incubation. For the metabolites formed prior to t = 30 min, a multiple detection in various time points was seen (Table 6.3). Metabolites **a** and **b** were also detected at t = 10 min and t = 30 min. Metabolite **c** was also seen at t= 30 min.

Metabolite	Detection time (min)		
a: M-Ala1	0	10	30
b: M-Ala1 + ring op. Cys3	5	10	30
c: M-Gly2_Ala1	-	10	30
d: M-Lys9	-	-	30

Table 6.3. Time of appearance and other detection times of the four metabolites detected for the [L-Orn4_Msa7_D-Trp8_D-Cys14]-SRIF14 (**13**) somatostatin analogue.

6.3.4 [Msa7_D-Trp8]-SRIF14 (7)

[Msa7_D-Trp8]-SRIF14 (**7**) had been previously synthesised in our group by Dr. Pablo Martín-Gago.[22] As mentioned in Chapter 2, this analogue was the first somatostatin analogue from which a major set of 3D structures could be determined in solution by NMR. Furthermore, its half-life had also been measured by RP-HPLC in collaboration with BCN Peptides S.A. being that of about 25 h.[21] However, that methodology was not sensitive enough to separate the peaks corresponding to the first metabolites (loss of the extracyclic part) from the one of the starting peptide. This lead to overestimate its half-life. To overcome this technical issue, we analysed the analogue again but using Lead Molecular Design's methodology[27] to have an accurate value of its half-life.

The half-life in human serum for **7** was established to be **27 min,** slightly higher than that of the natural hormone but two orders of magnitude lower than the value obtained by RP-HPLC (25 h).[21] Furthermore, this low half-life could be related to a similar degradation pattern than SRIF14.

Analogue **7** displayed three different metabolites (Figure 6.5); first and second generation metabolites were identified and the MS/MS data was acquired for the samples of the first five time points.

Although the modifications introduced did not imply huge differences within the peptide sequence with respect to the natural hormone, the fragmentation pattern changed drastically as only three metabolites were detected and identified. However, the first-formed metabolite, **a**, had been detected before for the natural hormone and both analogues **12** and **13** as a result of an amide bond breakage between the Ala1 and the Gly2. Moreover, metabolite **b** had also been identified in previously studied peptides.

Metabolite **c** could have been formed from either a double amide cleavage of metabolites **a** or **b**; thus cleaving the bonds in between Asn5_Phe6 and Thr12_Ser13.

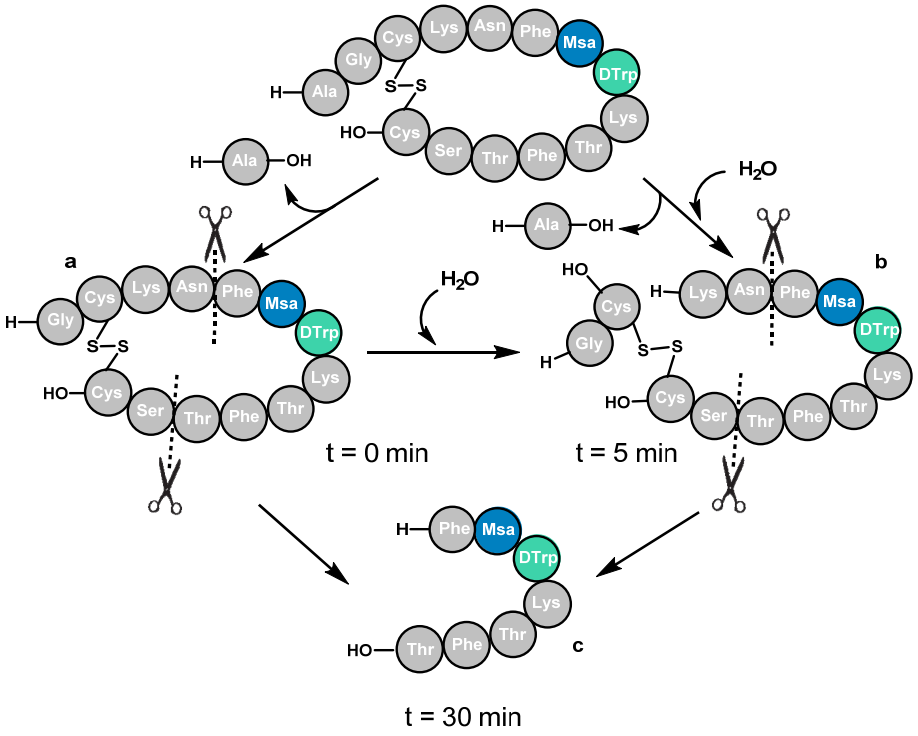

Figure 6.5. Proposed metabolites of [Msa7_D-Trp8]-SRIF14 (**7**) at different times after incubations in human serum detected using UPLC-MS/MS and analysed with WebMetabase and Mass MetaSite. **a**: M-71; **b**: M-53; **c**: M-661.

Metabolite **a** was detected at t = 0 min, **b** after 5 min and the last one, **c**, at time point t = 30 min. For the metabolites formed up to t = 30 min, a multiple detection was seen (Table 6.4). Metabolite **a** was also detected at three more time points (t = 5, 30 and 60 min), metabolite **b** was also identified at t = 30 and 60 min and metabolite **c** at t = 60 min.

Metabolite	**Detection time (min)**			
a: M-Ala	0	5	30	60
b: M-Ala + ring opening	-	5	30	60
c: Phe7-Thr12	-	-	30	60

Table 6.4. Time of appearance and other detection times of the three metabolites detected for the [Msa7_D-Trp8]-SRIF14 (**7**) somatostatin analogue.

6.3.5 [Msa7_D-Trp8_D-Cys14]-SRIF14 (8)

[Msa7_D-Trp8_D-Cys14]-SRIF14 (**8**) was synthesised with the aim to obtain higher half-life through a reinforcement of one end of the disulphide bridge with a D-amino acid. In this case, **8** had a half-life in human serum of **30 min** being twice as much the one obtained for the natural hormone. Although the $t_{1/2}$ had risen, the degradation pattern was similar to the one obtained for SRIF14.

For analogue **8** five different metabolites were detected and only first and second generation metabolites were identified (Figure 6.6). As for analogue **7**, the MS/MS data was acquired for five time points (t = 0, 5, 10, 30 and 60 min) as the experimentally obtained half-life was set to be 30min (doubling SRIF14's one).

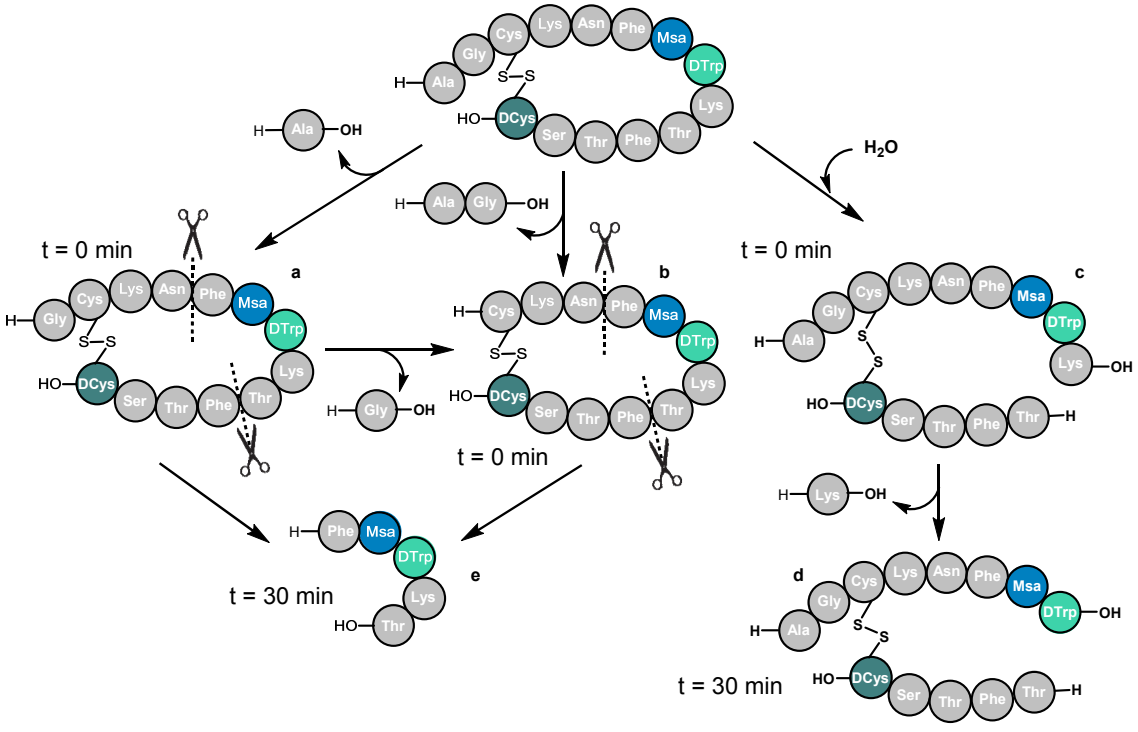

Figure 6.6. Proposed metabolites of [Msa7_D-Trp8_D-Cys14]-SRIF14 (**8**) at different times after incubations in human serum detected using UPLC-MS/MS and analysed with WebMetabase and Mass MetaSite. **a**: M-71; **b**: M-128; **c**: M+18; **d**: M-110; **e**: M-909.

The modifications introduced in the sequence of analogue **8** did not imply a huge difference with respect to the natural hormone. Having seen the fragmentation pattern of **7**, we hypothesised that the pattern for **8** would not change much even though the number of metabolites identified raised up to five. The metabolite resulting from the loss of the Ala1, **a**, had been detected before for the natural hormone and analogues **7**, **12** and **13** as a result of an amide bond breakage between Ala1 and Gly2.

Moreover, both metabolites **b** and **c** had also been identified in previously studied peptides. While **b** is formed by the loss of the Gly2 (from metabolite **a**) or by the loss of the pair Ala1_Gly2 from the starting peptide, metabolite **c** was formed through the ring opening between Lys9 and Thr10. In addition to that, metabolite **d** was formed as a result of the loss of Lys9, through which the ring was previously opened (metabolite **c**). The last identified metabolite, **e**, could have been formed from either a double amide cleavage of metabolites **a** or **b**; thus cleaving the bonds in between Asn5_Phe6 and Thr10_Phe11.

From the metabolites identified, three of them were detected at t = 0 min and the other two after 30 min of incubation. For the metabolites formed up to t = 30 min, a multiple detection in various time points was seen (Table 6.5). Metabolites **a, b** and **c** were also detected at three more time points (t = 5, 30 and 60 min) while metabolites **d** and **e** were also identified at t = 60 min.

Metabolite	**Detection time (min)**			
a: M-Ala1	0	5	30	60
b: M-Gly2_Ala1	0	5	30	60
c: ring opening Lys9	0	5	30	60
d: M-Lys9	-	-	30	60
e: Phe6-Thr10	-	-	30	60

Table 6.5. Time of appearance and other detection times of the five metabolites detected for the [Msa7_D-Trp8_D-Cys14]-SRIF14 (**8**) somatostatin analogue.

6.3.6 [D-Ala1_Msa7_D-Trp8_D-Cys14]-SRIF14 (9)

The modifications introduced in the sequence of analogue **8** triggered an increase in the peptide half-life of about 15min twice as much of that of the SRIF14. That increase combined with the fact that the extracyclic amino acids of the peptide were the first to be cleaved from the sequence, led us to introduce D-Ala in position one to prevent this breakage.

[D-Ala1_Msa7_D-Trp8_D-Cys14]-SRIF14 (**9**) half-life was obtained through the UPLC data[28] which showed a $t_{1/2}$ value of **39 min**. This was a slight improvement with respect to analogue **8** and a significant improvement versus SRIF14. Five different metabolites were detected for peptide **9**,[29] among which first and second generation fragments were identified (Figure 6.7). In this case, MS/MS data was acquired for five time points.

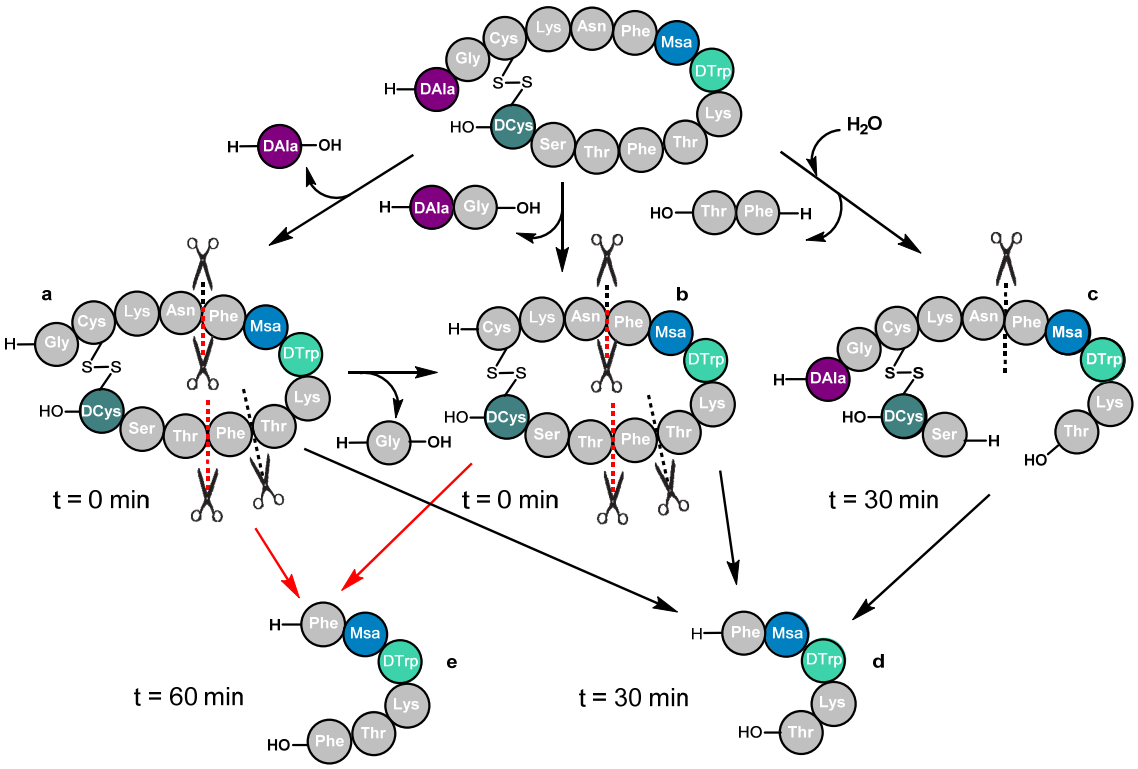

Figure 6.7. Proposed metabolites of [D-Ala1_Msa7_D-Trp8_D-Cys14]-SRIF14 (**9**) at different times after incubations in human serum detected using UPLC-MS/MS and analysed with WebMetabase and Mass MetaSite. **a**: M-71; **b**: M-128; **c**: M-230; **d**: M-909; **e**: M-762.

Contrary to what was expected, the metabolite resulting from the loss of D-Ala in position one, **a**, was the first to be identified, followed by the identification of metabolite **b** in which the pair D-Ala1_Gly2 was lost. Both metabolites were detected at t = 0 min. Metabolite **c** was detected after 30 min. This metabolite was formed as a result of two amide bond cleavage (Thr10_Phe11 and Thr12_Ser13) through the incorporation of water. When talking about metabolite **d**, it could have been formed from metabolites **a, b** and/or **c** through the breakage of Asn5_Phe6 and Thr10_Phe11 bonds (for **a** and **b**) or only the breakage of Asn5_Phe6 amide bond (metabolite **c**). Fragment **e** constitutes a similar case as it could derive from both **a** and/or **b** by breaking the amide bonds between Asn5_Phe6 and Phe11_Thr12.

Metabolites **a** and **b** were detected at t = 0 min, **c** and **d** after 30 min of incubation and **e** at t = 60 min. For the four metabolites formed prior to the first hour of incubation, a multiple detection was seen (Table 6.6). Metabolites **a** and **b** were also detected at three more time points (t = 5, 30 and 60 min) while metabolites **c** and **d** were also identified at t = 60 min.

Metabolite	Detection time (min)			
a: M-DAla1	0	5	30	60
b: M-Gly2_DAla1	0	5	30	60
c: M-Thr12_Phe11	-	-	30	60
d: Phe6-Thr10	-	-	30	60
e: Phe6-Phe11	-	-	-	60

Table 6.6. Time of appearance and other detection times of the five metabolites detected for the [D-Ala1_Msa7_D-Trp8_D-Cys14]-SRIF14 (**9**) somatostatin analogue.

6.3.7 [D-Cys3,14_Msa7_D-Trp8]-SRIF14 (10)

The modifications introduced in the sequence of analogues **8** and **9** increased their half-life in about 15min. Despite that increase, the loss of the extracyclic amino acids of peptide **9** guided the next substitution towards the reinforcement of the disulphide bridge by the introduction of another D-Cys in position three; thus having unnatural amino acids at

both sides of the bridge. We hypothesised that this modification would result in a higher increase of the peptide stability which was further confirmed by the UPLC data[28] as the obtained half-life for peptide **10** was **65 min**. Four metabolites were detected and characterised and first and second generation metabolites were formed during the incubation (Figure 6.8). In this case, the MS/MS data was only acquired for the first five time points.

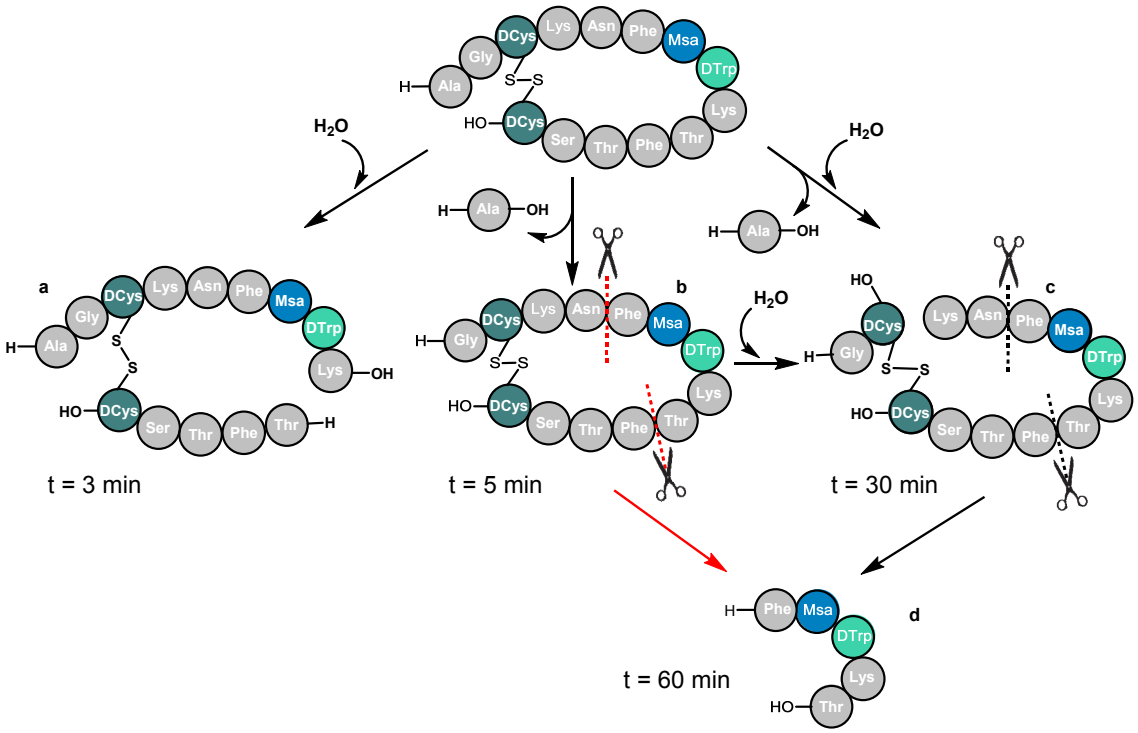

Figure 6.8. Proposed metabolites of [D-Cys3,14_Msa7_D-Trp8]-SRIF14 (**10**) at different times after incubations in human serum detected using UPLC-MS/MS and analysed with WebMetabase and Mass MetaSite. **a**: M+18; **b**: M-71; **c**: M-53; **d**: M-909.

Looking closer into the degradation pattern some differences regarding previous peptide metabolite formation was seen; metabolite **a** was not the result of the loss of neither Ala1 nor the pair Ala1_Gly2 but the consequence of an amide bond breakage in between Lys9 and Thr10. However, both metabolites **b** and **c** were formed after losing the extracyclic amino acid Ala1. Moreover, metabolite **c** also experienced a ring opening between D-Cys3 and Lys4. Furthermore, metabolite **c** could have been formed through two different pathways; directly from the starting peptide (loss of Ala1 and ring opening) or by a

cleavage of the amide bond between DCys3 and Lys4 from metabolite **b**. Metabolite **d** could have also been formed from both metabolites **b** and/or **c** through the breakage of two amide bonds (Asn5_Phe6 and Thr10_Phe11).

For the four metabolites formed prior to the first hour of incubation, a multiple detection was observed (Table 6.7).

Metabolite	Detection time (min)				
a: ring op. Lys9	3	10	30	60	120
b: M-Ala1	5	10	30	60	120
c: M-Ala1 + ring op. DCys3	-	-	30	60	120
d: Phe6-Thr10	-	-	-	60	120

Table 6.7. Time of appearance and other detection times of the four metabolites detected for the [D-Cys3,14_Msa7_D-Trp8]-SRIF14 (**10**) somatostatin analogue.

Metabolite **a** was detected at t = 3 min, **b** after 5 min of incubation, metabolite **c** at t = 30 min and metabolite **d** after an hour. Metabolites **a** and **b** were also detected at four more time points (t = 10, 30, 60 and 120 min) while metabolite **c** was identified at t = 60 and 120 min and **d** was also detected at t = 120 min.

6.3.8 [D-Ala1_D-Cys3,14_Msa7_D-Trp8]-SRIF14 (11)

In light of the findings from peptide **10**, we decided to synthesise one last peptide which agglutinated both the disulphide bridge and the extracyclic part reinforcement. This analogue was established to be [D-Ala1_Cys3,14_Msa7_D-Trp8]-SRIF14 (**11**) which only differed from **10** in the amino acid at position one. Our hypothesis was to obtain a further increase in **11**'s half-life with respect to peptide **10**. Somewhat surprisingly, the half-life of **11** in human serum was **2400 min** (40 h). To the best of our knowledge, this is the 14-amino acid somatostatin analogue with the highest half-life developed until now.

The obtained serum stability samples were further analysed and the degradation pattern obtained (Figure 6.9) in which six different metabolites were identified. From these six fragments, first and second generation metabolites were found. The MS/MS data was acquired for the samples up to t = 2880 min (t = 0 min, 5 min, 10 min, 30 min, 60 min, 120 min, 480 min, 1800 min and 2880 min).

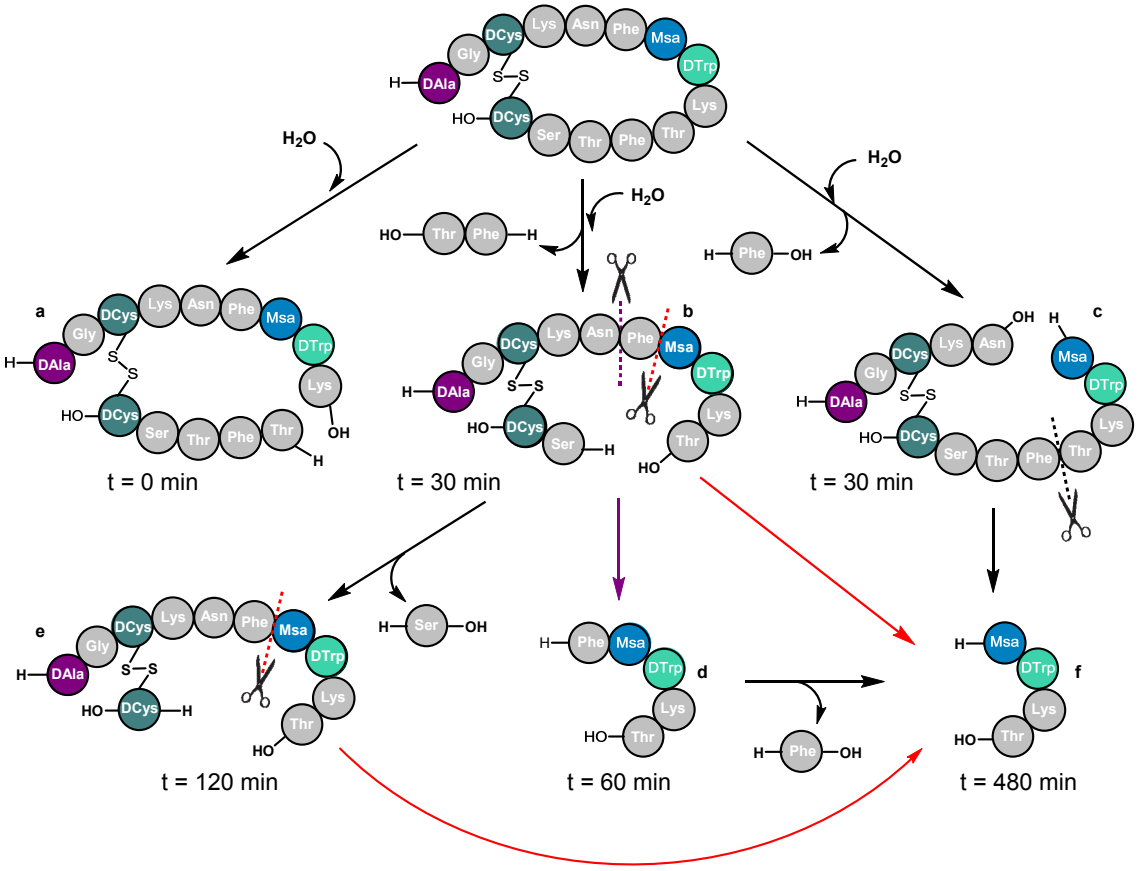

Figure 6.9. Proposed metabolites of [D-Ala1_D-Cys3,14_Msa7_D-Trp8]-SRIF14 (**11**) at different times after incubations in human serum detected using UPLC-MS/MS and analysed with WebMetabase and Mass MetaSite. **a**: M+18; **b**: M-230; **c**: M-129; **d**: M-909; **e**: M-317; **f**: M-1056.

Peptide **11** showed a different degradation pattern when compared to the other peptides of the family which could be attributed to its enhanced stability given by the D-Ala1 and the D-Cys at both sides of the disulphide bridge. Looking at the degradation pattern in more detail, a change into the most frequent fragmentation points was observed; the loss of D-Ala1 or D-Ala1_Gly2 pair was not observed in any of the metabolites formed (**11**). Moreover, the times in which the metabolites were detected also changed. Metabolites of

11 were detected from t = 30 min and onwards with the only exception of metabolite **a** which was detected at t = 0 min.

Metabolite **a** was formed after an amide bond cleavage in between Lys9 and Thr10. After 30 min of incubation, two metabolites, **b** and **c**, were detected thus corresponding to ring opening reactions followed by the loss of one or two amino acids. Metabolite **b** was formed after the ring opening and subsequent loss of the pair Phe11_Thr12 while the ring opening and the following loss of Phe6 resulted in the formation of metabolite **c**.

In fact, it was from this last metabolite, **c**, that the rest of the fragments (**d**, **e** and **f**) were formed. Metabolite **d** may have been formed after the amide bond breakage between Phe6 and Msa7. The cleavage of the amide bond Thr12_Ser13 resulted in the formation of metabolite **e** from which metabolite **f** could have been formed through the breakage of another amide bond (Phe6_Msa7). By the cleavage of the same bond from metabolite **d**, metabolite **f** was achieved. In addition to that, **f** could have been formed through the cleavage of Phe6_Msa7 from metabolite **c**.

For the six metabolites formed prior to the first eight hours of incubation, a multiple detection was observed (Table 6.8).

Metabolite	**Detection time (min)**								
a: ring op. Lys9	0	5	10	30	60	120	480	1800	2880
b: M-Thr12_Phe11	-	-	-	30	60	120	480	1800	2880
c: M-Phe6	-	-	-	30	60	120	480	1800	2880
d: Phe6-Thr10	-	-	-	-	60	120	480	1880	2880
e: M-Ser13-Phe11	-	-	-	-	-	120	480	1880	2880
f: Phe6-Thr10	-	-	-	-	-	-	480	1800	2880

Table 6.8. Time of appearance and other detection times of the six metabolites detected for the [D-Ala1_D-Cys3,14_Msa7_D-Trp8]-SRIF14 (**11**) somatostatin analogue.

Metabolite **a** was detected at t = 0 min, **b** and **c** after 30 min of incubation, **d** at t = 60 min, **e** after two hours (120 min) and **f** after eight hours (480 min). Metabolite **a** was also detected at t = 5, 10, 30, 60, 120, 480, 1800 and 2880 min. Metabolites **b** and **c** were also

detected at five more time points (t = 60, 120, 480, 1800 and 2880 min) while metabolite **e** was identified at t = 120, 480, 1800 and 2880 min and **f** at t = 480, 1800 and 2880 min.

6.4 Binding assays

The binding affinity of both analogues containing the natural amino acid L-Orn in position four (**12** and **13**) were not studied due to their low half-life which resembled the natural hormone.

As previously described for the Dmp and Pya's peptide families, the binding activity against all five somatostatin receptors (SSTR1-5) was measured for the new four analogues containing D-Cys (**8**-**11**) together with the previously synthesised[21] peptide **7** and somatostatin. They were performed following the protocol designed by Rens-Domiano *et al.*[30] as previously mentioned. These assays were performed externally by Eurofins Scientific.[31] As it happened with the binding assays of the other peptide families, the raw data obtained for these SRIF14 analogues had to be normalised.[32] Binding affinity values of the analogues containing D-amino acids together with the ones for the natural SRIF14, expressed as Ki values, are shown in Table 6.9.

Normalised data illustrates that all analogues (**7** - **11**) show an outstanding affinity against SSTR2 which resemble the one of the natural hormone for the same receptor while the activity against the other receptors decreases significantly. The only exception is the binding affinity that compound **7** displays for SSTR1, which also resembles SRIF14.

Therefore the stable analogue **11** showed even better binding profile versus SSTR2 than analogue **7**.

[30] S. Rens-Dominano, S. F. Law, Y. Yamada, S. Seino, G. I. Bell, T. Reisine, *Mol. Pharmacol.*, **1992**, *42*, 28 - 34.

[31] Eurofins Panlabs Taiwan Ltd., 158 Lide Road Beitou, District 112, Taipei, Taiwan. www.eurofins.com

[32] Ki values have been normalised using the protocol described in Chapter 3.4. Ki values of Table 3.2 and 4.1 have been obtained with the same normalization protocol.

	SSTR1 (nM)	SSTR2 (nM)	SSTR3 (nM)	SSTR4 (nM)	SSTR5 (nM)
Somatostatin-14	3.07	0.036	0.53	3.75	2.50
[Msa7_D-Trp8]-SRIF14 (7)*	2.36	0.054	7.47	$>10^3$	$>10^3$
[Msa7_D-Trp8_D-Cys14]-SRIF14 (8)	43.83	0.015	63.36	68.78	45.08
[D-Ala1_Msa7_D-Trp8_D-Cys14]-SRIF14 (9)	11.47	0.014	52.80	84.41	44.18
[D-Cys3,14_Msa7_D-Trp8]-SRIF14 (10)	22.45	0.023	49.37	150.07	43.73
[D-Ala1_D-Cys3,14_Msa7_D-Trp8]-SRIF14 (11)	10.69	0.034	6.86	25.95	14.02

Table 6.9. Normalised binding selectivity values (Ki values) of D-amino acid containing somatostatin analogues against SSTR1-5. Ki values express inhibition in a competitive assay of somatostatin analogues against radio-labelled SRIF. Due to the small number of repetitions, the values are shown without their error. Raw data is shown in Chapter 9, section 9.2.4 *Peptide previously synthesised.[22]

6.5 Structure determination

The outstanding stability and binding profile of peptide [D-Ala1_D-Cys3,14_Msa7_D-Trp8]-SRIF14 (**11**) led us to analyse it as a TFA salt by NMR spectroscopic techniques in phosphate buffer at pH = 6.5 and both bidimensional homonuclear ^{1}H-^{1}H TOCSY and ^{1}H-^{1}H NOESY were obtained. The process was as described in Chapter 3.3 of the present doctoral thesis. After identifying all the NOE signals,[33] peaks were integrated and the volumes introduced in the CNS program[34] using the StructCalc platform.[35] A variable number of calculations were set up until the lower energy structures were convergent, coherent with the experimental values and the dihedral angles did not violate the Ramachandran diagrams.[36]

[33] K. Wuethrich, G. Wider, G. Wagner, W. Braun, *J. Mol. Biol.*, **1982**, *155*, 311 - 319.

[34] A. T. Brunger, P. D. Adams, G. M. Clore, W. L. DeLano, P. Gros, R. W. Grosse-Kunstleve, J. S. Jiang, J. Kuszewski, M. Nilges, N. S. Pannu, R. J. Read, L. M. Rice, T. Simonson, G. L. Warren, *Acta Crystallogr. D Biol. Crystallogr.*, **1998**, *54*, 905 - 921.

[35] P. Martín-Malpartida, M. J. Macias, unpublished data.

[36] G. N. Ramachandran, C. Ramakrishnan, V. Sasisekharan, *J. Mol. Biol.*, **1963**, *7*, 95 - 99.

The acquired NMR data for [D-Ala1_D-Cys3,14_Msa7_D-Trp8]-SRIF14 analogue (**11**) clearly showed that this peptide was more rigid than the natural SRIF in solution due to the high density of NOE signals. Even though some conformational variability of the extra cyclic side chains was observed, the major set of conformations in solution could be elucidated with high convergence of the peptidic backbone and intracyclic side chains (Figure 6.10).

After assigning the NOE peaks, it could be confirmed that the inclusion of D-Trp in position 8 enhances the aliphatic-aromatic interaction between D-Trp8_Lys9 which is translated into a higher shielding of Hγ of Lys9 and it also triggers a stabilization of the β-turn of the peptide.

As previously seen in our group, the inclusion of Msa in position 7 favours the formation of rigid-enough 3D structures in solution.[21] As the modifications introduced in analogue **11** were introduced in the extracyclic part and in the disulphide bridge, we hypothesised that the 3D structure would show great similarity with the one previously obtained for the analogue **7**.

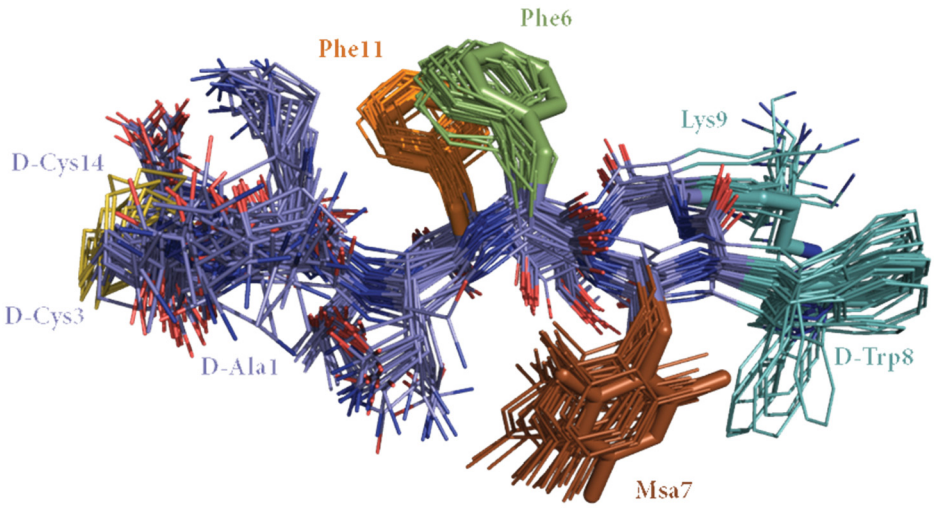

Figure 6.10. Superimposition of the 25 lower energy structures of [D-Ala1_D-Cys3,14_Msa7_D-Trp8]-SRIF14 (**11**) which are in agreement with experimental NMR data.

As it happened with the analogues from previous chapters, **11** also displayed sufficient information in the bidimensional NMR experiments to determine a major set of conformations in solution. As shown in Figure 6.10, there is a π-π aromatic interaction between Phe6 and Phe11 while Msa7 is placed at the other side of the molecule.

Altough the geometry of the most stable set of conformations is very similar to that of **7**, the geometry of the 6-to-11 interaction is different from the ones observed until now; an *offset-stacked* geometry which is not completely flat due the a close spatial proximity between Hβ of Phe11 with H_{AR} of Phe6 (Figure 6.11). At the same time, Msa7 does not participate in the aromatic interaction and is placed at the other side of the molecule with the same orientation than the Phe6_Phe11 pair.

This orientation was supported by some long-distance NOE signals: interaction of Hβ of Asn5 and Hγ of Thr12 with Hε of Msa7, Hφ of Msa7 with Hγ of Thr12 and Thr10. Furthermore, the D-Trp8_Lys9 pair shows high denisity of NOE signals between them which is translated in a closer proximity in space. As a consequence of the little volume of NOE signals between that pair and the rest of the molecule D-Trp8_Lys9 face the outside of the peptidic backbone. Due to this lack of NOE signals, two different populations of orientation of the pair were found being the most populated the one which was oriented to the same side of the molecule that Phe6 and Phe11.

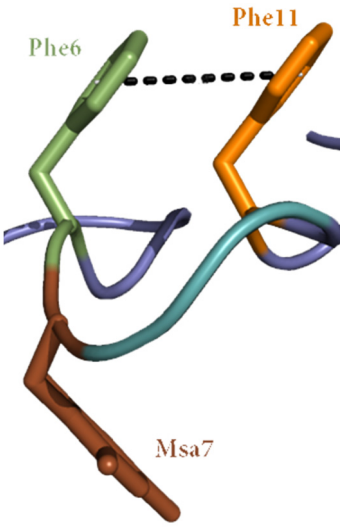

Figure 6.11. Lateral view of the *offset-stacked* π-π aromatic interaction between Phe6 and Phe11.

6.6 Discussion and conclusions

We have successfully synthesised five new analogues containing either L-Orn or the non-natural amino acids D-Ala and D-Cys in different positions. These substitutions were performed to positions believed to be key breakage points which were also important in the determination of the analogues' half-lives. Furthermore, peptide **11** reached a rigid-enough set of 3D structures in solution when containing the non-natural amino acids D-Ala and D-Cys as demonstrated by the NMR spectroscopy experiments. Moreover, the obtained set of conformations for peptide **11** resembled the one found for the previously synthesised [Msa7_DTrp8]-SRIF14 (**7**).

We have studied two new somatostatin analogues containing the natural amino acid L-Orn in their sequence in substitution of Lys4. Even though we expected to obtain peptides with increased half-life, the results showed an opposite behaviour of these analogues being really similar to the natural hormone (15 min for SRIF14 and **12** and 13 min for analogue **13**).

Due to the low $t_{1/2}$ of both **12** and **13**, we decided not to perform neither the binding nor the NMR studies as they would not represent an improvement to previously obtained analogues.

The most promising analogue to date, peptide 7 was analysed following the methodology applied for the new compounds. Analogue **7** half-life has been already published[21] but without being able to separate the parent compound from the first formed metabolite (loss of Gly2_Ala1). In the present doctoral thesis we used a more sensitive technique which enabled us to discriminate between these two compounds thus obtaining a more accurate value for the $t_{1/2}$. In our case, the experimentally obtained half-life was shown to be 27 min only two times higher than the natural hormone.

Therefore, our strategy was to introduce modifications one by one to be able to evaluate the effects in both the half -life and the degradation pattern of the analogue. The introduction of a D-Cys in position fourteen (**8**) induced a two-fold increase in the half-life when compared to the natural SRIF. Seeing that one of the major fragments formed was the one resulting from the loss of residue 1 or both residues 1 and 2 (present in **7**-**10** and **8**-**9** respectively), we decided to study the peptide which combined the introduction of a D-Ala at position one with a D-Cys at position fourteen (**9**). This analogue showed a half-life of 39 min comparable to that obtained for peptide **8**. In light of these findings, our hypothesis was that the sole introduction of the D-Ala at the extracyclic part did not introduce a significant change in the peptide structure to induce a significant increase of the $t_{1/2}$ value.

Seeing that metabolite **d** from somatostatin (Figure 6.2) was also present in peptides **7, 12** and **13,** we hypothesised that the introduction of the non-natural amino acid D-Cys at both sides of the disulphide bridge would trigger an enhancement of peptide's half-life as the amide bond cleavage between D-Cys3_Lys4 would be impeded as peptidases would not recognise the D-amino acid. The experimentally obtained half-life was 65 min which represented a four-fold increase when compared to the natural hormone and a two-fold increase with respect to previous analogues (**7**, **8** and **9**).

The formation of a metabolite in which the ring had been opened in between residues three and four (metabolite **d** of the natural hormone, Figure 6.2) was not detected for peptide **9**. For that reason, we decided to combine the modifications of peptide **9** with the ones of peptide **10**, thus obtaining the analogue [D-Ala1_D-Cys3,14_Msa7_D-Trp8]-SRIF14 (**11**). The results were unexpectedly good when introducing both modifications. The half-life for peptide **11** was established to be 2400 min (40h), a 160-fold increase when compared to the natural SRIF14 and a 37-fold increase with respect to peptide **10**. These results indicate that both the D-Ala1 and the D-Cys3,14

are necessary for the stabilisation of the analogue. Due to the modifications introduced in this analogue (**11**), the obtained fragmentation pattern differed from the ones obtained previously; only metabolite **a** was also present in the degradation pattern of the parent compound (metabolite **c**, Figure 6.2).

One of the main objectives of the synthesis of these D-Cys-containing analogues was the obtainment of 14-amino acid somatostatin analogues which retain the selective binding for SSTR2 that [Msa7_D-Trp8]-SRIF14 (**7**) displayed previously. The binding assays were externally performed and we were pleased to corroborate that, indeed, analogues **8**-**11** were still selective for SSTR2.

Considering the excellent binding profile and stability displayed by peptide **11**, we decided to acquire its NMR spectra. As the modifications were introduced at both the *C*- and *N*-terminal parts of the peptide, we hypothesised that the structure would not experiment major changes. After acquiring the NMR spectra and performing the theoretical structure calculations, we were able to establish that the structure of peptide **11** strongly resembles the one obtained for peptide **7.**[21] The main differences were that the π-π aromatic interaction on peptide **11** has an *offset-stacked* geometry while it was *edge-to-face* for peptide **7** and that **11** displays a more ordered extracyclic part than **7**.

In conclusion, using the degradation patterns and the formation of different metabolites of several peptides we have been able to design and synthesise a new analogue (**11**) which displayed a half-life of 2400 min which represented a 160-fold increase in the values of the $t_{1/2}$ obtained for the natural hormone. Furthermore, the four D-Cys-containing analogues (**8**-**11**) maintained the binding affinity for SSTR2 resembling the one of the natural hormone. In addition to this, a 3D structure in solution of the main set of conformations was also obtained for peptide **11**. Remarkably, these conformations strongly resemble the ones of peptide **7** the most promising 14-aa SRIF analogue to date.

Chapter 7

SRIF analogues as carriers or drug delivery systems (DDS)

7.1 Introduction

The concept of targeted drugs dates back to 1906 when Ehrlich[1] first postulated the 'magic bullet' concept. Nowadays this concept still endures and it is an indication of its appeal. However, it continues to be a challenge to be implemented in real clinic. Its difficulty lies in three different fronts: i) finding a proper target for the desired disease; ii) designing a drug that effectively treats the disease and iii) finding a proper carrier which can transport the drug in a stable form to the specific site while avoiding the immunogenic and non-specific interactions that could clear the drug from the body.

As drugs are distributed through the body by the blood circulation, only a small portion of the therapeutic agents reach the affected organ; in chemotherapy only ~1% of the administered drug reaches the tumour site.[2] Due to that inefficacy in reaching the desired target new strategies have been designed. Among these, targeted drug delivery seeks to concentrate the medication in the tissues of interest while reducing the relative concentration of the drug in the healthy tissues. A plausible approach would be avoiding the host's defence mechanisms and inhibiting the non-specific distribution in the liver,[3] so as the drug-delivery system can reach the intended site of action in higher concentrations; that way the efficacy could be improved and side-effects reduced.

Furthermore, the mechanism and pathway through which the drug would be released inside the body is also an element which has to be controlled and optimised. In that sense, light-assisted drug-delivery systems (DDS) have been developed. These DDS transport a pharmaceutical compound to a specific part of the body so as the drug can play its desired therapeutic effect after being released by a light source.

---

[1] P. Ehrlich, The collected papers of Paul Ehrlich, *Pergamon*, London, **1960**, 3.

[2] A. Trafton, MIT Tech Talk, **2009**, *53*, 4 - 4.

[3] N. Bertrand, J. C. Leroux, *J. Control. Release*, **2012**, *161*, 152 - 163.

To explore the suitability of somatostatin as a carrier or as a DDS, we considered that it would be useful to introduce a fluorophore or a photo-cleavable fluorophore into a somatostatin analogue's sequence to be able to follow its internalisation in cells. The synthesis of the 14-amino acid somatostatin analogues with different fluorescent groups and the *in vitro* studies will be discussed in this chapter.

7.2 Synthesis of SRIF14 analogues with fluorescent groups

Peptides modified with fluorescent dyes and photo-cleavable fluorescent groups are valuable tools with many uses in biochemical research. These compounds have become a promising tool for protein analysis in drug discovery, diagnostics and biological research in the last few years.[4] Furthermore, fluorescent derivatives of biologically active peptides have become useful experimental tools for studying biological structures and functions[5] as well as valuable tools for the visualization of intracellular processes or molecular interactions.[6,8,9]

7.2.1 Simple fluorescent groups

Coumarins are well-known for their extensive and diverse applications as fluorescent probes or labels.[7] These compounds exhibit an extended spectral range, are photo-stable and have high emission quantum yields. Fluorescent molecules are important for use as molecular probes and labels in biological research[8] and in commercial assays.[9] While a

[4] D. Stoll, J. Bachmann, M. F. Templin and T. O. Joos, DDT: Targets, **2004**, *3*, 24 - 31.

[5] J.-M. Soleilhac, F. Cornille, L. Martin, C. Lenoir, M.-C. FourniJ-Zaluski, B. P. Roques, *Anal. Biochem.*, **1996**, *241*, 120 - 127.

[6] a) G. Turcatti, H. Vogel and A. Chollet, *Biochemistry*, **1995**, *34*, 3972–3980; b) D. J. Cowley, A. J. Schulze, J. *Pept. Res.*, **1997**, *49*, 444 - 454.

[7] a) A. P. deSilva, H. Q. N. Gunaratne, T. Gunnlaugsson, A. J. M. Huxley, C. P. McCoy, J. T. Rademacher, T. E. Rice, *Chem. Rev.*, **1997**, *97*, 1515 - 1566; b) S. R. Trenor, A. R. Shultz, B. J. Love, T. E. Long, *Chem. Rev.*, **2004**, *104*, 3059 - 3077.

[8] D. L. Rousseau, *Optical Techniques in Biological Research*; Academic: New York, **1984**; Chapter 4.

[9] a) P. G. Mattingly, *Bioconjugate Chem.*, **1992**, *3*, 430 - 431; b) M. Adamczyk, J. Fishpaugh, C. Harrington, D. Hartter, D. Johnson, A. Vanderbilt, *J. lmmunol. Methods*, **1993**, *162*, 47 - 58; c) J. R. Fino, M. T. Shipchandler, L. D. Klein, C. L. Kirkemo, *Anal. Biochem.*, **1987**, *162*, 89.

variety of fluorescent probes have been reported,[10] coumarin derivatives are frequently used for their great fluorescence upon excitation above 330 nm.[11] The fluorescence is dependant of various factors: i) the pH of the medium, ii) the substituents of the coumarin and iii) the microenvironment of the fluorescent-probe.[12]

In this regard, we thought that it could be of interest to introduce the 4-methy-7-hydroxycoumarin (4-Methylumbelliferone, 4-MU, Figure 7.1) into a somatostatin derivative.[13] We hypothesised that the introduction of 4-MU at the *N*-terminal part of a 14-aa SRIF analogue would be helpful in the elucidation of the internalisation process.

The initial strategy was to synthesise a short model peptide (4-5 amino acids) and attach the 4-MU at the *N*-terminal part of the chain by a carbamate bond. To perform this coupling we thought that we could synthesise a carbamate at the amino moiety of the alanine so as to couple it to the rest of the peptidic chain by SPPS as a building block. The synthetic route for the obtainment of the carbamate compound is shown in Figure 7.1.

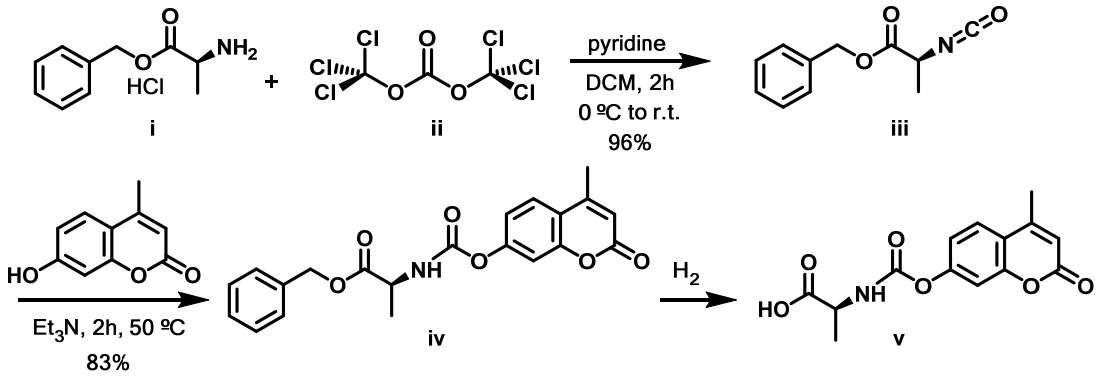

Figure 7.1. Synthesis of carbamate (**v**) from the isocyanate (**iii**) and 4-MU.

[10] R. P. Haughlund, Handbook of Fluorescent Probes, **1992**.

[11] a) Y. Forster, E. Haas, *Anal Biochem.,* **1993**, *209,* 9 - 14; b) J. E. T. Corrie, *J. Chem. Soc., Perkin Trans. 1,* **1994**, *0*, 2975 - 2982.

[12] a) S. A. Haroutounian, J. A. Katzenellenbogen, *Tetrahedron*, **1995**, *51*, 1585 - 1598; b) E. Musgrove, C. Rugg, D. Hedley, *Cytometry*, **1986**, *7*, 347 - 355.

[13] a) T. Nakamura, K. Takagaki, S. Shibata, K. Tanaka, T. Higuchi, M. Endo, *Biochem Biophys Res Commun.*, **1995**, *208*, 470 - 475; b) D. Kudo, A. Kon, S. Yoshihara, I. Kakizaki, M. Sasaki, M. Endo, K. Takagaki, *Biochem. Biophys. Res. Commun.*, **2004**, *321*, 783 - 787; c) D. Vigetti, M. Rizzi, M. Viola, E. Karousou, A. Genasetti, M. Clerici, B. Bartolini, V. C. Hascall, G. De Luca, A. Passi, *Glycobiology*, **2009**, *19*, 537 - 546; d) X. Cheng, N. Sato, S. Kohi, A. Koga, K. Hirata, *Oncol. Lett.*, **2018**, *15*, 6297 - 6301.

The synthesis of the isocyanate **iii** from the benzyl-protected alanine (**i**) and triphosgene (**ii**) proceeded without major problems and with excellent yield (96%) after 2h of reaction. In the same way, the carbamate formation (**iv**) took place within the same time (2h) and with good yield (83%). So, indeed, we managed to synthesise the desired compound (**iv**). However, after some tests we noticed that the carbamate bond was more labile than expected when introduced in aqueous media which we attributed to the leaving group properties of the phenol ring of the 4-MU. At that point, we decided to follow the decomposition reaction by ^{1}H-NMR which enabled us to see that the product degraded within 9 hours (Figure 7.2).

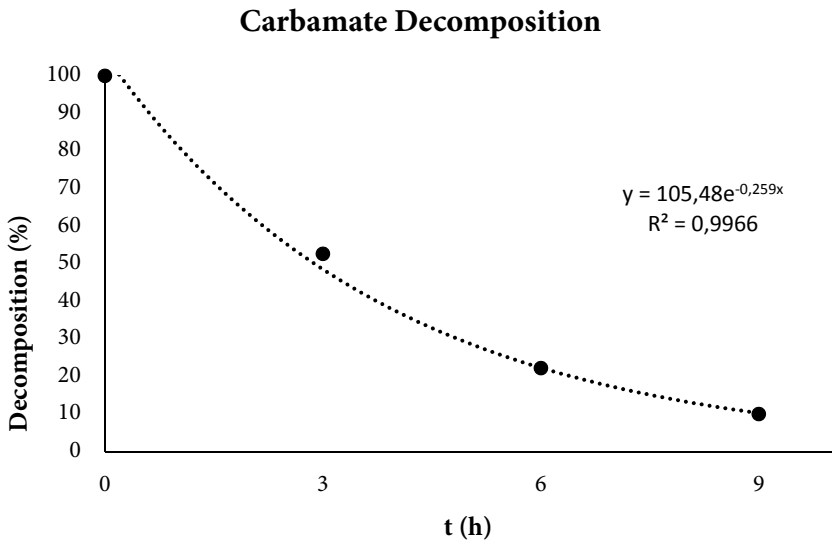

Figure 7.2. Decomposition of the carbamate bond in a buffer solution (NH_4HCO_3, 10 mM : H_2O, 1:1). Percentages of the remaining compound were obtained from the ^{1}H-NMR spectra.

With that results in hand, we decided to change the synthetic strategy and use another coumarin in which the bond between it and the linker or the SRIF14 analogue was not made through the phenol moiety. The new chosen fluorescent coumarin was the (7-methoxycoumarin-4-yl)-acetic acid (Mca, Figure 7.3) which has been previously proposed as a fluorophore for thimet peptidase, pitrilysin and MMP substrates.[14]

[14] a) C. G. Knight, F. Willenbrock, G. Murphy, *FEBS Lett.*, **1992**, *296*, 263–266; b) A. Anastasi, C. G. Knight, A. J. Barrett, *Biochem. J.*, **1993**, *290*, 601–607; c) H. Nagase, C. G. Fields, G. B. Fields, *J. Biol. Chem.*, **1994**, *269*, 20952–20957.

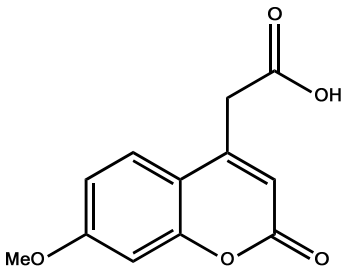

Figure 7.3. Chemical structure of (7-methoxycoumarin-4-yl)-acetic acid (Mca).

Mca has been used before as a fluorescent probe and its absorption and fluorescence data has been published elsewhere.[15] Katritzky *et al.* reported that when linked to a two-amino acid peptide the absorption and emission wavelengths were around 320 nm and 380 nm respectively. From that data, we hypothesised that the wavelengths would not suffer a dramatic change if the fluorophore was attached to a longer peptide with a linker in between.

Fluorescently labelled peptides can be achieved by the reaction of the peptide in solution with an activated form of the coumarin, however a potentially more effective approach is to assemble the peptide chain on a solid phase and incorporate the fluorophore onto the peptide attached to the solid support.[16] Two different compounds were synthesised; in the first one (**14**) the linker and the coumarin were attached to the natural hormone and in the second one (**15**), they were attached to our most stable peptide (**11**) described in Chapter 6.

We believed that compound **15** would be internalised together with the receptor as some other studies indicated for these type of transmembrane receptors.[17] The described mechanism of internalisation consisted of the binding of the compound (agonist) to the SSTR, which activated the G-proteins and inhibited the adenylyl cyclase (AC), activated

[15] A. R. Katritzky, M. Yoshioka, T. Narindoshvili, A. Chung, J. V Johnson, *Org. Biomol. Chem.*, **2008**, *6*, 4582 - 4586.

[16] a) J. Fernandez-Carneado, E. Giralt, *Tetrahedron Lett.*, **2004**, *45*, 6079–6081; b) P. J. A. Weber, J. E. Bader, G. Folkers, G. Beck-Sickinger, *Bioorg. Med. Chem. Lett.*, **1998**, *8*, 597–600.

[17] a) D. Calebiro, V. O. Nikolaev, L. Persani, M. J. Lohse, *Trends Pharmacol. Sci.*, **2010**, *31*, 221 - 228; b) F. Gatto, L. J. Hofland, *Endocr. Relat. Cancer*, **2011**, *18*, R233 - 51.

K^+ channels and inhibited Ca^{2+} channels. After agonist activation, the receptors were phosphorylated and recruited by the cytoplasmic proteins (arrestins). At that point, the internalised receptor was directed to the endosomes in which it was dephosphorylated, dissociated from the arrestins and directed to different intracellular compartments, leading to recycling or degradation. The receptor was recycled back to the plasma membrane as a functional receptor.

Compounds **14** and **15** were synthesised by SPPS while introducing a linker (Fmoc-8-amino-3,6-dioxaoctanoic acid, Fmoc-O2Oc-OH) between the somatostatin (or the analogue) and the fluorophore. Synthesis of compound **15** is shown as an example in Scheme 7.1.

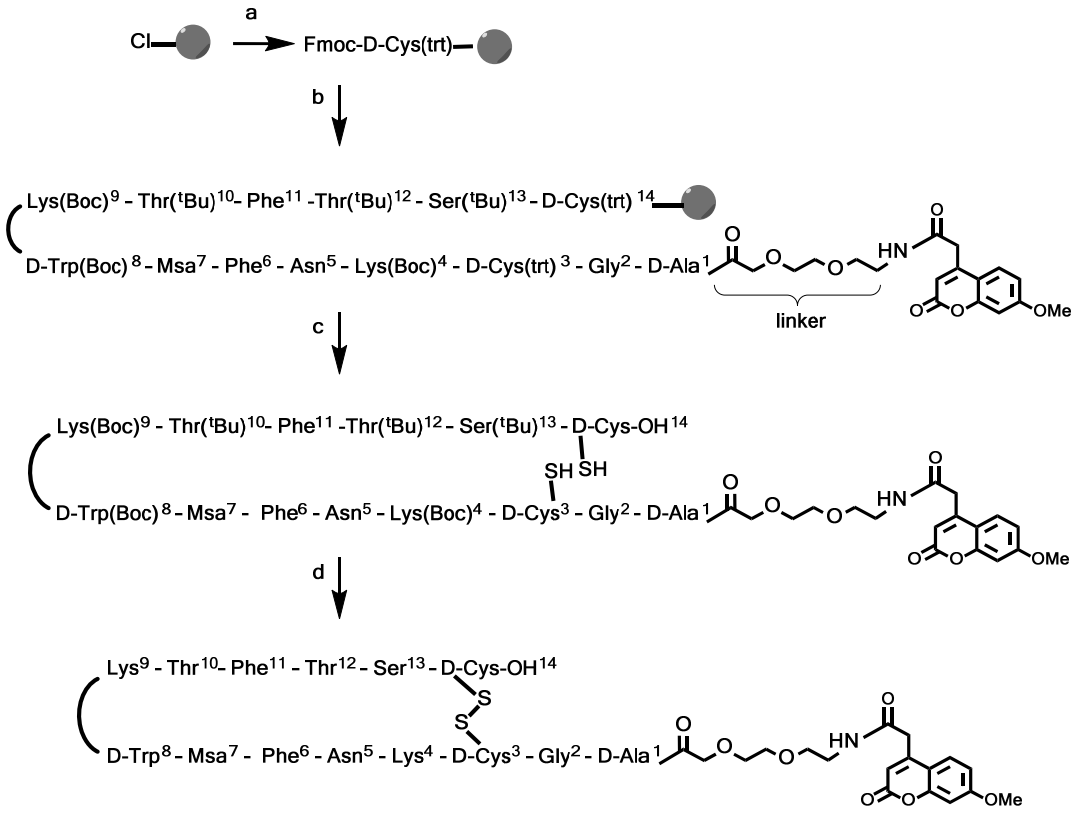

Scheme 7.1. SPPS of [D-Ala1_D-Cys3,14_Msa7_D-Trp8]-(8-amino-3,6-dioxaoctanoic acid)-((7-methoxy-coumarin-4-yl)-acetic acid) (**15**). a) 1. Fmoc-D-Cys(trt)-OH (3eq), DIEA (3eq), 2. MeOH; b) 1. Piperidine 20% in DMF, 2. Fmoc-AA-OH (1.5-3eq), DIPCIDI (3eq), HOBt (3eq), DMF; 3. Piperidine 20% in DMF, 4. Fmoc-O2Oc-OH (3eq), DIPCIDI (3eq), HOBt (3eq), DMF, 5. Piperidine 20% in DMF, 6. (7-Methoxycoumarin-4-yl)-acetic acid (3eq), DIPCIDI (3eq), HOBt (3eq), DMF c) DCM/TFE/AcOH, d) 1. I_2, 2. TFA/DCM/anisole/H_2O.

The completion of the linker and coumarin coupling reactions was followed by both Kaiser tests and UPLC-MS. The control mass spectra of the linear version of compound **15** is shown in Figure 7.4.

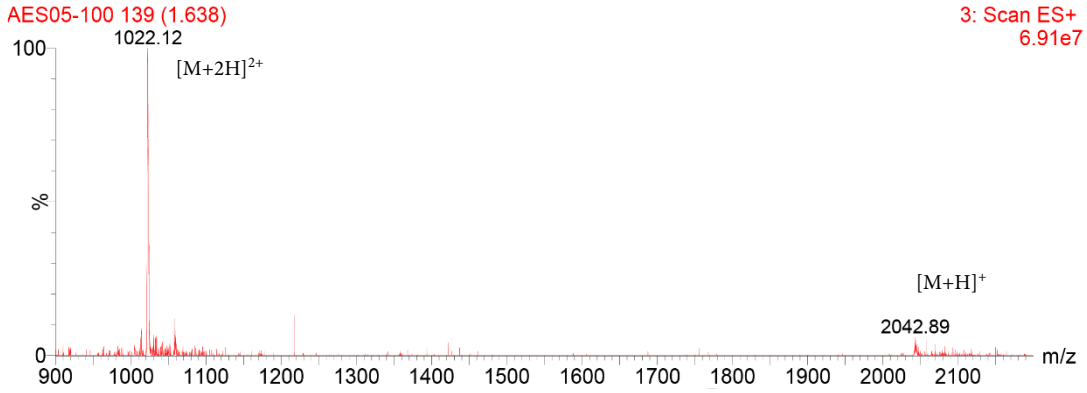

Figure 7.4. Mass spectra of the linear version of compound **15**. The expected mass of compound **15** is 2041.33; both $[M+H]^+$ (*m/z* 2042.89) and $[M+2H]^{2+}$ (*m/z* 1022.12) peaks were observed.

After the cyclisation and side chain deprotection, a purification was needed. Peptides **14** and **15** were purified by semi-prep RP-HPLC (25-60% ACN + 0.1% TFA in 30 min, 1 mL/min, λ = 220 nm) and obtained with purity above 95%. HRMS were also performed for both peptides thus corroborating that we had obtained the expected compounds.

From these two compounds, only **15** was tested *in vitro* due to the low half-life results obtained in Chapter 6 for the native somatostatin. Furthermore, SRIF14 is not receptor-selective while peptide **11** was selective for SSTR2 as demonstrated in the previous chapter. We hypothesised that both compounds **14** and **15** would maintain the same biological activity and binding selectivity that their parent compounds (natural hormone and peptide **11** respectively).

To test the compound **15,**[18] CHO-K1 cells (wild type and with the SSTR2 overexpressed) were incubated with 10 μM of the fluorescent compound **15** for one hour at 37ºC and with 5% of CO_2. After that time, the compound was supposed to be internalized and the

[18] Compound **14** was discarded for these experiments due to the low half-life of the natural hormone found in Chapter 6 of the present thesis.

cells were observed using a TIRF-ScanR Olympus microscope. A cell or a set of cells was selected for each type (Figure 7.5 a and b) and observed under the same conditions. Both cell types were irradiated at λ = 377/50 nm and absorbance detected at λ = 447/60 nm.

Under these conditions, we observed that CHO-K1 cells with SSTR2 overexpressed (CHO-K1 ST) showed fluorescence (Figure 7.5 d) while for the wild type CHO-K1 cell line (CHO-K1 WT) any fluorescence was observed (Figure 7.5 c).

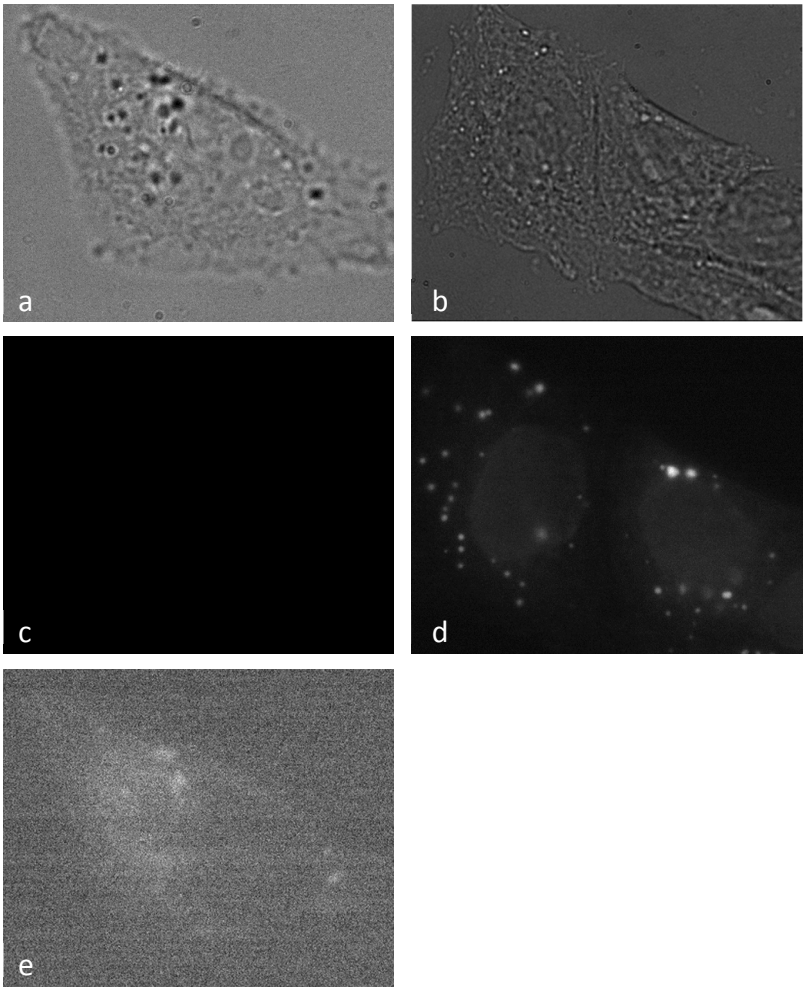

Figure 7.5. Microscope images of the cellular internalisation of compound **15**: a) bright field image of CHO-K1 wild type cell; b) bright field image of CHO-K1 ST cells; c) fluorescence image of CHO-K1 WT cells; d) fluorescence image of CHO-K1 ST cells; e) fluorescence image of CHO-K1 WT cells close to the background level.

From this studies we hypothesized that peptide **15** was a selective analogue for cells overexpressing the SSTR2 and that it had no activity against the wild type cell line. However, when the detection level was decreased close to the background level, a tenuous fluorescence was observed in the CHO-K1 WT cells (Figure 7.5 e). This weak fluorescence could be due to the passive diffusion of compound **15** into the cell or due to other internalisation mechanisms rather than through the G-protein-coupled transmembrane receptors.

7.2.2 Photo-labile fluorescent groups

The *p*-hydroxyphenacyl (*p*HP) group has been used as an efficient photo-trigger for the study of fast biological processes like the release of nucleotides[19] and the release of neurotransmitters and secondary messengers.[20] Furthermore, *p*HP group is well-known for its rapid and clean release, its high photochemical efficiency, its synthetic accessibility, its easy introduction on most substrates and the formation of a transparent (causing no inner-filter effect) biocompatible photoproduct. The cleavage of *p*HP group takes place in a four-step mechanism displayed in Figure 7.6;[21,22] a) formation of a triplet intermediate, b) deprotonation of the phenolic group, c) bond reorganisation to a putative spirodienedione (Favorskii intermediate) and d) hydrolytic ring opening of the spirodiketone leading to the *p*-hydroxyphenylacetic acid. However, its major drawbacks are its nonfluorescent character and its excitation wavelength below 400 nm. [22]

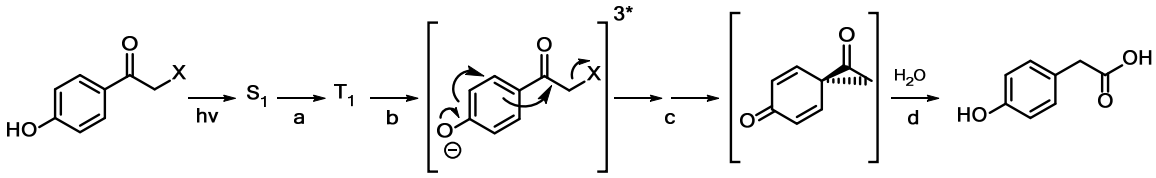

Figure 7.6. Photo-release of the pHP group by the photo-Favorskii mechanism.

[19] a) K. Zou, S. Cheley, R. S. Givens, H. Bayley, *J. Am. Chem. Soc.*, **2002**, *124*, 28, 8220 - 8229; b) R. S. Givens, C. H. Park, *Tetrahedron Lett.*, **1996**, *37*, 6259 - 6262.

[20] R. S. Givens, A. Jung, C.-H. Park, J. Weber, W. Bartlett, *J. Am.Chem. Soc.*, **1997**, *119*, 8369 - 8370.

[21] J. C. Anderson, C. B. Reese, *Tetrahedron Lett.*, **1962**, *3*, 1 - 4.

[22] S. Barman, S. K. Mukhopadhyay, S. Biswas, S. Nandi, M. Gangopadhyay, S. Dey, A. Anoop, N. D. A. Pradeep Singh, *Angew. Chem. Int. Ed.*, **2016**, *55*, 4194 - 4198.

Barman *et al.*[22] designed an analogous *p*HP-benzothiazole compound the excitation wavelength of which was above 400 nm and which also maintained the above mentioned properties. The resulting compound should exhibit a rapid and clean release of the active molecules in the visible wavelength region and with a strong fluorescence. They claimed that their new photo-trigger would be a better option than the existing *o*-nitrobenzyl,[23] coumaryl-methyl[24] and quinoline[25] derivatives as photo-responsive drug-delivery systems. Barman *et al.*'s analogue included an excited-state intermolecular proton transfer (ESIPT) substituent by incorporating the 2-benzothiazole (BTH) moiety on the *p*HP group. This *p*HP-BTH group has also shown a dual emission behaviour which is sensitive to polar solvents and to pH values. ESIPT processes have been gaining importance due to their properties; a) a fluorescence band with a large Stokes shift, b) a low inner-filter effect and c) low self-quenching. ESIPT process consists of an ultrafast enol-keto phototautomerisation which occurs on the excited-state surface of many intramolecular H-bonded molecules (Figure 7.7).

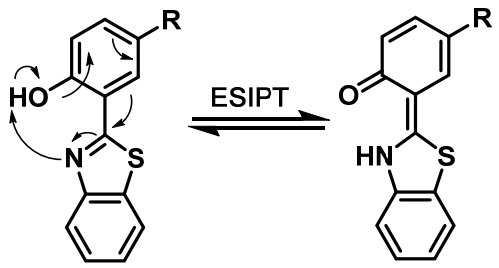

Figure 7.7. ESIPT mechanism of the fast enol-keto phototautomerisation of the *p*HP-BTH.

In the case of the *p*HP-BTH group, the introduction of the ESIPT substituent makes the system have some advantages over the previously mentioned *p*HP group; with the BTH moiety its excitation wavelength increases over 400 nm and both chromophores (*p*HP and BTH) can act as an environment-sensitive fluorophore. Furthermore, the combination of both moieties led to a dual colour fluorescence which would be useful for

[23] a) S. K. Choi, M. Verma, J. Silpe, R. E. Moody, K. Tang, J. J. Hanson, J. R. Baker, Jr., *Bioorg. Med. Chem.*, **2012**, *20*, 1281 - 1290; b) G. Liu, C.-M. Dong, *Biomacromolecules*, **2012**, *13*, 1573 - 1583.

[24] S. Atta, A. Jana, R. Ananthakirshnan, P. S. Narayana Dhuleep, *J. Agric. Food Chem.*, **2010**, *58*, 11844 - 11851.

[25] M. J. Devis, C. H. Kragor, K. G. Reddie, H. C. Wilson, Y. Zhu, T. M. Dore, *J. Org. Chem.*, **2009**, *74*, 1721 - 1729.

real-time monitoring of drug release mechanisms.[22] This duality in the fluorescence emission colours is due the fluorescence originating from the enol form and the fluorescence from its tautomeric keto form (Figure 7.7).[22] For all these reasons, Barman *et al.* designed a novel DDS in which they incorporated the BTH moiety into the *p*HP group to obtain a built-in ESIPT substituent (Figure 7.8).

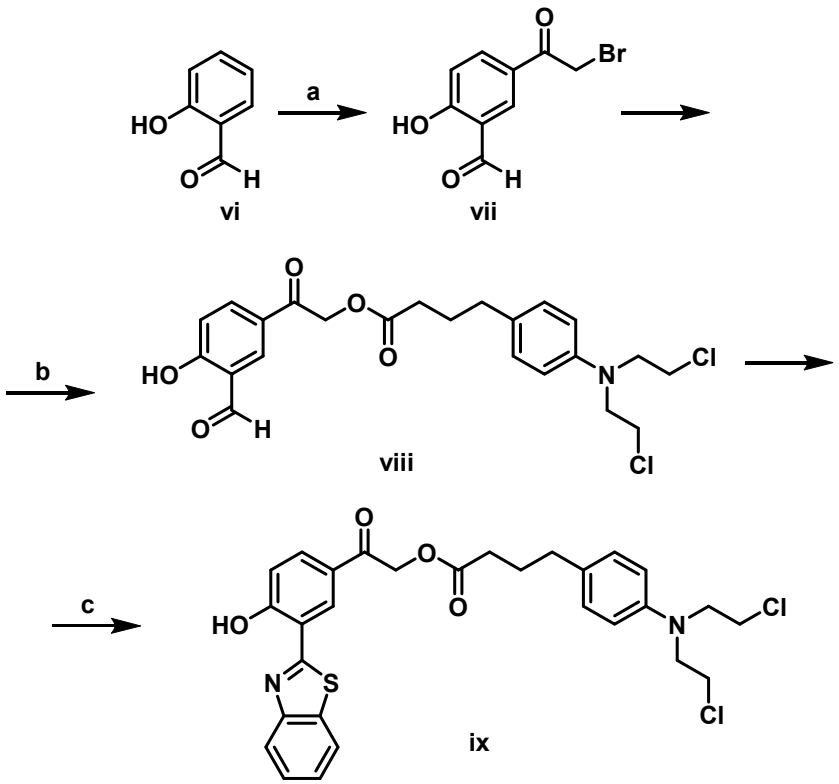

Figure 7.8. Synthetic route of the DDS *p*-hydroxyphenacyl-benzothiazole-chlorambucil (*p*HP-BTH-Cbl) with the built-in ESIPT substituent. a) bromoacetyl bromide, $AlCl_3$, DCM, 35 ºC, 15h; b) chlorambucil, K_2CO_3, DMF, r.t., 4h; c) 2-aminothiophenol, DMSO, reflux, 110 ºC, 1h.

As depicted in the figure above, Barman *et al.* converted salicylaldehyde (**vi**) into compound **vii** by a Friedel-Crafts acylation using bromoacetyl bromide. In the next step, **vii** was treated with chlorambucil (Cbl, an anticancer drug) in the presence of potassium carbonate in dry DMF to afford **viii**. Finally, its treatment with 2-aminothiophenol in DMSO yielded the desired DDS (**ix**), in moderate yield (70%).

Due to the outstanding properties of the *p*HP-BTH fluorophore group mentioned above, we thought that it could be useful to introduce it in the SRIF14's sequence or in a selective analogue's sequence to evaluate them as carriers and drug delivery systems. The most important features of the system would be the rapid release once inside the cell and the easier real-time monitoring of the process due to the duality in the fluorescence's colours which it gives to the final compound. At that point we designed a synthetic strategy with the aim of coupling the *p*HP-BTH fluorescent moiety to the *N*-terminal part of one of our peptides (Scheme 7.2).

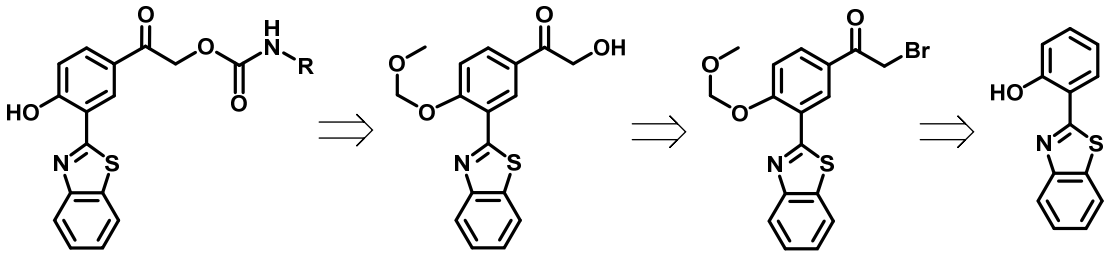

Scheme 7.2. Retrosynthetic route for the synthesis of the *p*HP-BTH coupled peptide. R = SRIF14 or SRIF14 analogue.

Although Pradeep and co-workers[22] started the synthesis of their fluorescent compound from the salicylaldehyde (Figure 7.8), we decided to start from the 2-(2'-hydroxy-phenyl)benzothiazole (HPB) moiety, as shown in Figure 7.9, because the aldehyde would not survive to the peptide chemistry.

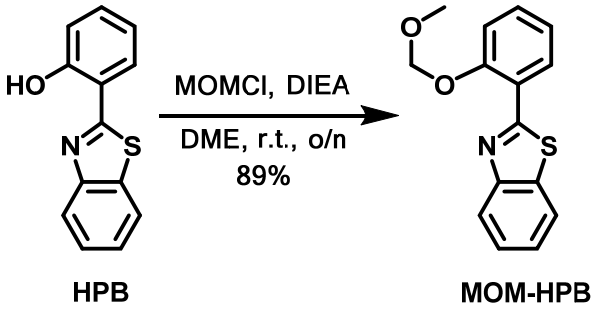

Figure 7.9. Hydroxyl protection with a MOM group which is resistant to the basic conditions used in the synthesis of peptides in solid phase (SPPS).

The protection of the hydroxyl group on the commercially available HPB proceeded as expected giving the desired compound (**MOM-HPB**) as a greenish oil in good yield

(89%). To obtain that product, an excess of MOMCl (5eq) and DIEA were used. Once the **MOM-HPB** was obtained, a Friedel-Crafts acylation with bromoacetyl bromide was performed (Figure 7.10). Even though two conditions were tested, neither of them led to the desired compound. When one equivalent of $AlCl_3$ was used, no reaction was observed while if 4 eq were used, the product with the deprotected phenol (**19**) was obtained.

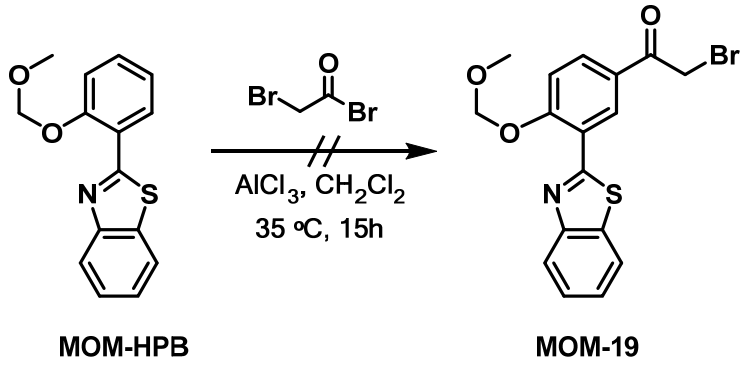

Figure 7.10. Friedel-Crafts acylation of the MOM-protected 2-(2'-hydroxyphenyl)benzothiazole compound (**MOM-19**). Two different conditions were used: a) 1eq of $AlCl_3$ and b) 4eq of $AlCl_3$.

In light of these findings, we decided to perform the Friedel-Crafts acylation directly over the 2-(2'-hydroxyphenyl)benzothiazole (**HPB**) moiety and protect the hydroxyl group afterwards (Figure 7.11). In this case, the acylation reaction was performed with 4 eq of $AlCl_3$ and it proceeded without problems giving the desired compound **19** with good yields (97%). After the Friedel-Crafts acylation, the hydroxyl moiety was protected with the MOM group using the conditions previously described in Figure 7.9. **MOM-19** was obtained with good yields (85%).

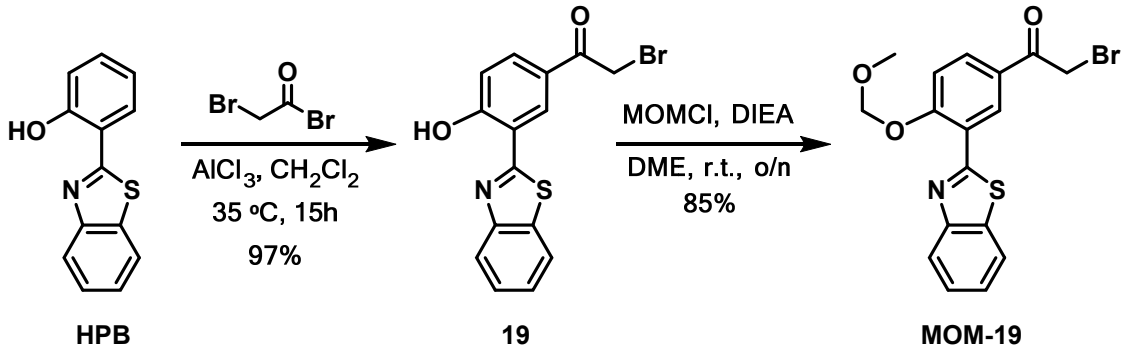

Figure 7.11. Friedel-Crafts acylation over the unprotected 2-(2'-hydroxyphenyl)benzothiazole (**HPB**) moiety using 4 eq of $AlCl_3$ to give compound **19** and the subsequent hydroxyl protection to give **MOM-19** compound.

The next step was the nucleophilic substitution of the bromine moiety by a hydroxyl group as shown in the retrosynthetic analysis of Scheme 7.2. For that particular reaction, two different conditions were tested starting from **MOM-19** but none of them worked (Table 7.1, entries 1 and 2). With these results in hand, we decided to perform the reaction again but starting from compound **19**, which had the free hydroxyl group (Table 7.1, entries 3-7). However, we did not obtain the desired compound in any case.

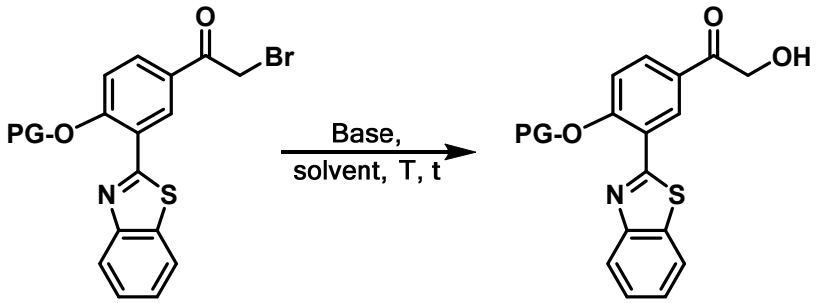

Entry	Starting material	Protecting Group (PG)	Base	Solvent	T	t
1	MOM-19	MOM	HCOOK	MeOH	reflux	overnight
2	MOM-19	MOM	Ag_2CO_3	H_2O/Acetone	55 ºC	overnight
3	19	-	HCOOK	EtOH	reflux	24h
4	19	-	Ag_2CO_3, NaOH (1N)	EtOH	r.t.	4h
5	19	-	Ag_2CO_3, NaOH (1N)	Dioxane	r.t.	24h
6	19	-	Ag_2CO_3, NaOH (1N)	^{t}BuOH	r.t.	24h
7	19	-	Ag_2CO_3, NaOH (1N)	ACN	r.t.	24h

Table 7.1. Reaction conditions of the nucleophilic substitution of the bromine moiety by a hydroxyl group. r.t. = room temperature, ~25 ºC

Unfortunately, none of these reactions led to the desired compound. The conversion for all the entries were close to zero except for entry 4. In this last case, the obtained product was not the alcohol but the ethyl ether.

Seeing that we were not able to obtain the desired alcohol neither from the MOM-protected (**MOM-19**) nor from unprotected phenol (**19**), we thought that another strategy could be synthesising a formate and then reduce it to an alcohol starting from the bromo-compound **19**. The formate compound **25** was achieved easily through two different conditions (Figure 7.12, A and B).

To avoid side reactions taking place within the carbonyl group, we decided to protect the ketone with a diol and then form the formate (Figure 7.12, C). However, the obtained compound was not stable enough to be characterised and only the unprotected one (**25**) was viable enough to proceed with further steps of the synthesis.

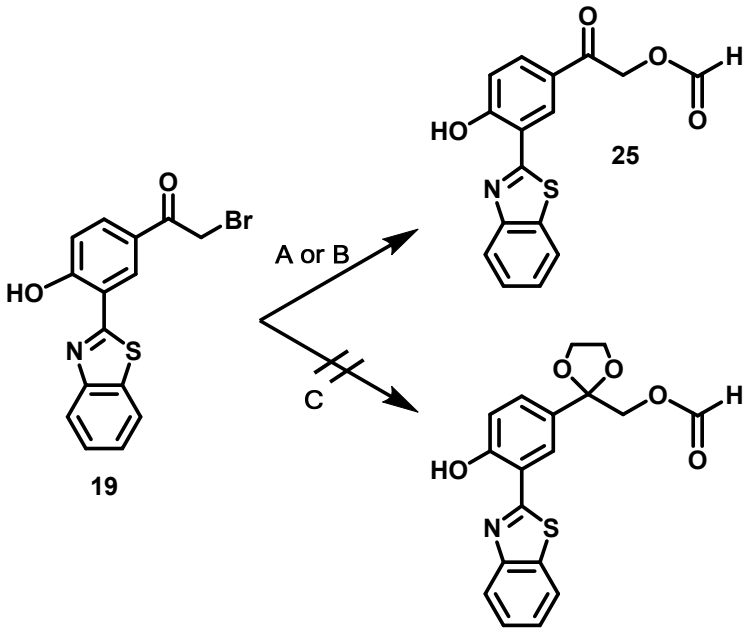

Figure 7.12. Reaction conditions of the nucleophilic substitution of the bromine moiety of compound **19** by a formate group. A) Formic acid, DBU, DCM, room temperature, overnight, 23% yield; B) Potassium formate, DMF, 90 ºC, overnight, 86% yield; C) i. Ethylene glycol, triethyl orthoformate, *p*-toluensulfonic acid, DCM, 50 ºC, 48h; ii. Potassium formate, DMF, 90 ºC, overnight, 44% yield.

After the formate **25** formation, we performed the hydroxyl group protection with a MOM group, using the same conditions depicted in Figure 7.9. This reaction worked without problems to give the desired MOM-protected formate **26** in excellent yield (96%) (Figure 7.13).

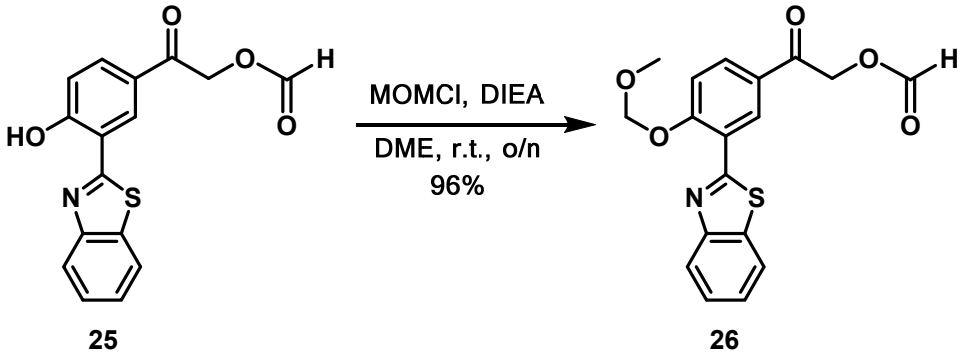

Figure 7.13. Reaction conditions of the hydroxyl protection of **25** with a MOM group to obtain **26**.

With compound **26** in hand, we designed two different strategies to reduce it; a) reducing both the ketone and the formate to obtain a diol (Figure 7.14 A) and b) reducing only the formate and obtain an alcohol (Figure 7.14 B). Even though both reactions seem plausible and easy to perform, none of them enabled us to obtain the desired product with good yields. The diol formation worked but the crude was not clean and the mixture of products obtained was not easy to separate and identify. Furthermore, while the diol formation proceeded fast, the sole reduction of the formate did not work at all as we could confirm by TLC and NMR.

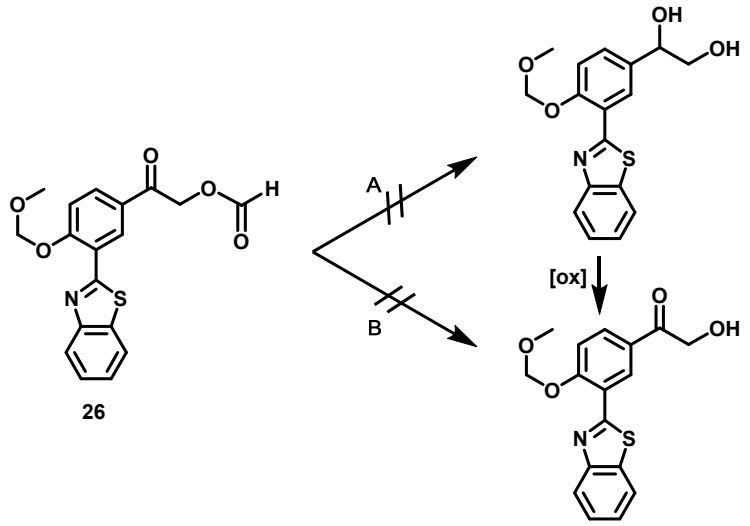

Figure 7.14. Reaction conditions for the reductions of the MOM-protected formate compound. A) NaBH4, MeOH, THF, room temperature, 20 min. B) NaOH (5M) excess, AcOEt, 90 ºC, 8 h.

For that reason, we decided to change the synthetic approach for obtaining the final *p*HP-HBT coupled peptide. Our idea was to synthesise an isocyanate (**xi**) from the benzyl-protected alanine (**x**) and couple it to the *tert*-butyl 2-hydroxyacetate (**xii**) (Scheme 7.3).

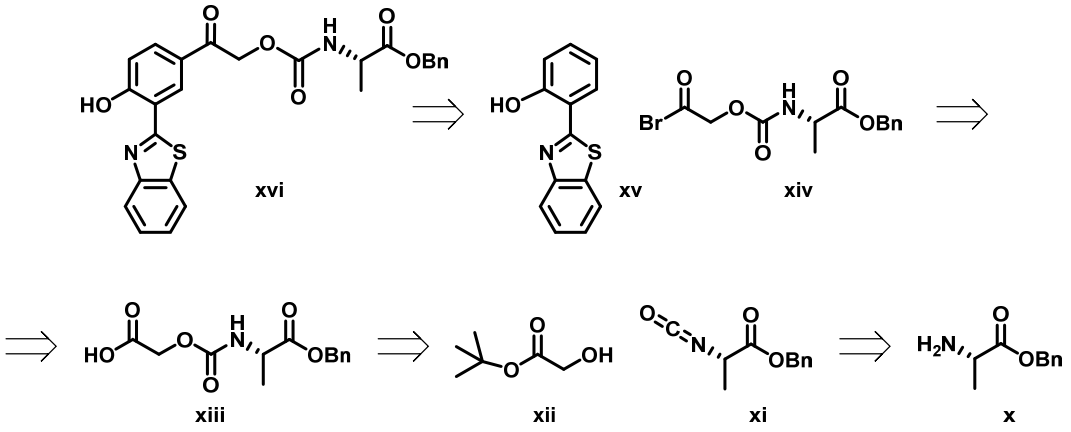

Scheme 7.3. New retrosynthetic route for the synthesis of the *p*HP-BTH coupled peptide.

Even though the carbamate bond between the isocyanate (**xi**) and the alcohol (**xii**) was formed in relatively good yield, 65%, (compound **xiii**, Scheme 7.3), we had to discard this route due to the decomposition experimented by that carbamate (**xiii**) before being able to introduce the bromo moiety to obtain (**xiv**) and be able to couple it with the 2-(2'-hydroxyphenyl)-benzothiazole (**xv**) to achieve the desired compound **xvi**.

Far from desisting, we thought that we could synthesise the desired compound with the peptide attached to a solid support and using the SPPS conditions to couple the *p*HP-BHT moiety to our analogue. With this aim in mind, we designed another synthetic strategy (Figure 7.15) in which the side chain of an aspartic acid and the **MOM-19** compound would be involved.

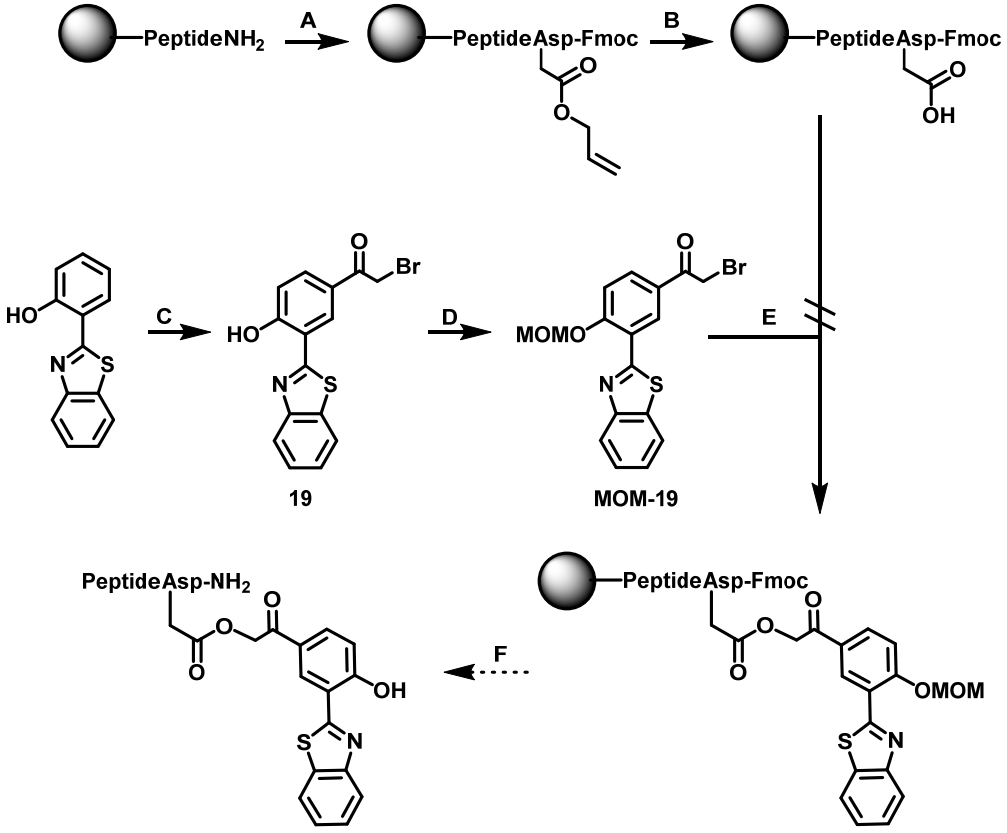

Figure 7.15. New strategy for the *p*HP-BTH coupled peptide. A) Fmoc-L-Asp(OAll)-OH (3 eq), HOBt (3 eq), DIPCIDI (3eq), DMF, room temperature, 1h; B) $Pd(PPh_3)_4$ (0.1 eq), $PhSiH_3$ (10 eq), DCM, room temperature, 2x15 min; C) Bromoacetyl bromide (1.2 eq), $AlCl_3$ (4 eq), DCM, 35ºC, 15h; D) MOMCl (5 eq), DIEA (5 eq), DME, room temperature, overnight; E) See Table 7.2; F) *i.* Piperidine 20% in DMF, *ii.* DCM/TFE/AcOH (70:20:10), *iii.* I_2, *iv.* TFA/DCM/anisole/H_2O (55:30:10:5).

Steps A and B were performed following the SPPS conditions and both reactions gave the desired product in quantitative yields. Steps C and D were performed previously obtaining both **19** and **MOM-19** compounds. Reactions conditions for step E had to be optimised but even though four different conditions (Table 7.2) were tested, none of them gave the desired compound.

Entry	Protecting Group (PG)	Base	Solvent
1	**Fmoc**	DIPEA	DMF
2	**Boc**	DIPEA	DMF
3	**Fmoc**	DIPEA	Dry DCM
7	**Boc**	DIPEA	Dry DCM

Table 7.2. Reaction conditions for the coupling between aspartic acid and **MOM-19** compounds.

With these results in hand, we decided to design a similar synthetic pathway in which SPPS would be also involved but in a later step to obtain the *p*HP-HBT coupled peptide. This route (Figure 7.16) consisted of coupling compound **19** and Fmoc-L-Asp(OAll)-OH in solution and, once the side chain was deprotected, introduce it onto the resin as another amino acid using the standard SPPS conditions.

As stated before, step A gave the desired compound **19,** with good yields (97%), which was then transformed to compound **20** by a nucleophilic substitution of the bromine moiety. For that particular reaction, two solvents were tested (dry DMF and ACN) but only the one described in Figure 7.16 gave the desired compound **20** in moderate yields (55%). The hydroxyl protection was performed to obtain compound **21** in good yield (84%) using the same conditions described in Figure 7.13. Once the phenol had been protected with a MOM group (**21**), we could perform the deprotection of the acid using tetrakis(triphenylphosphine)palladium(0) and phenyl silane in dichloromethane to remove the allyl group and obtain compound **22** in quantitative yields.

At that point, compound **22** needed to be coupled to the desired peptide (**11** without the alanine in position 1 as it would be replaced by the aspartic acid) to obtain compound **23.** The lineal peptide was then transformed to compound **24** by selective deprotection of the cysteines, cleavage from the resin, cyclisation and side chain deprotection. The synthesis of compound **24** is shown in Figure 7.16.

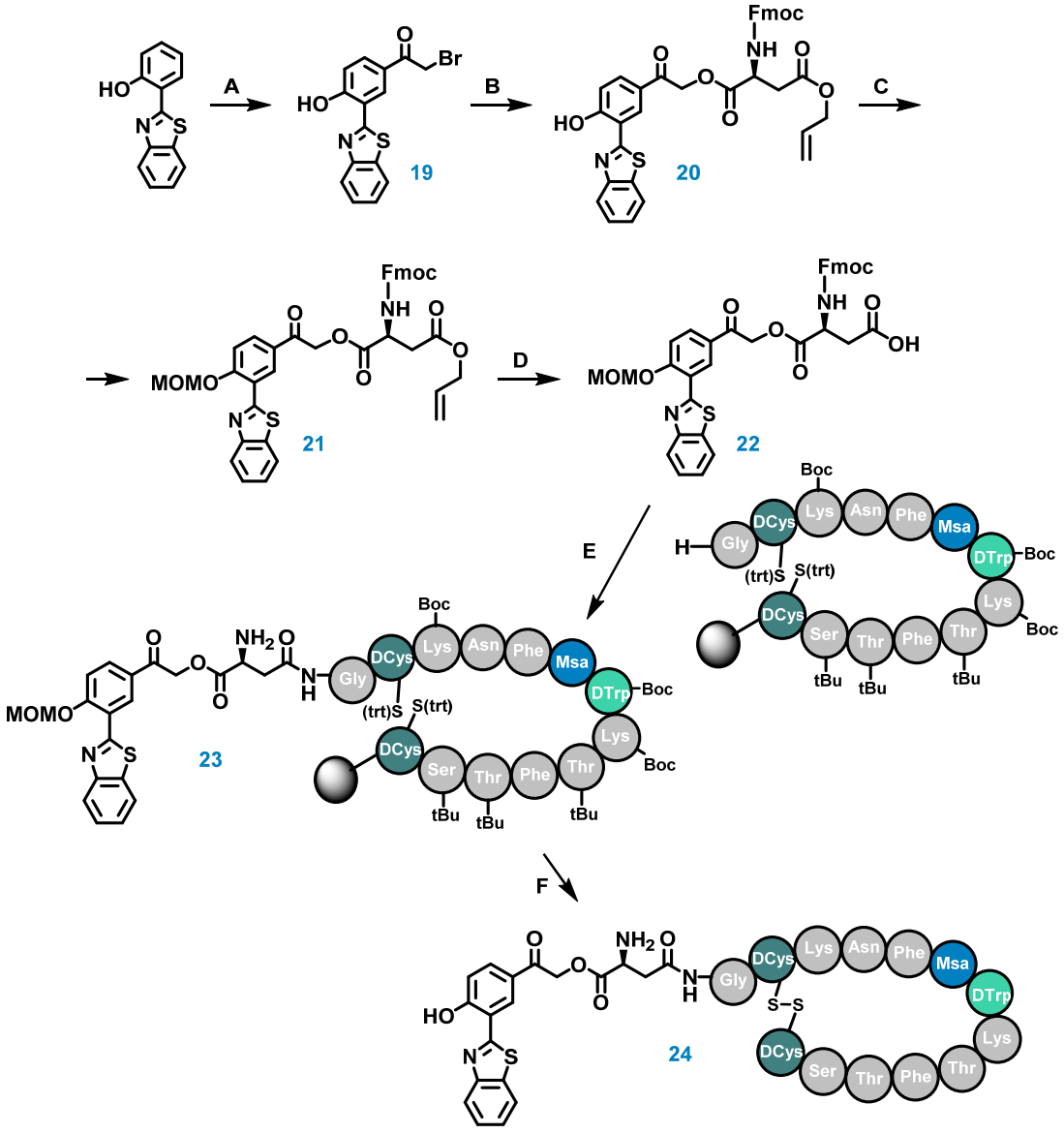

Figure 7.16. New strategy for the *p*HP-HBT coupled peptide. A) Bromoacetyl bromide (1.2 eq), $AlCl_3$ (4 eq), DCM, 35ºC, 15 h h; B) Fmoc-L-Asp(OAll)-OH (1 eq), K_2CO_3 (3 eq), ACN, room temperature, overweekend; C) MOMCl (5 eq), DIEA (5 eq), DME, room temperature, overnight; D) $Pd(PPh_3)_4$ (0.1 eq), $PhSiH_3$ (10 eq), DCM, room temperature, 5h; E) a) Compound **22** (3 eq), HOBt (3 eq), DIPCIDI (3eq), DMF, room temperature, 1h; b) Piperidine 20% in DMF; F) *i.* DCM/TFE/AcOH, *ii.* I_2, *iii.* TFA/DCM/anisole/H_2O.

Light-sensitive compounds **23** and **24** could only be characterised by MALDI-TOF or high resolution mass spectrometry (HRMS) as the UV light from the HPLC-MS and the infrared light of the IR cleaved the bond between the peptide and the photo-cleavable fluorophore. Furthermore, step F had to be performed protecting the reaction vessel from the visible and UV light to avoid premature cleavage of the light-sensitive fluorophore from happening.

We hoped that compound **24** would be internalised together with the receptor as it happened for compound **15** and as indicated for these type of transmembrane receptors.[17] Once we had corroborated by HR-MS that the compound **24** was formed, we decided to test it *in vitro* with the CHO-K1 cells (both WT and ST cell lines) following the procedure described by Barman *et al.*[22] in which cells were incubated with 10 μg/mL of the light-sensitive compound for 4 h, irradiated with UV-visible light for previously set times and then observed using confocal microscopy.

Singh and co-workers[22] proposed a mechanism for the photochemical release of the drug attached to the *p*HP-BHT moiety in aqueous solution which we have adapted for our peptide release in Figure 7.17. With the exception of the first step involving a rapid ESIPT process and a deprotonation, their proposed mechanism was similar to that suggested by Givens and co-workers.[26]

Preliminary real time monitoring studies of drug release by our DDS (*p*HP-HBT-Peptide) inside CHO-K1 WT and CHO-K1 ST cells were performed and analysed by confocal microscopy (Figure 7.18). A control experiment without compound and without irradiation was done for both cell types (Figure 7.18 a and b) to check if the cells themselves showed any kind of green and/or blue autofluorescence.

[26] P. G. Conrad, R. S. Givens, J. F. W. Weber, K. Kandler, *Org. Lett.*, **2000**, *2*, 1545 - 1547.

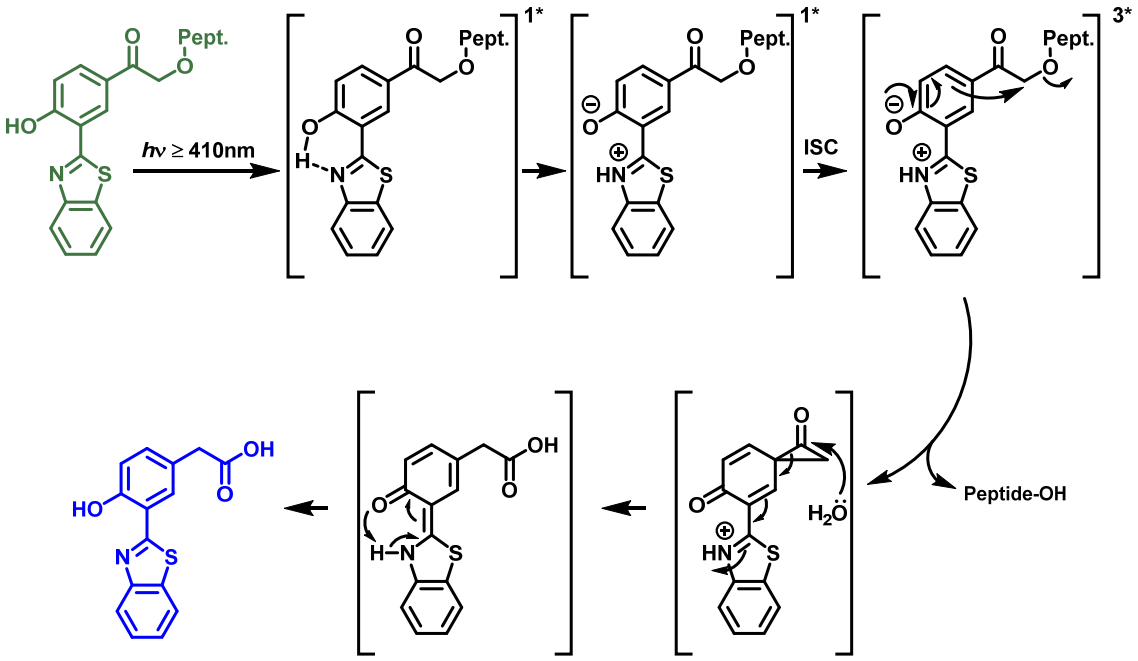

Figure 7.17. Possible photo-release mechanism of the drug delivery system *p*HP-Benz-Peptide adapted from the one proposed by Singh and co-workers. ISC = intersystem crossing.

Initially, the CHO-K1 ST cells showed green fluorescence due to the cellular uptake of the *p*HP-HBT-Peptide compound **24** (Figure 7.18 d). After exposing them to visible light (≥ 410 nm) for 15 min, both green and blue fluorescence were observed, thus indicating the partial release of the peptide by our drug delivery system (Figure 7.18 f).

However, after 30 min of irradiation (Figure 7.18 h), blue fluorescence was observed while the green fluorescence intensity had decreased and almost disappeared which indicated a greater photorelease of our peptide. Nevertheless, CHO-K1 WT cells showed different results; initially only a tenue green fluorescence was observed (Figure 7.18 c). After 15 min of irradiation with UV-Visible light (Figure 7.18 e), both green and blue fluorescence was observed but to not as intense as the one detected for the CHO-K1 ST cells. After 30 min of irradiation (Figure 7.18 g), the green fluorescence had almost disappeared while the blue could still be detected even though its intensity was not comparable to the one detected for the ST cells. Even though both green and blue fluorescence was detected for both wild type (WT) and cells with the SSTR2 overexpressed (ST), the intensity was not the same (more intense fluorescence for the ST cells than the WT), thus indicating that

the internalisation was more efficient in the cells overexpressing the somatostatin receptor SSTR2 than for the WT ones. The observed fluorescence in the WT cells could be due to the internalisation of compound **24** through passive diffusion.

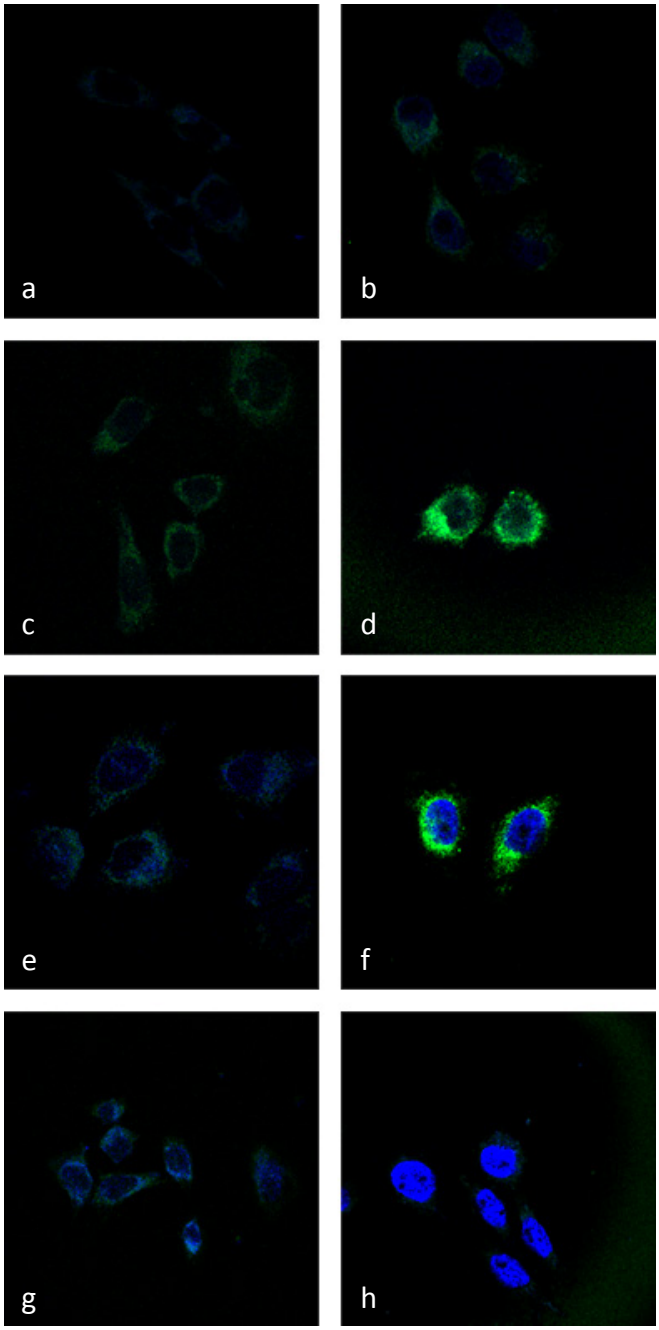

Figure 7.18. Confocal images of the cellular internalisation and photo-release of compound **24**: a) Non-treated and non-irradiated CHO-K1 WT cells; b) Non-treated and non-irradiated CHO-K1 ST cells; c) Non-irradiated treated CHO-K1 WT cells; d) Non-irradiated treated CHO-K1 ST cells; e) Treated CHO-K1 WT cells after 15min of irradiation; f) Treated CHO-K1 ST cells after 15min of irradiation; g) Treated CHO-K1 WT cells after 30 min of irradiation; h) Treated CHO-K1 ST cells after 30min of irradiation.

7.3 Synthesis of SOM1-PH, SOM2-PH and SOM3-PH

The p38 mitogen-activated protein kinases (MAPKs) are activated by a wide range of cellular stresses as well as in response to inflammatory cytokines.[27] Their signalling pathway plays various important roles in the ability of cells to assimilate external stimuli and elaborate suitable responses. In addition, this pathway also plays an important role in the stress response, but inflammatory cytokines and many different non-stress stimuli can also activate p38 MAPK signalling, leading to the regulation of numerous cellular processes.[28] The p38α pathway can also control the production of extracellular signalling molecules, such as cytokines, chemokines, and growth factors, at different levels.[29]

New evidence suggests that p38α can contribute to the homeostasis of cancer cells, facilitating their survival and proliferation and it may also enable invasion, angiogenesis and metastasis at different levels.[29b] Cancer is a complex disease that arises through a multistep, mutagenic process, which involves changes in the wiring of signalling pathways that are normally tightly regulated to maintain tissue homeostasis. These mutations could affect protein kinases directly involved in promoting cancer cell growth.[28b]

To go one step further in the study of somatostatin and its analogues as carriers, we set up a collaboration with Dr. Ángel Nebreda research group and decided to incorporate an analogue (PH) of a previously reported drug (PH-797804),[30] an inhibitor of the p38α MAPK, to the natural somatostatin sequence and two of its analogues (Figure 7.19).

---

[27] A. Cuenda, S. Rousseau, *Biochim. Biophys. Acta - Mol. Cell Res.,* **2007**, *1773*, 1358 - 1375.

[28] a) A. Cuadrado, A. R. Nebreda, *Biochem. J.,* **2010**, *429*, 403 - 417; b) A. Igea, A. R. Nebreda, *Cancer Res.,* **2015**, *75*, 3997 - 4002.

[29] a) E. F. Wagner, Á. R. Nebreda, *Nat. Rev. Cancer,* **2009**, *9,* 537 - 549; b) C. Youssif, M. Cubillos-Rojas, M. Comalada, E. Llonch, C. Perna, N. Djouder, A. R. Nebreda, *EMBO Mol. Med.*, **2018**, *10*, e8403.

[30] a) S. R. Selness, R. V. Devraj, B. Devadas, J. K. Walker, T. L. Boehm, R. C. Durley, H. Shieh, L. Xing, P. V. Rucker, K. D. Jerome, A. G. Benson, L. D. Marrufo, H. M. Madsen, J. Hitchcock, T. J. Owen, L. Christie, M. A. Promo, B. S. Hickory, E. Alvira, W. Naing, R. Blevis-Bal, D. Messing, J. Yang, M. K. Mao, G. Yalamanchili, R. Vonder Embse, J. Hirsch, M. Saabye, S. Bonar, E. Webb, G. Anderson, J. B. Monahan, *Bioorg. Med. Chem. Lett.*, **2011**, *21*, 4066 - 4071; b) L. Xing, *JSM Chemnistry*, **2014**, *2*, 1 - 3; c) W. MacNee, R. J. Allan, I. Jones, M. C. De Salvo, L. F. Tan, *Thorax*, **2013**, *68*, 738 - 745; d)

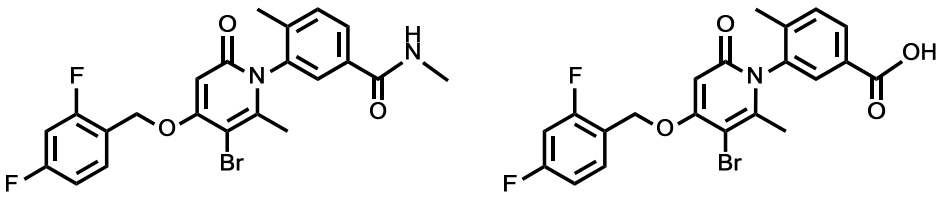

Figure 7.19. Chemical structures of PH-797804 (left) and its analogue PH (right) developed and synthesised by Craig Donoghue from our research group.

In that sense, three different analogues containing the PH moiety were synthesised and tested in vitro (Figure 7.20).

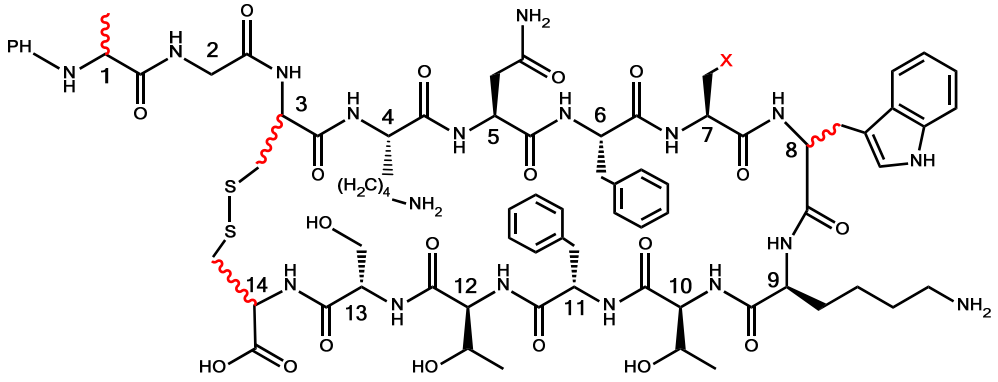

	1	3	7	8	14
SOM1-PH (16)	L-Ala	L-Cys	Phe	L-Trp	L-Cys
SOM2-PH (17)	-	L-Cys	Phe	L-Trp	L-Cys
SOM3-PH (18)	D-Ala	D-Cys	Msa	D-Trp	D-Cys

Figure 7.20. Somatostatin derivatives containing the PH analogue coupled at the *N*-terminal part of the peptide.

As previously mentioned in Chapter 4, Fmoc-L-Msa-OH was synthesised following the asymmetric synthesis protocol previously developed in our group (Scheme 4.1, page 73)[31] while the rest of amino acids, including Fmoc-D-Trp(Boc)-OH, Fmoc-D-Ala-OH and Fmoc-D-Cys(trt)-OH were commercially available from different suppliers.

[31] R. Ramón, M. Alonso, A. Riera, *Tetrahedron: Asymmetry*, **2007**, *18*, 2797 - 2802.

The three new peptides with the inhibitor introduced in the sequence, were synthesised by solid phase peptide synthesis (SPPS) following the well-known Fmoc/^{t}Bu strategy using 2-chlorotrytyl chloride resin. The synthesis of compound **16** is shown as a general example in Scheme 7.4.

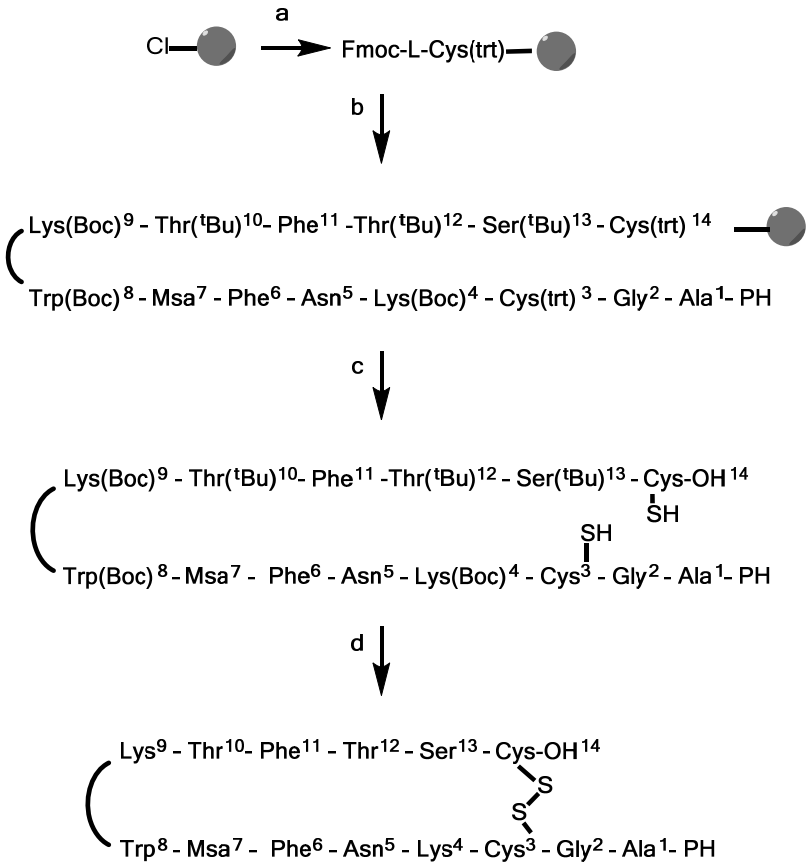

Scheme 7.4. SPPS of SOM1-PH (**16**). a) 1. Fmoc-L-Cys(trt)-OH (3eq), DIEA (3eq), 2. MeOH; b) 1. Piperidine 20% in DMF, 2. Fmoc-AA-OH (1.5-3eq), DIPCIDI (3eq), HOBt (3eq), DMF; 3. Piperidine 20% in DMF, 4. PH analogue (3eq), DIPCIDI (3eq), HOBt (3eq), DMF, c) DCM/TFE/AcOH, d) 1. I_2, 2. TFA/DCM/anisole/H_2O.

Contrary to what happened during the synthesis of [L-Dmp11_D-Trp8]-SRIF14 (**3**) and [Msa6_L-3'Pya7_D-Trp8]-SRIF14 (**5**), the coupling of Fmoc-Asn-OH in position 5 in the PH-containing sequences was not problematic so the recoupling step was not needed. For peptides **16**-**18**, the coupling of the drug was followed by UPLC-MS.[32]

[32] A mini-cleavage was performed: 5mg of resin were placed in an eppendorf tube which contained TFA 95% and let it react for 1h. After that, the TFA was evaporated and the peptide precipitated with cold ether. The solution was decanted and the pellet dissolved with H_2O:ACN (1:1) and then analysed by UPLC-MS.

Once the peptides containing the PH moiety were synthesised, we decided to test their capacity of inhibiting the function of the p38α by monitoring the phosphorylation of its downstream target ATF2. The p38 mitogen activated protein kinase (MAPK) has been reported to play a key role in the biosynthesis of several key pro-inflammatory cytokines such as tumour necrosis factor-α (TNFα) and interleukin-1β (IL-1β).[33] Modulation of p38α by ATP competitive small molecules has led to the generation of a variety of novel p38α inhibitors as potential therapeutics for the treatment of inflammatory conditions including Crohn's disease and rheumatoid arthritis (RA).[34] The inhibitor that we choose for that purpose was PH (Figure 7.19), an analogue of PH-797804 designed and synthesised by Pfizer Corporation.[30a]

With the purpose of testing our three PH-containing analogues as p38α inhibitors, we performed an initial inhibitory kinase assay for compound **16** and **17**.[35] As shown in Figure 7.21, the inhibitory potency of **16** and **17** was comparable with that of PH for the 5 μM concentration and slightly less potent for the lowest concentration.

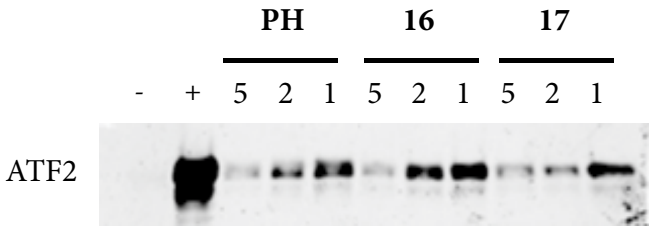

Figure 7.21. Western Blot of the kinase assay for the two somatostatin derivatives (**16** and **17**) containing the PH coupled at the *N*-terminal part of the peptide. PH itself was used as a control. Concentrations used: 5 μM, 2 μM and 1 μM; + : positive control; - : negative control.

The phosphorylation of the downstream target of p38α, ATF2, was quantified and the results plotted in Figure 7.22-a. In order to evaluate all three compounds, it was important

[33] a) J. C. Lee, J. T. Laydon, P. C. McDonnell, T. F. Gallagher, S. Kumar, D. Green, D. McNulty, M. J. Blumenthal, J. R. Heys, S. W. Landvatter, *Nature*, **1994**, *372*, 739 - 746; b) J. L. Adams, A. M. Badger, S. Kumar, J. C. Lee, *Prog Med Chem*, **2001**, *38*, 1–60; c) J. Saklatvala, *Curr. Opin. Pharmacol.*, **2004**, *4*, 372 - 377.

[34] S. Kumar, J. Boehm, J. C. Lee, *Prog Med Chem*, **2001**, *38*, 1 - 60.

[35] Methodology described in Chapter 9 of the present thesis.

to quantify the inhibition of the phosphorylation of ATF2 triggered by each compound. For that reason, the inverse of the phosphorylation was plotted in Figure 7.22-b. As extracted from these figures, the higher the phosphorylation got, the lower the inhibition was.[36]

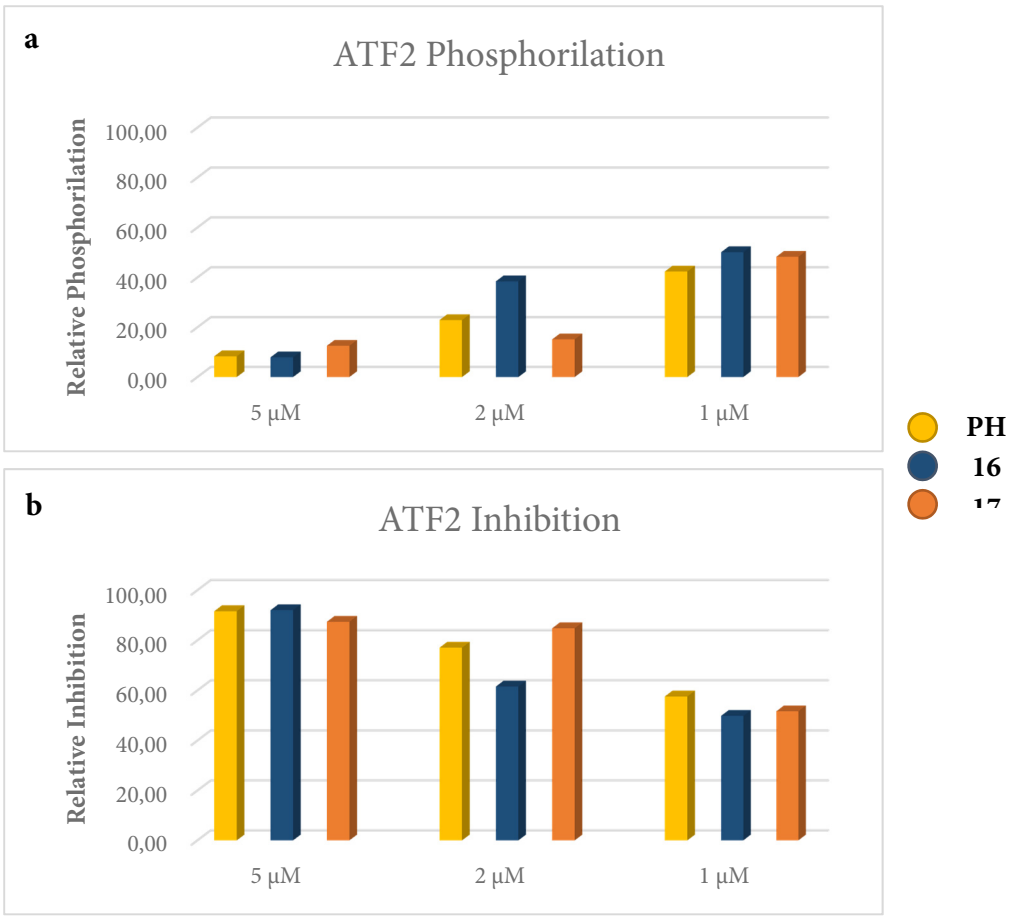

Figure 7.22. a) Quantified phosphorylation of ATF2 by PH, **16** and **17** at different concentrations; b) Quantified inhibitory effect of PH, **16** and **17** over ATF2 at different concentrations. Results have been grouped by concentrations for an easier comparison.

As stated before, this initial experiment showed a similar inhibition of the phosphorylation of ATF2 by the three compounds for both the highest concentration (5 µM) and the lowest one (1 µM) while for the 2 µM concentration the behaviour was slightly different; being **16** the one with less inhibitory activity and **17** the compound which triggered more inhibition.

[36] From now on, only ATF2 inhibition (and not both phosphorylation and inhibition) results will be shown.

With these results in hand, we decided to test **16**, **17** and **18** in an *in vitro* p38α cellular assay.[37] For these assays, we tested all three compound with wild type (WT) and overexpressing SSTR2 (ST) cell lines in order to elucidate if the inhibition of p38α would be selective only for the ST cells, as our compounds have shown some selectivity towards this receptor. For this type of assay, each compound was tested separately and using only two different concentrations (2 μM and 10 μM).

Inhibitory activity against p38α of compound **16** was the first to be tested (Figure 7.23). GAPDH was used as a control to ensure a similar protein loading in each lane and detect possible loading errors. In that experiment, PH was used as a control inhibitor to compare it to the results obtained for the somatostatin analogues. As done with the initial inhibitory kinase assay, the results (Figure 7.23) for both p38α and its downstream target, Hsp27, were quantified and then plotted in Figure 7.24 for a clearer visualisation.

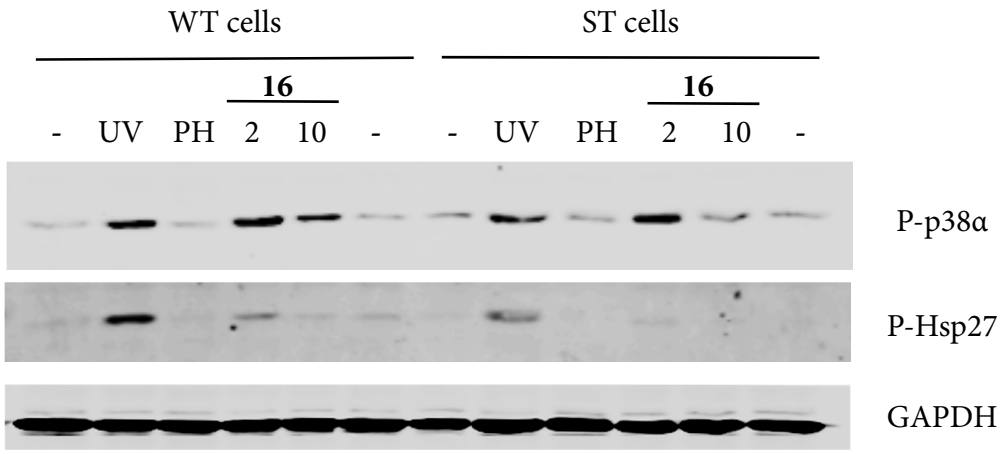

Figure 7.23. Western Blot of the p38α cellular assay for compound **16** at two different concentrations (2 μM and 10 μM). PH was used as a positive control for the inhibition of the phosphorylation of Hsp27. GADPH was used as a loading control. Negative controls (-) were also introduced.

Even though in Figure 7.23 it looks like **16** in a 10 μM concentration was slightly more active in ST cells than in the WT, the results were slightly different after the quantification (Figure 7.24).

[37] Methodology described in Chapter 9 of the present thesis.

After the quantification of the western blot, compound **16** at 10 μM concentration had the same inhibitory activity in WT than in ST cell lines and similar to PH. However, when at 2 μM **16** was a slightly better inhibitor for the phosphorylation of Hsp27 in ST cells (Figure 7.24).

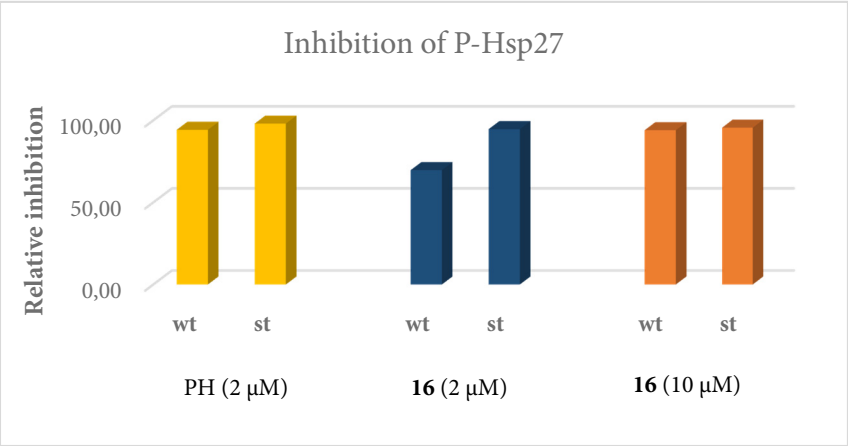

Figure 7.24. Quantified inhibitory effect of P-Hsp27 by PH and **16** at 2 μM and 10 μM. Results have been grouped by concentrations for an easier comparison between WT and ST cells.

After testing compound **16** and seeing the good inhibitory results obtained against the phosphorylation of Hsp27, we decided to test compound **17** in the same conditions. As in the previous experiment, GAPDH was also used as a control for the protein loading and PH was used as a control inhibitor. The obtained results (Figure 7.25) for both p38α and its downstream target, Hsp27, were quantified and then plotted in Figure 7.26 for a clearer visualisation.

Compared to **16, s**imilar results were obtained for compound **17** when referring to the higher concentration (10 μM); in both cases almost null phosphorylation of Hsp27 was detected which was similar to the values obtained for the PH (Figure 7.25). These results were translated into an inhibitory activity comparable to that obtained for the PH and similar between WT and ST cells (Figure 7.26).

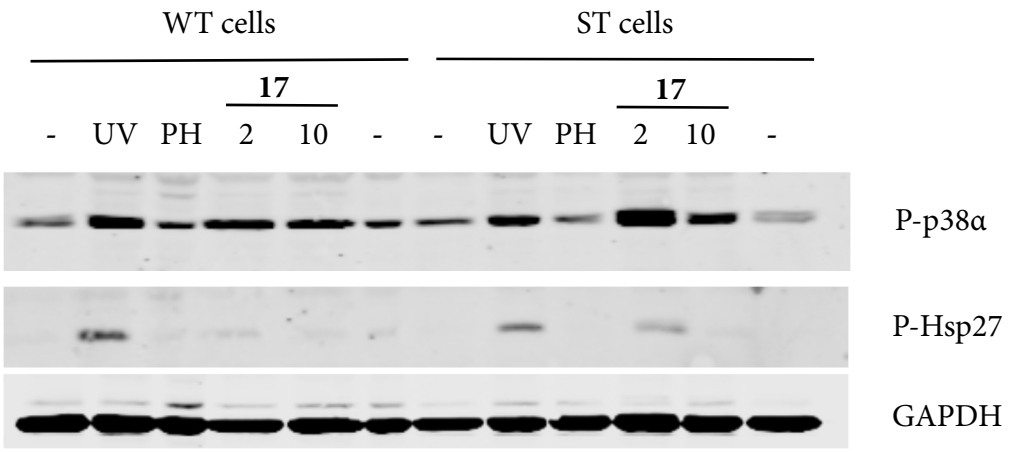

Figure 7.25. Western Blot of the p38α cellular assay for compound **17** at two different concentrations (2 μM and 10 μM). PH was used as a positive control for the inhibition of the phosphorylation of Hsp27. GADPH was used as a loading control. Negative controls (-) were also introduced.

However, 2 μM concentration of **17** gave small differences between WT and ST cell lines. Compound **17** triggered higher phosphorylation of Hsp27 in the cell line overexpressing the SSTR2 receptor (Figure 7.25) than in the WT ones, thus being less potent as an inhibitor for the ST cells than for the WT ones (Figure 7.26). From these results we could extract that the behaviour of **17** was the opposite of **16** for that particular concentration.

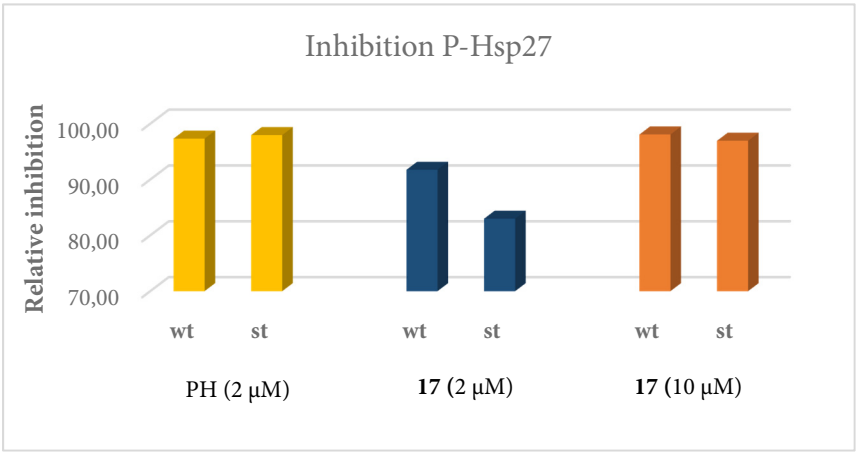

Figure 7.26. Quantified inhibitory effect of P-Hsp27 by PH and **17** at 2 μM and 10 μM. Results have been grouped by concentrations for an easier comparison between WT and ST cells.

At that point, we were wondering what could make these two analogues so potent even resembling the values obtained for the PH inhibitor itself. As it has been demonstrated in Chapter 6 (Section 6.3.1, Figure 6.2), one of the first metabolites to be formed when incubating the natural somatostatin in human serum was the one in which the extracyclic part (residues 1 and 2) had been lost.

Knowing this, we hypothesised that the high inhibitory activity of both **16** and **17** could be due to the loss of the first two amino acids (Ala1-Gly2) which intrinsically implied losing the PH. This fact would led to an internalisation of a smaller compound, Gly2_Ala1_PH or PH itself, into the cells which would be responsible of the great activity showed by analogues **16** and **17**.

For that reason, we decided to test compound **18** under the same conditions. Compound **18** was synthesised from peptide **11**, the one with a half-life of 2400 min and for which the loss of the extracyclic part was not detected (Chapter 6, Section 6.3.8, Figure 6.9).

If our hypothesis was right, we should observe a decrease in the inhibitory activity of our compound when compared to PH, **16** and **17** as only the analogue (**18**) would be internalised into the cell and not PH alone thus giving a false positive result.

Contrary to what happened for **16** and **17**, where almost full inhibition of the phosphorylation of Hsp27 was observed, a concentration-dependent inhibition could be observed for compound **18** (Figure 7.27)**.** Furthermore, we were also able to see some differences between the activity against WT and ST cell lines which indicated that the mechanism of internalisation of the analogue was different. The results for analogue **18** were quantified and then plotted in Figure 7.28 and grouped by concentrations for a clearer visualisation.

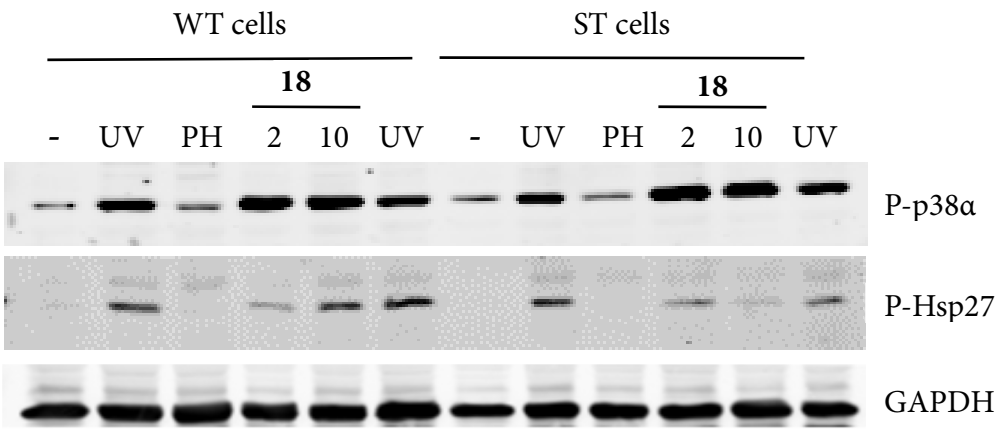

Figure 7.27. Western Blot of the p38α cellular assay for compound **18** at two different concentrations (2 μM and 10 μM). PH was used as a positive control for the inhibition of the phosphorylation of Hsp27. GADPH was used as a loading control. Negative controls (-) were also introduced.

After the quantification was made, we saw that at 10 μM concentration, compound **18** was more active in the inhibition of the phosphorylation of Hsp27 in the WT cell line than in the ST and slightly lower than PH. Furthermore, for the lower concentration (2 μM), a bigger difference was observed; the inhibition of the phosphorylation of Hsp27 was higher in the cells overexpressing SSTR2 (ST) than in the wild type (WT) cell line (Figure 7.28).

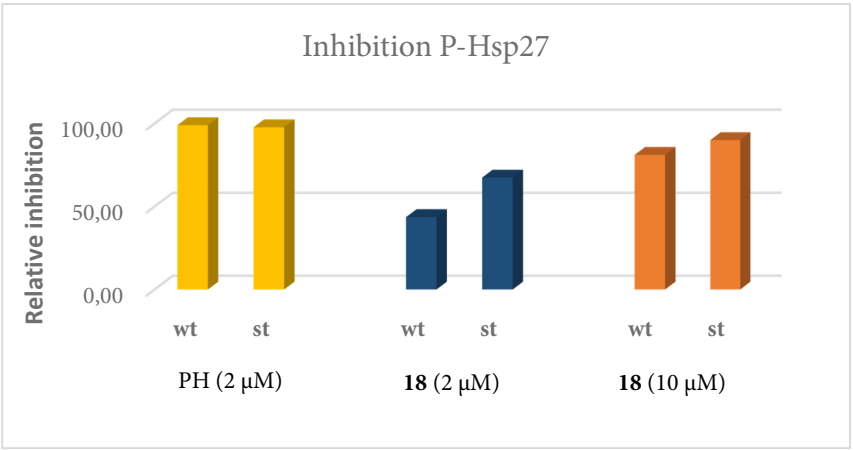

Figure 7.28. Quantified inhibitory effect of P-Hsp27 by PH and **18** at 2 μM and 10 μM. Results have been grouped by concentrations for an easier comparison between WT and ST cells.

Compound **18** was the only of the three analogues which showed higher inhibition in the ST cells than in the WT ones at different concentrations. This could be due to the stability

of the extracyclic part of the peptide which prevents PH from being cleaved and entering the cell alone.

7.4 Conclusions

After some failed attempts, we have been able to synthesise a fluorescent probe stable enough to resist the harsh acidic conditions of the cyclisation of the peptide after solid phase peptide synthesis. We have synthesised two analogues (**14** and **15**) containing the fluorescent coumarin at the *N*-terminal part of the peptide. The compound **15** has also demonstrated its stability within the cell culture medium and under the *in vitro* assay conditions.

The introduction of the fluorescent prove (7-Methoxycoumarin-4-yl)-acetic acid (Mca) at the *N*-terminal part of the peptide has enabled us to corroborate the internalisation of somatostatin analogues inside the cells. Furthermore, we have observed a difference in the compound **15**'s internalisation between WT and ST cells. As shown in Figure 7.5, the fluorescent compound was internalised in the cells overexpressing the SSTR2 while its internalisation in the WT cells was almost inexistent unless the detection level was decreased close to the background level, where a tenue fluorescence was observed for these cells. This fluorescence has been hypothesised to be due to the internalisation by passive diffusion.

When referring to the two-colour fluorescence compound (**24**), we have also been able to synthesise it after several attempts and attach it at the *N*-terminal part of the desired and stable peptide. It has also proved to be resistant to the acidic conditions of the peptide cyclisation. We have also treated WT and ST cells with this compound and evaluated the results under confocal microscopy. As for compound **15**, analogue **24** was internalised in ST cells more efficiently than in the WT cells where passive diffusion may have happened. Moreover, we have detected a fluorescence colour change under the irradiation of WT and ST cells with UV-visible light for previously set times (0-to 30min). In the smaller

irradiation time points, green fluorescent was predominant and more intense in ST cells than in WT cells. As the irradiation time increased, the blue fluorescent became predominant and, as for smaller time points, more intense in ST cells than in WT cells.

We have also been able to attach an inhibitor at the *N*-terminal part of both somatostatin and one of our analogues (**11**) though solid phase peptide synthesis (SPPS) and it has proven to be resistant to the cleavage and cyclisation conditions used. Biological studies have been performed for the three PH-containing analogues (**16**, **17** and **18**) to test them as p38α inhibitors.

Preliminary inhibitory kinase assays showed that both **16** and **17** had an inhibition potency close to the PH itself against ATF2 (p38α downstream target).

We also tested **16** and **17** in an *in vitro* p38α cellular assay. This assay should enabled us to see some differences between the CHO-K1 WT and CHO-K1 ST cells. However, compounds **16** and **17** displayed similar action for both cell lines at 10 μM concentrations and similar to PH. When talking about the 2 μM concentration, **17** was more active in WT cells than in ST cells while **16** gave better results for the ST ones. With these results in hand, we hypothesised that **16** and **17** were as potent as PH due to the loss of the extracyclic part of the peptide thus leading to PH release. To corroborate this hypothesis, we planned to perform fragmentation studies on these two compounds (currently ongoing).

Contrary to what happened for both **16** and **17, 18** inhibited the phosphorylation of Hsp27 to a higher extent in ST cells than in the WT for both 2 μM and 10 μM. Among these three compounds, **18** was the one which was consistent at both concentrations (more active in ST than in WT cells). Even though **18** was slightly less potent than **16** and **17**, it was more selective for the ST cells which could lead to a decrease in the side effects of a hypothetic treatment.

Chapter 8

Global Conclusions

It has been demonstrated that the inclusion of a non-natural electron-rich aromatic amino acid, specifically L-β-3',5'-dimethylphenylalanine, at positions 7 and 11 of the peptidic sequence of the natural somatostatin (SRIF14), triggers the formation of a major conformation in solution with a variable biological profile. The introduction of the same amino acid in position 6 led to the obtainment of two different major conformations which decreased the analogue's selectivity. All three peptides (**1** - **3**) were characterised by NMR spectroscopy.

The introduction of non-natural electron-poor amino acids, like L-β-4'-pyridylalanine and L-β-3'-pyridylalanine, favours a conformational restriction of the 14-amino acid somatostatin analogues in aqueous solution. Although Pya's are more hydrophilic than Phe leading to a decrease in the π-π aromatic interactions, the difference in the electronic density distribution counteracted that decrease, leading to highly structured analogues. These highly structured major structures were characterised by nuclear magnetic resonance spectroscopy.

Even though we have been able to synthesise the L-3-(3'-quinolyl)-alanine, a non-natural electron-deficient amino acid, its introduction in position 8 to substitute Trp, did not lead to rigid-enough peptides. For that reason, its effect in the binding affinity could not be studied.

From all the analogues studied, the family of peptides containing the non-natural amino acid D-Cys (**8** - **11**) have exhibited an interesting biological profile; all of them being selective for SSTR2 thus resembling [Msa7_D-Trp8]-SRIF14 (**7**) previously synthesised in our group and also selective for SSTR2. Even though structure calculations were only performed for compound **11**, all the NMR spectra showed high density of NOE signals which should correlate to the obtainment of rigid 3D structures in solution. Furthermore, peptide **11** has shown to have the highest half-life value (2400 min) from all the 14-amino acids somatostatin analogues reported until now. Moreover, the fragmentation studies had enabled us to disclose the key breakage points within the

somatostatin sequence and design new and more stable peptides which could be more suitable as drug delivery systems and/or drug carriers.

All three fluorescent compounds, **14**, **15** and **24**, proved to be resistant to the cyclisation and side chain deprotection acidic conditions and under the *in vitro* cell assay conditions. It has been demonstrated that both **15** was a receptor selective analogue as it has been internalised into ST cells to a greater extent than into WT cells as fluorescence was only detected for the cells overexpressing the SSTR2. Furthermore, the photo-release of **24** could be demonstrated by the fluorescence colour change detected while irradiating the two types of CHO-K1 cells with UV-visible light for different times. As for compound **15**, analogue **24** was selective for the ST cells as green and blue fluorescence was only detected for this type of cells.

The synthesis of somatostatin analogues with an inhibitor attached has been performed successfully. Furthermore, preliminary inhibitory kinase assays showed that analogues **16** and **17** had an inhibition potency close to the PH itself against ATF2 being **17** the one that triggered more inhibition. Compounds **16**, **17** and **18** showed an inhibitory effect against the phosphorylation of Hsp27 and even though **18** was slightly less potent than **16** and **17**, it was more selective for the ST cells which should lead to a decrease in the side effects of a hypothetic treatment.

Chapter 9

Experimental Section

9.1 General information & instruments

Non-aqueous reactions were carried out under inert nitrogen atmosphere and with dry solvents. Anhydrous tetrahydrofuran (THF), diethyl ether (Et_2O) and dichloromethane (CH_2Cl_2/DCM) were prepared by Solvent Purification System (SPS PS-MD-3). The rest of the anhydrous solvents were purchased from Sigma Aldrich. Non-anhydrous solvents were obtained from Panreac, Sigma Aldrich, Carlo Erba or Scharlab. The reactions that took place in aqueous media, were performed with bi-distilled water.

Commercially available reagents were purchased from Sigma-Aldrich, Alfa Aesar, Fluorochem, abcr GmbH, TCI Europe, Chem-Impex International, Iris-Biotech GmbH and Acros Organics without further purification.

The reactions were monitored by thin layer chromatography (TLC) using silica gel TLC-aluminum sheets (Merck 60 F_{254}). The TLC stains used have been:

- UV 254 nm and 365 nm
- Ninhydrin: 2 g ninhydrin in 1000 mL of acetone
- Potassium permanganate: 3 g $KMnO_4$, 20 g K_2CO_3, 300 mL H_2O and 5 mL of 5% $NaOH_{aq}$.
- p-Anisaldehyde: 9.2 mL of p-anisaldehyde, 3.8 mL of concentrated acetic acid, 12.5 mL sulfuric acid (98%) and 338 mL of absolute ethanol.

If further purification was needed, the crudes were purified by normal-phase column chromatography upon silica or by using the automated column chromatography system (Combiflash®, Teledyne Isco or PuriFLASH® 430, Interchim) using Hexane/Ethyl acetate mixtures in both cases. Some crudes needed to be purified over basic silica gel (SiO_2/Et_3N 2.5% v/v) using Hexane/Ethyl acetate mixtures or DCM as solvents.

Depending on the temperature needed, different options were considered:

- For T = 15-25ºC, room temperature (rt) was supposed.
- For T > 25ºC, a silicone bath was used in combination with a hot plate magnetic stirrer.
- For T < 0ºC, ice bath were used.
- For T < -10ºC, ice-brine baths or ice-acetone baths were used.

Reactions in high H_2 pressure were carried out in a Buchi Glas Uster Miniclave Steel reactor.

NMR spectra were acquired at room temperature on a Varian Mercury 400. ^{1}H and ^{13}C spectrums were referenced by its solvent residual peak. ^{1}H and ^{13}C monodimensional spectra were acquired to assign the signals of the ^{13}C NMR, as well as bidimensional homonuclear COSY, TOCSY, HSQC and HMBC.

Melting points were measured either in a Büchi M-540 or by DSC in a Mettler-Toledo DSC-822e apparatus without recrystallization of the final solids.

HRMS experiments were carried out both in the Mass Spectrometry Core Facility located in the Institute for Research in Biomedicine (IRB) and in the *Espectrometria de masses de caracterització molecular* Unit of the *Centres Científics i Tecnològics de la Universitat de Barcelona* (CCiTUB) located in the Faculty of Chemistry of the University of Barcelona (UB). In the IRB Barcelona, the samples were introduced by automatic nano-electrospray into an LTQ-FT Ultra mass spectrometer. Conditions: spray voltage 1.7 kV, capillary voltage 40 V, capillary temperature 200ºC, 120 V tube lense, m/z range 200 – 2000 u.m.a. and positive ionization. The software used for the data acquisition was Xcalibur (ThermoScientific). In the UB, the equipment used was an Agilent LC/MSD-TOF. The samples were introduced directly without chromatography by electrospray (ion spray) (ESI-MS). Conditions: capillary voltage 4 kV, capillary temperature 325ºC, N_2 pressure 15 psi, fragmentor voltage 215 V. This equipment is equipped with a double nebulizer for

the exact mass determination; this permits the simultaneous introduction of the internal reference by an independent nebulizer (internal reference masses (+) m/z = 121.050873 (Purine) and 922.009798 (HP-0921), internal reference masses (-) m/z = 112.6523 (TFA Anion), 119.0363 (Purine) and 1033.9881 (HP-0921).

Chiral HPLC experiments were performed on an analytical Agilent HP1100 with an automatic injector and a UV detector and a quaternary pump. The software used to process the data was Chemstation. The columns used were a Chiralpak IA (250 mm x 4.6 mm, 5 μm), a Chiralpak ADH (250 mm x 4.6 mm, 5 μm) and a Chiralcel OJ (250 mm x 4.6 mm, 10 μm). Isocratic gradients of Heptane and IPA (90:10), Heptane and Ethanol (70:30), Heptane and Ethanol - 0.2% DEA (70:30), Heptane and Ethanol - 0.2% TFA (90:10), Heptane and Ethanol - 0.2% TFA (70:30) and Heptane and Ethanol - 0.2% TFA (60:40) over 30 min where used to run the experiments with a flow rate of 0.5 mL/min and the UV detection was carried out at 254 nm.

Acidic HPLC-MS were carried out on an analytical Agilent Infinity 1260/MS 6130 with an automatic injector, a DAD/MS-ESI and APCI detector and a quaternary pump. The software used to process the data was Chemstation. The column used was a Gemini C18 (30 mm x 4,6 mm, 3μm). A linear gradient of H_2O (0.1% Formic Acid) and CAN over 10 min was used to run the experiments with a flow rate of 1.5 mL/min and the UV detection was carried out at 210 nm, 254 nm and 550 nm.

Basic HPLC-MS were carried out on an analytical Agilent HP1200/MS 6110 with an automatic injector, a UV/MS-ESI detector and a quaternary pump. The software used to process the data was Chemstation. The columns used were a Gemini-NX (30 mm x 4.6 mm, 3 μm) and a Kinetex EVO (50 mm x 4.6 mm, 2.6 μm). Linear gradients of NH_4HCO_3 (pH 8) and ACN over 8 min where used to run the experiments with a flow rate of 2 mL/min and the UV detection was carried out at 210 nm.

All **IR** spectrums have been obtained using a Thermo Nicolet Nexus FT-IR Fourier transform spectrometer. The samples were prepared by dissolution in solvent and

subsequent formation of a film on a NaCl disc by evaporation of the prepared solution. Absorptions are given in wavenumbers (cm^{-1}).

Absorption spectra were performed with UV-250-1PC, UV-VIS recording spectrophotometer Shimadzu.

The experimental procedure used for the synthesis of Fmoc-L-Dmp-OH, Fmoc-L-Msa-OH and Fmoc-L-Qla-OH were the previously used in our group[1] and the ones described in the literature.[2] The non-natural amino acids Fmoc-D-Trp(Boc)-OH, Fmoc-L-3'Pya-OH, Fmoc-L-4'Pya-OH, Fmoc-D-Cys(trt)-OH, Fmoc-L-Orn-OH, Boc-D-Ala-OH and Fmoc-D-Ala-OH were commercially obtained by either Sigma Aldrich, Iris-Biotech GmbH or Fluorochem.

9.2 Synthesis of somatostatin analogues (SRIF-14 analogues)

9.2.1 General methods & instruments

The natural amino acids were supplied by BCN Peptides S. A. or bought from Sigma Aldrich, Iris-Biotech and Fluorochem. Reagents used for the peptide synthesis where bought from Sigma Aldrich or Fluorochem without further purification. Dichloromethane (DCM) and dimethylformamide (DMF) were obtained from Carlo Erba and/or Panreac. Milli-Q water was obtained from an ultrapure water purification Milli-Q Advantage A10 system and used for the synthesis when needed. SST14 and octreotide were supplied by BCN Peptides S. A. following the same synthesis strategy described herein. 2-chlorotrityl chloride resin (2-CTC) was indistinctively bought from

[1] a) R. Ramon, M. Alonso, A. Riera, *Tetrahedron: Asymmetry*, **2007**, *18*, 2797-2802; b) P. Martín-Gago, M. Gómez-Caminals, R. Ramón, X. Verdaguer, P. Martín-Malpartida, E. Aragón, J. Fernández-Carneado, B. Ponsati, P. López-Ruiz, M. Alicia Cortés, B. Colás, M. J. Macías, A. Riera, *Angew. Chem. Int. Ed.*, **2012**, *51*, 1820-1825; c) P. A. Martín-Gago, doctoral thesis *Synthesis of highly structured and receptor-selective tetradecapeptidic analogs of somatostatin: Fine tuning the non-covalent interactions among their aromatic residues*, Univeristat de Barecelona, **2013**; d) R. Ramón, P. Martín-Gago, X. Vedaguer, M. J. Macias, P. Martín-Malpartida, J. Fernández-Carneado, M. Gómez-Caminals, B. Ponsati, P. López-Ruiz, M. A. Cortés, B. Colás, A. Riera, *ChemBioChem*, **2011**, *12*, 625-632.

[2] T. Li, Y. Tsuda, K. Minoura, Y. In, T. Ishida, L. H. Lazarus, Y. Okada, *Chem. Pharm. Bull.*, **2006**, *54*, 873-877.

Iris Biotech GmbH or supplied by BCN Peptides S. A. To perform the ion exchange the Dowex Monosphere 550A OH resin from The Dow Chemical Company was used.

Peptide mini-cleavages were performed at different points of the peptidic chain to check the progress of the couplings. A solution of TFA:TIS:H_2O (95:2.5:2.5) was added to a small portion of resin and let it react for 1h at room temperature followed by a TFA evaporation with N_2 flow. Cold ether was added to precipitate the peptide, the mixture centrifuged and the supernatant removed. H_2O:ACN (1:1) was added to dissolve the precipitate and then analysed by HPLC/HPLC-MS or UPLC/UPLC-MS.

For the analysis of intermediate peptides **HPLC** experiments were performed on a Waters Alliance 2695 (Waters, Milford, MA) with an automatic injector and a photodiode array detector (Waters 2998 or Waters 996). The software used to process the data was the Empower2. The column used was a Sunfire™ C18 3.5 µm (4.6 mm x 100 mm) reverse-phase analytical column. A linear gradient of H_2O (0.045% TFA) and ACN (0.036% TFA) over 8-min was used to run the experiments with a flow rate of 1 mL/min. The UV detection was carried out at 220 and 254 nm. Some others were performed in an Agilent HP1200 with an automatic injector and a photodiode array detector. The software used in this case was Chemstation. The columns used were a Luna C18 (250 mm x 4.6 mm, 5 µm) and a Kromasil C18 100 (150 mm x 4mm, 5µm) reverse phase columns. A linear gradient of H_2O (0.1% TFA) and ACN (0.1% TFA) over 30 min was used to run the experiments with a flow rate of 1 mL/min. The UV detection was carried out at 220 nm.

HPLC-ESI-MS of the intermediate peptides were also performed. The equipment used was a Waters system Alliance 2695 with a photodiode detector Waters 2998, the ESI-MS model was Micromass ZQ and using Masslynx v4.1 as the software (Waters). The column used was a Sunfire™ C18 3.5 µm (2.1 mm x 100 mm) using linear gradients of H_2O (0.1% FA) and ACN (0.07% FA) over 8 min with a flow rate 1 mL/min. The UV detection was at 220 and 254 nm.

UPLC chromatograms were obtained on a Waters Acquity system (PDA eλ detector, sample manager FNT and Quaternary solvent manager). The software used to process the data was the Empower2. The column used was an Acquity BEH C18 1.7 μm (2 mm x 50 mm). Linear gradients of H_2O (0.045% TFA) and ACN (0.036% TFA) were used over 2 min with a flow rate of 0.6 mL/min. The UV detection was performed at 220 and 254 nm.

UPLC-ESI-MS spectra of some peptide were performed on a Waters Acquity sytsem (PDA eλ detector, sample manager FNT and Quaternary solvent manager) and ESI-MS model SQ Detector2. The column used was an Acquity BEH C18 1.7 μm (2 mm x 50 mm) with linear gradients of H_2O (0.1% FA) and ACN (0.07% FA) over 2 min with a flow rate of 0.6 mL/min. The UV detection was at 220 and 254 nm.

For the purification of peptides semi-preparative RP-HPLC were performed on an Agilent 1260 Infinity comprising an automatic injector with two loops, two preparative pumps, a multiple wavelength detector and a fraction collector (Agilent 1260 Infinity) with an OpenLAB system controller. The column used was a Pursuit 10 C18 (150 mm x 21.2 mm, 10 μm) using linear gradients of H_2O (0.1% TFA) and ACN 90% (0.1% TFA) over 45 min with a flow rate 20 mL/min. The UV detection was performed at 220 nm and 254 nm.

In some cases, the fractions of the purification were analysed by **MALDI-TOF**. These experiments were carried out in the *Espectrometria de masses de caracterització molecular* Unit of the *Centres Científics i Tecnològics de la Universitat de Barcelona* (CCiTUB) located in the Faculty of Chemistry of the University of Barcelona (UB). The determination of the molecular weight of some peptides was performed on a MALDI TOF/TOF 4800 Plus (ABSciex) with a solid state laser of 355 nm (200 Hz, 3-7ns pulses) calibrated with Calmix (Calmix 4700 Proteomics Analyzer Calibrating Misture) using α-cyano- 4-hydroxycinnamic acid (ACH) matrix (10 mg/mL of ACH in ACN-H_2O (1:1, v/v) containing 0.1% TFA). The spectra were obtained by reflector positive mode in an

m/z range between 500 and 3000 u.m.a. Data was analysed by Data Explorer software. Sample preparation: 1 μL of sample solution (0.5 – 2 mg/mL) mixed with 0.5 μL of matrix were seeded on the MALDI-TOF plate and air-dried.

Homonuclear bidimensional TOCSY (50 ms) and NOESY (200 and 350 ms) experiments were acquired in a Bruker Avance III 600 MHz at 285 K using either a 100 mM phosphate buffer at pH = 6.5 in 10% D_2O or deuterated DMSO. Peptide's final concentration = 2 mM. Before and after the 2D experiments, ^1H monodimensional experiments were acquired to ensure that aggregation and/or precipitation did not occur during the acquisition which could modify the concentration of the peptide.

9.2.2 General considerations for the solid-phase peptide synthesis

Peptide analogues were synthesised following the solid-phase peptide synthesis strategy via the well-known Fmoc/^{t}Bu[3] methodology using polypropylene syringes with a polyethylene filter and connected to a vacuum system. Reactors of different volumes (2, 5, 10 or 20 mL) were used depending on the scale used for the synthesis. The solvents and/or reagents were added to the SPPS reactor containing the resin and stirred in an orbital shaker. After the treatment, the excess of solvents and reagents was removed by filtration through the vacuum system.

For the coupling of the first amino acid, a known quantity of resin was weighted and swelled with anhydrous DCM. Afterwards, 0.3 eq of the Fmoc-aa-OH and 3 eq of DIEA were dissolved in $DCM_{anh.}$ and added onto the resin. After determining the resin load by UV monitoring of the Fmoc removal at 301 nm, the unreacted sites were capped with methanol. For the *N*-Fmoc group deprotection once the coupling was finished, the strategy of piperidine washings was used using piperidine in DMF (40%) for 5 min and piperidine in DMF (20%) for 10 min. Some washings had to be performed after every

[3] G. B. Fields, R. L. Noble, *Int. J. Protein Res.*, **1990**, *35*, 161-214.

coupling and deprotection steps; these washings consisted of six washings with DMF, two with DCM and a final and longer wash with DMF to equilibrate the resin.

Both the coupling and the deprotection of the *N*-Fmoc group during the elongation of the peptidic chain were monitored by Kaiser test[4] or ninhydrin test, a colorimetric test which allows the detection of free primary amine groups on the resin. After DCM washings, a small portion of resin was placed in a glass tube to which 5 μL of solution A (40 g of phenol in 10 mL of EtOH), 10 μL of solution B (20 mL of 10 mM KCN aq in 100 mL of pyridine) and 5 μL of solution C (2.5 g of ninhydrin in 50 mL of EtOH) where added and heated to 100ºC for 3 min. The colour of the resin or the supernatant was evaluated: a yellow colour indicates absence of free primary amines (coupling finished) whilst a blue colour is a positive result indicating incomplete coupling or *N*-Fmoc group deprotection finished. Due to the sensitivity of this test, a negative result indicates a coupling rate greater than 99.5%. To double check the progress of the elongation, mini-cleavages were performed after some key aa's.

9.2.3 General methodology for the synthesis of somatostatin analogues

All the synthesis were performed by SPPS using the 2-chlorotrityl chloride resin (2-CTC) via the Fmoc/^{t}Bu strategy. In most cases, a decrease of the commercial resin loading (from 1.6 mmol/g to ~0.50 mmol/g) was carried out to avoid aggregation problems further on. Variable quantities of 2-CTC resin were used (from 0.2 g to 3.0 g) and swelled with an appropriate quantity of anhydrous DCM for 30 min. Having done that, 0.3 eq of Fmoc-aa-OH and 3 eq of DIEA in $DCM_{anh.}$ were added and stirred for 1 h. After determining the resin loading by UV detection, the remaining active sites were end-capped with cocktail solution of MeOH/DCM/DIEA (15:80:5). Once the washings and the Fmoc deprotection had been done, the second amino acid could be coupled by adding Fmoc-aa-OH (4 eq regarding the determined resin load), HOBt (3.9 eq) and DIPCDI (3.9 eq) in

[4] E. Kaiser, R. L. Colescott, C. D. Bossinger, P. I. Cook, Anal. Biochem., **1970**, *34*, 595-598.

DMF under agitation for 1 h. Kaiser test was performed to verify the coupling completion. If a recoupling was needed, Fmoc-aa-OH (3 eq), HATU (3 eq) and DIEA (6 eq)[5] in DMF would be added and stirred for 30 min after some washings of the resin with DMF. Once the amino acid is completely coupled to the previous one and the Fmoc-group deprotected, the same strategy is followed to couple the rest of the residues until de *N*-terminal one. For the coupling of the last amino acid, a Boc-aa-OH was used. For the non-natural amino acids, 3.0 eq were used together with 2.9 eq HOBt and 2.9 eq DIPCDI in the appropriate quantity of DMF.

The release of the complete fully-protected peptidic chain was achieved using a soft cleavage cocktail solution (DCM/TFE/AcOH, 70:20:10 v/v) over two hours. This cocktail solution released the linear peptide from the resin and deprotected the Cys side chains (protected with a trityl group) enabling them to form the disulphide bridge by an oxidation mechanism. This bridge formed by the oxidation of two thiol side chains was achieved using I_2 (10 eq) in solution at room temperature over 15 min and then quenched with $Na_2S_2O_3$ 1N. The aqueous layer was extracted with DCM, the combined organic layers washed with a 5% aqueous solution of Citric Acid/NaCl 1:1 and then evaporated under reduced pressure.

Finally, total side chain deprotection was achieved with an acidolysis reaction mediated by a TFA solution (TFA/DCM/Anisole/H_2O, 55:30:10:5 v/v) over 4 hours. Then, the remaining solution was washed with heptane and drip filtered over cold Et_2O (-10ºC) to precipitate the final cyclic peptide. The resulting suspension was centrifuged at 4ºC and 3500rpm two times, changing the cold diethyl ether each time. Ether was decanted, H_2O:ACN (70:30) added and then lyophilised to obtain the final crude peptide, which could be analysed, purified and analysed again.

[5] This strategy cannot be used for the recoupling of Fmoc-L-Cys(trt)-OH, Fmoc-L-Ser(^{t}Bu)-OH or Fmoc-L-Asn-OH, due to racemization problems (Cys and Ser) or formation of autocondensation products (Asn).

To perform the ion-exchange from TFA^- to AcO^-, purified peptides were dissolved in aqueous 0.1N AcOH, added over an ion exchange Dowex resin and recovered by filtration after lyophilising the obtained aqueous phase.

9.2.4 Biological assays' methodologies

SSTR2 transfection into CHO-K1 cell line

CHO-K1 cells were maintained in Kaighn's modification of Ham's F-12K medium (F-12K) supplemented with a 10% of fetal bovine serum (FBS). *N*-terminal 3xHA-tagged human Somatostatin receptor 2 (SSTR2) cloned into pcDNA3.1+ (Invitrogen) at KpnI (5') and XhoI (3') vectors were obtained from *Missouri S&T cDNA Resource Center* (Missouri University of Science and Technology, MO, USA). CHO-K1 cells were transfected with these vectors by using a solution of sodium chloride (NaCl) and Polyethylenimine (PEI). Stable clones were selected in F-12K medium containing geneticin (1 mg/mL) as an antibiotic and maintained in the same media. Expression was detected by Western Blot and immunofluorescence.

SRIF14 analogues – SSTR1-5 binding affinity assays

CHO-K1 cell line independently expressing SSTR1-5 was used for the assay. Cell membranes were extracted and incubated in the assay buffer (25 mM HEPES, pH 7.4, 5 mM $MgCl_2$, 1 mM $CaCl_2$, 0.1% BSA), together with a fixed concentration of [^{125}I-Tyr11]-SRIF14 radio-ligand and the analogues with concentrations ranging from 10^{-12} to 10^{-6} M for 2-4 hours at 25°C. The total binding was determined when only the [^{125}I-Tyr11]-SRIF14 was present. When 1 μM of SRIF14 was added, the non-specific binding was determined. The difference between these two values gave the specific binding.

The Ki values of each compound were determined as Cheng and Prusoff described.[6] These assays were performed by Eurofins Panlabs Taiwan, Ltd. using the above mentioned conditions.

Raw data obtained

	SSTR1 (nM)	**SSTR2 (nM)**	**SSTR3 (nM)**	**SSTR4 (nM)**	**SSTR5 (nM)**
Somatostatin-14 (Batch S1401)	2.88	0.21	0.99	4.18	2.00
[Dmp11_D-Trp8]-SRIF14 (1)	4.75	0.84	2.06	25.00	3.82
[Dmp7_D-Trp8]-SRIF14 (2)	1.70	0.55	0.67	19.90	1.58
[Dmp6_D-Trp8]-SRIF14 (3)	7.53	3.39	0.76	7.02	2.31
[Msa6_4Pya7_DTrp8]-SRIF (4)	32.00	4.32	4.86	14.80	3.48

	SSTR1 (nM)	**SSTR2 (nM)**	**SSTR3 (nM)**	**SSTR4 (nM)**	**SSTR5 (nM)**
Somatostatin-14 (Batch S0509)	0.75	0.036	0.20	1.20	1.11
[Msa7_D-Trp8_D-Cys14]-SRIF14 (7)	10.7	0.0146	24.00	22.00	20.00
[D-Cys3,14_Msa7_D-Trp8]-SRIF14 (8)	5.48	0.023	18.7	48.00	19.40
[D-Ala1_Msa7_D-Trp8_D-Cys14]-SRIF14 (9)	1.80	0.0144	20.00	27.00	19.60
[Msa6_3Pya7_D-Trp8]-SRIF14 (5)	18.1	12.6	0.85	2.58	2.70

	SSTR1 (nM)	**SSTR2 (nM)**	**SSTR3 (nM)**	**SSTR4 (nM)**	**SSTR5 (nM)**
Somatostatin-14 (Batch S1402)	3.69	0.20	1.10	6.94	4.64
[D-Ala1_D-Cys3,14_Msa7_D-Trp8]-SRIF14 (10)	11.80	0.19	14.30	48.00	26.00

[6] Y. Cheng, W. H. Prusoff, *Biochem. Pharmacol.*, **1973**, *22*, 3099-3108.

Inhibitory Kinase assay

Sample preparation

p38 activation: Bacterially-expressed GST-p38a MAPK is activated with MBP-MKK6 DD (5:1)

Kinase buffer: 50 mM Tris HCl pH = 7.5, 10 mM $MgCl_2$, 2 mM DTT, supplemented with protease and phosphate inhibitors: sodium vanadate (100 μM), PMSF (1 mM), aprotinin (10 μg/mL) and leupeptin (10 μg/mL).

Reaction (can be scaled up as needed)*:* mix 17.9 μL of kinase buffer, 1 μL (4 μg) of GST-p38a (4.3 μg/μL), 0.4 μL of ATP 10 mM (the final concentration will be 200 μM, pH = 7.5 adjusted with HCl or NaOH) and 0.7 μL (1 μg) of MBP-MKK6 DD (1.5 μg/μL) over ice. Incubate at 30ºC for 1 h and store at -80ºC. 1 μL of this prep has approx. 200 ng of p38 and 50 ng of MKK6-DD.

Kinase assay preparation

The kinase assay was carried out using 1 μL of activated p38 protein in approx. 12 μL of buffer, supplemented with 100 μM of cold ATP and 2 μCi ^{32}P-γ-ATF2. A negative control (ATF2 alone) a positive control (ATF2 and p38 active) and a PH control (ATF2, p38 active and PH [2 μM]) were also prepared. The samples containing the calculated amounts (0.5 to 10 μL) of inhibitors' solutions in DMSO were also prepared. All the samples were incubated at 30ºC for 30 min. After this, the reaction was quenched by adding 5 μl loading buffer (Blue, x5 loading) and then placing the samples in ice.

Polyacrylamide gel electrophoresis SDS-PAGE

Protein electrophoresis in a sodium dodecyl sulphate polyacrylamide gel (SDS-PAGE) has been widely used for separating proteins based on their molecular weight.[7] SDS buffer

[7] U. K. Laemmli, *Nature*, **1970**, *227*, 680-685.

(acting as a detergent) is added to the sample before the electrophoresis to ensure the denaturalisation of the proteins and provide a negative charge to maintain the charge-to-mass ratio. By binding to the proteins the detergent destroys their secondary, tertiary and/or quaternary structure denaturing them and turning them into negatively charged linear poly peptide chains. When subjected to an electric field in PAGE, the negatively charged polypeptide chains travel toward the anode with different mobility depending on their weight.

For this type of electrophoresis two gels need to be prepared with different pH and acrylamide concentration; stacking and separating gel. Acrylamide concentration is lower in stacking gel forming bigger pores in the acrylamide mesh which enables proteins to travel fast inside it and to enter the separating gel all at once. The net formed by the separating gel is thicker and it separates the proteins by their weight. Acrylamide concentration in that gel varies depending on the sample to separate (6%, 7.5%, 10%, or 12.5%).

Gel preparation

2 gels		
Separating 12,5%		**Stacking 4%**
6.3 mL	H_2O Milli-Q	6.0 mL
5.0 mL	Tris 1.5 M	-
-	Tris 0.5 M	2.5 mL
8.3 mL	Acrilamide 30%	1.33 mL
200 µL	SDS 10%	100 µL
200 µL	APS	100 µL
20 µL	TEMED	10 µL

2 gels		
Separating 10%		**Stacking 4%**
9.8 mL	H_2O Milli-Q	7.6 mL
5.0 mL	Tris 1.5 M	-
-	Tris 1.0 M	1.25 mL
5.0 mL	Acrilamide 40%	1.0 mL
100 µL	SDS 20%	50 µL
200 µL	APS 10%	100 µL
16 µL	TEMED	10 µL

After mounting the electrophoresis glass plates as indicated in the manufacturer's instructions, the separating gel is prepared, placed between the plates (3/4 of total volume) and left to polymerise (APS and TEMED are the polymerisation catalysts) which usually takes between 10-15 min. Before it polymerises, isopropanol is added at the top to flatten the gel layer, eliminate the possible air bubbles and prevent the oxygen from inhibiting the polymerisation

Once the separating gel has polymerised, isopropanol is decanted and the stacking gel is prepared and added on top of the other gel. Immediately after that, the appropriate comb is placed to form the wells. When samples are ready, remove the comb.[8] While waiting for the gel to be polymerised, the samples are boiled (95ºC, 5min), spinned and placed in ice before loading into wells. Part of the sample is kept in the freezer in case something needs to be repeated.

Electrophoresis

Glass plates with gels are placed inside apparatus, and the tank filled with running buffer 1x[9] up to top of inner space between gel plates and then just above the metal wire. At that point, samples can be loaded. A pre-stained buffer (loading buffer) was loaded in parallel to visualise protein separation and establish the approximate molecular weight of the proteins present in the sample. If only one gel was loaded, a plastic well needed to be used to imitate using 2 gels at a time. The rest of tank was filled with running buffer and then lid placed on top.

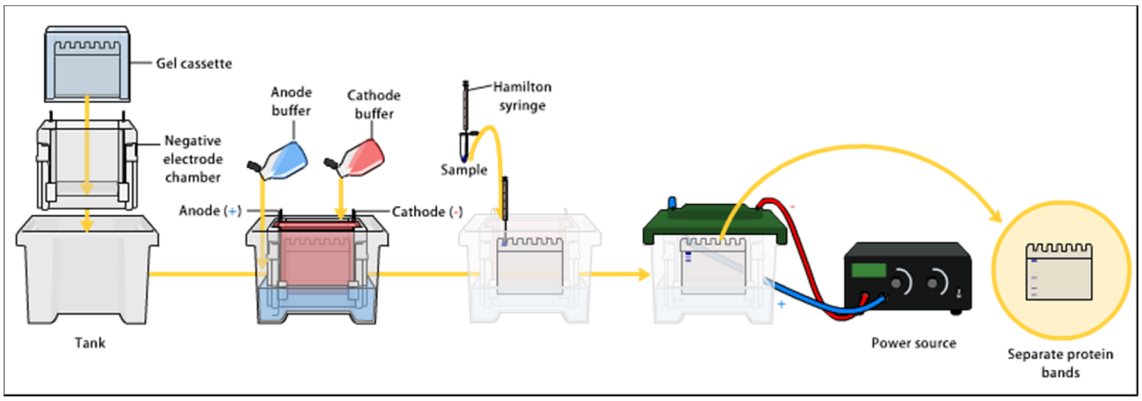

Electrophoresis was ran at 100 V for the first 15 minutes during initial loading of proteins onto gel and then ramped up to 120 V during the rest of the run. Once proteins were separated, run was stopped. Running buffer can be reused.

[8] Gels can be wrapped in wet paper, and stored in a sealed plastic bag at 4ºC for some days. Be sure to test transparency and condition, especially about the comb, before using premade gels.

[9] 900 mL H_2O + 100 mL running buffer 10x (Tris-Base 250 mM, glycine 1.9 M, SDS 0.1%).

Western Blot

Western-blot analysis enables the selective identification of a protein, previously separated by electrophoresis, by the use of an antibody that specifically binds to it. In order to perform this recognition, proteins must be transferred to a nitrocellulose membrane so they are immobilised by adsorption. Once the transfer is done, the membrane must be incubated with a primary antibody which presence is revealed by a peroxidase-conjugated secondary antibody. In presence of substrate the secondary antibody generates fluorescence. Western Blot analysis consists of two steps; protein transfer to a membrane and detection by antibodies.

Transfer Blot

First thing to be done was prepare Whatman® papers using a cardboard stencil and wash all material with water. Plastic sandwich was placed inside a plastic tray filled with transfer buffer[10] solution (black part on bottom), and then a sponge was soaked in transfer buffer too. After that, 2 Whatman® papers were soaked in the buffer solution and placed on top of sponge. Gel was removed from the glass, wells region scraped away, and the gel transferred on top of the Whatman® papers. Membrane was, then soaked in transfer buffer solution and placed directly on top of the gel taking care to remove bubbles by rolling a falcon down from the middle outwards. To finish, 2 more Whatman® papers were soaked as well as a second sponge and placed on top of membrane,[11] then the transparent part of the sandwich was closed.

[10] 700 mL H2O + 200 mL MeOH + 100 mL Transfer Buffer 10x (Glycine 1.9 M, Tris Base 250 mM).

[11] Membrane must not be touched with wet hands or without gloves when handling/cutting. If dark stains appear when soaking it in the solution, discard it and cut another one.

Transfer tank and plastic holder were set up and the sandwich placed inside the tank,[12] using frozen falcons to prevent the temperature from rising. Tank was then filled with transfer buffer solution. Transference was done at 0.25A over 1.5-2 hours.

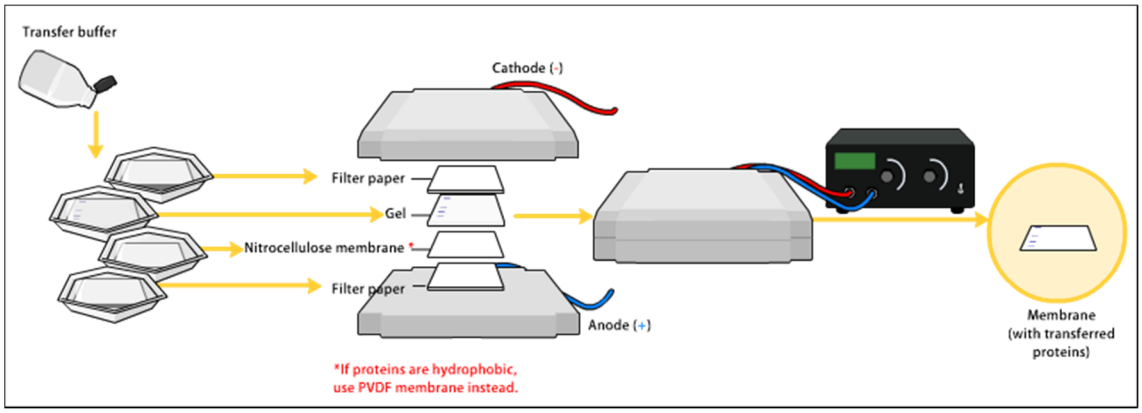

After run was finished, membrane was removed (papers and gel may be discarded, transfer buffer reused, plastic and sponges washed) and placed into a small plastic tray. Membrane was covered with Ponceau red stain and left for several minutes, before removing stain (which can be poured directly back into bottle) and washing twice with water to remove any unbound protein. At that point, membrane was scanned inside a polypocket to provide a loading control.

At that point, membrane was washed with PBS to remove remaining Ponceau and cut to size. To block membrane, 10-15 mL of milk solution (5% skimmed milk in PBS solution) were poured over it and shacked for 45 min - 2 h at room temperature or at 4ºC chamber overnight. Milk was removed and membrane washed with PBS (quick wash, 5min wash and quick wash).

[12] When placing sandwich inside tank, check black plastic matches black part of tank, and transparent part of sandwich with red of tank. When placing lid of container colours must match again.

Primary antibody

5% BSA (Bovine Serum Albumin) was prepared by weighing 2.5 g and dissolving them in 50 mL PBS. From this stock, 1% BSA was prepared (1:5 dilution using PBS). About 5 mL per membrane were needed.

To prepare primary antibody solution, 5 μL of antibody (p-ATF-2 p38α Rabbit) were added to 5 mL of 1% BSA solution (1:1000 dilution). Then, membrane was covered with this solution in a tray, covered with parafilm, labelled, and left shaking for 2 hours at room temperature or at a 4ºC chamber overnight.

Secondary antibody

If sample was in a cold-room, it was left shaking at room temperature for 5 - 10 min. Then antibody solution removed (this may be reused 3-4 times, it needs to be stored in a falcon at 4ºC). Membrane was washed PBS as before (quick wash, 5 min wash shaking and quick wash).

To prepare secondary antibody solution, 1 μL of antibody (goat anti-rabbit) was added to 5 mL of 1% BSA solution (1:5000 dilution). Membrane was covered with the solution, the tray covered with tinfoil because of fluorescence and left shacking for 45 min at room temperature or overnight in a 4ºC chamber.

After the incubation, secondary antibody solution was removed, membrane washed with PBS (quick wash, 5min wash shacking, quick wash) and blot scanned.

p38 Kinase cellular assay

Cell splitting

After viewing cells under the microscope to estimate confluency, the split needed to be done so as they were around 50% confluent for the assay. CHO-K1 wild type (CHO-K1 WT) and CHO-K1 with the SSTR2 transfected (CHO-K1 ST) cell lines grew very fast, so

the splits needed to be diluted enough for the cells not to grow up more than to 50% confluency. 10 cm culture plates with 6 mL of media were used for cell normal growth but only 2 mL of media were used before the experiment.

Once the 50% confluency was achieved, cell media was removed and cells washed twice with PBS (2 mL each time). PBS was completely removed (to avoid inhibition of trypsin in the next step) and 1 mL, or volume enough to cover the surface of the plate, of trypsin added. Then cells were left in the incubator for 5 min (37ºC, 5% CO_2). Culture plates were removed from the incubator, and it was checked that the cells have detached from the plastic plate on the microscope. Media was added to inhibit trypsin (same quantity as trypsin added previously). Cells were transferred to a falcon and centrifuged (1300 rpm, 5 min) to remove the trypsin-containing media. Supernatant was removed, 6 mL of new media were added and cells re-suspended. From that suspension of cells, 250 µL were placed in a culture plate containing 3 mL of media and placed into the incubator at 37ºC.

Treatment of cells

Cell media was removed (3 mL) and 2 mL of fresh media was added (except in negative controls, where 3 mL can be kept). After that, inhibitors were added directly into the media (2mM, therefore 2 µM would be 1:1000 dilution, 4 µM is 2:1000 dilution, 4 µl added to 2 mL solution in plate). Cell culture plates were returned to incubator for 1 hour.

Cell irradiation

Cells were removed from incubator, cell media removed and kept in labelled Eppendorf tubes so that the media may be returned to the cell plates after radiation. Controls had 3 mL, so 2 mL were kept and 1 mL discarded.

Cell plates were placed in the UV irradiator, lids removed to allow UV to penetrate and cells blasted 80 J of energy. Then media was added back and plates left in the incubator at 37ºC 5% CO_2 for 45 min.

Pellet treatment

Media was removed and two washes with 1 mL of PBS were done. PBS was removed and trypsin added to the cells and incubated at 37ºC for 5 min. Once the cells were removed from the incubator, 0.8 -1 mL of media was added to inhibit trypsin. Cells should be completely detached from the plate so they were transferred to Eppendorf tubes. After centrifuging the cells (1200 rpm, 5 min), supernatant was removed, PBS added and centrifuged again for 5 more min. Once the second centrifugation was finished, supernatant was removed carefully so as not to touch the cells and the pellet kept at -20ºC overnight for further treatment.

Cell lysis and protein extraction

RIPA Lysis buffer[13] was thawed and kept over ice. Lysing of cells was performed using 50 µL of above mentioned buffer. Agitation was used to dissolve pellet which was, then, left 15 min on ice (after last sample had been lysate). Centrifugation was performed at 4ºC at 13200 rpm for 15 min and final solutions were transferred to new labelled eppendorf tubes.

Protein quantification

Protein Assay Reagents A, B and S were used.[14] A mix had to be premade: 500 µL reagent A + 10 uL reagent S. Once the mix was prepared, 25 µL were added to the 96-well plate, followed by the addition of 2 µL of sample and 200 µL of reagent B. Every sample was loaded twice and the average value was used for concentration calculation. A BSA

[13] For 10 mL RIPA Buffer: 300 µL NaCl (5 M), 500 µL TRIS pH = 7.4 (1 M), 100 µL EDTA 0.5 M, 1 mL NP-40 (10%), 8.1 mL H_2O. Inhibitors for 1 mL RIPA: 1 µL leupeptin (10 mg/mL), 1 µL pepstatin A (10 mg/mL), 1 µL aprotinin (10 mg/mL), 1 µL PMSF (1 M), 1 µL NaV_3 (1 M), 1 µL DTT (1 M), 1 µL microcystin (1 mM), 5 µL benzamide (0.5 M) and 40 µL NaF (0.5 M).

[14] Bio Rad DC Protein Assay Kit. Reagent A: alkaline copper tartrate solution, Reagent B: dilute Folin Reagent.

calibration curve was performed as well, using different quantities of BSA (0-8 µg BSA). The plate was left to react for 5-10 min after what it was red trough Gen5 2.09 programme.

Once the proteins had been quantified, SDS-PAGE and Western Blot protocols were followed and same antibodies (primary and secondary) and concentrations were also used as did before for the inhibitory kinase assay.

Immunofluorescence

Immunofluorescence (IF) or cell imaging techniques rely on the use of antibodies to label a specific target antigen with a fluorescent dye (also called fluorophores or fluorochromes) such as fluorescein isothiocyanate (FITC). Antibodies that are chemically conjugated to fluorophores are commonly used in IF. The fluorophore allows visualization of the target distribution in the sample under a fluorescent microscope (e.g. confocal microscopes). Two IF methods depending on whether the fluorophore is conjugated to the primary or the secondary antibody can be distinguished:

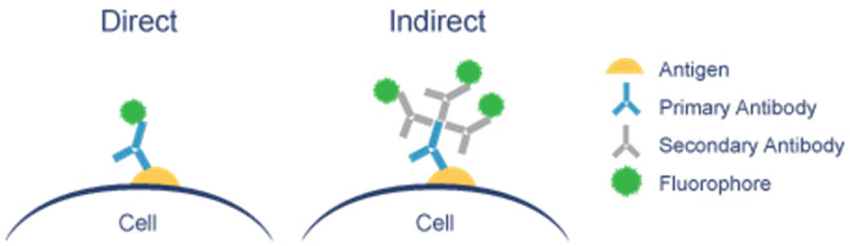

Direct IF which uses a single antibody (conjugated with a fluorophore) directed against the target of interest (known as primary antibody).

Indirect IF which uses two antibodies; the primary antibody unconjugated and a fluorophore-conjugated secondary antibody directed against the primary antibody which is used for detection.

In our case, the experiment was carried out in sterile 10 mm coverslips and with differentiated and grown cells. Coverslips were transferred to 6-well plates and were washed twice with PBS. It was really important to control the orientation of the cells (which were attached to only one side of the coverslip) and avoid adding solutions directly over them. Cells were fixed with 4% p-formaldehyde in PBS during 15min at room temperature and then washed three times with PBS over 10 min.[15]

Once the washings were done, a blocking was done with 10% FBS in PBS over 30 min. This step was done to block unspecific bindings of primary and/or secondary antibodies. While the blocking was ongoing, primary antibodies' solutions were prepared in eppendorf tubes with PBS-10%FBS. For each coverslip, 25 µL of solution were needed. To discard possible antibody aggregation, the solution was centrifuged at 4ºC for 5 min.

Cell incubation with primary antibody solution was performed in clean parafilm over which 25 µL of the antibody solution were added as a drop. Coverslip was transferred from the 6-well plate to the parafilm making sure the side with cells was in contact with the solution. Cells were incubated at room temperature for 45 min-1 h.[16] Coverslips were transferred back into the 6-well plate and three 5 min washed with PBS were done.

Secondary antibody incubations with cells was performed following the same protocol as for the primary but, this time, protecting cells from light due to chromophore's photosensitivity. From this point, samples were handled protected from light. After three 10 min washes with PBS, coverslips were incubated with PBS-DAPI (15 µL DAPI / 30 mL PBS) for 10 min and washed with PBS over 10 more minutes and a quick wash with Milli-Q H_2O was performed as well. Later, coverslips with cells facing up were left on an absorbent paper and let air dry at room temperature protected from light.

[15] At this point, coverslips can be stored at 4ºC overnight.

[16] Negative controls (incubating cells with irrelevant antibody or directly with a secondary antibody) could be included at that point.

Once the coverslips were dry, the mounting could be done by adding 5-10 µL of Mowiol over the microscope slides and placing the coverslips on top each drop (cells facing the solution). The mounting was left to dry overnight in a horizontal position and stored at 4ºC protected from light. Sample observation was done in a Leica TCS 4D laser fluorescence confocal microscope with a 63x lense in the *Servei de Microscopia Confocal* of the *Serveis Cientificotècnics* of the University of Barcelona.

Live fluorescence *in vitro* assays. Internalisation assay

To study the cellular uptake and the localization of the compound **15**, CHO-K1 WT and CHO-K1 ST cells were first seeded in 10 mm coverslips inside 3 cm cell culture plates. Once 50% confluence was achieved (~24 h), both cell lines were incubated with 10 µM of compound 15 and left inside the incubator at 37 ºC in a 5% CO_2 incubator for 1h. Positive and negative controls for both cell lines were prepared by incubating the cells with 10 µM of the free coumarin (7-methoxy-coumarin-4-yl)-acetic acid) or without adding any compound, respectively.

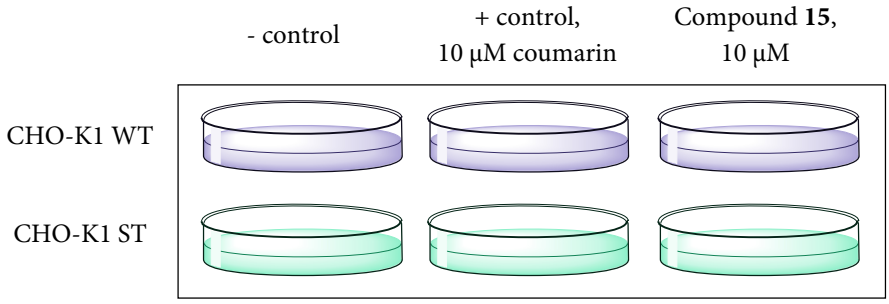

Sample observation was done in a TIRF-ScanR Olympus microscope with a 100x oil lense with an excitation wavelength of 377/50 nm and an emission wavelength of 447/60 nm in the *Servei de Microscopia Confocal* of the *Serveis Cientificotècnics* of the University of Barcelona.

Real time cellular uptake or photo-release *in vitro* assays

To study the cellular uptake of compound **24**, cells were first seeded in 10 mm coverslips inside 3 cm cell culture plates. Once 50% confluence was achieved (~24 h), both cell lines were incubated with 10 μg/mL of compound **24** for 4 hours at 37 ºC in a 5% CO_2 incubator. After incubation, cells were irradiated with UV-visible light (≥ 410 nm) for 0, 15 and 30 min. In this case, a negative control was also prepared by incubating the cells alone and without irradiating them with UV-Visible light. Thereafter, cells were fixed using 4% *p*-formaldehyde for 30 min, washed twice with phosphate buffered saline (PBS) and then the mounting was done by adding 5-10 μL of Mowiol over the microscope slides and placing the coverslips on top each drop (cells facing the solution). The slides were left to dry overnight and stored at 4ºC protected from light.

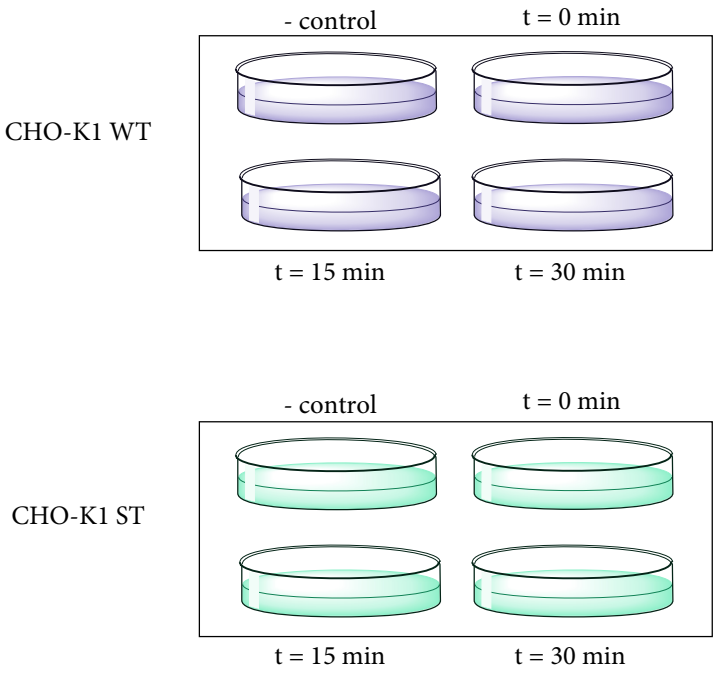

Sample observation was done in a Leica TCS 4D laser fluorescence confocal microscope with a 63x lense in the *Servei de Microscopia Confocal* of the *Serveis Cientificotècnics* of the University of Barcelona.

9.2.5 Somatostatin (SRIF14) analogues

L-Dmp family

[L-Dmp11_D-Trp8]-SRIF (1): SRIF14 analogue **1** was synthesised following the general synthesis protocol using 1.0 g of 2-CTC resin (1.6 mmol/g), Fmoc-L-Cys(trt)-OH as a *C*-terminal amino acid and Boc-L-Ala-OH as *N*-terminal aa. Peptide was purified by semi-prep. RP-HPLC and 51.4 mg were obtained with purity above 95%. HPLC: t_R = 12.3 min, gradient: 25-60% ACN (0.1% TFA) in 30 min, 1 mL/min, λ = 220 nm. HRMS: calculated for $C_{78}H_{108}N_{18}O_{19}S_2$: 1664.7480; found: 833.3818 $[M+2H]^{2+}$ and 555.9249 $[M+3H]^{3+}$.

	HN	Hα	Hβ	Hγ	Hδ	Hε	Hζ	Hη
1 Ala	-	3.95	1.35	-	-	-	-	-
2 Gly	8.49	3.82	-	-	-	-	-	-
3 Cys	8.28	4.44	2.93 (β2) 2.74 (β3)	-	-	-	-	-
4 Lys	8.47	4.43	1.46	1.16 (γ2) 1.04 (γ3)	1.26	2.58	7.25	-
5 Asn	8.41	4.66	2.45	-	7.35 (δ21) 6.75 (δ22)	-	-	-
6 Phe	8.36	4.49	2.73 (β2) 2.52 (β3)	-	6.57	6.93	6,80	-
7 Phe	8.06	4.35	2.78 (β2) 2.74 (β3)	-	7.03	7.17	7.12	-
8 DTrp	8.31	4.23	2.87 (β2) 2.71 (β3)	-	6.93	10.02 (ε1) 7.40 (ε3)	7.30 (ζ2) 6.97 (ζ3)	7,05
9 Lys	8.13	3.95	1.41 (β2) 1.03 (β3)	0.31 (γ2) 0.10 (γ3)	1.11	2.46 (ε2) 2.39 (ε3)	7.26	-
10 Thr	7.60	4.24	3.95	0.92	-	-	-	-
11 Dmp	8.22	4.79	2.58	2.01*	6.53	-	6.69	-
12 Thr	8.34	4.33	4.04	1.00	-	-	-	-
13 Ser	8.27	4.44	3.75	-	-	-	-	-
14 Cys	8.06	4.34	3.05 (β2) 2.96 (β3)	-	-	-	-	-

Chemical shifts in ppm for the detected protons in TOCSY and/or NOESY spectrum. *Hφ of Dmp have been placed in Hγ column for a clearer visualisation.

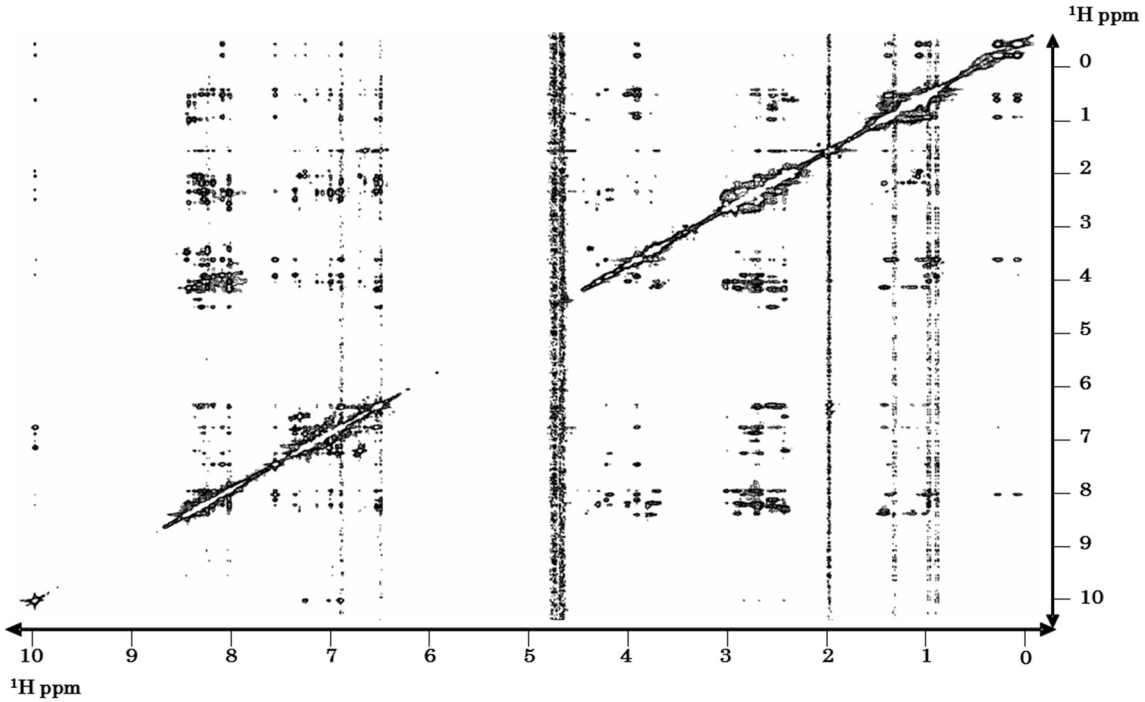

Bidimensional homonuclear NOESY 350 ms spectra for [L-Dmp11_D-Trp8]-SRIF (**1**) acquired in a Bruker Avance III 600 MHz at 285 K.

Distance restrictions:

Intraresidual: 0

Sequential: 97

Medium-range (1<dist≤4): 32

Long-range (dist>4): 34

Total: 163

Dihedral angle restrictions: 18

Statistics for 20 best structures

Energies (kcal/mol):	**RMSD*:**
Total energy: -251.3 ± 9.673	Bonds (Å): $7.02 \times 10^{-3} \pm 2.322 \times 10^{-4}$
Van der Waals: -34.51 ± 5.60	Angles (°): 1.180 ± 0.01737
Electrostatic: -483.7 ± 9.55	Impropers (°): 4.466 ± 0,04302
Bonds: 11.45 ± 0.76	Dihedrals (°): 41.19 ± 0.1704
Angles: 87.57 ± 2.59	NOEs: $1.163 \times 10^{-2} \pm 2.782 \times 10^{-4}$

Parameters' study for 20 structures with lower energy calculated for [L-Dmp11_D-Trp8]-SRIF (**1**). *Average deviation for 20 structures with lower energy when compared to lowest energy structure.

[L-Dmp7_D-Trp8]-SRIF (2): SRIF14 analogue **2** was synthesised following the general synthesis protocol using 1.0 g of 2-CTC resin (1.6 mmol/g), Fmoc-L-Cys(trt)-OH as a *C*-terminal amino acid and Boc-L-Ala-OH as *N*-terminal aa. Peptide was purified by semi-prep. RP-HPLC and 69.6 mg were obtained with purity above 95%. HPLC: t_R = 13.2 min, gradient: 25-60% ACN (0.1% TFA) in 30 min, 1 mL/min, λ = 220 nm. HRMS: calculated for $C_{78}H_{108}N_{18}O_{19}S_2$: 1664.7480; found: 833.3803 $[M+2H]^{2+}$ and 555.9257 $[M+3H]^{3+}$.

	HN	Hα	Hβ	Hγ	Hδ	Hε	Hζ	Hη
1 Ala	-	3.95	1.35	-	-	-	-	-
2 Gly	8.50	3.82	-	-	-	-	-	-
3 Cys	8.31	4.48	2.96 (β2) 2.80 (β3)	-	-	-	-	-
4 Lys	8.44	4.32	1.48	1.17 (γ2) 1.08 (γ3)	1.32	2.63	7.27	-
5 Asn	8.28	4.59	2.51	-	7.39 (δ21) 6.78 (δ22)	-	-	-
6 Phe	8.17	4.44	2.75 (β2) 2.66 (β3)	-	6.75	7.02	6,99	-
7 Dmp	8.00	4.32	2.72	2.09*	6.69	-	6.81	-
8 DTrp	8.07	4.24	2.85 (β2) 2.74 (β3)	-	6.92	10.01 (ε1) 7.37 (ε3)	7.30 (ζ2) 6.97 (ζ3)	7,05
9 Lys	8.04	3.94	1.36 (β2) 1.06 (β3)	0.42 (γ2) 0.29 (γ3)	1.15	2.48	7.28	-
10 Thr	7.73	4.16	3.95	0.93	-	-	-	-
11 Phe	8.18	4.66	2.81 (β2) 2.67 (β3)	-	6.94	7.09	7.05	-
12 Thr	8.11	4.23	4.00	0.97	-	-	-	-
13 Ser	8.10	4.34	3.71	-	-	-	-	-
14 Cys	8.08	4.33	3.05 (β2) 2.92 (β3)	-	-	-	-	-

Chemical shifts in ppm for the detected protons in TOCSY and/or NOESY spectrum. *Hφ of Dmp have been placed in Hγ column for a clearer visualisation.

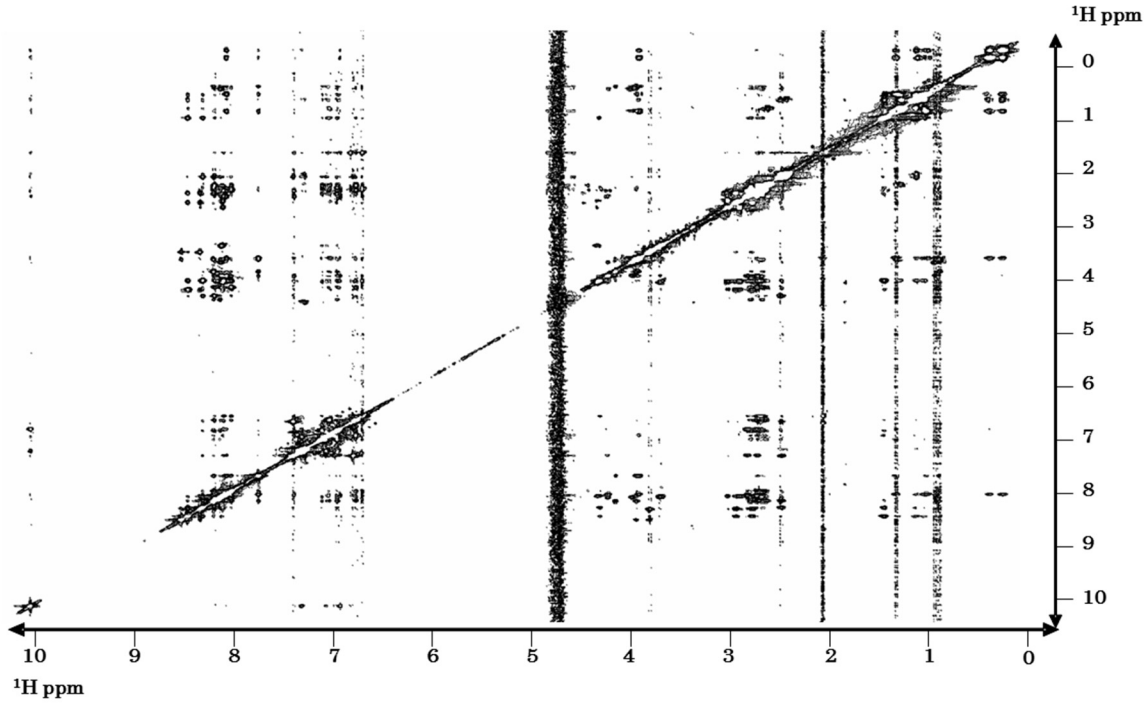

Bidimensional homonuclear NOESY 350 ms spectra for [L-Dmp7_D-Trp8]-SRIF (**2**) acquired in a Bruker Avance III 600 MHz at 285 K.

Distance restrictions:	
Intraresidual: 0	
Sequential: 79	
Medium-range (1<dist≤4): 33	
Long-range (dist>4): 37	
Total: 149	
Dihedral angle restrictions: 8	
Statistics for 20 best structures	
Energies (kcal/mol):	**RMSD*:**
Total energy: -219.8 ± 21.79	Bonds (Å): 8.089 x10^{-3} ± 8.418 x10^{-4}
Van der Waals: -17.42 ± 10.18	Angles (º): 1.212 ± 0.1089
Electrostatic: -437.2 ± 34.13	Impropers (º): 3.16 ± 0,5008
Bonds: 9.19 ± 2.52	Dihedrals (º): 43.86 ± 0.7308
Angles: 93.14 ± 17.09	NOEs: 8.089 x10^{-3} ± 1.563x10^{-3}

Parameters' study for 20 structures with lower energy calculated for [L-Dmp7_D-Trp8]-SRIF (**2**). *Average deviation for 20 structures with lower energy when compared to lowest energy structure.

[L-Dmp6_D-Trp8]-SRIF (3): SRIF14 analogue **3** was synthesised following the general synthesis protocol using 1.0 g of 2-CTC resin (1.6 mmol/g), Fmoc-L-Cys(trt)-OH as a *C*-terminal amino acid and Boc-L-Ala-OH as *N*-terminal aa. Peptide was purified by semi-prep. RP-HPLC and 66.2 mg were obtained with purity above 98%. HPLC: t_R = 12.5 min, gradient: 25-60% ACN (0.1% TFA) in 30 min, 1 mL/min, λ = 220 nm. HRMS: calculated for $C_{78}H_{108}N_{18}O_{19}S_2$: 1664.7480; found: 833.3827 $[M+2H]^{2+}$ and 555.9248 $[M+3H]^{3+}$.

	HN	Hα	Hβ	Hγ	Hδ	Hε	Hζ	Hη
1 Ala	-	3.95	1.35	-	-	-	-	-
2 Gly	8.50	3.82	-	-	-	-	-	-
3 Cys	8.28	4.45	2.94 (β2) 2.79 (β3)	-	-	-	-	-
4 Lys	8.41	4.34	1.43	1.15 (γ2) 1.05 (γ3)	1.29 (δ2) 1.22 (δ3)	2.61	7.25	-
5 Asn	8.27	4.60	2.47	-	7.34 (δ21) 6.75 (δ22)	-	-	-
6 Dmp	8.16	4.52	2.73 (β2) 2.61 (β3)	1.98*	6.47	-	6,67	-
7 Phe	8.12	4.39	2.79	-	7.03	7.17	7.12	-
8 DTrp	8.32	4.27	2.90 (β2) 2.82 (β3)	-	6.94	10.02 (ε1) 7.41 (ε3)	7.30 (ζ2) 6.97 (ζ3)	7,05
9 Lys	8.08	3.93	1.39 (β2) 1.04 (β3)	0.37 (γ2) 0.21 (γ3)	1.13	2.49 (ε2) 2.44 (ε3)	7.26	-
10 Thr	7.83	4.24	3.98	0.94	-	-	-	-
11 Phe	8.27	4.73	2.73 (β2) 2.61 (β3)	-	6.82	7.06	6.97	-
12 Thr	8.23	4.25	3.98	0.97	-	-	-	-
13 Ser	8.16	4.34	3.73	-	-	-	-	-
14 Cys	8.07	4.32	3.04 (β2) 2.94 (β3)	-	-	-	-	-

Chemical shifts in ppm for the detected protons in TOCSY and/or NOESY spectrum. *Hφ of Dmp have been placed in Hγ column for a clearer visualisation.

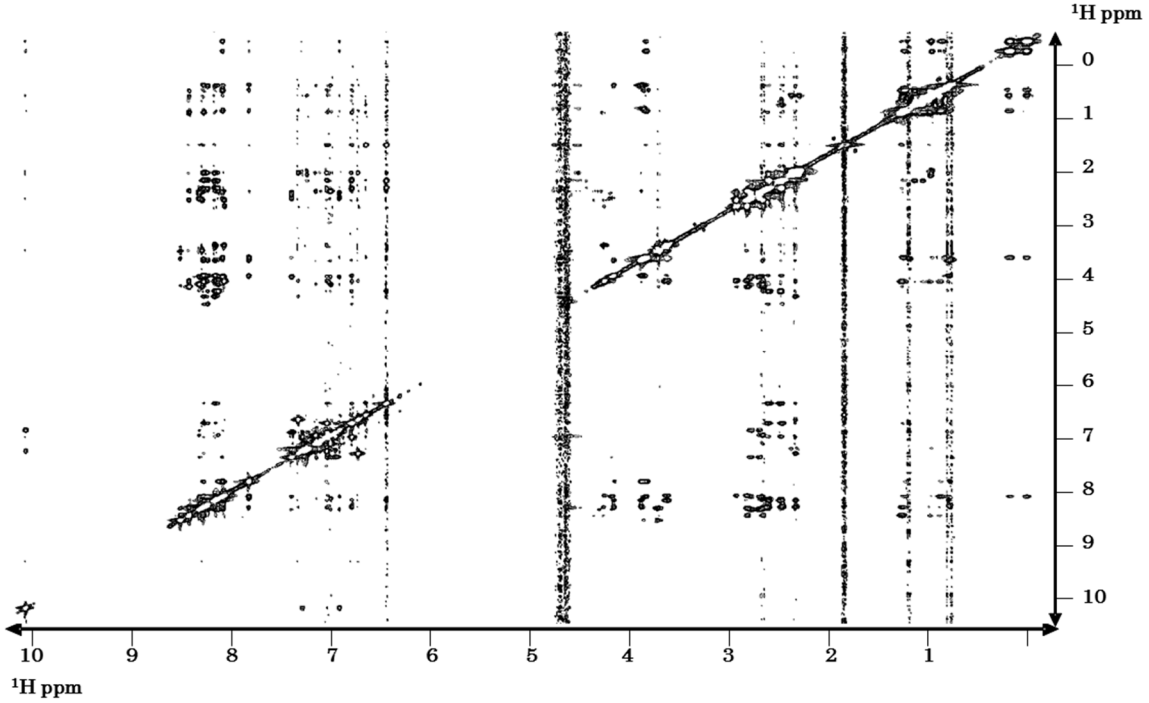

Bidimensional homonuclear NOESY 350 ms spectra for [L-Dmp6_D-Trp8]-SRIF (**3**) acquired in a Bruker Avance III 600 MHz at 285 K.

Distance restrictions:	
Intraresidual: 0	
Sequential: 84	
Medium-range (1<dist≤4): 27	
Long-range (dist>4): 22	
Total: 133	
Dihedral angle restrictions: 22	
Statistics for 20 best structures	
Energies (kcal/mol):	**RMSD*:**
Total energy: -167.1 ± 30.18	Bonds (Å): $8.193 \times 10^{-3} \pm 5.179 \times 10^{-4}$
Van der Waals: -4.20 ± 7.20	Angles (º): 1.425 ± 0.04258
Electrostatic: -442.0 ± 29.36	Impropers (º): 2.832 ± 0,2698
Bonds: 15.63 ± 1.96	Dihedrals (º): 41.90 ± 0.2836
Angles: 1527.8 ± 7.54	NOEs: $9.726 \times 10^{-3} \pm 7.428 \times 10^{-4}$

Parameters' study for 20 structures with lower energy calculated for [L-Dmp6_D-Trp8]-SRIF (**3**). *Average deviation for 20 structures with lower energy when compared to lowest energy structure.

Pya family

[Msa6_L-4'Pya7_D-Trp8]-SRIF (4): SRIF14 analogue **4** was synthesised following the general synthesis protocol using 1.0 g of 2-CTC resin (1.6 mmol/g), Fmoc-L-Cys(trt)-OH as a *C*-terminal amino acid and Boc-L-Ala-OH as *N*-terminal aa. Peptide was purified by semi-prep. RP-HPLC and 96.7 mg were obtained with purity above 94%. HPLC: t_R = 11.9 min, gradient: 0-40% ACN (0.1% TFA) in 25 min, 1 mL/min, λ = 220 nm. HRMS: calculated for $C_{78}H_{109}N_{19}O_{19}S_2$: 1679.7589; found: 840.8859 $[M+2H]^{2+}$ and 560.9273 $[M+3H]^{3+}$.

	HN	Hα	Hβ	Hγ	Hδ	Hε	Hζ	Hη
1 Ala	-	4.04	1.43	-	-	-	-	-
2 Gly	8.53	3.89	-	-	-	-	-	-
3 Cys	8.34	4.50	2.98 (β2) 2.88 (β3)	-	-	-	-	-
4 Lys	8.43	4.42	1.56 (β2) 1.48 (β3)	1.27 (γ2) 1.17 (γ3)	1.43 (δ2) 1.35 (δ3)	2.76	7.37	-
5 Asn	8.33	4.63	2.45 (β2) 2.33 (β3)	-	7.35 (δ21) 6.76 (δ22)	-	-	-
6 Msa	7.97	4.58	2.90 (β2) 2.84 (β3)	-	2.06*	6.75	-	1.94
7 4Pya	8.46	4.75	3.18 (β2) 3.08 (β3)	-	7.70	8.28	-	-
8 DTrp	8.66	4.55	3.09 (β2) 3.06 (β3)	-	7.07	10.07 (ε1) 7.54 (ε3)	7.39 (ζ2) 7.05 (ζ3)	7,14
9 Lys	8.29	4.08	1.55	0.50 (γ2) 0.34 (γ3)	1.23 (δ2) 1.18 (δ3)	2.59 (ε2) 2.52 (ε3)	7.33	-
10 Thr	7.95	4.24	4.07	1.02	-	-	-	-
11 Phe	8.44	4.93	2.67	-	6.73	7.06	6.86	-
12 Thr	8.16	4.26	3.97	0.97	-	-	-	-
13 Ser	8.19	4.32	3.79	-	-	-	-	-
14 Cys	8.10	4.41	3.09 (β2) 2.97 (β3)	-	-	-	-	-

Chemical shifts in ppm for the detected protons in TOCSY and/or NOESY spectrum. *Hφ of Msa have been placed in Hδ column for a clearer visualisation.

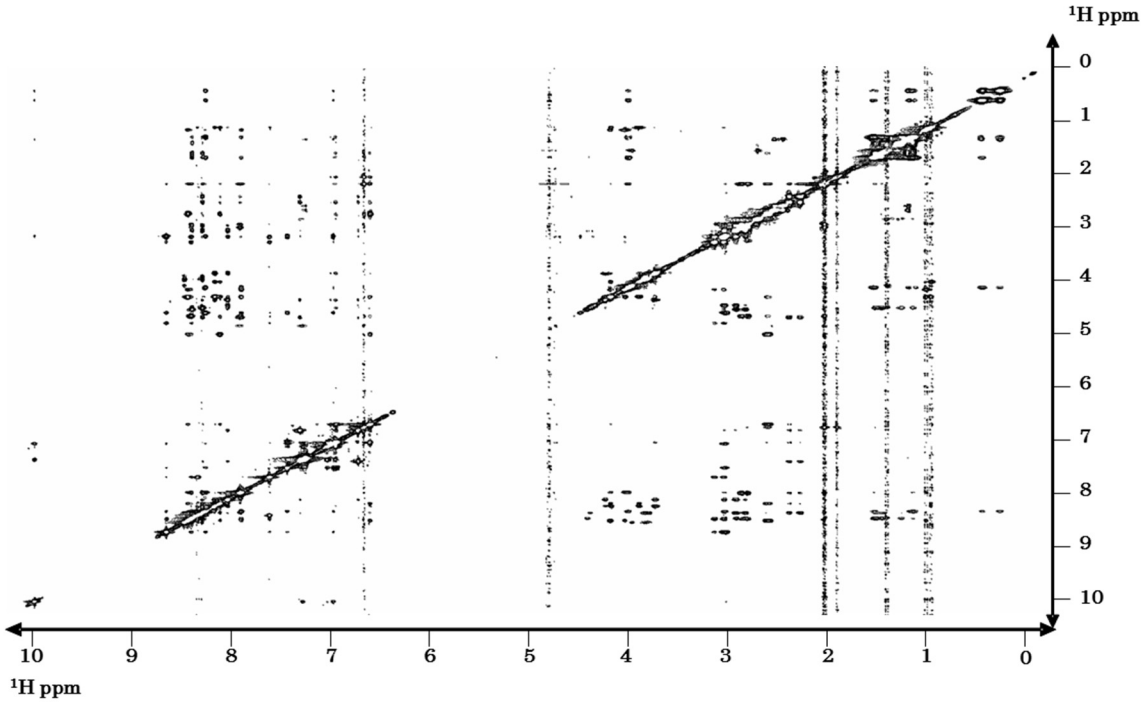

Bidimensional homonuclear NOESY 350 ms spectra for [L-4'Pya6_Msa7_D-Trp8]-SRIF (4) acquired in a Bruker Avance III 600 MHz at 285 K.

Distance restrictions:	
Intraresidual: 0	
Sequential: 49	
Medium-range (1<dist≤4): 10	
Long-range (dist>4): 19	
Total: 78	
Dihedral angle restrictions: 22	
Statistics for 20 best structures	
Energies (kcal/mol):	**RMSD*:**
Total energy: -392.4 ± 9.101	Bonds (Å): 4.487 x10^{-3} ± 4.40 x10^{-4}
Van der Waals: -40.63 ± 6.57	Angles (º): 1.129 ± 0.0304
Electrostatic: -542.3 ± 9.49	Impropers (º): 2.772 ± 0,221
Bonds: 4.75 ± 0.96	Dihedrals (º): 40.77 ± 0.3551
Angles: 81.03 ± 4.40	NOEs: 2.997 x10^{-3} ± 1.037x10^{-3}

Parameters' study for 20 structures with lower energy calculated for [L-4'Pya6_Msa7_D-Trp8]-SRIF (**4**). *Average deviation for 20 structures with lower energy when compared to lowest energy structure.

[Msa6_L-3'Pya7_D-Trp8]-SRIF (5): SRIF14 analogue **5** was synthesised following the general synthesis protocol using 1.0 g of 2-CTC resin (1.6 mmol/g), Fmoc-L-Cys(trt)-OH as a *C*-terminal amino acid and Boc-L-Ala-OH as *N*-terminal aa. Peptide was purified by semi-prep. RP-HPLC and 52.7 mg were obtained with purity above 98%. HPLC: t_R = 12.2 min, gradient: 0-40% ACN (0.1% TFA) in 25 min, 1 mL/min, λ = 220 nm. HRMS: calculated for $C_{78}H_{109}N_{19}O_{19}S_2$: 1679.7589; found: 840.8869 $[M+2H]^{2+}$ and 560.9282 $[M+3H]^{3+}$.

	HN	Hα	Hβ	Hγ	Hδ	Hε	Hζ	Hη
1 Ala	-	3.88	1.36	-	-	-	-	-
2 Gly	8.56	3.85	-	-	-	-	-	-
3 Cys	8.27	4.61	3.13 (β2) 2.88 (β3)	-	-	-	-	-
4 Lys	8.24	4.58	1.56 (β2) 1.48 (β3)	1.24	1.42 (δ2) 1.38 (δ3)	2.64	7.62	-
5 Asn	8.31	4.69	2.81 (β2) 2.61 (β3)	-	7.73 (δ21) 7.24 (δ22)	-	-	-
6 Msa	8.21	4.17	2.71	-	1.97*	6.67	-	2.12
7 3Pya	7.93	4.35	3.05 (β2) 2.76 (β3)	-	7.64	7.22	8.43	-
8 DTrp	8.06	4.45	3.11 (β2) 2.94 (β3)	-	7.11	10.76 (ε1) 7.55 (ε3)	7.29 (ζ2) 6.93 (ζ3)	7,04
9 Lys	8.07	4.28	1.54 (β2) 1.43 (β3)	1.09 (γ2) 1.02 (γ3)	1.23	2.65	7.66	-
10 Thr	7.88	4.35	3.91	0.99	-	-	-	-
11 Phe	8.19	4.71	3.08 (β2) 2.81 (β3)	-	7.18	7.30	7.22	-
12 Thr	8.11	4.25	4.01	1.01	-	-	-	-
13 Ser	7.81	4.34	3.63	-	-	-	-	-
14 Cys	8.27	4.49	3.11 (β2) 2.96 (β3)	-	-	-	-	-

Chemical shifts in ppm for the detected protons in TOCSY and/or NOESY spectrum. *Hφ of Msa have been placed in Hδ column for a clearer visualisation.

Qla Peptide

[Msa7_L-Qla8]-SRIF (6): SRIF14 analogue **6** was synthesised following the general synthesis protocol using 1.0 g of 2-CTC resin (1.6 mmol/g), Fmoc-L-Cys(trt)-OH as a *C*-terminal amino acid and Boc-L-Ala-OH as *N*-terminal aa. Peptide was purified by semi-prep. RP-HPLC and 50.7 mg were obtained with purity above 95%. HPLC: t_R = 9.5 min, gradient: 25-60% ACN (0.1% TFA) in 30 min, 1 mL/min, λ = 220 nm. HRMS: calculated for $C_{80}H_{110}N_{18}O_{19}S_2$: 1690.7636; found: 846.3892 $[M+2H]^{2+}$ and 564.5967 $[M+3H]^{3+}$.

	HN	Hα	Hβ	Hγ	Hδ	Hε	Hζ	Hη
1 Ala	-	4.18	1.58	-	-	-	-	-
2 Gly	8.53	3.90	-	-	-	-	-	-
3 Cys	8.36	4.56	3.03 (β2) 2.86 (β3)	-	-	-	-	-
4 Lys	8.52	4.18	1.56	1.25 (γ2) 1.20 (γ2)	1.42	2.77 (ε2) 2.73 (ε3)	7.42	-
5 Asn	8.15	4.47	3.13 (β2) 2.87 (β3)	-	7.46 (δ21) 6.80 (δ22)	-	-	-
6 Phe	8.14	4.57	3.02 (β2) 2.89 (β3)	-	7.09	7.18	7.12	-
7 Msa	7.99	4.19	2.77 (β2) 2.73 (β3)	-	2.02*	6.70	-	1.98
8 LQla	8.04	4.26	2.56	-	6.69	7.47 (ε3)	7.35 (ζ2) 6.75 (ζ3)	6.79 (η2) 6.87 (η3)
9 Lys	8.10	4.39	3.03 (β2) 2.88 (β3)	1.56 (γ2) 1.23 (γ3)	1.46 (δ2) 1.36 (δ3)	3.58	7.41	-
10 Thr	7.98	4.25	4.07	1.04	-	-	-	-
11 Phe	7.96	4.60	3.09 (β2) 2.79 (β3)	-	6.90	6.97	7.07	-
12 Thr	8.09	4.36	3.75	1.11	-	-	-	-
13 Ser	7.98	4.31	3.99	-	-	-	-	-
14 Cys	8.15	4.45	3.11 (β2) 2.87 (β3)	-	-	-	-	-

Chemical shifts in ppm for the detected protons in TOCSY and/or NOESY spectrum. *Hφ of Msa have been placed in Hδ column for a clearer visualisation.

Msa / D-Cys family

[Msa7_D-Trp8]-SRIF (7): SRIF14 analogue **7** was synthesised following the general synthesis protocol using 1.0 g of 2-CTC resin (1.6 mmol/g), Fmoc-**L**-Cys(trt)-OH as a *C*-terminal amino acid and Boc-L-Ala-OH as *N*-terminal aa. Peptide was purified by semi-prep. RP-HPLC and 46.1 mg were obtained with purity above 99%. HPLC: t_R = 15.9 min, gradient: 0-40% ACN (0.1% TFA) in 25 min, 1 mL/min, λ = 220 nm. HRMS: calculated for $C_{79}H_{110}N_{18}O_{19}S_2$: 1678.7636; found: 1679.7718 $[M+H]^+$, 840.3884 $[M+2H]^{2+}$ and 560.5960 $[M+3H]^{3+}$. This peptide has been synthesised before in our group.[1c] Peptide structure was determined by 2D-NMR and the obtained chemical shifts were as follows:

	HN	Hα	Hβ	Hγ	Hδ	Hε	Hζ	Hη
1 Ala	-	3.89	1.30	-	-	-	-	-
2 Gly	8.47	3.73	-	-	-	-	-	-
3 Cys	8.24	4.39	2.92 (β2) 2.67 (β3)	-	-	-	-	-
4 Lys	8.41	4.43	1.34 (β2) 1.23 (β3)	1.04 (γ2) 0.92 (γ3)	1.15	2.43	7.13	-
5 Asn	8.36	4.61	2.43 (β2) 2.30 (β3)	-	7.36 (δ21) 6.76 (δ22)	-	-	-
6 Phe	8.25	4.52	2.71 (β2) 2.58 (β3)	-	6.73	6.93	6.85	-
7 Msa	8.18	4.38	2.80 (β2)	-	2.04*	6.66	-	1.93
8 DTrp	8.26	4.28	2.87 (β2) 2.82 (β3)	-	6.88	10.00 (ε1) 7.37 (ε3)	7.26 (ζ2) 6.93 (ζ3)	7.01
9 Lys	8.14	3.92	1.39 (β2) 0.99 (β3)	0.29 (γ2) 0.07 (γ3)	1.07	2.44 (ε2) 2.36 (ε3)	7.22	-
10 Thr	7.80	4.22	3.95	0.89	-	-	-	-
11 Phe	8.07	4.98	2.43 (β2) 2.40 (β3)	-	6.79	7.05	6.99	-
12 Thr	8.34	4.26	4.02	0.96	-	-	-	-
13 Ser	8.29	4.43	3.75 (β2) 3.69 (β3)	-	-	-	-	-
14 Cys	7.97	4.26	2.98 (β2) 2.94 (β3)	-	-	-	-	-

Chemical shifts in ppm for the detected protons in TOCSY and/or NOESY spectrum. *Hφ of Msa have been placed in Hδ column for a clearer visualisation.

[Msa7_D-Trp8_D-Cys14]-SRIF (8): SRIF14 analogue **8** was synthesised following the general synthesis protocol using 1.0 g of 2-CTC resin (1.6 mmol/g), Fmoc-D-Cys(trt)-OH as a *C*-terminal amino acid and Boc-L-Ala-OH as *N*-terminal aa. Peptide was purified by semi-prep. RP-HPLC and 63.6 mg were obtained with purity above 98%. HPLC: t_R = 12.7 min, gradient: 25-60% ACN (0.1% TFA) in 30 min, 1 mL/min, λ = 220 nm. HRMS: calculated for $C_{79}H_{110}N_{18}O_{19}S_2$: 1678.7636; found: 840.3896 $[M+2H]^{2+}$ and 560.5966 $[M+3H]^{3+}$.

	HN	Hα	Hβ	Hγ	Hδ	Hε	Hζ	Hη
1 Ala	-	3.90	1.37	-	-	-	-	-
2 Gly	8.59	3.88	-	-	-	-	-	-
3 Cys	8.28	4.60	3.14 (β2) 2.88 (β3)	-	-	-	-	-
4 Lys	8.21	4.50	1.58 (β2) 1.50 (β3)	1.24 (γ2) 0.85 (γ3)	1.42	2.65	7.65	-
5 Asn	8.22	4.66	2.74 (β2) 2.58 (β3)	-	7.57 (δ21) 7.12 (δ22)	-	-	-
6 Phe	8.09	4.42	2.98 (β2) 2.82 (β3)	-	6.76	7.48	7.14	-
7 Msa	8.04	4.37	3.02 (β2) 2.83 (β3)	-	2.22*	6.74	-	2.16
8 DTrp	8.20	4.38	3.05 (β2) 2.83 (β3)	-	7.06	10.78 (ε1) 7.49 (ε3)	7.31 (ζ2) 6.97 (ζ3)	7.05
9 Lys	8.03	4.25	1.55 (β2) 1.33 (β3)	0.98	1.39	2.62	7.63	-
10 Thr	7.85	4.36	3.93	1.02	-	-	-	-
11 Phe	8.20	4.79	3.04 (β2) 2.84 (β3)	-	7.19	7.50	7.31	-
12 Thr	8.05	4.35	4.06	1.00	-	-	-	-
13 Ser	7.97	4.38	3.68	-	-	-	-	-
14 DCys	8.07	4.49	3.08 (β2) 2.96 (β3)	-	-	-	-	-

Chemical shifts in ppm for the detected protons in TOCSY and/or NOESY spectrum. *Hφ of Msa have been placed in Hδ column for a clearer visualisation.

[D-Ala1_Msa7_D-Trp8_D-Cys14]-SRIF (9): SRIF14 analogue **9** was synthesised following the general synthesis protocol using 1.0 g of 2-CTC resin (1.6 mmol/g), Fmoc-D-Cys(trt)-OH as a *C*-terminal amino acid and Boc-D-Ala-OH as *N*-terminal aa. Peptide was purified by semi-prep. RP-HPLC and 55.4 mg were obtained with purity above 99%. HPLC: t_R = 12.7 min, gradient: 25-60% ACN (0.1% TFA) in 30 min, 1 mL/min, λ = 220 nm. HRMS: calculated for $C_{79}H_{110}N_{18}O_{19}S_2$: 1678.7636; found: 840.3886 $[M+2H]^{2+}$ and 560.5961 $[M+3H]^{3+}$.

	HN	Hα	Hβ	Hγ	Hδ	Hε	Hζ	Hη
1 Ala	-	3.95	1.36	-	-	-	-	-
2 Gly	8.59	3.84	-	-	-	-	-	-
3 DCys	8.29	4.64	3.13 (β2) 2.87 (β3)	-	-	-	-	-
4 Lys	8.26	4.55	1.59 (β2) 1.51 (β3)	1.25	0.86	2.28	7.63	-
5 Asn	8.24	4.66	2.76 (β2) 2.60 (β3)	-	7.58 (δ21) 7.12 (δ22)	-	-	-
6 Phe	8.10	4.42	2.98 (β2) 2.83 (β3)	-	6.75	7.20	7.01	-
7 Msa	8.06	4.49	3.08 (β2) 2.95 (β3)	-	2.22*	7.19	-	2.49
8 DTrp	8.01	4.38	3.02 (β2) 2.84 (β3)	-	7.07	10.78 (ε1) 7.49 (ε3)	7.31 (ζ2) 6.98 (ζ3)	7.06
9 Lys	8.03	4.27	1.56 (β2) 1.34 (β3)	0.99	1.37	2.63	7.64	-
10 Thr	7.87	4.35	3.93	1.01	-	-	-	-
11 Phe	8.21	4.80	3.06 (β2) 2.85 (β3)	-	7.04	7.20	7.12	-
12 Thr	8.05	4.36	4.07	1.02	-	-	-	-
13 Ser	7.88	4.37	3.91	-	-	-	-	-
14 DCys	8.23	4.47	2.83 (β2) 2.75 (β3)	-	-	-	-	-

Chemical shifts in ppm for the detected protons in TOCSY and/or NOESY spectrum. *Hφ of Msa have been placed in Hδ column for a clearer visualisation.

[D-Cys3,14_Msa7_D-Trp8]-SRIF (10): SRIF14 analogue **10** was synthesised following the general synthesis protocol using 1.0 g of 2-CTC resin (1.6 mmol/g), Fmoc-D-Cys(trt)-OH as a *C*-terminal amino acid and Boc-L-Ala-OH as *N*-terminal aa. Peptide was purified by semi-prep. RP-HPLC and 50.3 mg were obtained with purity above 99%. HPLC: t_R = 12.3 min, gradient: 25-60% ACN (0.1% TFA) in 30 min, 1 mL/min, λ = 220 nm. HRMS: calculated for $C_{79}H_{110}N_{18}O_{19}S_2$: 1678.7636; found: 1701.7466 $[M+Na]^+$ and 1678.7636 [M].

	HN	Hα	Hβ	Hγ	Hδ	Hε	Hζ	Hη
1 Ala	-	3.89	1.35	-	-	-	-	-
2 Gly	8.59	3.82	-	-	-	-	-	-
3 DCys	8.26	4.60	3.09 (β2) 2.96 (β3)	-	-	-	-	-
4 Lys	8.24	4.48	1.59 (β2) 1.51 (β3)	1.23	0.84	2.26	7.59	-
5 Asn	8.27	4.63	2.72 (β2) 2.53 (β3)	-	7.53 (δ21) 7.05 (δ22)	-	-	-
6 Phe	8.01	4.43	2.94 (β2) 2.79 (β3)	-	6.73	7.12	7.01	-
7 Msa	8.10	4.42	3.11 (β2) 2.95 (β3)	-	2.20*	7.13	-	2.49
8 DTrp	8.11	4.35	3.00 (β2) 2.82 (β3)	-	7.02	10.73 (ε1) 7.48 (ε3)	7.31 (ζ2) 6.87 (ζ3)	7.06
9 Lys	8.09	4.23	1.55 (β2) 1.33 (β3)	0.90	1.37	2.63	7.64	-
10 Thr	7.93	4.29	3.88	0.98	-	-	-	-
11 Phe	8.19	4.80	3.01 (β2) 2.80 (β3)	-	7.01	7.17	7.12	-
12 Thr	8.07	4.23	4.09	1.06	-	-	-	-
13 Ser	7.92	4.27	3.86	-	-	-	-	-
14 DCys	8.23	4.48	2.81 (β2) 2.75 (β3)	-	-	-	-	-

Chemical shifts in ppm for the detected protons in TOCSY and/or NOESY spectrum. *Hφ of Msa have been placed in Hδ column for a clearer visualisation.

[D-Ala1_D-Cys3,14_Msa7_D-Trp8]-SRIF (11): SRIF14 analogue **11** was synthesised following the general synthesis protocol using 1.0 g of 2-CTC resin (1.6 mmol/g), Fmoc-D-Cys(trt)-OH as a *C*-terminal amino acid and Boc-D-Ala-OH as *N*-terminal aa. Peptide was purified by semi-prep. RP-HPLC and 57.1 mg were obtained with purity above 99%. HPLC: t_R = 12.0 min, gradient: 25-60% ACN (0.1% TFA) in 30 min, 1 mL/min, λ = 220 nm. HRMS: calculated for $C_{79}H_{110}N_{18}O_{19}S_2$: 1678.7636; found: 840.3892 $[M+2H]^{2+}$ and 560.5949 $[M+3H]^{3+}$.

	HN	Hα	Hβ	Hγ	Hδ	Hε	Hζ	Hη
1 Ala	-	3.91	1.33	-	-	-	-	-
2 Gly	8.53	3.77	-	-	-	-	-	-
3 DCys	8.13	4.49	3.06 (β2) 2.87 (β3)	-	-	-	-	-
4 Lys	8.04	4.29	1.42 (β2) 1.33 (β3)	1.13 (γ2) 0.98 (γ3)	0.86	2.53	6.69	-
5 Asn	8.27	4.55	2.44 (β2) 2.33 (β3)	-	7.26 (δ21) 7.69 (δ22)	-	-	-
6 Phe	8.22	4.56	2.76 (β2) 2.30 (β3)	-	6.81	6.96	6.83	-
7 Msa	8.21	4.43	2.81 (β2)	-	2.05*	6.69	-	1.96
8 DTrp	8.27	4.29	2.85(β2) 2.83(β3)	-	6.89	10.03 (ε1) 7.39 (ε3)	7.26 (ζ2) 6.94 (ζ3)	7.03
9 Lys	8.16	3.91	1.40 (β2) 1.00 (β3)	1.07 (γ2) 0.99 (γ3)	0.29 (δ2) 0.05 (δ3)	2.05	6.70	-
10 Thr	7.88	4.19	3.93	0.91	-	-	-	-
11 Phe	8.15	4.89	2.57 (β2) 2.49 (β3)	-	6.78	7.03	6.95	-
12 Thr	8.27	4.28	4.08	0.99	-	-	-	-
13 Ser	8.31	4.42	3.74	-	-	-	-	-
14 DCys	7.76	4.22	3.09 (β2) 2.86 (β3)	-	-	-	-	-

Chemical shifts in ppm for the detected protons in TOCSY and/or NOESY spectrum. *Hφ of Msa have been placed in Hδ column for a clearer visualisation.

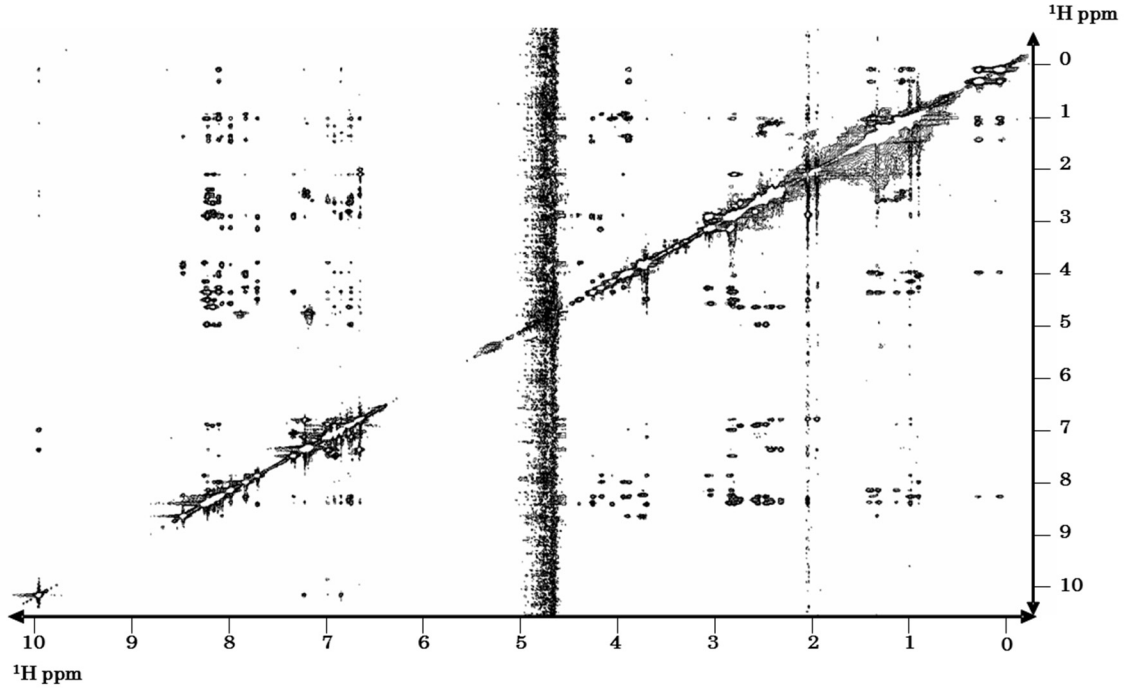

Bidimensional homonuclear NOESY 200 ms spectra for [D-Ala1_D-Cys3,14_Msa7_D-Trp8]-SRIF (**10**) acquired in a Bruker Avance III 600 MHz at 285 K.

Distance restrictions:

Intraresidual: 0

Sequential: 61

Medium-range (1<dist≤4): 12

Long-range (dist>4): 10

Total: 83

Dihedral angle restrictions: 12

Statistics for 20 best structures

Energies (kcal/mol):	**RMSD*:**
Total energy: -349.5 ± 10.80	Bonds (Å): 6.30 x10^{-3} ± 4.87 x10^{-4}
Van der Waals: -20.04 ± 9.429	Angles (º): 1.172 ± 0.05003
Electrostatic: -528.9 ± 26.4	Impropers (º): 1.968 ± 0,2704
Bonds: 9.376 ± 1.49	Dihedrals (º): 42.21 ± 1.283
Angles: 87.8 ± 7.529	NOEs: 1.09 x10^{-2} ± 1.021x10^{-3}

Parameters' study for 20 structures with lower energy calculated for [D-Ala1_D-Cys3,14_Msa7_D-Trp8]-SRIF (**10**). *Average deviation for 20 structures with lower energy when compared to lowest energy structure.

[L-Orn4_Msa7_D-Trp8]-SRIF (12): SRIF14 analogue **12** was synthesised following the general synthesis protocol using 1.0 g of 2-CTC resin (1.6 mmol/g), Fmoc-L-Cys(trt)-OH as a *C*-terminal amino acid and Boc-L-Ala-OH as *N*-terminal aa. Peptide was purified by semi-prep. RP-HPLC and 60.9 mg were obtained with purity above 98%. HPLC: t_R = 15.9 min, gradient: 0-40% ACN (0.1% TFA) in 25 min, 1 mL/min, λ = 220 nm. HRMS: calculated for $C_{78}H_{108}N_{18}O_{19}S_2$: 1664.7480; found: 1665.7539 $[M+H]^+$, 1687.7290 $[M+Na]^+$ and 833.3810 $[M+2H]^{2+}$.

[L-Orn4_Msa7_D-Trp8_D-Cys14]-SRIF (13): SRIF14 analogue **13** was synthesised following the general synthesis protocol using 1.0 g of 2-CTC resin (1.6 mmol/g), Fmoc-D-Cys(trt)-OH as a *C*-terminal amino acid and Boc-L-Ala-OH as *N*-terminal aa. Peptide was purified by semi-prep. RP-HPLC and 61.4 mg were obtained with purity above 98%. HPLC: t_R = 12.5 min, gradient: 25-60% ACN (0.1% TFA) in 30 min, 1 mL/min, λ = 220 nm. HRMS: calculated for $C_{78}H_{108}N_{18}O_{19}S_2$: 1664.7480; found: 1665.7521 $[M+H]^+$, 833.3810 $[M+2H]^{2+}$ and 555.9237 $[M+3H]^{3+}$.

SOM-linker-coumarin family

SOM - (3,6-dioxaoctanoic acid)-((7-methoxy-coumarin-4-yl)-acetic acid) (14): SRIF14 analogue **14** was synthesised following the general synthesis protocol using 0.25 g of 2-CTC resin (1.6 mmol/g), Fmoc-L-Cys(trt)-OH as a *C*-terminal amino acid and Fmoc-L-Ala-OH as *N*-terminal aa. After removing Fmoc group from *N*-terminal aa, Fmoc-O2Oc-OH linker was added, Fmoc removed and ((7-methoxy-coumarin-4-yl)-acetic acid) added. Peptide was purified by semi-prep. RP-HPLC and 62.5 mg were obtained with purity above 95%. HPLC: t_R = 14.8 min, gradient: 25-60% ACN (0.1% TFA) in 30 min, 1 mL/min, λ = 220 nm. HRMS: calculated for $C_{94}H_{123}N_{19}O_{26}S_2$: 1997.8328; found: 999.9226 $[M+2H]^{2+}$ and 666.9528 $[M+3H]^{3+}$.

[DAla1_D-Cys3,14_Msa7_DTrp8]-(3,6-dioxaoctanoic acid)-((7-methoxy-coumarin-4-yl)-acetic acid) (15): SRIF14 analogue **15** was synthesised following the general synthesis protocol using 0.53 g of 2-CTC resin (1.6 mmol/g), Fmoc-D-Cys(trt)-OH as a *C*-terminal amino acid and Fmoc-D-Ala-OH as *N*-terminal aa. After removing Fmoc group from *N*-terminal aa, Fmoc-O2Oc-OH linker was added, Fmoc removed and ((7-methoxy-coumarin-4-yl)-acetic acid) added. Peptide was purified by semi-prep. RP-HPLC and 43.5 mg were obtained with purity above 97%. HPLC: t_R = 17.1 min, gradient: 25-60% ACN (0.1% TFA) in 30 min, 1 mL/min, λ = 220 nm. HRMS: calculated for $C_{97}H_{129}N_{19}O_{26}S_2$: 2039.8798; found: 1020.9470 $[M+2H]^{2+}$ and 680.9674 $[M+3H]^{3+}$.

SOM-PH family

SOM1 - PH (16): SRIF14 analogue **16** was synthesised following the general synthesis protocol using 0.37 g of 2-CTC resin (1.6 mmol/g), Fmoc-L-Cys(trt)-OH as a *C*-terminal amino acid and Fmoc-L-Ala-OH as *N*-terminal aa. After removing Fmoc group from *N*-terminal aa, PH-797804 was added. Peptide was purified by semi-prep. RP-HPLC and 80.2 mg were obtained with purity above 92%. HPLC: t_R = 20.9 min, gradient: 25-60% ACN (0.1% TFA) in 30 min, 1 mL/min, λ = 220 nm. HRMS: calculated for $C_{97}H_{118}BrF_2N_{19}O_{22}S_2$: 2081.7292; found: 1041.8721 $[M+2H]^{2+}$ and 694.9172 $[M+3H]^{3+}$.

SOM2 - PH (17): SRIF14 analogue **17** was synthesised following the general synthesis protocol using 0.35 g of 2-CTC resin (1.6 mmol/g), Fmoc-L-Cys(trt)-OH as a *C*-terminal amino acid and Fmoc-Gly-OH as *N*-terminal aa[17]. After removing Fmoc group from *N*-terminal aa, PH-797804 was added. Peptide was purified by semi-prep. RP-HPLC and 80.2 mg were obtained with purity above 93%. HPLC: t_R = 21.8 min, gradient: 25-60% ACN (0.1% TFA) in 30 min, 1 mL/min, λ = 220 nm. HRMS: calculated for $C_{94}H_{113}BrF_2N_{18}O_{21}S_2$: 2010.6921; found: 1006.3535 $[M+2H]^{2+}$ and 671.2382 $[M+3H]^{3+}$.

[17] Note that this analogue has one amino acid less than natural somatostatin, the sequence is the same but only until amino acid two (Alanine not coupled).

[D-Ala1_D-Cys3,14_Msa7_D-Trp8] - PH (18): SRIF14 analogue **18** was synthesised following the general synthesis protocol using 0.35 g of 2-CTC resin (1.6 mmol/g), Fmoc-D-Cys(trt)-OH as a *C*-terminal amino acid and Fmoc-D-Ala-OH as *N*-terminal aa. After removing Fmoc group from *N*-terminal aa, PH-797804 was added. Peptide was purified by semi-prep. RP-HPLC and 32.1 mg were obtained with purity above 96%. HPLC: t_R = 22.7 min, gradient: 25-60% ACN (0.1% TFA) in 30 min, 1 mL/min, λ = 220 nm. HRMS: calculated for $C_{100}H_{124}BrF_2N_{19}O_{22}S_2$: 2123.7761; found: 1062.8952 $[M+2H]^{2+}$ and 708.9330 $[M+3H]^{3+}$.

9.2.6 Photo-labile compound and Somatostatin (SRIF14) analogue

2-bromo-1-(3-(2'-benzothiazole)-4-hydroxyphenyl)ethan-1-one (19)

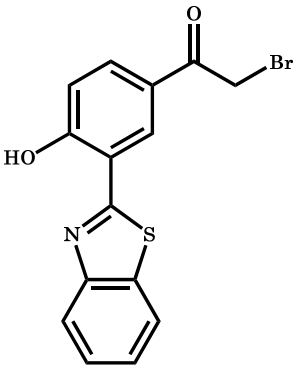

To a cold (10ºC) suspension of $AlCl_3$ (52.8 mmol) in DCM (200 mL), bromoacetyl bromide (15.8 mmol) was added dropwise. Once the addition finished, the mixture was heated up to 30ºC and stirred for 1h. After that, a solution of 2-(2-hydroxyphenyl)-benzothiazole (13.2 mmol) in DCM (25 mL) was added while the mixture was heated up to 35ºC and stirred for 24h. Reaction was quenched with H_2O at 0ºC, aqueous phase extracted two times with DCM and organic phase evaporated thus obtaining a yellow solid which was resuspended in heptane and stirred for 15 min. Solid was filtered, washed with heptane and air dried obtaining 4.46 g of **19** (97%).

MP: 162.5 – 163.7 ºC

^{1}H NMR (400 MHz, $CDCl_3$) δ; 8.44 (d, *J* = 2.1 Hz, 1H), 8.06 – 7.99 (m, 2H,), 7.96 (d, *J* = 8.0, 1H), 7.56 (ddd, *J* = 8.3, 7.3, 1.3 Hz, 1H), 7.47 (ddd, *J* = 8.4, 7.3, 1.2 Hz, 1H), 7.18 (d, *J* = 8.7 Hz, 1H), 4,44 (s, 2H).

^{13}C NMR (101 MHz, $CDCl_3$) δ; 189.3 (C), 168.3 (C) , 162.6 (C), 151.4 (C), 133.4 (CH), 132.6 (C), 130.3 (CH), 127.0 (CH), 126.2 (CH), 125.8 (C), 122.4 (CH), 121.7 (CH), 118.3 (CH), 117.1 (C), 30.20 (CH_2).

IR: 3410.3 cm^{-1} (O-H st), 2914.8 cm^{-1} (C-H st), 2845.3 cm^{-1} (C-H st), 1673.3 cm^{-1} (C=O st), 1580.7 cm^{-1} (C=N st), 650 cm^{-1} (C-Br st).

HRMS (ESI$^+$): calculated for $C_{15}H_{10}BrNO_2S$: 346.9616; found: 347.9692 $[M+H]^+$, 369.9506 $[M+Na]^+$ and 716.9130 $[2M+Na]^+$.

4-Allyl 1-(2-(3-(2'-benzothiazole)-4-hydroxyphenyl)-2-oxoethyl) Fmoc-L-aspartate (20)

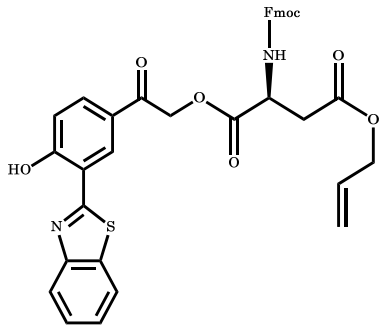

To a solution of Fmoc-Asp(All)-OH (1.44 mmol) in ACN (15 mL), K_2CO_3 was added and mixture stirred for 10 min at room temperature. After that, compound **19** (1.44 mmol) in ACN (5 mL) was added dropwise and stirred at room temperature overweekend. Once the reaction was finished, H_2O and AcOEt were added and aqueous phase extracted twice with AcOEt. The organic phase was dried over $MgSO_4$, filtered, and concentrated to dryness obtaining 0.41g of **20** as a yellow solid (55%).

MP: 160.9 – 162.5 ºC **$[\alpha]_D$:** - 7.25

^{1}H NMR (400 MHz, CD_3COCD_3) δ; 8.48 (d, *J* = 1.7 Hz, 1H), 8.22 – 8.08 (m, 3H), 7.85 (d, *J* = 7.0 Hz, 2H), 7.71 (d, *J* = 7.5 Hz, 2H), 7.64 (t, *J* = 7.5 Hz, 1H), 7.56 (t, *J* = 7.7 Hz, 1H), 7.36 (dt, *J* = 34.3, 7.6 Hz, 4H), 7.22 (d, *J* = 8.8 Hz, 1H), 7.04 (d, *J* = 9.4 Hz, 1H), 6.02 – 5.92 (m, 1H), 5.69 – 5.50 (m, 2H), 5.35 (dd, *J* = 17.3, 1.6 Hz, 1H), 5.21 (d, *J* = 9.6 Hz, 1H), 4.94 – 4.86 (m, 1H), 4.64 (d, *J* = 5.6 Hz, 2H), 4.41 – 4.21 (m, 3H), 3.20 – 2.95 (m, 2H).

^{13}C NMR (101 MHz, CD_3COCD_3) δ; 192.19 (CO, 1C), 170.60 (CO, 1C), 169.63 (CO, 1C), 166.59 (C, 1C), 162.12 (CO 1C), 151.44 (C, 1C), 144.09 (C, 1C), 141.18 (C, 1C), 137.93

(C, 1C), 132.89 (C, 1C), 132.53 (CH, 1C), 132.49 (CH, 1C), 129.01 (CH, 1C), 127.62 (CH, 2C), 127.16 (CH, 1C), 127.04 (CH, 2C), 126.25 (CH, 1C), 125.25 (CH, 1C), 125.23 (CH, 1C), 122.25 (CH, 1C), 122.11 (CH, 1C), 119.89 (CH, 2C), 118.04 (CH, 1C), 117.25 (CH_2, 1C), 116.88 (C, 1C), 109.99 (C, 1C), 91.22 (C, 1C), 75.83 (C, 1C), 66.72 (CH_2, 1C), 66.51 (CH_2, 1C), 65.04 (CH_2, 1C), 50.81(CH, 1C), 47.04 (CH, 1C), 36.25 (CH_2, 1C).

IR: 3425.4 cm^{-1} (O-H st), 3059.7 cm^{-1} (N-H st), 2929.1 cm^{-1} (C-H st), 2846.4 cm^{-1} (C-H st), 1718.9 cm^{-1} (C=O st), 1588.4 cm^{-1} (C=N st), 1501.3 cm^{-1} (C=C st), 1266.3 cm^{-1} (C-O st), 1187.9 cm^{-1} (C-N st).

HRMS (ESI$^+$): calculated for $C_{37}H_{30}N_2O_8S$: 662.1723; found: 663.1793 $[M+H]^+$, 1325.3518 $[2M+H]^+$ and 1347.3351 $[2M+Na]^+$.

4-Allyl 1-(2-(3-(2'-benzothiazole)-4-MOMO-phenyl)-2-oxoethyl) Fmoc-L-aspartate (21)

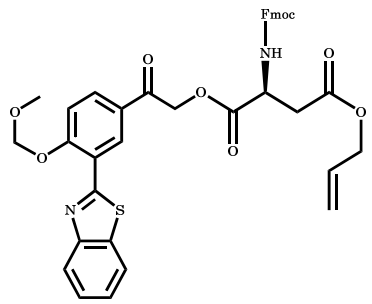

Chloromethyl methyl ether (2.80 mmol) was dissolved in DME (2 mL) and stirred at room temperature for 10 min. After that, DIEA (2.99 mmol) and compound **20** (0.543 mmol) in DME (8 mL) were added. The obtained reddish and transparent solution was stirred overnight at room temperature. The reaction was quenched with Na_2CO_3 (7 mL) and H_2O (5.5 mL). Aqueous phase was extracted twice with DCM and organic phase washed with brine, dried over Na_2SO_4 and concentrated to dryness obtaining 0.33 g of **21** as a yellow solid (84 %).

MP: 120.3 – 122.0 ºC **$[\alpha]_D$:** - 31.90

^{1}H NMR (400 MHz, CD_3COCD_3) δ (ppm); 9.20 (d, *J* = 2.3 Hz, 1H), 8.17 (dd, *J* = 8.8, 2.4 Hz, 1H), 8.12 (d, *J* = 9.2 Hz, 2H), 7.86 (dd, *J* = 7.7, 4.9 Hz, 2H), 7.70 (d, *J* = 7.5 Hz, 2H), 7.58 (ddd, *J* = 8.2, 7.2, 1.2 Hz, 1H), 7.53 – 7.45 (m, 2H), 7.40 (t, *J* = 7.3 Hz, 2H), 7.35 – 7.29

(m, 2H), 7.05 (d, *J* = 8.7 Hz, 1H), 5.95 (ddd, *J* = 17.3, 10.7, 5.5 Hz, 1H), 5.64 (d, *J* = 11.7 Hz, 3H), 5.55 (d, *J* = 16.2 Hz, 1H), 5.35 (dq, *J* = 17.3, 1.6 Hz, 1H), 5.21 (d, *J* = 10.5 Hz, 1H), 4.94 – 4.86 (m, 1H), 4.63 (dt, *J* = 5.6, 1.5 Hz, 2H), 4.36 (t, *J* = 6.9 Hz, 2H), 4.25 (t, *J* = 7.3 Hz, 1H), 3.59 (s, 3H), 3.22 – 2.95 (m, 2H).

^{13}C NMR (101 MHz, CD_3COCD_3) δ (ppm); 191.34 (CO, 1C), 171.51 (CO, 1C), 170.53 (CO, 1C), 162.22 (C, 1C), 159.36 (CO, 1C), 152.99 (C, 1C), 144.96 (C, 1C), 142.10 (C, 1C), 137.04 (C, 1C), 133.45 (C, 1C), 132.36 (CH, 1C), 132.35 (CH, 1C), 130.39 (CH, 1C), 128.53 (CH, 2C), 127.95 (CH, 1C), 127.23 (CH, 1C), 126.14 (CH, 2C), 123.87 (CH, 1C), 123.60 (CH, 1C), 122.45 (CH, 1C), 120.82 (CH, 1C), 120.80, (CH, 2C) 118.17 (CH, 1C), 115.78 (CH_2, 1C), 114.50 (C, 1C), 110.91 (C, 1C), 95.51 (CH_2, 1C), 91.52 (C, 1C), 76.47 (C, 1C), 67.75 (CH_2, 1C), 67.41 (CH_2, 1C), 65.96 (CH_2, 1C), 57.30 (CH_3, 1C), 47.96 (CH, 1C), 37.19 (CH, 1C), 29.84 (CH_2, 1C).

IR: 3059.7 cm^{-1} (N-H st), 2924.8 cm^{-1} (C-H st), 2846.4 cm^{-1} (C-H st), 1727.7 cm^{-1} (C=O st), 1601.5 cm^{-1} (C=N st), 1501.3 cm^{-1} (C=C st), 1261.9 cm^{-1} (C-O st), 1157.4 cm^{-1} (C-N st), 957.2 cm^{-1} (C-O-C st sy).

HRMS (ESI$^+$): calculated for $C_{39}H_{34}N_2O_9S$: 706.1985; found: 707.2059 $[M+H]^+$.

1-(2-(3-(2'-benzothiazole)-4-MOMO-phenyl)-2-oxoethyl) Fmoc-L-aspartic acid, HBB (22)

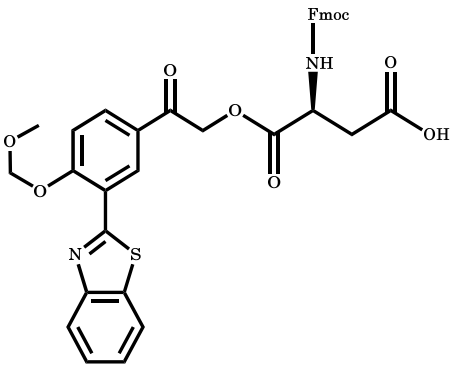

To a round bottom flask containing compound **21** (0.071 mmol) dissolved in dry DCM (1.5 mL) and under N_2 atmosphere, phenylsilane (0.71 mmol) was added and the mixture stirred for 30 seconds. At that point, $Pd(PPh_3)_4$ (7.1x10^{-3} mmol) was dissolved in DCM (0.5 mL) and added to de solution. The reaction was stirred at room temperature for three hours. Once the reaction was finished, the resulting dark brown solution was filtered three times through a nylon filter and evaporated to dryness thus

obtaining the compound **22** as a brownish solid. This product was used without further purification.

^{1}H NMR (400 MHz, CD_3COCD_3) δ (ppm); 9.20 (d, *J* = 2.3 Hz, 1H), 8.17 (dd, *J* = 8.6, 2.3 Hz, 1H), 8.12 (d, *J* = 8.2 Hz, 2H), 7.85 (d, *J* = 7.9 Hz, 2H), 7.60 (d, *J* = 5.8 Hz, 2H), 7.55 (d, *J* = 3.2 Hz, 1H), 7.50 (d, *J* = 2.6 Hz, 1H), 7.40 (t, *J* = 7.6 Hz, 2H), 7.32 (t, *J* = 7.2 Hz, 2H), 7.03 (d, *J* = 9.0 Hz, 1H), 5.66 (s, 2H), 5.60 (m, 2H), 4.88 (td, *J* = 8.1, 4.4 Hz, 1H), 4.40-4.29 (m, 2H), 4.25 (t, *J* = 7.1 Hz, 1H), 3.59 (s, 3H), 3.17 – 2.93 (m, 2H).

[HBB1_D-Cys(trt)3,14_Msa7_D-Trp8]-SRIF14 (23)

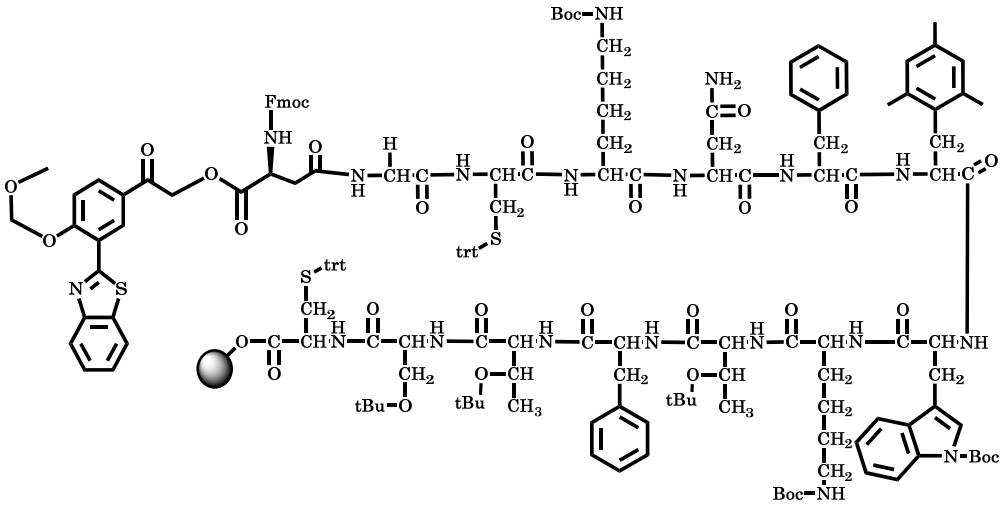

To 35 mg of 2-CTC resin containing the linear peptide (SOM 2-14), compound **22** (1.79 mmol) was added together with HOBt (1.74 mmol) and DIPCDI (1.74 mmol) in DMF (5 mL). Mixture was stirred for 1.5 hours at room temperature giving compound **23**. Reaction progress was checked by Kaiser test and mini cleavage protecting the mixture from light.

MALDI-TOF: calculated for $C_{110}H_{131}N_{19}O_{25}S_3$ (**23-PGs**[18]): 2215,5; found: m/z = 2215.9 $[M]^+$, m/z = 2237.9 $[M+Na]^+$ and m/z = 2253.8 $[M+K]^+$.

[18] Note that due to the acidic conditions of the mini-cleavage, all the protecting groups are deprotected.

[HBB1_D-Cys3,14_Msa7_D-Trp8]-SRIF14 (24)

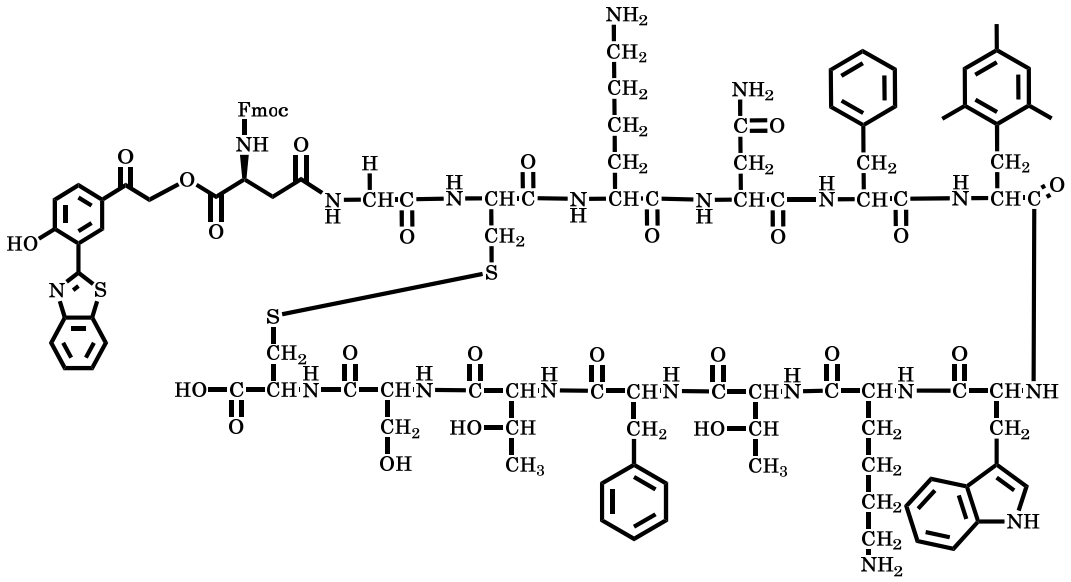

Following the protocol described in section 9.2.3, peptide was cleaved from the resin, cyclised and side chains deprotected to obtain the light-sensitive final compound **24**. This part of the synthesis had to be done protected from light so as not to trigger a light-mediated release of benzothiazolic part.

HRMS (ESI$^+$): calculated for $C_{110}H_{129}N_{19}O_{25}S_3$: 2211.8569; found: 1117.9244 $[M+H+Na]^{2+}$, 1106.9362 $[M+2H]^{2+}$ and 738.2952 $[M+3H]^{3+}$.

2-bromo-1-(3-(2'-benzothiazole)-4-MOMO-phenyl)ethan-1-one, (MOM-19)

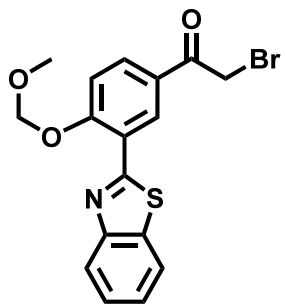

To a solution of MOMCl (29.58 mmol) in DME (15 mL), a solution of compound **19** (5.74 mmol) and DIEA (31.59 mmol) in DME (17 mL) was added at room temperature and stirred for 18 h. Reaction was quenched with a saturated solution of Na_2CO_3 (32 mL) and H_2O (24 mL), aqueous phase extracted four times with DCM and the organic phase washed with brine and evaporated thus obtaining a yellow solid. The solid was filtered and air dried obtaining 1.91 g of **MOM-19** (85%).

MP: 132.4 – 133.8 ºC

^{1}H NMR (400 MHz, $CDCl_3$) δ (ppm); 9.14 (d, *J* = 2.3 Hz, 1H), 8.17 – 8.10 (m, 2H), 7.97 – 7.94 (m, 1H), 7.54 (ddd, *J* = 8.3 Hz, 7.2 Hz, 1.2 Hz, 1H), 7.45 – 7.37 (m, 2H), 5.52 (s, 2H), 4.85 (s, 2H), 3.59 (s, 3H).

^{13}C NMR (101 MHz, $CDCl_3$) δ; 189.70 (C, 1C), 158.52 (C, 1C), 151.98 (C, 1C), 136.08 (C, 1C), 132.01 (CH, 1C), 130.55 (CH, 1C), 128.41 (C, 1C), 126.26 (CH, 1C), 125.16 (CH, 1C), 123.16 (CH, 1C), 122.90 (C, 1C), 121.23 (CH, 1C), 114.79 (CH, 1C), 110.0 (C, 1C), 94.39 (CH_2, 1C), 57.02 (CH_3, 1C), 46.11 (CH_2, 1C).

IR: 3056.6 cm^{-1} (C-H st), 2917.7 cm^{-1} (C-H st), 1693.6 cm^{-1} (C=O st), 1595.2 cm^{-1} (C=N st).

HRMS (ESI$^+$): calculated for $C_{17}H_{14}BrNO_3S$: 390.9878; found: 390.9865 $[M+H]^+$.

2-(2'-MOMO-phenyl)-benzothiazole, (MOM-HPB)

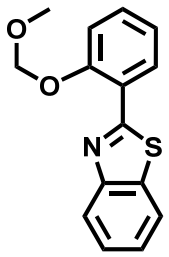

To a solution of MOMCl (11.33 mmol) in DME (3.3 mL), a solution of 2-(2'-hydroxyphenyl)benzothiazole (HPB) (2.2 mmol) and DIEA (12.1 mmol) in DME (5.54 mL) was added at room temperature and stirred for 18 h. Reaction was quenched with a saturated solution of Na_2CO_3 (7.5 mL) and H_2O (5.5 mL), aqueous phase extracted two times with DCM and the organic phase washed with brine and evaporated thus obtaining a 0.54g of **MOM-HPB** as a greenish oil.

^{1}H NMR (400 MHz, $CDCl_3$) δ (ppm); 8.54 (dd, *J* = 7.9 Hz, 1.7 Hz, 1H), 8.10 (ddd, *J* = 8.2 Hz, 1.2 Hz, 0.7 Hz, 1H), 7.93 (ddd, *J* = 8.0 Hz, 1.3 Hz, 0.6 Hz, 1H), 7.49 (ddd, *J* = 8.3 Hz, 7.2 Hz, 1.3 Hz, 1H), 7.44 (ddd, *J* = 8.5 Hz, 7.2 Hz, 1.8 Hz, 1H), 7.38 (ddd, *J* = 8.1 Hz, 7.2 Hz, 1.2 Hz, 1H), 7.28 (dd, *J* = 8.4 Hz, 1.0 Hz, 1H), 7.18 (ddd, *J* = 8.2 Hz, 7.3 Hz, 1.1 Hz, 1H), 5.43 (s, 2H), 3.58 (s, 3H).

^{13}C NMR (101 MHz, $CDCl_3$) δ (ppm); 162.98 (C, 1C), 154.78 (C, 1C), 152.17 (C, 1C), 136.10 (C, 1C), 131.69 (CH, 1C), 129.61 (CH, 1C), 125.94 (CH, 1C), 124.68 (CH, 1C), 122.90 (C, 1C), 122.88 (CH, 1C), 122.17 (CH, 1C), 121.16 (CH, 1C), 114.67 (CH, 1C), 94.42 (CH_2, 1C), 56.66 (CH_3, 1C).

IR: 3064.1 cm^{-1} (C-H st), 2955.3 cm^{-1} (C-H st), 2885.6 cm^{-1} (C-H st), 1597.1 cm^{-1} (C=N st), 1501.3 cm^{-1} (C=C st), 1235.8 (C-O st).

HRMS (ESI$^+$): calculated for $C_{15}H_{13}NO_2S$: 271.0667; found: 272.0738 $[M+H]^+$.

(3-(2'-benzothiazole)-4-hydroxyphenyl)-2-oxoethyl formate, (25)

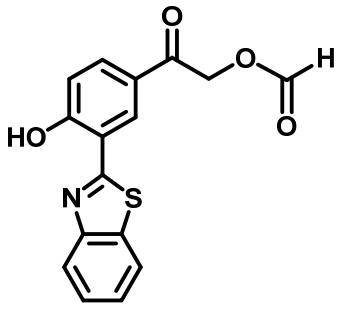

Following the previously described strategy,[19] compound **19** (2.87 mmol) and DBU (0.87 mL, 5.85 mmol) were combined and placed in a 250 mL round bottom flask and dissolved in 50 mL of 1:1 CH_2Cl_2/1,4-dioxane and cooled to 0° C. Once the acid and base solutions were cool, the formic acid (0.16 mL, 4.31 mL) was slowly added to the base making sure to keep the flask cold. When the acid had dissolved, the solution was stirred for 21h at room temperature. When the reaction was judged to be complete, equal volumes (5 mL) of CH_2Cl_2 and H_2O were added to the reaction mixture. The organic layer was washed 3 times with H_2O, once with a saturated $NaHCO_3$ solution, once with 0.1N HCl and, finally, washed once with brine, dried over $MgSO_4$, filtered and the solvent was removed. Purification was performed using column chromatography (6:4 hexane/EtOAc) to yield 0.206 mg of **25** as a white crystalline solid (23% yield).

MP: 174.1 - 174.7 °C

[19] M. Remeš, J. Roithová, D. Schröder, E. D. Cope, C. Perera, S. N. Senadheera, K. Stensrud, C. C. Ma, R. S. Givens, *J. Org. Chem.,* **2011**, *76*, 2180 - 2186.

^{1}H NMR (400 MHz, $CDCl_3$) δ (ppm); 8.36 (d, *J* = 2.1 Hz, 1H), 8,29 (s, 1H), 8.03 (d, *J* = 8.1 Hz, 1H), 7.97 – 7.91 (m, 2H), 7.56 (ddd, *J* = 8.2, 7.3, 1.3 Hz, 1H), 7.47 (ddd, *J* = 7.8, 7.3, 1.2 Hz, 1H), 7.18 (d, *J* = 8.7 Hz, 1H), 5.45 (s, 2H).

^{13}C NMR (101 MHz, $CDCl_3$) δ (ppm); 188.9 (CO, 1C), 168.2 (C, 1C), 162.6 (C, 1C), 160.1 (COH, 1C), 151.4 (C, 1C), 132.6 (C, 1C), 132.0 (CH, 1C), 129.1 (CH, 1C), 127.1 (CH, 1C), 126.2 (CH, 1C), 125,9 (C, 1C) 122.4 (CH, 1C), 121.7 (CH, 1C), 117,1 (C, 1C), 118.4 (CH, 1C), 65.1 (CH_2, 1C).

IR: 3425.4 cm^{-1} (O-H st), 2916.1 cm^{-1} (C-H st), 2878.5 cm^{-1} (C-H st), 1727.7 (C=O st) 1688.5 cm^{-1} (C=O st), 1589.1 cm^{-1} (C=N st), 1501.3 cm^{-1} (C=C st).

HRMS (ESI$^+$): calculated for $C_{16}H_{11}NO_4S$: 313.0409; found: 314.0479 $[M+H]^+$.

(3-(2'-benzothiazole)-4-MOMO-phenyl)-2-oxoethyl formate, (26)

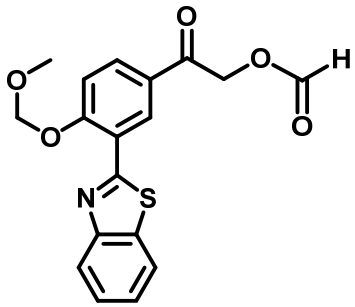

To a solution of MOMCl (0.822 mmol) in DME (3 mL), a solution of compound **25** (0.159 mmol) and DIEA (0.878 mmol) in DME (5 mL) was added at room temperature and stirred for 18 h. Once the reaction was judged to be complete, the solvent was evaporated. The resulting crude was dissolved in CH_2Cl_2 and then, quenched with a saturated solution of Na_2CO_3 (7.5 mL) and H_2O (5.5 mL), aqueous phase extracted two times with DCM and the organic phase washed with brine, dried over Na_2SO_4 and the solvent evaporated. 55.5 mg of compound **26** were obtained as a white solid (97% yield).

MP: 133.9 - 134.5 ºC

^{1}H NMR (400 MHz, $CDCl_3$) δ (ppm); 9.12 (d, *J* = 2.3 Hz, 1H), 8.29 (s, 1H), 8.16 – 8.08 (m, 2H), 7.96 (d, *J* = 7.9 Hz, 1H), 7.54 (ddd, *J* = 8.3, 7.2, 1.3 Hz, 1H), 7.45 – 7.42 (m, 1H), 7.40 (d, *J* = 8.8 Hz, 1H), 5.58 (s, 2H), 5.52 (s, 2H), 3.59 (s, 3H)

^{13}C NMR (101 MHz, $CDCl_3$) δ (ppm); 194.7 (CO, 1C), 168.6 (C, 1C), 162.2 (C, 1C), 151.5 (C, 1C), 132.6 (CH, 1C), 129.5 (CH, 1C), 127.1 (C, 1C), 126.9 (CH, 1C), 126.0 (CH, 1C), 122.3 (CH, 1C), 121.7 (CH, 1C), 118.0 (CH, 1C), 116.8 (C, 1C), 110,0 (C, 1C), 73.9 (CH_2, 1C), 67.3 (CH_2, 1C), 15.0 (CH_3, 1C).

IR: 3331.5 cm^{-1} (O-H st), 2917.7 cm^{-1} (C-H st), 2848.3 cm^{-1} (C-H st), 1690.7 cm^{-1} (C=O st), 1592.3 cm^{-1} (C=N st), 1499.7 cm^{-1} (C=C st).

HRMS (ESI^+): calculated for $C_{18}H_{15}NO_5S$: 357.0671; found: 358.0743 $[M+H]^+$.

9.2.7 Serum stability

Half-life times were carried out in Lead Molecular Design S.L. (Molecular Discovery Ltd, Middlesex, UK) in collaboration with Gabrielle Cruciani's research group in the University of Perugia (Italy).

A peptide solution of 6 mg/mL in Milli-Q water (solution **A**) was prepared in an eppendorf tube while human serum (Sigma, 4522) was incubated at 37ºC. A 1:10 dilution was prepared; i.e. for preparing 3 mL of study solution, 300 µL of solution **A** were added to 2700 µL of human serum, obtaining a final concentration of 0.6 mg/mL (solution **B**). Just after that, 200 µL of **B** were dispensed in eppendorf tubes and incubated at 37ºC. At specified times (0, 5 min, 10 min, 30 min, 1 h, 2 h, 4 h, 8 h, 24 h, 30 h and 48 h) aliquots were taken, and precipitated with 400 µL of cold ACN and 0.6 M solution of labetalol (Sigma, L1011) added as an internal standard (final peptide concentration 0.12 mg/mL).

Samples were cooled down in an acetone-dry ice bath for some seconds before centrifuging them at 10000 rpm for 5 min and 4ºC (Eppendorf 5810 R). Samples were analysed by RP-UPLC (Thermo Scientific Ultimate 3000 ultra-performance liquid chromatography) equipped with a Zorbax Eclipse Plus C18 column (150 x 2.1 mm, 1.8 µm) using H_2O-0.1%TFA and ACN-0.1%TFA as eluents over 20 min. Negative controls were prepared under the same conditions containing serum, ACN and labetalol. Half-

lives of peptides in human serum were calculated from the analysis of the degradation data. Analysis of this data was carried out using a linear regression of the natural logarithm of the percentage of peak area integration with respect to time. The determination of the slope, corresponding to the experimental constant, allowed the calculation of the half-life:

$$t_{1/2} = \ln 2 / Ke$$

where $t_{1/2}$ is the half-life and Ke the decay constant.

9.2.8 Fragmentation studies

Metabolism studies to obtain probable fragmentations of synthesised peptides were carried out in Lead Molecular Design S.L. (Molecular Discovery Ltd, Middlesex, UK) in collaboration with Gabrielle Cruciani's research group in the University of Perugia (Italy).

Serum stability samples were further analysed and were used for these assays. Samples were analysed using a data-dependent MS/MS method. Chromatographic separation of the metabolites was performed in a Thermo Ultimate 3000 UPLC system equipped with a Zorbax Exlipse C18 column (150 mm x 2.1 mm, 18 μm) heating the system up to 40ºC. Linear gradients of H_2O-0.1%TFA and ACN-0.1%TFA over 20 min were used to run the experiments with a flow rate of 0.25 mL/min.

All data obtained from the LC-MS/MS was processed using Mass-MetaSite 5.1.9 and WebMetabase 3.2.9 (Molecular Discovery Ltd, Middlesex, UK) where all the samples from the same experiment were clustered together for further analysis and interpretation. Each experiment was composed of a set of different samples (i.e. one sample per time point). Mass-MetaSite processed every sample file as a separate unit collecting the metabolic scheme, the structural fragment assignment and the chromatogram (retention time, MS area, MS relative are and ppm).

WebMetabase consolidated all the data related to the same experiment and analysed which metabolite peaks from each sample could be grouped based on the retention time and *m/z*. Once the experiment results were interpreted and approved in WebMetabase, peptides and metabolites were stored in the database. Identification of metabolites and its correspondence with the parent compound was performed as previously described.[20]

The application of Mass-MetaSite for the interpretation of small molecules metabolic stability data has been reported before.[21] In our case, not only amide bond cleavage has been studied but also disulphide bridge breakage.

[20] T. Radchenko, A. Brink, Y. Siegrist, C. Kochansky, A. Bateman, F. Fontaine, L. Morettoni, I. Zamora, *PlosOne*, **2017**, article number: 0186461.

[21] a) B. Bonn, C. Leandersson, F. Fontaine, I. Zamora, *Rapid. Commun. Mass. Spectrom.*, **2010**, *24*, 3127-3138; b) E. N. Cece-Esencan, *et al.*, *Rapid. Commun. Mass. Spectrom.*, **2016**, *30*, 301-310; c) I. Zamora, F. Fontaine, B. Serra, G. Plasencia, *Drug Discov. Today Technol.*, **2013**, *10*, e199-205; d) V. Zelesky, R. Schneider, J. Janiszewski, I. Zamora, J. Ferguson, M. Troutman, *Bioanalysis*, **2013**, *5*, 1165-1179; e) M. Ahlqvist, C. Leandersson, M. A. Hayes, I. Zamora, R. A. Thompson, *Rapid. Commun. Mass. Spectrom.*, **2015**, *29*, 2083-2089; f) A. Brink, *Drug Discov. Today Technol.*, **2013**, 10, e207-217; g) A. Brink, *et al.*, *Rapid. Commun. Mass. Spectrom.*, **2014**, *28*, 2695-2703.

Appendix 1

Final observations

Upon completion of the present doctoral thesis entitled *Somatostatin analogues as drug delivery systems for receptor-targeted cancer therapy*, Chapter 6 (corresponding to the derivatives of the D-amino acids family) was in the pre-publication phase, being *First Stable and Selective 14-amino acid Somatostatin Analogue* the provisional title.

Appendix 2

List of peptides

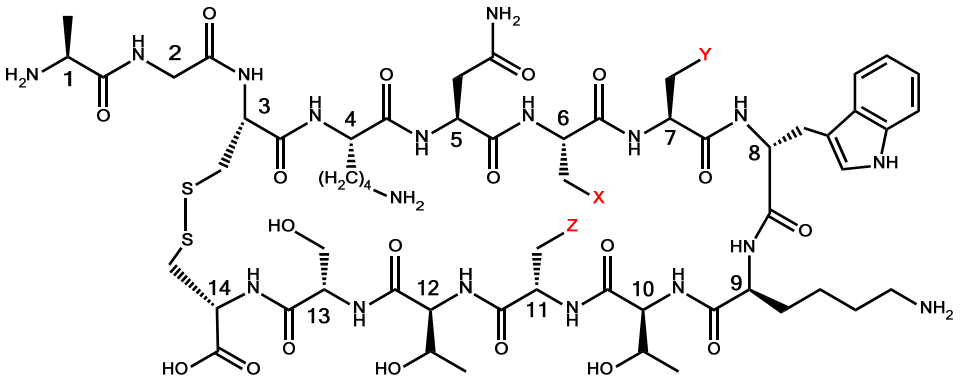

Dmp family
[L-Dmp6_D-Trp8]-SRIF14 (1)
[L-Dmp7_D-Trp8]-SRIF14 (2)
[L-Dmp11_D-Trp8]-SRIF14 (3)
Pya family
[Msa6_L-4'Pya7_D-Trp8]-SRIF14 (4)
[Msa6_L-3'Pya7_D-Trp8]-SRIF14 (5)
Qla family
[Msa7_L-Qla8]-SRIF14 (6)
[L-Qla8_4'Pya11]-SRIF14 (6.1)
[L-Qla8_3'Pya11]-SRIF14 (6.2)
D-amino acid family
[Msa7_D-Trp8]-SRIF14 (7)*
[Msa7_D-Trp8_D-Cys14]-SRIF14 (8)
[D-Ala1_Msa7_D-Trp8_D-Cys14]-SRIF14 (9)
[D-Cys3,14 _Msa7_D-Trp8]-SRIF14 (10)
[D-Ala1_D-Cys3,14_Msa7_D-Trp8]-SRIF14 (11)
[L-Orn4_Msa7_D-Trp8]-SRIF14 (12)
[L-Orn4_Msa7_D-Trp8_D-Cys14]-SRIF14 (13)

*Peptide previously synthesised by Dr. Martín-Gago.

Appendix 3

Selected examples of ^{1}H-^{1}H assignation

[L-Dmp11_D-Trp8]-SRIF14 (3)

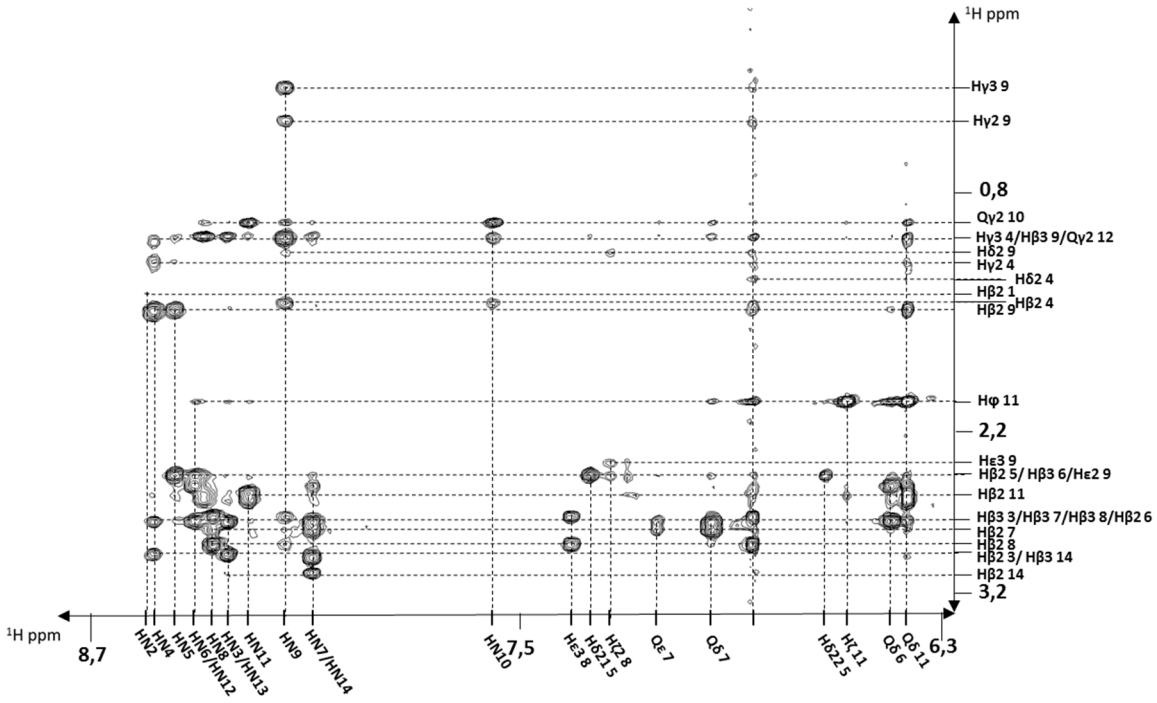

Bidimensional homonuclear NOESY 350 ms spectrum for [L-Dmp11_D-Trp8]-SRIF14 (**3**). Enlargement of the upper left sector.

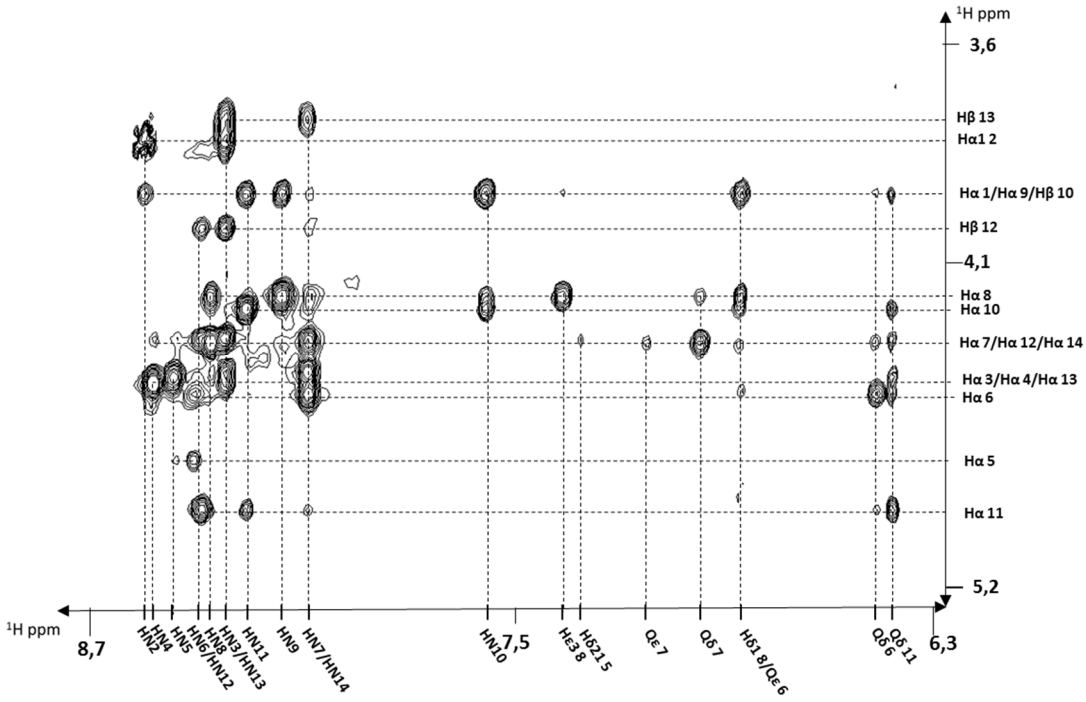

Bidimensional homonuclear NOESY 350 ms spectrum for [L-Dmp11_D-Trp8]-SRIF14 (**3**). Enlargement of the central left sector.

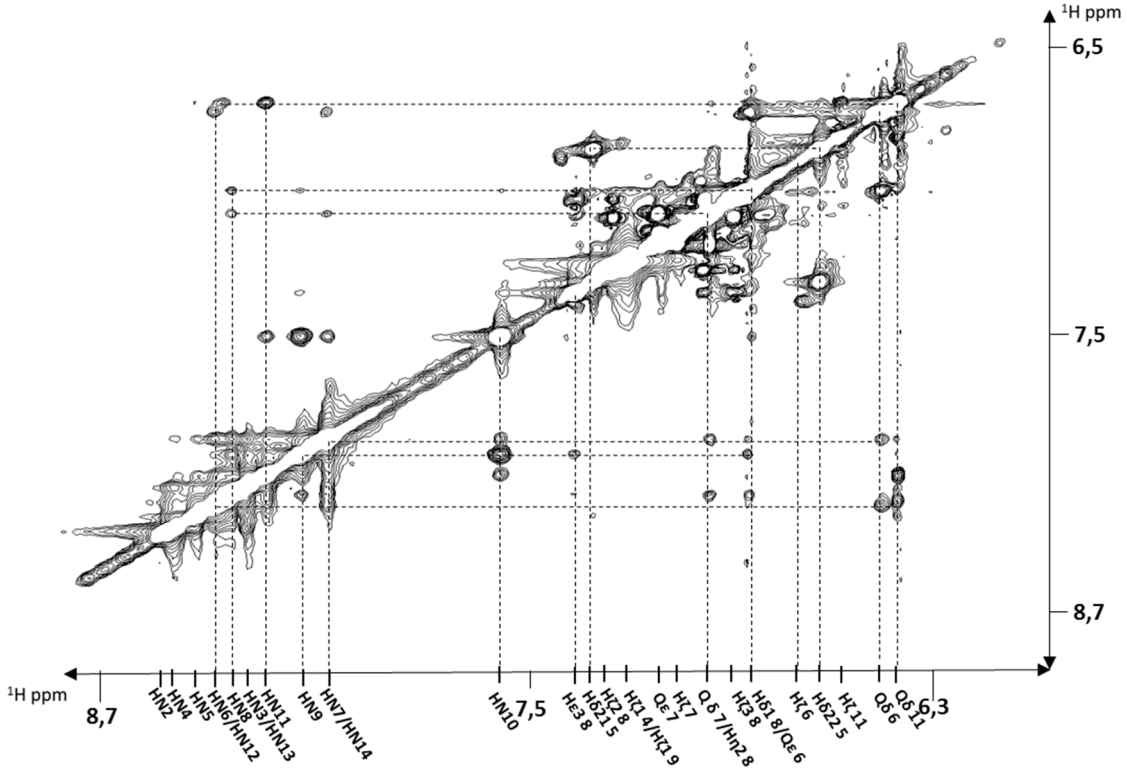

Bidimensional homonuclear NOESY 350 ms spectrum for [L-Dmp11_D-Trp8]-SRIF14 (**3**). Enlargement of the lower left sector.

[Msa6_L-4'Pya7_D-Trp8]-SRIF14 (4)

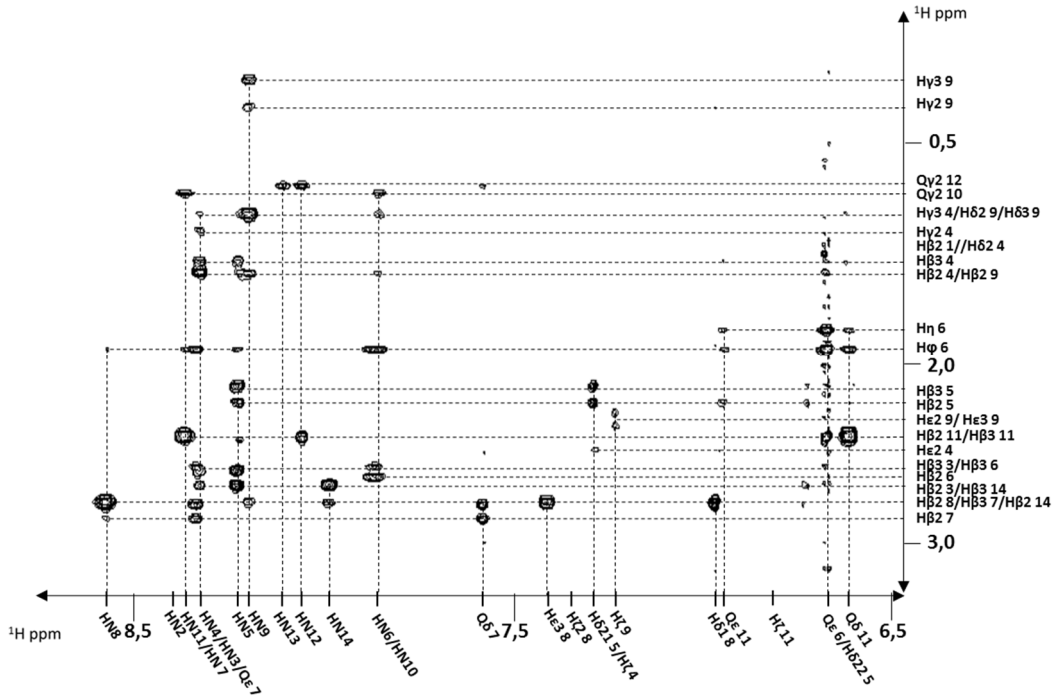

Bidimensional homonuclear NOESY 150 ms spectrum for [Msa6_L-4'Pya7_D-Trp8]-SRIF14 (**4**). Enlargement of the upper left sector.

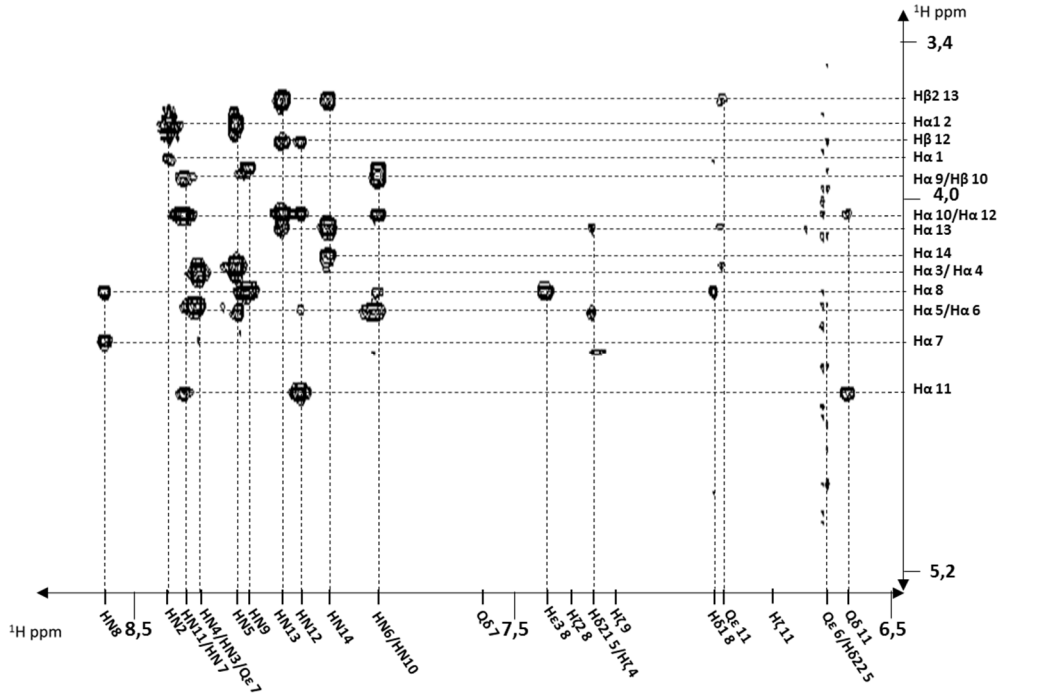

Bidimensional homonuclear NOESY 150 ms spectrum for [Msa6_L-4'Pya7_D-Trp8]-SRIF14 (**4**). Enlargement of the central left sector.

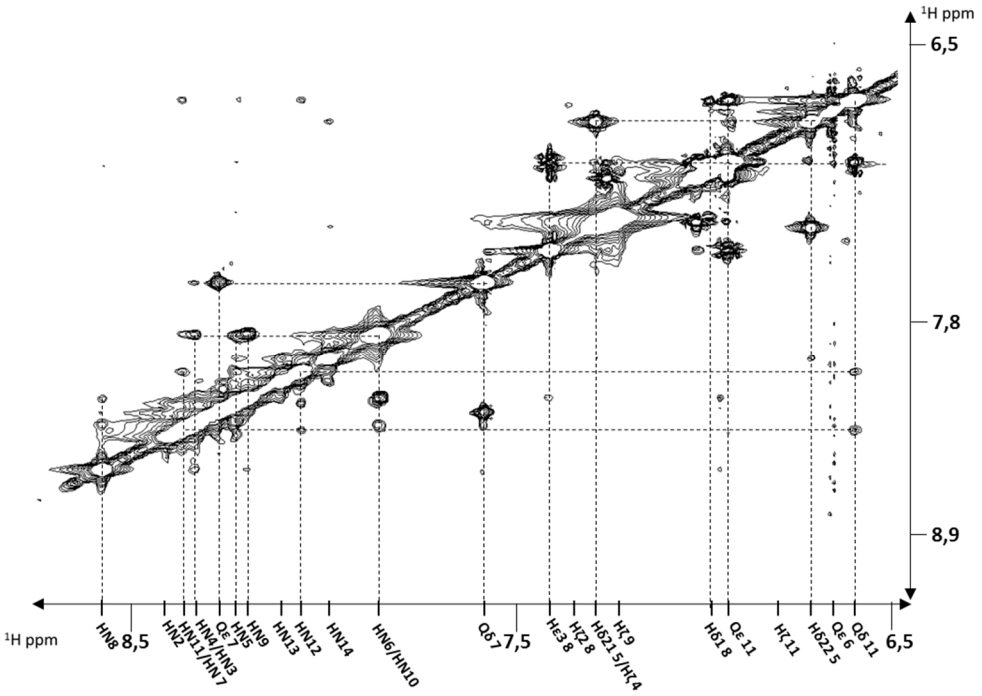

Bidimensional homonuclear NOESY 150 ms spectrum for [Msa6_L-4'Pya7_D-Trp8]-SRIF14 (**4**). Enlargement of the lower left sector.

[D-Ala1_D-Cys3,14_Msa7_D-Trp8]-SRIF14 (11)

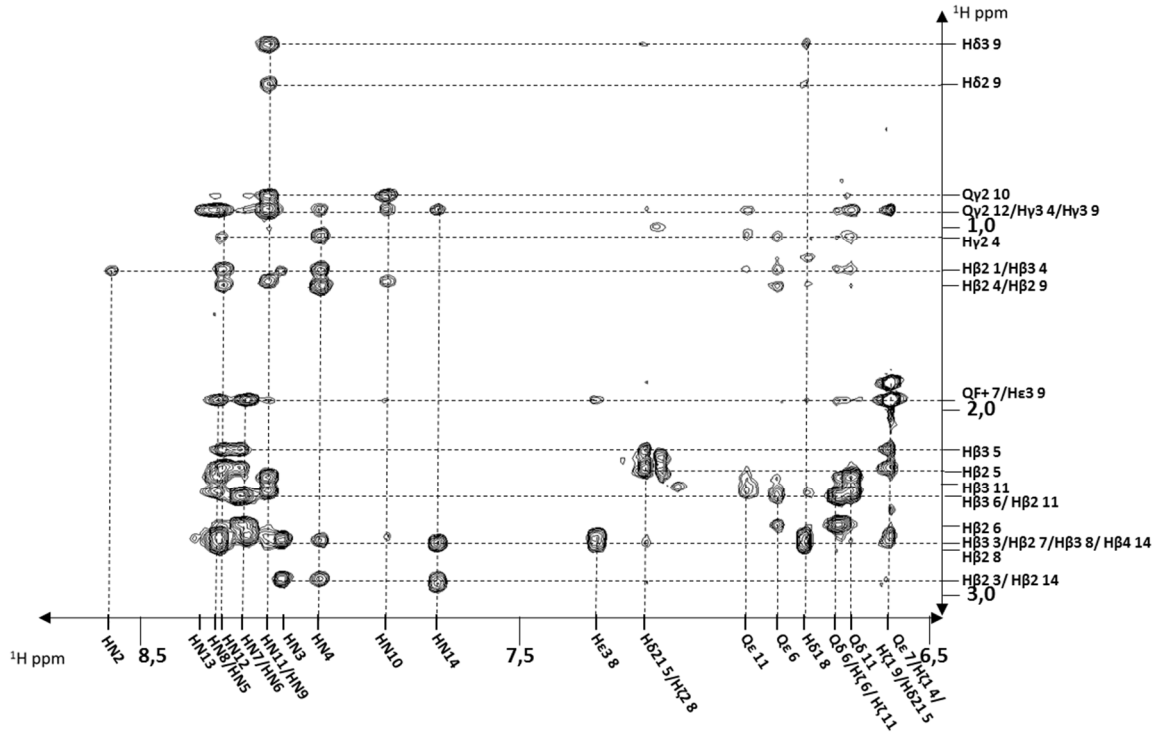

Bidimensional homonuclear NOESY 350 ms spectrum for [D-Ala1_D-Cys3,14_Msa7_D-Trp8]-SRIF14 **(11)**. Enlargement of the upper left sector.

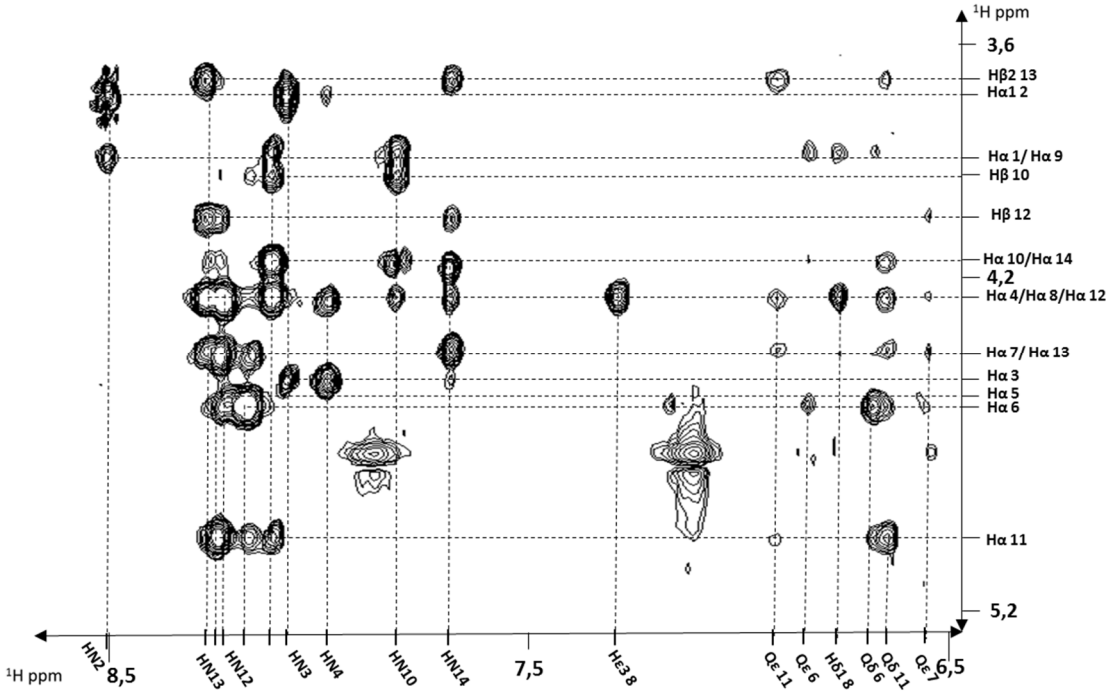

Bidimensional homonuclear NOESY 350 ms spectrum for [D-Ala1_D-Cys3,14_Msa7_D-Trp8]-SRIF14 **(11)**. Enlargement of the central left sector.

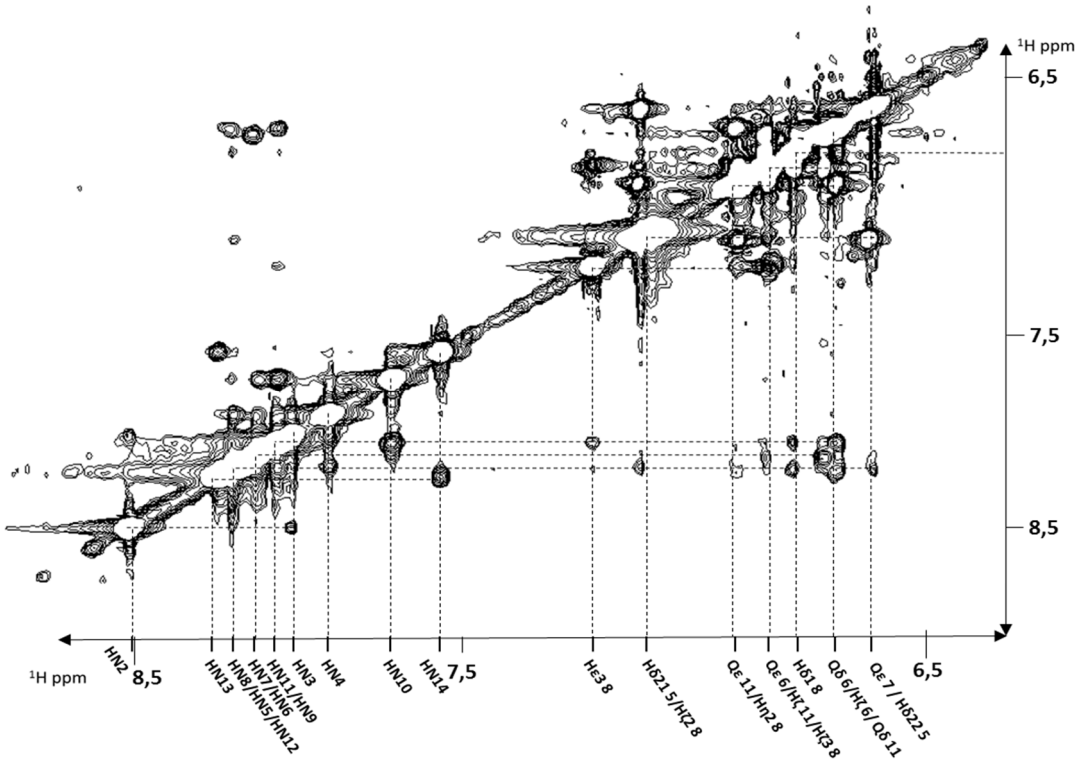

Bidimensional homonuclear NOESY 350 ms spectrum for [D-Ala1_D-Cys3,14_Msa7_D-Trp8]-SRIF14 **(11)**. Enlargement of the lower left sector.